THE UNIVERSITY
of EDINBURGH

SPATIAL AND TEMPORAL REGULATION OF CEREBRAL CORTEX DEVELOPMENT BY THE TRANSCRIPTION FACTOR PAX6

By Petrina A. Georgala

Thesis submitted for the degree of Doctor of Philosophy

University of Edinburgh

September 2010

DISCLAIMER

I (Petrina Georgala) performed all of the experiments presented in this thesis unless otherwise clearly stated in the text. No part of this work has been, or is being submitted for any other degree of qualification.

Signed:

Date:

ACKNOWLEDGEMENTS

First and foremost, I offer my sincerest gratitude to David Price who has supported me throughout my PhD research. I appreciate his knowledge of the field, patience towards student training and enthusiasm about science. One could simply not wish for a better advisor. I am extremely grateful to Martine Manuel and John Mason, members of my thesis committee, for their critical comments and helpful suggestions throughout my studies. I would like to acknowledge Tom Pratt and Peter Kind for thoughtful discussions and invaluable suggestions during this work.

My special thanks to my friends and colleagues in DBUG. It was a great pleasure to work with such wonderful people, thank you for providing an atmosphere that makes science fun, as well as for your excellent advice and collaborations. I would like to thank Mike Molinek for providing me with excellent technical advice. A very special thanks goes to Chris Conway for making my time in Edinburgh a more enjoyable experience. I would also like to thank Natasha Tian and Dario Magnani for being excellent friends and great fun throughout my PhD years.

I am deeply indebted to my parents for their encouragement and never-ending support that has been a powerful source of inspiration and energy throughout my entire life. A special thought is also devoted to my brother and best friend, Babis. Without you life would not be nearly as beautiful.

ABSTRACT

Lamina formation in the developing cortex requires precise generation, migration and differentiation of cortical neurons. Cortical projection neurons originate from progenitors of the embryonic dorsal telencephalon. The transcription factor Pax6 is expressed in apical progenitors (APs) throughout corticogenesis in a rostro-lateral^{high} to caudo-medial^{low} gradient. The current studies focus on elucidating the spatial and temporal role of Pax6 in cortical development. I first analysed the cortex of PAX77 transgenic mice that overexpress Pax6 in its normal domains of expression. I show that Pax6 overexpression acts cell-autonomously to reduce the proliferation of late cortical progenitors specifically, resulting in the formation of thinner superficial layers in the PAX77 cortex. Increased levels of Pax6 lengthen the cell cycle of APs and drive the system towards neurogenesis. These effects are specific to late stages of corticogenesis, when superficial layer neurons are normally generated, in cortical regions that express Pax6 at the highest levels. The number of superficial layer neurons is reduced in postnatal PAX77 mice, while radial migration and lamina specification of cortical neurons are not affected by Pax6 overexpression. Then, Pax6 was conditionally inactivated in cortical progenitors at mid- or late-stages of corticogenesis by using a tamoxifen-inducible Emx1-CreER line. I report a novel requirement of Pax6 for continuous suppression of ventral fates and concurrent maintenance of an appropriate dorsal identity in cortical progenitors. Pax6 ablation at either mid- or late-stages of corticogenesis increases the proliferation of late cortical progenitors at all levels across the rostral-caudal axis. In the absence of Pax6 from mid-corticogenesis, late-born neurons are severely under-represented and misspecified in superficial layers of the mutant cortex. Notably, Pax6 inactivation during late corticogenesis also affects superficial laminar fate; although the numbers of late-born cortical neurons are not severely affected in superficial layers of the mutant cortex, substantial numbers of late-born cells fail to migrate to appropriate laminar positions and accumulate in the ventricular zone (VZ) of the postnatal mutant cortex. Collectively, these gain- and loss-of-function studies suggest that disruption of Pax6 levels during different developmental time points leads ultimately to impaired formation of superficial cortical layers but through different cellular and molecular mechanisms.

TABLE OF CONTENTS

TABLE OF FIGURES

CHAPTER 1

CHAPTER 3

CHAPTER 4

CHAPTER 5

CHAPTER 6

ABBREVIATIONS

APs: Apical progenitors

BPs: Basal progenitors

BrdU: 5-bromo-2'-deoxyuridine

CGE: Caudal ganglionic eminence

cKO: Conditional knock-out

CNS: Central nervous system

CP: Cortical plate

CR: Cajal-Retzius

DAB: Diaminobenzidine

dLGE: Dorsal lateral ganglionic eminence

dTel: Dorsal telencephalon

Emx: Empty spiracles homeobox gene

ER^{T2}: Tamoxifen-responsive Estrogen Receptor

GABA: γ-aminobutyric acid

GAD-67: Glutamic Acid Decarboxylase 67

GFP: Green Fluorescent Protein

IdU: 5-iodo-2'-deoxyuridine

hGFAP: Human glial fibrillary acidic protein

I.p.: Intraperitoneal

IZ: Intermediate zone

FACS: Fluorescent activating cell sorting

FGF: Fibroblast growth factor

FP6: Floxed Pax6

LGE: Lateral ganglionic eminence

MGE: Medial ganglionic eminence

MZ: Marginal zone

Ngn: Neurogenin

Olig2: Oligodendrocyte lineage transcription factor 2

Pax: Paired-box gene

PCNA: Proliferating cell nuclear antigen

PFA: Paraformaldehyde

PH3: Phosphorylated histone H3

PBS: Phosphate-buffered saline

PSPB: Pallial-subpallial boundary

RGCs: Radial glial cells

R26: Rosa 26 (reporter allele)

SHH: Sonic hedgehog

SP: Subplate

SVZ: Subventricular zone

Tbr: T-box brain gene

Tg: β-globin transgene

VP: Ventral pallium

dTel: Ventral telencephalon

VZ: Ventricular zone

YFP: Yellow Fluorescent Protein

CHAPTER 1

General Introduction

1.1 Overview

Development of distinct brain regions is a multistep process that starts with the specification of progenitor cells in the regionalized neuroectoderm, followed by intense progenitor cell proliferation that will ultimately give rise to neural progeny constructing the entire brain. Secretion of extracellular signalling factors and expression of transcription factor genes in graded patterns across the field of progenitor cells specify spatial identity. The primary focus of this thesis is on the genetic control of cerebral cortex development, a mammal-specific structure that arises from the dorsal part of the embryonic telencephalon. The neocortex (hereafter referred to as cortex) is the phylogenetically most recent development of the cerebral cortex and is responsible for the higher functions in humans. It contains an extraordinary number of neurons arrayed in a six-layered sheet, with neurons in each layer organized into a complex network of local circuits and subcortical connections. The discovery of regulatory genes that are expressed in characteristic gradients and master cortical development from the earliest stages has provided evidence that intrinsic information regulates important aspects of cortical development in a both temporal and spatial manner, and contributes to the transformation of a simple neuroepithelial sheet to a complex structure subdivided into distinct functional domains. The spatial and temporal roles of the transcription factor Pax6 during cortical development were addressed in this study through analyses of gain- and loss-of-function mutant mice.

1.2 Pax6: a transcription factor expressed in the CNS from early developmental stages

Pax6 is one of a variety of transcription factors required for the normal development of the mammalian brain. It is a member of the paired-box family of transcription factors and therefore has two DNA binding domains, the paired-box and the homeobox. These domains are separated by a glycine-rich linker sequence and can bind DNA both independently and cooperatively (Callaerts et al. 1997; Jun and Desplan 1996). Pax6 expression is first seen as early as embryonic day (E) 8.5 in

mouse. It is widely expressed in the developing CNS including the forebrain, hindbrain and ventral neural tube (Walther and Gruss 1991; Grindley et al. 1995; Warren and Price 1997). It is also expressed in the developing olfactory system and in the lens, cornea and retina of the developing eye. *Pax6* null mice die immediately after birth exhibiting a range of abnormalities, including absence of eyes and nasal structures, a severely malformed cortex, and failure of the diencephalon (the major region of the brain relaying sensory information to the cortex) to innervate the mutant cortex (Schmahl et al. 1993; Warren and Price 1997; Pratt et al. 2000; Tyas et al. 2003).

The paired-box domain, which characterises the *Pax* gene family, was first discovered in the *Drosophila* gene paired and was found to be conserved in a number of functionally related genes (Bopp et al. 1986, 1989). The paired-box domain was subsequently found to be conserved across a wide variety of species from turtle and zebrafish to mammals. The first murine *Pax* gene, *Pax1*, was identified by Deutsch et al. (1988), and to date nine members of the *Pax* gene family have been identified in both mouse and human (for review see Lang et al. 2007). Mutations in *Pax* genes have indicated a link between a number of mouse and human conditions (Chalepakis et al. 1993). The human condition aniridia and its homologous mouse phenotype, *small eye* (*Sey*), were long believed to be caused by mutations in the same gene. Analysis of a candidate gene for aniridia predicted that its protein product would have the characteristics of the paired box family of transcription factors (Ton et al. 1991) and murine cDNA was subsequently found to be 92% homologous to the aniridia gene at the nucleotide level and produced an almost identical amino acid sequence (Ton et al. 1992). Analysis of the *Pax6* gene in mice with a variety of *Sey* alleles confirmed that *Pax6* is the gene responsible for this phenotype (Hill et al. 1991). Identification of the *Drosophila* homolog of *Pax6*, *eyeless*, which is critical for eye formation in the fly, shows a high degree of functional conservation of this gene across species (Quiring et al. 1994).

The conservation of *Pax6* function and the importance of its regulatory role during development are evident from the phenotypes caused by mutations in this gene. In mice, heterozygosity results in reduced eye size and ocular abnormalities including

iris hypoplasia, corneal opacification and cataracts (Hogan et al. 1988). Humans with heterozygous mutations in *PAX6* suffer from aniridia, displaying a variable eye phenotype similar to that seen in heterozygous mice, and so *Sey* (*Pax6*$^{+/-}$) mice provide a good model to study aniridia (Glaser et al. 1990; van der Meer-de Jong et al. 1990). Interestingly, eye development is extremely sensitive to Pax6 dosage with both elevated and decreased levels inducing abnormal phenotypes (Schedl et al. 1996). There is also a variety of structural brain abnormalities associated with *PAX6* haploinsufficiency in humans. Interhemispheric connections through the anterior commissure or the corpus callosum seem to be reduced in aniridia patients (Sisodiya et al. 2001). Consistent with the known function of the anterior commissure to also contain olfactory and auditory fibres, aniridia patients frequently have reduced olfaction or deficient auditory interhemispheric transfer, although the latter is often associated with an absent/hypoplastic anterior commissure and/or a reduced corpus callosum (Sisodiya et al. 2001; Bamiou et al. 2004).

1.3 Early patterning of the embryonic telencephalon

The brain constitutes the major part of the central nervous system (CNS) and develops from the rostral (anterior) region of the neural plate. The neural plate is a flat neuroepithelial sheet that folds to form the neural tube. After neural tube closure, the most rostral portion of the tube undergoes drastic changes inducing distinct swellings of the neural tube that lead to the formation of three primary vesicles: the forebrain (prosencephalon), the midbrain (mesencephalon) and the hindbrain (rhombencephalon) (for review, see Martinez and Puelles 2000). The forebrain is the most rostral region of the developing CNS that will eventually give rise to the two adult cerebral hemispheres; it is subdivided into the telencephalon and the more caudally positioned diencephalon. The midbrain remains a single unit caudal to the diencephalon. The hindbrain develops into the rostral metencephalon and the myelencephalon, the caudal-most division of the brain.

Patterning is a process by which equipotent cells proliferate and organise themselves in distinct territories in response to positional information. The early phases of brain

development involve conferring rostral-caudal identity in the neuraxis through opposing signals. Once the telencephalic neuroepithelium is established rostrally, patterning centres assign dorsal-ventral positional identity to progenitor cells. Such flow of positional information occurs through the secretion of morphogens (diffusible molecules that act in a concentration-dependent manner to specify cell fate) from signalling centres. Morphogens specify cell fate through the establishment and maintenance of transcription factor expression in a region-specific manner throughout the telencephalic neuroepithelium (Fig. 1) (reviewed in Hebert and Fishell 2008; Hoch et al. 2009; Sansom and Livesey 2009; Borello and Pierani 2010). Signalling centres around the borders of the cortical neuroepithelium include the anterior neural ridge, the cortical hem and the anti-hem (localized at the pallial-subpallial boundary) (reviewed in Subramanian et al. 2009; Borello and Pierani 2010). Opposing gradients of morphogen-regulated transcription factor expression orchestrate cortical development from the earliest stages and ultimately lead to the formation of distinct functional domains along the rostral-caudal axis of the cortex. The impact of signalling molecules in the arealization of the cortex is demonstrated, for instance, by findings that increased endogenous Fgf8 levels rostrally result in expansion of rostral cortical identities and shrinkage of the caudal ones, whereas decreased levels have the opposite effect (Fukuchi-Shimogori and Grove 2001; Garel et al. 2003).

The telencephalic primordium, which will subsequently give rise to the cortex dorsally and the ganglionic eminences ventrally, becomes specified at approximately E8.5 in mouse. On a molecular level, this early event can be identified by the expression of Foxg1, the earliest telencephalic marker that is induced by Fgf signalling; Foxg1 expression remains in telencephalic cells throughout development (Shimamura and Rubenstein 1997; Storm et al. 2003). Loss of Foxg1 leads to severe growth defects in the entire telencephalon, although the ventral telencephalon is far more affected compared to the cortex (Xuan et al. 1995; Martynoga et al. 2005; Hanashima et al. 2007). Critical for conferring early regional identity in the developing telencephalon are the transcription factors *Pax6* and *Emx2* (expressed dorsally), and *Gsh2* and *Nkx2.1* (expressed ventrally). Pax6 is expressed in a rostro-

FIGURE 1

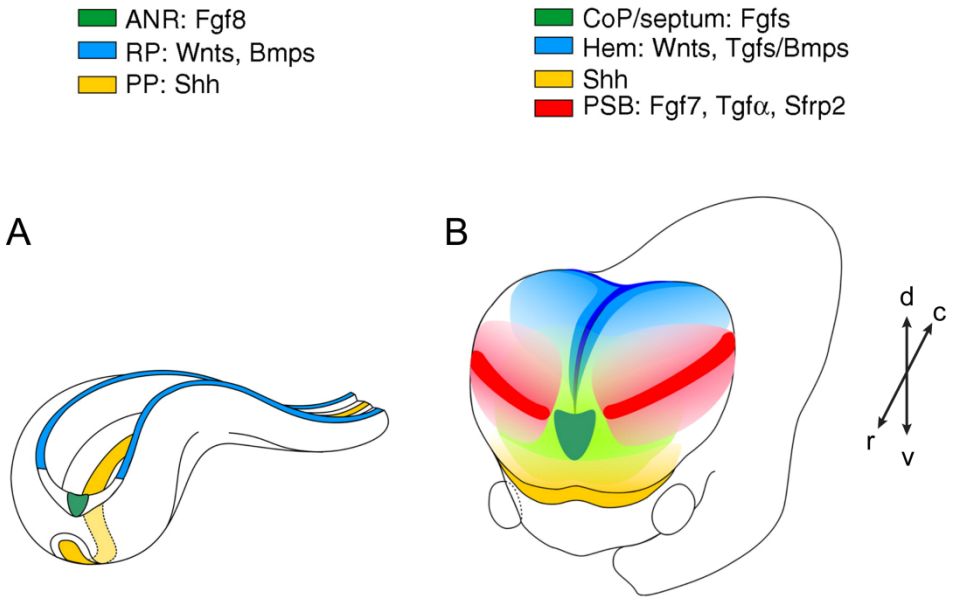

Figure 1. Localized patterning centres regionalize the early telencephalon through secretion of key signalling molecules. (A) Early patterning events during neural tube closure. The anterior neural ridge (ANR), which forms after neural induction and localizes at the rostral midline, promotes telencephalic identity mainly through secretion of fibroblast growth factor (Fgf) 8 and subsequent induction of transcription factor expression. The roof plate (RP), at the dorsal midline, is a source of bone morphogenetic proteins (Bmps) and Wnts. The prechordal plate (PP), at the ventral midline, is a source of sonic hedgehog (Shh) signalling, a key ventralizing factor throughout the neural tube. (B) At E10.5-E12.5, after telencephalic vesicle evangination, Fgf signalling is produced from the commissural plate (CoP) and the septum, at the rostral pole of the telencephalon. At this stage, dorsal and ventral telencephalic territories are separated by the pallial-subpallial boundary (PSB), a region where the patterning centre known as anti-hem is localized. The anti-hem is a source of signalling molecules such as Fgf7, Tgfa and Sfrp2 (Wnt antagonist). At the caudal midline of the dorsal telencephalon, the hem produces Wnts and Bmps; this signalling centre is adjacent to the hippocampal anlage and is important for its development. Shh is expressed along the ventral midline of the CNS throughout development. (From Borello and Pierani 2010). D, dorsal; v, ventral; r, rostral; c, caudal.

lateral (high) to caudo-medial (low) gradient, whereas Emx2 is expressed in a caudo-medial (high) to rostro-lateral (low) gradient (Bishop et al. 2000). At the onset of its expression, Pax6 is detected throughout the anterior neural plate, whereas by E9.5 it is excluded from the ventral-most region of the telencephalic neuroepithelium (Corbin et al. 2003). By E10.5, the graded expression of Pax6 and Emx2 is confined to mutually exclusive dorsal telencephalic domains (Cecchi 2002; Corbin et al. 2003). Nkx2.1 is expressed in more medial domains whereas Gsh2 defines more lateral domains of the ventral telencephalon (Fig. 2). Although cross-repressing mechanisms between transcription factors lead ultimately to the establishment of molecularly distinct progenitor domains within the telencephalon, at early stages (E10.5) the expression of Pax6 and Gsh2 and that of Gsh2 and Nkx2.1 overlaps in a substantial number of cells located in the boundary of these expression domains (see Corbin et al. 2003). *Pax6*$^{-/-}$ embryos exhibit patterning defects from the earliest stages of telencephalic development. Expression of Wnts is upregulated in the caudal-medial field, while signals such as the Wnt antagonist SFRP-2 are absent from the cortical anti-hem of *Pax6*$^{-/-}$ mice (Muzio et al. 2002a). Emx2 promotes caudomedial identities through interaction with molecules released from the anterior neural ridge and the cortical hem. FGF8 regulates rostral area identity at least partly through repression of Emx2 (Fukuchi-Shimogori and Grove, 2003), while BMP and Wnt signalling in the caudal midline positively regulate *Emx2* expression in the developing telencephalon (Ohkubo et al. 2002; Theil et al. 2002). Complimentary patterning defects in *Pax6* and *Emx2*-deficient mice are consistent with their opposing expression gradients in the cortical neuroepithelium. Early patterning defects in *Pax6*$^{-/-}$ and *Emx2*$^{-/-}$ mice above lead to severe abnormalities in the maturation of distinct functional areas in the mutant cortices, described in 1.7.2.

1.4 Regionally enriched transcription factors specify dorsal and ventral telencephalic identities

Along its dorsal-ventral axis, the telencephalon is divided into a dorsal (pallial) and a ventral (subpallial) region, giving rise to the cerebral cortex and basal ganglia,

FIGURE 2

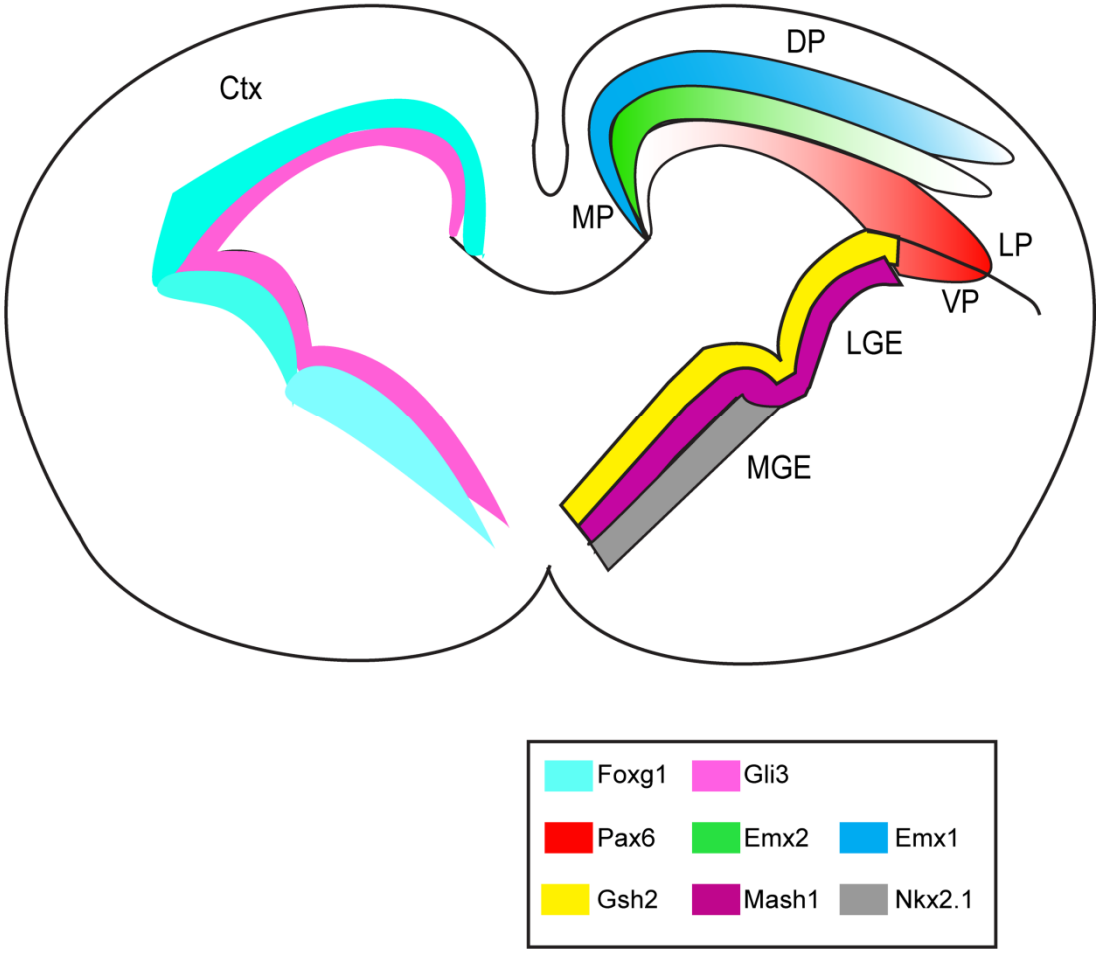

Figure 2. Schematic representation of transcription factor expression on a coronal section through the mouse telencephalon at midgestation (E12.5). Foxg1 and Gli3 are expressed throughout the telencephalon. Dorsally expressed genes include Pax6, Emx2 and Emx1. Pax6 is expressed in a lateral (high) to medial (low) gradient, whereas Emx2 is expressed in the opposite gradient. Graded expression of Emx1 in the cortical neuroepithelium is highly similar to that of Emx2. The expression domain of Pax6 extends to more lateral cortical regions such that its levels are highest at the lateral and ventral pallium (LP and VP, respectively). The LP is a region around the lateral ventricular angle (the anatomical position of the angle region is illustrated through an extended line). The VP is a small domain located immediately dorsal to the LGE. Emx2 and Emx1 are highly expressed at the medial pallium (MP), the hippocampal anlage. Ventrally expressed genes include Gsh2, Mash1 and Nkx2.1. At this early stage, the domain of Gsh2 expression overlaps with that of Pax6 at the border region between the pallium and the subpallium. Gsh2 and Mash1 are expressed in progenitors throughout the ventral telencephalon, whereas Nkx2.1 expression is localized in MGE progenitors. Ctx, cortex; LGE, lateral ganglionic eminence; MGE, medial ganglionic eminence.

respectively (Fig. 2) (for review, see Campbell 2003). At rostral levels, the lateral and medial ganglionic eminences (LGE and MGE) are formed in the ventral telencephalon, whereas caudally there is a single eminence called the caudal ganglionic eminence (CGE). Cortical projection neurons are generated locally from dorsal telencephalic progenitors, whereas inhibitory GABAergic interneurons are born in the ventral telencephalon and migrate long distances to reach the cortex (Marin and Rubenstein 2001; Gorski et al. 2002). The LGE is the source of interneurons that migrate through the rostral migratory stream to the olfactory bulb (Wichterle et al. 2001).

The earliest division to occur within the embryonic telencephalon is the formation of the pallial-subpallial boundary (PSPB), marked by gene expression patterns from as early as E9.5 in mouse (Toresson et al. 2000; Yun et al. 2001). The PSPB does not lie at the angle region between the pallium and the LGE, but it is rather located at the dorsal-most part of the LGE as revealed by molecular expression. A large number of transcription factors exhibit restricted expression in either dorsal or ventral domains of the embryonic telencephalon and their expression patterns have a sharp border (Fig. 2). Pax6 exhibits a lateral-high to medial-low gradient of expression in the cortical field with its highest levels evident in the ventral pallium, located on the dorsal side of the PSPB; Gsh2 is expressed in the ventral telencephalon with its highest levels present in the dorsal LGE (Toresson et al. 2000; Yun et al. 2001). The PSPB has been suggested to be formed through cross-repression of Pax6 function at its pallial side and Gsh2 function at the subpallial side.

In *Pax6*$^{-/-}$ mutant mice, the PSPB fails to form and marker genes no longer have a sharp expression boundary in this region (Stoykova et al. 1996; Stoykova et al. 2000). Subpallial marker expression is expanded dorsally, while pallial marker gene expression is downregulated. By E12.5 the subpallial markers *Gsh*2, *Dlx* and *Mash1* are all ectopically expressed in progenitor cells of the ventrolateral cortex (Stoykova et al. 2000; Toresson et al. 2000; Yun et al. 2001). This ectopic expression continues to expand dorsally so that by E14.5 it includes the ventricular zone (VZ) of the dorsolateral cortex (Toresson et al. 2000). Pallial *Ngn2* expression is lost in the areas of ectopic *Gsh2* expression and is downregulated in the remainder of the cortical VZ

(Stoykova et al. 2000; Toresson et al. 2000; Kroll and O'Leary 2005). Previous studies suggested that the ectopic ventral marker expression in the cortex of *Pax6*$^{-/-}$ mice is due to aberrant migration of ventral telencephalic cells into the mutant cortex and suggested that Pax6 is required to restrict cell migration from ventral to dorsal telencephalic domains (Chapouton et al. 1999). However, more recent fate-mapping studies by Kroll and O'Leary (2005), using an *Emx1-Cre* to trace progenitors of pallial origin in *Pax6*$^{-/-}$ mice, have suggested that cortical progenitors are re-specified to acquire a ventral cell identity in the absence of Pax6. Such a role for Pax6 in specifying dorsal character in progenitor cells and preventing them from acquiring ventral identity has also been indicated by Muzio et al. (2002b), whereas studies by Quinn et al. (2007) have suggested that Pax6 is cell-autonomously required to regulate this process.

Gsh2$^{-/-}$ mice show a phenotype that is opposite to that of *Pax6*$^{-/-}$ embryos; pallial markers such as *Pax6*, *Tbr2*, *Ngn1/2* are ectopically expressed in ventral telencephalic progenitor cells at E10.5, coinciding with loss of *Dlx* and *Mash1* expression from the LGE (Toresson et al. 2000; Yun et al. 2001). The misspecification of these cells is less pronounced at E12.5 and by E14.5 pallial genes are no longer ectopically expressed, possibly due to the effect of ectopic Gsh1 expression (Yun et al. 2001). Gsh1 is normally only expressed in ventral parts of the LGE, but it is expressed more strongly in the Gsh2 mutant and at later stages it expands into the dorsal LGE where it is thought to compensate for Gsh2, thereby reducing the molecular abnormalities in the mutant LGE. In *Pax6*$^{-/-}$/*Gsh2*$^{-/-}$ double mutant mice, striatal development is improved compared with the *Gsh2*$^{-/-}$ single mutants; cortical progenitors remain misspecified although the double mutants exhibit a less severe phenotype compared to *Pax6*$^{-/-}$ mice.

Although Emx2 exhibits an expression gradient throughout the cortical neuroepithelium, complimentary to that of Pax6, its inactivation does not overly affect dorsal-ventral specification as in *Pax6*$^{-/-}$ mice (Muzio et al. 2002b). However, concurrent inactivation of *Pax6* and *Emx2* results in dramatic morphological and molecular defects with complete loss of dorsal identity in the double mutant cortex, which instead acquires features unique to those of the striatum (Muzio et al. 2002b).

These studies have suggested that at least one copy of *Pax6* or *Emx2* is required for activation of cortical morphogenetic programmes and repression of adjacent ventral telencephalic structures. It also appears that Pax6 functions at a high hierarchical level for repressing ventral telencephalic identity and it seems that it does so in cooperation with Emx2, although the two genes seem to function along parallel pathways.

Pax6 seems to also cooperate with another gene, Tlx, in the formation of the PSPB. Although Tlx is expressed in VZ cells on both sides of the PSPB, loss-of-function mutants show a misspecification of the ventral pallium that is similar to, but less severe than, that seen in *Pax6*$^{-/-}$ mutants. Gsh2 expression is expanded dorsally so that it overlaps with Pax6 expression in a wider region compared to wild-types (Stenman et al. 2003). A stream of Pax6-positive cells, which appear to originate from the region of overlapping Pax6 and Gsh2 expression, extends out along the PSPB from the subventricular zone (SVZ) towards the pial surface as part of the lateral cortical stream (LCS) (Carney et al. 2006). In *Tlx*$^{-/-}$ mice, where this overlapping region is increased, a much wider stream of cells can be seen (Stenman et al. 2003), while there is a marked decrease in these cells in *Gsh2*$^{-/-}$ mice (Toresson et al. 2000). Heterozygous mutations in either *Pax6* or *Tlx* do not appear to have any effect on the development of the PSPB; however, compound heterozygotes display a mild phenotype with some ectopic Gsh2 and Mash1 positive cells present in the ventral pallium. Loss of one copy of *Pax6* on the *Tlx*$^{-/-}$ background results in a phenotype that, while worse than *Tlx*$^{-/-}$ on its own, is less severe than that of *Pax6*$^{-/-}$ mice (Stenman et al. 2003). However, the loss of one or both copies of *Tlx* on the *Pax6*$^{-/-}$ background does not affect the patterning defects seen in Pax6 mutants. This is probably due to a much broader requirement for Pax6 than for Tlx in patterning the dorsal telencephalon.

1.5 Progenitor cell proliferation in the developing cortex

The production of appropriate numbers of neurons during development is a prerequisite to ensure proper functioning in the mature brain. Projection neurons

account for approximately 80% of cortical neurons and are generated during embryogenesis from progenitor cells surrounding the lateral ventricles of the embryonic cerebral wall (Sidman et al. 1959). Cortical progenitor cells proliferate in two adjacent cell layers: an inner-most layer, the ventricular zone (VZ), and the overlying subventricular zone (SVZ). On the basis of the location cortical progenitors undergo division they can be classified into two major groups, the apical and basal progenitors. Other than the site of cell division, apical and basal progenitors differ in their molecular expression, with apical progenitors expressing Pax6 and basal progenitors expressing the transcription factor Tbr2 (Fig. 3) (Gotz and Barde 2005; Englund et al. 2005).

1.5.1 Apical progenitors

Apical progenitors (APs) are considered as neural stem cells since they meet the two main criteria applied to define stem cells: (i) they self-renew through an extended number of proliferative divisions, and (ii) are multipotent in their ability to produce different neuronal subtypes (Gotz and Huttner 2005). APs include neuroepithelial cells, radial glial cells and short neural precursors (reviewed in Fishell and Kriegstein 2003; Kriegstein and Gotz 2003; Pinto and Gotz 2007). Neuroepithelial cells represent the earliest subtype of APs in the cortical neuroepithelium and they are successively replaced by radial glia, a transition that occurs at around E10 in mouse, prior to neurogenesis (Pinto and Gotz 2007). APs exhibit a characteristic bipolar morphology in the apical-basal axis. In all three subtypes, the apical process is a short endfoot attached to the ventricular surface. In contrast, neuroepithelial cells and radial glial cells, but not short neural precursors, extend long pia-connected basal processes. An important feature of APs is their apical-basal polarity which is crucial for their succession through different phases of the cell cycle, a process called interkinetic nuclear movement (Fig. 3) (Takahashi et al. 1993; reviewed in Gotz and Huttner 2005; Guillemot 2005). The characteristic radial movement of cell nuclei accounts for the pseudostratified appearance of the VZ, the proliferative layer where APs reside. Pax6 is a critical regulator of interkinetic nuclear migration, and its loss

FIGURE 3

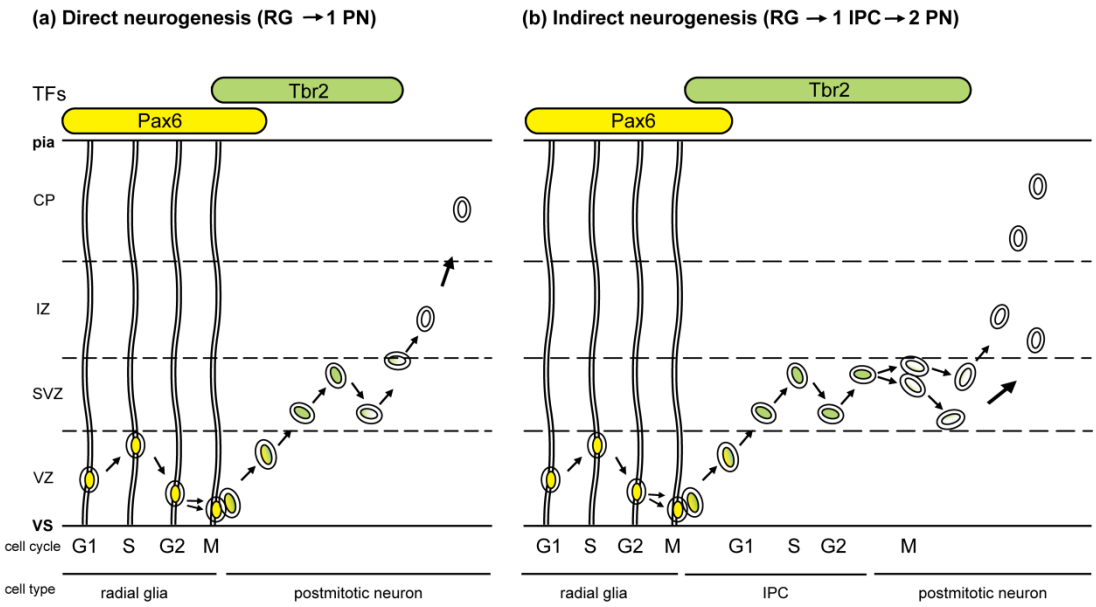

Figure 3. The two modes of cortical neurogenesis correlate with cell cycle phases and the expression of the transcription factors Pax6 and Tbr2. (a) Generation of postmitotic neurons directly from radial glia. Radial glial cells exhibit interkinetic nuclear migration where the cell nucleus moves along the apical-basal axis in concert with the cell cycle. Cell nuclei in G1 phase of the cell cycle move toward the basal VZ to undergo S-phase, and as they proceed to G2 phase, they migrate to the ventricular surface (VS) to enter mitosis (M-phase). Asymmetric division results in the production of a postmitotic neuron, which migrates through the subventricular zone (SVZ) and intermediate zone (IZ) to reach its final laminar position in the cortical plate (CP). (b) Generation of postmitotic neurons though indirect neurogenesis from radial glia. The scheme illustrates a radial glial cell dividing asymmetrically to produce a basal progenitor cell (BP) and a daughter radial glial progenitor. In contrast to BPs, radial glia extend a basal process that spans the thickness of the cortical wall and is maintained during mitosis. The BP nucleus migrates to the SVZ to divide symmetrically and produce two neurons which subsequently migrate to the CP. Sequences of transcription factor (TF) expression are indicated by shading of bars and nuclei. Pax6 is expressed in radial glia and its expression overlaps with that of Tbr2 at stages immediately after the production of (a) postmitotic neurons and (b) BPs. During the transition of newly generated BPs from the VS to the SVZ, Pax6 is downregulated and expression of Tbr2 is initiated. VS, ventricular surface; VZ, ventricular zone; SVZ, subventricular zone; IZ, intermediate zone; CP, cortical plate. (Adapted from Hevner 2006).

of function results in reduced numbers of apical-surface divisions and concurrent increase of ectopic non-surface divisions (Estivill-Torrus et al. 2002; Tamai et al. 2007; Tuoc et al. 2009).

At the earliest stages of development, the neural plate contains a single layer of neuroepithelial cells that forms the neuroepithelium. Neuroepithelial cells undergo extensive proliferation through symmetric divisions to establish a pool of progenitor cells. Symmetric divisions occur with a cleavage plane vertical or close-to-vertical to the epithelium that results in equal distribution of cell fate determinants to daughter cells (Chenn and McConnell 1995; Zhong et al. 1997). With the onset and progress of cortical neurogenesis (corticogenesis), asymmetric divisions of APs, with the cleavage plane oriented parallel to the epithelium, predominate to generate neural progeny (Chenn and McConnell 1995; Fuerstenberg et al. 1998). Through either symmetric or asymmetric divisions, APs self-renew to either expand or maintain the progenitor population. Pax6 promotes asymmetric, neurogenic cell divisions and constitutes an important neurogenetic determinant in radial glial cells (Heins et al. 2002; Hack et al. 2004).

Corticogenesis in mouse occurs between E11.5 and E17.5 (Caviness 1982; Takahashi et al. 1996), followed by gliogenesis that occurs mostly at postnatal ages from radial glial cells (for review, see Costa et al. 2010). Lineage analyses have shown that radial glia are a heterogenous group of progenitor cells in terms of the progeny they give rise to. While they generate distinct cell types in the cortex including pyramidal neurons, oligodendrocytes and astrocytes, individual radial glial cells are restricted in their lineage potential (Price and Thurlow 1988; Parnavelas et al. 1991; Grove et al. 1993; McCarthy et al. 2001; for review, see Kriegstein and Gotz 2003). Radial glial cells are also present in brain regions other than the cortex, including the striatum where they exhibit a multipolar morphology and cell cycle parameters different from those of their counterparts in the cortex (Gotz et al. 1998; Hartfuss et al. 2001). Pax6 is specifically expressed in radial glial progenitors in the cortex, whereas radial glial cells in ventral telencephalic regions express Gsh2 (in the LGE) or Olig2 (in the MGE) (Gotz et al. 1998; Malatesta et al. 2003). It should be noted that radial glia comprise the majority of APs in the cortical VZ and most

pyramidal neurons in the cortex are born from this progenitor cell type (Hartfuss et al. 2001; Tamamaki et al. 2001; Noctor et al. 2002; Malatesta et al. 2003). In contrast, radial glia in the ventral telencephalon mainly generate glial cells and only a few neurons (Malatesta et al. 2003). *Pax6*-deficient cortical radial glia acquire morphological and molecular features characteristic of their counterparts in the ventral telencephalon (Gotz et al. 1998; Malatesta et al. 2003; Quinn et al. 2007); loss of Pax6 function results in a prominent reduction in number of cortical neurons (Gotz et al. 1998; Fukuda et al. 2000; Heins et al. 2002; Malatesta et al. 2003; Hack et al. 2005; Quinn et al. 2007).

1.5.2 Basal progenitors

Basal progenitors (BPs), also known as intermediate progenitor cells, are generated from asymmetric divisions of APs and their potential is restricted in that they only generate neural progeny through symmetric divisions (Fig. 3) (Haubensak et al. 2004; Miyata et al. 2004; Noctor et al. 2004; Kriegstein et al. 2006). Pax6 function is critical for the production of Tbr2-expessing BPs (Quinn et al. 2007). APs that give rise to BPs transiently express the transcription factor Neurogenin 2 (Ngn2), a proneural gene that is expressed in the mammalian telencephalon and promotes cortical neurogenesis (Nieto et al. 2001; reviewed in Guillemot 2007). Thus, a sequential Pax6→Ngn2→Tbr2 expression correlates with the transition of APs to BPs (Englund et al. 2005).

BPs arise at around E12, the onset of corticogenesis, and their generation peaks as corticogenesis progresses. A defining feature of BPs is that they undergo cell division in the SVZ and basal positions of the VZ, away from the ventricular surface, and thus they constitute the non-surface progenitors in the developing cortex (Fig. 3). Notably, this progenitor cell subtype is almost exclusive to the telencephalon, since only few BPs exist in limited regions of the CNS such as the hindbrain and spinal cord (Smart 1972, 1973; Haubensak et al. 2004). BPs also differ in cell morphology from their parental APs; after final mitosis of APs, newly generated BPs migrate to basal positions and retract their apical process prior to mitosis, and thus they appear as round progenitor cells randomly distributed in the basal VZ and the SVZ. The vast

majority of these progenitors produce two neurons, with only around 10% undergoing a second round of symmetric division to generate two BPs (Haubensak et al. 2004; Miyata et al. 2004; Noctor et al. 2004). Their restricted potential to divide only symmetrically is thought to arise due to their lack of apical-basal polarity, which also leads to a substantial number of symmetric divisions with a cleavage plane not strictly vertical to the ventricular surface (Attardo et al. 2008).

1.5.3 Determinants of neuronal output

In mice, APs generate cortical neurons between E11.5 and E17.5, a 6-day period that comprises the neurogenetic interval (Caviness 1982; Takahashi et al. 1996). The number of proliferating cells present at the onset of corticogenesis constitutes the founder population. The entire neurogenetic interval involves a total of 11 cell cycles (CC_1 – CC_{11}) and the cell cycle of APs lengthens from about 8 h at the onset of neurogenesis to about 20 h at its termination (Caviness and Takahashi 1995; Caviness et al. 2009). The maturation of the developing cortex occurs in a gradient such that, at its given stage during the neurogenetic interval, progenitors in rostrolateral regions have longer cell cycles compared to caudomedial ones (Caviness et al. 2009). Once the neurogenetic interval initiates, the daughter cells generated at each given time are separated into two complementary fractions, one that leaves the cell cycle (Q cells) and another one that continues to proliferate (P cells, equal to 1-Q). By definition, the neurogenetic interval initiates when Q exceeds zero and the P value becomes lower than 1.0; at the completion of CC_{11}, APs are abolished and all postmitotic cells exit the VZ as Q cells. The progression in Q exit occurs in a non-linear fashion throughout the course of corticogenesis such that Q and P values become 0.5 at the course of CC_8, a critical point that corresponds to E14.5 and signals the depletion of the proliferative population (Caviness and Takahashi 1995). In theory, the total number of neurons produced from APs during the entire course of the neurogenetic interval depends upon four parameters: (1) the size of the founder progenitor population, (2) the proportion of VZ cells that are actually cycling (that is the growth fraction), (3) the cell cycle length that determines the cell cycle progression, and (4) the Q fraction. Since the growth fraction in the VZ

is normally 1.0 throughout the course of corticogenesis, it is now established that the total cell cycle number and the Q exit are the principal determinants of the final neuronal output (Caviness and Takahashi 1995; Takahashi et al. 1995; Takahashi et al. 1996). The balance between cell-cycle exit and re-entry as well as the rate of cell cycle progression are controlled by positive and negative cell-cycle regulators including various cyclins/cyclin-dependent kinases (Cdks) complexes and Cdk inhibitors, respectively, as well as by a number of extracellular cell fate determinants (for review, see Nguyen et al. 2006; Salomoni and Calegari 2010).

The increase in cell cycle length during the progress of corticogenesis reflects a progressive lengthening of the G1 phase that reaches a fourfold increase towards the end of neurogenesis; the length of S phase varies at around 4 h as corticogenesis advances, while the combined length of G2 and M phase is constant at about 2 h throughout corticogenesis (Takahashi et al. 1995; Miyama et al. 1997). In essence, cell cycle length influences the rate of cell division during corticogenesis. Accumulating evidence suggests that G1-phase length of cortical progenitors also correlates with the mode of division and influences the important decision of whether to proliferate or differentiate (reviewed in Salomoni and Calegari 2010). For instance, forced shortening of G1-phase length in VZ progenitors, through overexpression of cyclins, is sufficient to increase cell-cycle re-entry of Pax6-expressing APs at the expense of neurogenic divisions, whereas lengthening of G1 has the opposite effect (Pilaz et al. 2009). Similar results have also been reported by other studies, suggesting that G1 lengthening functions as a cause of neurogenesis and concurrent inhibition of proliferative activity (Calegari and Huttner, 2003; Calegari et al. 2005; Glickstein et al. 2009; Lange et al. 2009). Interestingly, shortening G1 duration acts as a trigger for proliferative divisions of Tbr2-expressing BPs (Pilaz et al. 2009), although self-renewing of BPs rarely occurs under normal conditions. In accord with the “cell cycle length hypothesis”, the enhanced neurogenic potential during a longer G1 could reflect the ability of cell fate determinants to act for a sufficient period of time in cortical progenitors, resulting in the stimulation of an appropriate cellular response (Calegari and Huttner 2003).

1.6 Cortical neuron migration

What distinguishes the cerebral cortex form other brain regions is its remarkable diversity of cellular subtypes arrayed in a stereotypical laminar and radial organization. After terminal mitosis, cortical precursors leave their site of origin to migrate towards their final laminar position. Neuronal migration is a dynamic and directional process occurring during embryonic development and early postnatal ages and involves multiple cellular and molecular mechanisms. Cell populations involved in guidance of migrating cortical precursors include Cajal-Retzius cells, subplate neurons and radial glia. On the other hand, the integrity of multiple molecular mechanisms, such as cell cycle exit, cell-cell adhesion, interaction with extracellular matrix protein, neurotransmitter release, is critical for normal neuronal migration. Tight interplay between such complex mechanisms probably explains the heterogeneity of clinical human conditions underlying defective cortical neuron migration (reviewed in Walsh and Goffinet 2000; Olson and Wash 2002; Gressens 2006). Whereas cortical projection neurons, which secrete the excitatory neurotransmitter glutamate, are born locally from cortical progenitors and migrate radially to the cortical plate, GABAergic interneurons originate in the subpallium and migrate long distances to reach their final residency in the cortex (Fig. 4a). Although projection neurons account for approximately 80% of all cortical neurons, the existence of appropriate numbers of GABAergic interneurons is a requirement for a proper balance between excitation and inhibition in the mature cortex. Disruption of this fine balance leads to altered neural circuitry that has been associated with many neurodevelopmental disorders, such as epilepsy, schizophrenia and autism (for review, see Di Cristo 2007; Lewis et al. 2008).

1.6.1 Mechanisms of radial neuron migration in the developing cortex

During cortical development, the first postmitotic neurons form the preplate, whereas successive waves of subsequently-born neurons form the cortical plate which splits the preplate into a superficial marginal zone and a deep subplate (Fig. 4b, c). Postmitotic neurons migrate from their site of origin in an order according to their

birthdate, such that they bypass earlier born-neurons located in the cortical plate to form the cortical layers in a deep-first superficial-last sequence (Angevine and Sidman 1961). Cortical neurons transport their cell bodies to their final laminar position by following a relatively direct radial path. Two major modes of radial migration have been described: somal translocation and glia-guided locomotion (Nadarajah et al. 2001; Borell et al. 2006; Rakic et al. 2007). A major difference between these two modes is that translocation requires stable attachment of the migrating cell's radial process to the pial surface or the marginal zone, whereas locomoting cells are freely migrating cells closely attached to radial glia fibres (Fig. 4b, c).

Somal translocation is the predominant mode during early corticogenesis. Bipolar cells connect the ventricular and pial surfaces by extending a radial process that spans the thickness of the cortical wall (Fig. 4b). During somal translocation, migrating cells lose their attachment to the ventricular surface and are directed outwards through their leading process. Time-lapse imaging studies have revealed that, during early corticogenesis, dividing radial glia maintain their fibres towards the pial surface during mitosis and that postmitotic neurons may inherit the radial process from their radial glial progenitor (Miyata et al. 2001; Noctor et al. 2001; Miyata and Ogawa 2007). Symmetric proliferative divisions at the ventricular surface give rise to a daughter cell that inherits the radial process, while the other extends a new process to the pial surface (Miyata et al. 2001). Postmitotic cells are bipolar shortly after birth but they become unipolar upon loosing ventricular attachment and start migrating (Miyata and Ogawa 2007). Interestingly, external mechanical forces appear to cause twisting and stretching of the pial process in cells transitioning from bipolar to unipolar morphology (Miyata and Ogawa 2007). As postmitotic neurons are en route to the cortex, cytoskeletal dynamics provide a pulling force and are critical to regulate two main events of migration: movement of the centrosome into the leading process to maintain a position in front of the transported nucleus, followed by nuclear movement towards the centrosome (reviewed in Tsai and Gleeson 2005).

FIGURE 4

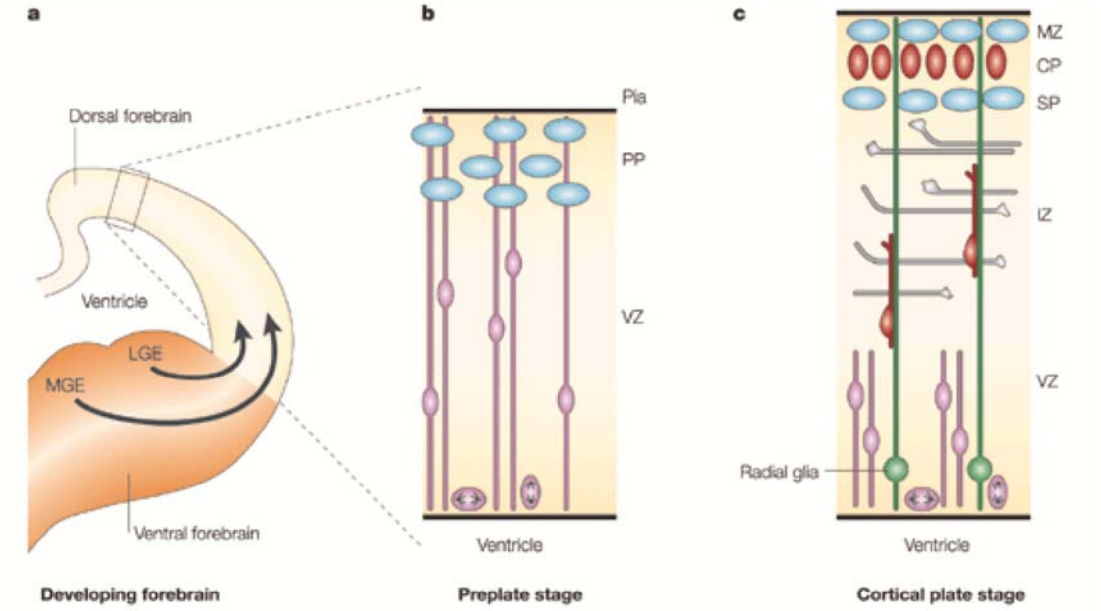

Figure 4. Neuronal migration in the developing cortex. (a) Schematic of a coronal section through the mouse telencephalon showing tangential migration of cortical interneurons from ventral telencephalic progenitor domains. (b, c) In the ventricular zone (VZ) of the dorsal telencephalon, postmitotic cortical precursors arise through asymmetric division of apical progenitors, which occurs with a cleavage parallel to the ventricular surface. (b) The earliest-born cortical neurons migrate radially towards the pial surface through somal translocation to form a layered structure called the preplate (PP). (c) As corticogenesis progresses and cortical width increases, newly generated neurons migrate to the developing CP along radial glial fibres (glial-guided migration). Successive waves of subsequently-born neurons form the cortical plate (CP) that splits the preplate into a superficial marginal zone (MZ) and a deep subplate (SP). The SP is a transient structure that disappears in the adult cortex; during CP development, the SP is the recipient area of afferent axons from subcortical structures. The CP, which will give rise to cortical layers VI-II, is separated from the proliferative layer by the intermediate zone (IZ), an axon-rich zone that will eventually form the white matter underneath the bottom of layer VI. (From Nadarajah and Parnavelas 2002).

As corticogenesis progresses, glia-guided locomotion predominates, a more complex migratory mode that relies on a tight physical interaction between migratory neurons and radial glia (Fig. 4c). However, glia-guided migrating neurons switch to somal translocation once their leading process reaches the pial surface. Rakic described the guidance role of radial glial cells during neuronal migration (Rakic 1971, 1972; for review, see Hatten 1999) and the term "radial glia" was assigned to acknowledge both the radial morphology and the glial nature of the previously described epithelial cells (for review, see Fishell and Kriegstein 2003). Although radial glia were initially thought to just serve as a migratory scaffold, it now appears that the majority of cortical projection neurons are generated by radial glia (Noctor et al. 2002). Cell polarity is a major feature of radial glia progenitor cells in the VZ, as evidenced by interkinetic nuclear movements during which cells progress through different phases of the cell cycle (Sidman et al. 1959; Fujita 1964). Coordination between polarity proteins and cytoskeletal dynamics in the migratory cell is crucial for establishing and maintaining the direction of glia-guided locomotion (for review, see Solecki et al. 2006). Time-lapse studies have revealed that cortical neurons generated at relatively late stages of corticogenesis pass through distinct phases during radial migration (Noctor et al. 2004). Initially, postmitotic neurons generated at the ventricular surface move radially away from the ventricle toward the SVZ, where the pause for 24 h or longer and acquire a highly dynamic multipolar morphology. Then, they move back towards the ventricle and undergo a multipolar-to-bipolar morphological transition while they extend a pia-directed leading process and initiate migration as radial glia-guided locomoting cells. In this mode of migration, cytoskeletal dynamics seem to be important for multipolar-bipolar transition of postmitotic neurons (Noctor et al. 2004; Ohshima et al. 2007). Furthermore, cell-cell adhesion molecules are important for appropriate interaction of migrating neurons with glial processes during radial migration (Anton et al. 1999; Dulabon et al. 2000), and interestingly some molecules exert their function in restricted temporal windows during laminar formation (Takeuchi and O'Leary 2006). Cell adhesion molecules are also present in the extracellular matrix, suggesting that appropriate environmental cues are also necessary for the fine regulation of a cell's migratory behaviour (Hynes 2002).

1.6.2 Cajal-Retzius cells: a transient neuronal population with important roles in the laminar organization of the cerebral cortex

The earliest-born cortical neurons are mostly Cajal-Retzius (CR) cells localized in the marginal zone (MZ) of the developing cortex (for review, see Super et al. 1998). Early cortical progenitors first generate CR cells between E10.5 and E11.5, and then they give rise to projection neurons. However, the main sites of origin for CR cells are the hem, the pallial-subpallial boundary and the septum, regions that flank the borders of the developing cortex and coincide with patterning centres; the MGE has also been described as an extracortical embryonic source for CR cell production (Bielle et al. 2005; for review, see Huang 2009). CR cells migrate long distances through tangential migration such that by E11.5 they reach the cortical primordium (Hevner et al. 2003). Their multiple sites of origin are mirrored by the fact that they express a combination of pallial (Tbr1, Emx2) and subpallial (Lhx6) transcription factors and that they exhibit different neurochemical properties due to their expression of glutamate or GABA (del Rio et al. 1995; Lavdas et al. 1996; Mallamaci et al. 1998; Meyer et al. 1998; Hevner 2001). However, recent data showing that CR cells mostly express pallial markers and consistently contain high levels of glutamate clearly point to a link between CR cells and pallial origin (Hevner et al. 2003; Hanashima et al. 2004).

CR cells are a transient neuronal population with a strategic location in the MZ that serve to guide migration of later-born neurons during cortical development, yet they disappear postnatally after neuronal migration is complete (Wood et al. 1992; Price et al. 1997). Their role in guiding neuronal migration is largely due to their synthesis and secretion of the extracellular matrix protein Reelin, which acts as a necessary signal for cortical lamination (for review, see Soriano and del Rio 2005). Reelin functions in combination with a number of molecules in a common signalling pathway to regulate neuronal migration (reviewed in Soriano and del Rio 2005; Huang et al. 2009). Downstream components of this pathway affect radial migration at least partially due to regulating cytoskeletal proteins (for review, see Tsai and Gleeson, 2005). The most characteristic phenotype is that of the *reeler* mouse mutant cortex, where the preplate fails to split and cortical lamination occurs in an outside-inside sequence that leads to the formation of an inverted cortex (Caviness 1982;

reviewed in Rice and Curran 2001; Tissir and Goffinet 2003). Reelin appears to have multiple functions during neuronal migration (Dulabon et al. 2000; for review, see Huang 2009). At early phases, it acts as an attractive cue so that the movement of neurons from their birthplace can be stimulated and the migration process itself can be initiated. As soon as migrating neurons reach their final residency in the cortical plate, reelin appears to induce detachment of neurons from their guides, the radial glia processes, while at the final phase of migration it functions as a stop signal to prevent neurons from entering layer I and to also trigger the initiation of neuronal differentiation. However, elegant experiments by the Rakic group, where reelin microbeads were injected into the rodent cortex, directly demonstrated that increased concentration of reelin induces arrest of neuronal migration (Dulabon et al. 2000). Such findings imply that the concentration gradient of reelin, which is high around layer I and most likely decreases gradually from the top of the cortical plate down to the VZ, is crucial for controlling different phases of migration.

1.6.3 Integration of interneurons into the cortex via complex migratory paths

The two broad classes of neurons that exist in the cortex are glutamatergic projection neurons, which exhibit a characteristic pyramidal morphology and extend axons to distant intracortical, subcortical and subcerebral targets, and GABAergic non-pyramidal interneurons, which appear as short-axon cells and project locally. Although the radial mode of neuronal migration in the cortex was first described a long time ago, more recent studies observed that the two major classes of cortical neurons follow distinct migratory paths en route to their final residency in the cortex. Initially, lineage tracing studies indicated that clonally related neurons can disperse widely across cortical layers (Walsh and Cepko 1988; 1992; 1993). Time-lapse imaging of VZ labelled cells during late corticogenesis provided the first direct evidence of non-radial, tangential migration of cortical neurons *in vitro* (O'Rourke et al. 1992). Subsequently, lineage tracing of clonally related populations indicated that glutamatergic neurons are arranged in radial columns across the cortex whereas the widely dispersed cells identified by previous studies represent cortical interneurons (Tan et al. 1998). It now appears that, at least in non-primate mammals, interneurons

originate exclusively from distant germinal domains in the ganglionic eminences and follow tangential migratory routes to reach the developing cortex (Anderson et al. 1997; Wichterle et al. 1999; for review, see Nadarajah and Parnavelas 2002). The large majority of cortical interneurons arise from the embryonic MGE, although the CGE has also been described as a site of origin (Sussel et al. 1999; Anderson et al. 2001; Nery et al. 2002; Fogarty et al. 2007; Miyoshi et al. 2007, 2010). Temporal and spatial gene expression in subpallial proliferative regions from which interneurons derive appears to correlate with the specification of cortical interneuron subtypes with regard to morphological, electrophysiological and molecular features (Xu et al. 2004; Butt et al. 2005; Fogarty et al. 2007; Miyoshi et al. 2007; for review see Flames and Marin 2005; Wonders and Anderson 2006; Batista-Brito and Fishell 2009).

Genetic fate-mapping studies have reported that cortical interneurons are born as early as E9.5 in discrete progenitor pools within the MGE (Miyoshi et al. 2007), whereas production of CGE-derived interneurons initiates from E12.5 in mouse (Miyoshi et al. 2010). Interestingly, interneurons sort themselves in cortical layers in an inside-out manner (Valcanis and Tan 2003; Xu et al. 2004; Yozu et al. 2004; Miyoshi et al. 2007), similarly to their pyramidal neuron counterparts. Recent work indicates that the inside-out migration to laminar positions applies mostly to MGE-derived interneurons, whereas CGE-derived interneurons distribute to superficial layers in not such an ordered sequence (Miyoshi et al. 2010). In support of a coupled integration of projection neurons and interneurons in laminar positions, interneurons settle in the *reeler* cortex in an inverted outward-inward laminar pattern as projection neurons, although intracortical migration of interneurons is independent of reelin signalling (Hevner et al. 2004; Pla et al. 2006). Both early- and late-born projection neurons adopt laminar positions well before MGE-derived interneurons born synchronically, favouring a model in which projection neurons provide positional information to regulate the laminar distribution of interneurons (Pla et al. 2006). Consistent with this concept, both early- and late-born MGE-derived interneurons heterochronically transplanted into the cortical VZ have the capacity to change their developmental potential according to the host environment, revealing that interneurons are not fully committed with regard to their laminar fate as they start

migrating from their birthplace and that their phenotypic choices can be influenced by instructive cues in the cortical VZ (Valcanis and Tan 2003; Pla et al. 2006).

The migratory path of cortical interneurons from their site of origin to final laminar destinations appears rather complex compared to the radial migration of projection neurons in a straight line. Interneurons migrate tangentially along the SVZ-intermediate zone (IZ), then turn and undergo pial surface-directed migration through the CP (Wichterle et al. 2001). Many interneurons position themselves in the MZ and disperse in many directions before descending to the CP and settling in their final laminar positions (Tanaka et al. 2003). Recent time-lapse imaging studies have shown that interneurons that have reached the MZ migrate to laminar positions in a rather undirected manner, meeting criteria for a random wandering behaviour (Tanaka et al. 2009). Alternatively, interneurons may travel long distances tangentially in the direction of the cortical VZ, where they pause and then resume migration to integrate radially into the CP (Nadarajah et al. 2002). Such ventricle-directed migration has suggested that populations of interneurons might actively seek the cortical VZ to acquire spatial information before resuming migration and integrating to cortical layers. This process would explain the inside-out laminar patterning of cortical interneurons and further support the notion that environmental cues are in place in the cortex to guide migrating interneurons to correct laminar positions.

The cellular and molecular mechanisms that are involved in directing the migration of interneurons to cortical laminar positions are not entirely clear. Close association of migratory neurons with axonal tracts involves a symbiotic relationship that could be influenced by adhesion molecules contained in axons. Both in vitro and in vivo evidence suggest that expression of the chemoattractant molecule Neuregulin 1 in the developing cortex as well as along the migratory path that interneurons follow to reach the cortex is necessary for interneuron migration (Flames et al. 2004). In contrast, the adhesion molecule TAG-1 was found to be required for axon-dependent guidance of migrating interneurons in vitro (Denaxa et al. 2001), but interneuron migration is not affected in mice knock-out for the same molecule (Fakamauchi et al. 2001; Denaxa et al. 2005). Therefore, cell adhesion molecules appear to act as

guidance cues for migrating interneurons but the lack of certain molecules might be compensated for by others present in axons. Furthermore, although many interneurons migrate through the IZ, an axon-rich compartment, substantial numbers migrate in multiple directions through the VZ/SVZ and MZ and are presumably guided by other cellular and molecular substrates (Tanaka et al. 2003; Tanaka et al. 2006). Loss of Pax6 leads to severe axon pathfinding defects in both corticofugal and thalamocortical tracts (Hevner et al. 2002; Jones et al. 2002; Pratt et al. 2002) and also to reduced expression of Neuregulin 1 in the mutant cortex (Flames et al. 2004). Interestingly, recent work has indicated that interneurons follow a disorganized migratory route within the *Pax6*$^{-/-}$ cortex, although the number of cortical interneurons is unaltered in these mutants (Gopal and Golden 2008). Previous viral LGE injections in *Pax6*$^{-/-}$ mice indicated increased migration of cells directed from ventral to dorsal telencephalic domains (Chapouton et al. 1999) but subsequent lineage-tracing studies showed that the LGE is not a source of cortical interneurons but rather a site of origin for olfactory bulb interneurons (Anderson et al. 2001; Wichterle et al. 2001; Nery et al. 2002). Thus, it appears that Pax6 loss does not affect the rate of interneuron migration to the mutant cortex but it does affect the intracortical route that interneurons follow. Such defective direction of migrating interneurons may arise due to both axon defects in *Pax6*$^{-/-}$ mice, also reported by Gopal and Golden (2008), and lack of molecular guidance as reported by Flames and colleagues (2004). The abnormal morphology of radial glial cells (Gotz et al. 1998) as well as paraventricular and subpial ectopias containing cells of ventral identity (Kroll and O'Leary 2005) further contribute to severe cellular disorganization in the *Pax6*$^{-/-}$cortex that could account for pathfinding defects of migrating interneurons.

1.7 Radial and tangential organization of the cerebral cortex

Radially, otherwise vertically to the pial surface, the cortex is composed of neurons arrayed in a six-layered sheet, with individual layers differing in their molecular gene expression, cytoarchitecture and connectivity. Along the tangential (horizontal) plane, the cortex can be subdivided into small vertical columns that span the depth of cortical layers and consist of clonally related projection neurons generated in the

cortical proliferative layers. Neurons within the same columnar unit are highly interconnected and share common functions, and groups of radial cortical columns are organized tangentially into functionally distinct areas. According to the "radial unit hypothesis" (Rakic 1988), the total number of columns determines the surface area of the cortex, whereas the number of neurons within each column determines the thickness of the cortex. The massive cortical expansion during mammalian evolution is achieved through an increase in the numbers of cortical columns, with little change in cortical thickness (Rakic 1988; Mountcastle et al. 1997). Although the relative cortical area sizes differ between human and rodents, in both species the cortex is divided into three major areas across the rostral-caudal axis: the rostral (motor) cortex, the central (somatosensory) cortex and the caudal (visual) cortex.

1.7.1 Radial organization in layers

The radial distribution of cortical projection neurons in laminar positions is temporally related to their birthdate. Projection neurons are born between E11.5 and E17.5 in mouse (Caviness et al. 1982; Takahashi et al. 1996) and migrate to the CP in a tightly controlled sequential order such that each successive generation bypasses earlier-born neurons and settles at the top of the CP (Fig. 5). Thus, the cortical layers VI-II are formed in a deep-first superficial-last sequence (Anvegine and Sidman 1961; Rakic 1974; McConnell 1995). When projection neurons arrive in their final laminar positions, they undergo terminal differentiation that involves elaboration of their dendrites and axons to establish connections and eventually form the cortical circuitry. Projection neurons in each layer tend to exhibit similar gene expression patterns, morphologies, and organization of afferent and efferent connections (Fig. 5). Based on morphology, cortical projection neurons are subdivided into two broad classes: pyramidal cells and spiny stellate cells. A defining difference between these two groups is that spiny stellate cells lack long apical dendrites, a typical characteristic of pyramidal cells that enables them to reach distant targets. Spiny stellate are small cells abundant in layer IV of the primary somatosensory cortex and constitute the main recipient of thalamic input. Pyramidal cells are the predominant

FIGURE 5

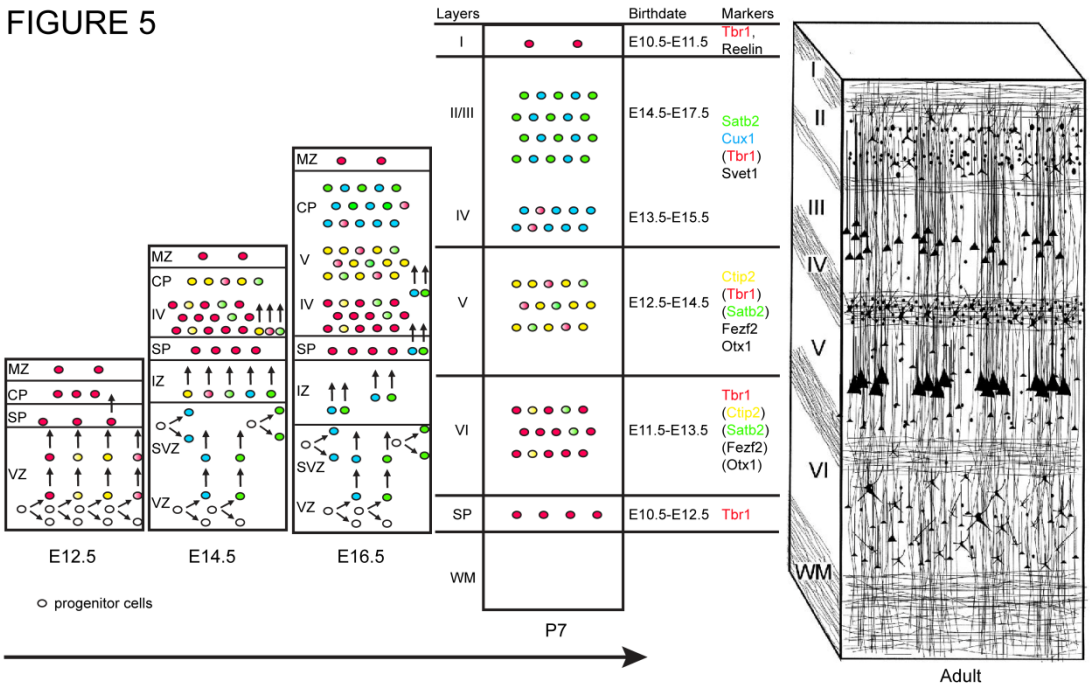

Figure 5. Schematic depicting sequential generation of cortical projection neurons, molecular expression in cortical layers, and cytoarchitecture in the adult cortex. Layer VI/II projection neurons are sequentially generated in the ventricular zone (VZ)/subventricular zone (SVZ) such that their birthdate highly correlates with their final laminar position. However, there is some overlap in the temporal windows of distinct layer neuron production; times indicated here are approximations given the neurogenetic gradient across the cortical neuroepithelium. During early corticogenesis (E12.5), deep layer neurons destined for layer VI are generated first, followed by production of layer V neurons. Neurons destined for layer VI highly express Tbr1 (red); however, low levels of Ctip2 (graded yellow) and Satb2 (graded green) are also present in layer VI neurons. Neurons destined for layer V express Ctip2 at high levels (yellow); Tbr1 and Satb2 are expressed at much lower levels (graded red or green, respectively). Genes in parentheses at P7 also indicate low levels of gene expression. Left to right in the E12.5 VZ indicates successively generated neurons; migrating neurons are illustrated by radial arrows. By E12.5 the production of marginal zone (MZ) neurons (Cajal-Retzius cells) is complete; this time also marks the end of subplate (SP) neuron generation. MZ and SP cells express Tbr1. E14.5 signals the start of generation of most superficial layer (IV/II) neurons, which highly express Cux1 (blue) and Satb2 (green). At this time, layer VI neurons have settled at the bottom of the CP, while layer V neurons are migrating through the intermediate zone (IZ), the SP and the CP to settle superficially. In each migratory zone, left to right indicates migratory neurons born successively; in reality, migrating cells are intermixed with neurons that have adopted their final laminar positions. At E16.5, layer III/II neurons are being born; the migration of layer V neurons is also complete at this time. Such sequential generation and migration of cortical neurons leads to the inside/out sequence of laminar formation. Classical drawings by Cajal (from Bentivoglio et al. 2003) illustrate the cytoarchitecture in a vertical column from the adult cortex. The white matter (WM) constitutes bundles of axons underneath layer VI (the SP has disappeared by this time).

type of neuron in the cortex and their size varies depending on laminar position, with layer V corticospinal neurons comprising the largest pyramidal cells (Fig. 5). Although pyramidal cells share many anatomical characteristics, they exhibit remarkable diversity in terms of morphology and connectivity both across and within layers (reviewed in Thomson and Bannister 2003; Bannister 2005). In simplified terms, depending on axonal targets, projection neuron connections fall into two main categories: (1) intracortical, which includes *ipsilateral* connections between neurons localized in different layers, and cortico-cortical projections to the *contralateral* cortex mainly through the corpus callosum, and (2) corticofugal, which includes *subcortical* projections to the thalamus and the striatum, and *subcerebral*, through extension of axons to distant targets such as the midbrain (including the tectum) and the spinal cord (for review, see O'Leary and Koester 1993; Thomson and Bannister 2003; Bannister 2005). Callosal neurons are widespread across layers VI-II but are particularly abundant in superficial layers II/III, with many forming both ipsilateral and contralateral cortical connections (Mitchell and Macklis 2005). While late-born superficial layer neurons form only intracortical connections, early-born pyramidal neurons in layers VI and V project to subcortical and subcerebral targets. Layer VI contains corticothalamic projection neurons, whereas layer V pyramidal neurons constitute the major cortical output. Layer V contains two broad classes of subcerebral projection neurons that are area-specific in the mature cortex: (1) corticospinal neurons are only located in layer V at the rostral and central levels of the cortex, corresponding to motor and somatosensory areas, and (2) corticotectal neurons that are found in layer V of the visual cortex, caudally (O'Leary and Koester 1993; Molnar and Cheung 2006). Cytoarchitectonic differences between different areas reflect changes in cortical circuits; for instance, the motor cortex has a prominent layer V, whereas layer IV is more prominent in the somatosensory cortex.

The developmental potential of cortical progenitors to generate neurons of different laminar fates becomes progressively restricted as corticogenesis advances. Early cortical progenitors heterochronically transplanted into older brains adopt a laminar fate appropriate to the host environment, whereas at later stages cortical progenitors are unable to generate deep-layer neurons when transplanted into a young host and continue to give rise to superficial laminar fates characteristic of the donor age

(McConnell and Kaznowski 1991; Frantz and McConnell 1996; Desai and McConnell 2000). This work revealed that early cortical progenitors, which normally generate deep-layer neurons, are multipotent prior to their final mitotic division and can generate neurons across layers VI-II when subjected to appropriate environmental influences; in contrast, during superficial layer neuron generation, laminar fate specification appears to be dictated by instructive cues that are intrinsic to cortical progenitors. Although laminar distribution of projection neurons correlates with the time of their origin, it does not predict neuronal subtype identity since even a single layer can comprise a mixture of projection neuron phenotypes, i.e., layer V contains callosal and subcortically projecting neurons (Koester and O'Leary 1993; Alcamo et al. 2008; Britanova et al. 2008). This illustrates that cortical neurons can follow completely distinct differentiation programmes despite being produced by progenitors at the same time and being exposed to the same environmental cues.

The discovery of genes that control the specification of distinct projection neuron subtypes has started unravelling the intrinsic mechanisms that control the fate specification process (Arlotta et al. 2005; Britanova et al. 2005; for review, see Molyneaux et al. 2007; Fishell and Hanashima 2008; Leone et al. 2008). For instance, the transcription factor Tbr1 is expressed in migratory cortical precursors born at early stages and its presence is required for the differentiation of PP and layer VI neurons; at postnatal ages, Tbr1 is highly expressed in layer VI neurons (mostly corticothalamic) and its loss-of-function results in defective axon targeting of layer VI neurons (Hevner et al. 2001). More recent studies have identified a number of key transcriptional regulators expressed exclusively in subtypes of corticofugal pyramidal neurons or callosal neurons. *Ctip2* and *Fezf2* are expressed at high levels in layer V subcerebral neurons, including corticospinal neurons, as well as at low levels in layer VI corticothalamic neurons (Arlotta et al. 2005). Although *Fezf2* is expressed in early cortical progenitors and their neuronal progeny, loss-of-function analyses have suggested that *Fezf2* is required to direct the differentiation programme of subcerebral projection neurons rather than affecting initial phases in the production of early-born neurons and their subsequent migration to deep layer laminar positions (Chen et al. 2005a; Molyneaux et al. 2005). Mice knock-out for either *Ctip2* or *Fezf2* fail to form appropriate corticofugal connections (Chen et al.

2005a; Chen et al. 2005b; Molyneaux et al. 2005). The transcription factor *Satb2* is expressed in callosal neurons and *Satb2*-deficient mice ectopically activate expression of deep layer markers (including that of Ctip2) in superficial layers of the mutant cortex, accompanied by concurrent loss of a number of superficial layer markers (Alcamo et al. 2008; Britanova et al. 2008). *Satb2*-deficient neurons fail to form callosal axons and instead extend axons to subcortical targets (Alcamo et al. 2008). Similarly, ectopic activation of either *Ctip2* of *Fezf2* is sufficient to alter the axon targeting of superficial layer neurons from intracortical to corticofugal connections, highlighting the impact of postmitotic gene control in specifying neuron subtype features at the post-migratory stage (Chen et al. 2005b; Chen et al. 2008). Except for *Fezf2*, all of the markers above are expressed exclusively in postmitotic cells, indicating that the differentiation programmes projection neurons follow are influenced by postmitotic gene control. However, little is known as to what extent molecular control at the progenitor level affects aspects of projection neuron fate. Elegant studies from Gaspard et al. (2008) have provided strong evidence that laminar identity and projection neuron subtypes are intrinsically specified within cortical progenitors with no influence from the cortical environment.

The two germinal zone compartments in the embryonic cortex contain progenitor cell subtypes that exhibit distinct proliferative properties and molecular gene expression patterns. The corresponding patterns of gene expression between early VZ cells and deep-layer neurons, and SVZ cells and superficial-layer neurons, have further suggested that pyramidal neuron fates are determined at the time of their origin. In agreement with the proposed contribution of SVZ progenitors to superficial layer neuron production, the SVZ forms at around E13.5 (Smart and McSherry 1982), after the onset of basal progenitor production. *Svet1* marks a subset of SVZ progenitors as well as their neural progeny adopting superficial laminar fates (Tarabykin et al. 2001). In the *reeler* cortex, *Svet1* is expressed normally in the SVZ but within the CP it is detected in deep laminar positions, consistent with the previously reported inverted neuronal migration in these mutants. The transcription factor *Cux1* is specifically expressed in the majority of superficial layer neurons II/IV and is also localized in SVZ progenitors (Tarabykin et al. 2001; Nieto et al. 2004). In *Pax6*$^{-/-}$ mice, *Svet1* and *Cux1* expression is lost in both the SVZ and superficial layers,

whereas *Otx1*-labelled VZ progenitors and their lineage in deep layers are present in the mutant cortex (Tarabykin et al. 2001). Such evidence, along with migration defects of late-born neurons in the *Pax6*$^{-/-}$cortex (Caric et al. 1997), supported a role for Pax6 in conferring superficial laminar identity. In agreement with such a model, recent studies have shown that the production of correctly specified SVZ progenitors occurs in a Pax6-dependent manner (Englund et al. 2005; Quinn et al. 2007).

1.7.2 Tangential subdivision into functional areas

The discovery of area-specific molecular markers expressed in a gradient throughout the rostral-caudal axis of the early neuroepithelium provided evidence that regionalization is intrinsic in the cortex, a notion that led to the "protomap" hypothesis (Rakic 1988; for review, see O'Leary and Sahara 2008). In contrast, heterotopic transplantation experiments indicated that the capacity of the embryonic cortex to acquire area-specific features largely depends on thalamocortical innervation and supported the "protocortex" model (Schlaggar and O'Leary 1991). Thalamocortical afferents arrive in the mouse cortex at around E14.5, and by E15.5 they reach their final target in the cortical plate. It is now well-established that area-specific positional information intrinsic to the cortical proliferative zone is required for the establishment of cortical areas, but thalamocortical innervation is needed at later stages for refinement of the final pattern of synaptic organization (for review, see Rakic et al. 2009).

Two genes that function as key determinants for conferring area-specific cortical identities are the transcription factors *Pax6* and *Emx2*, expressed in the cortical VZ throughout corticogenesis in opposing and complementary gradients (Fig. 6) (Bishop et al. 2000; Mallamaci et al. 2000). Consistent with their graded expression in the rostral-caudal and medial-lateral axis, loss of *Pax6* or *Emx2* function in mutant mice results in rostral and caudal shifts of cortical areas, respectively (illustrated in Fig. 6) (Bishop et al. 2000, 2002; Malllamaci et al. 2000; Muzio et al. 2002b). Gain-of-function studies in *nestin-Emx2* (*ne-Emx2*) transgenic mice have shown a striking areal shift without affecting the overall cortical surface area, further supporting the role of Emx2 in cortical arealization and also suggesting that Emx2 operates in a

concentration-dependent manner in cortical progenitors in order to specify sizes and positioning of caudomedial cortical domains (Fig. 6) (Hamasaki et al. 2004). Surprisingly, transgenic mice carrying several copies of the *PAX6* locus do not exhibit any significant defects in the positioning and sizes of the caudal cortical domains (Fig. 6) (Manuel et al. 2007). Collectively, it appears that cortical arealization is Emx2 dosage-dependent; with regard to Pax6, relative and not absolute levels of Pax6 expression seem to be required for the spatial identity of cortical progenitors. Other regulators conferring cortical area identities include the transcription factors COUP-TF1 and Sp8, which are also expressed in a gradient throughout the caudal-rostral and medial-lateral axes (Armentano et al. 2007; Zembrzycki et al. 2007). Such mutant phenotypes highlight the importance of transcription factors levels for normal cortical arealization and possibly other important aspects of cortical development.

FIGURE 6

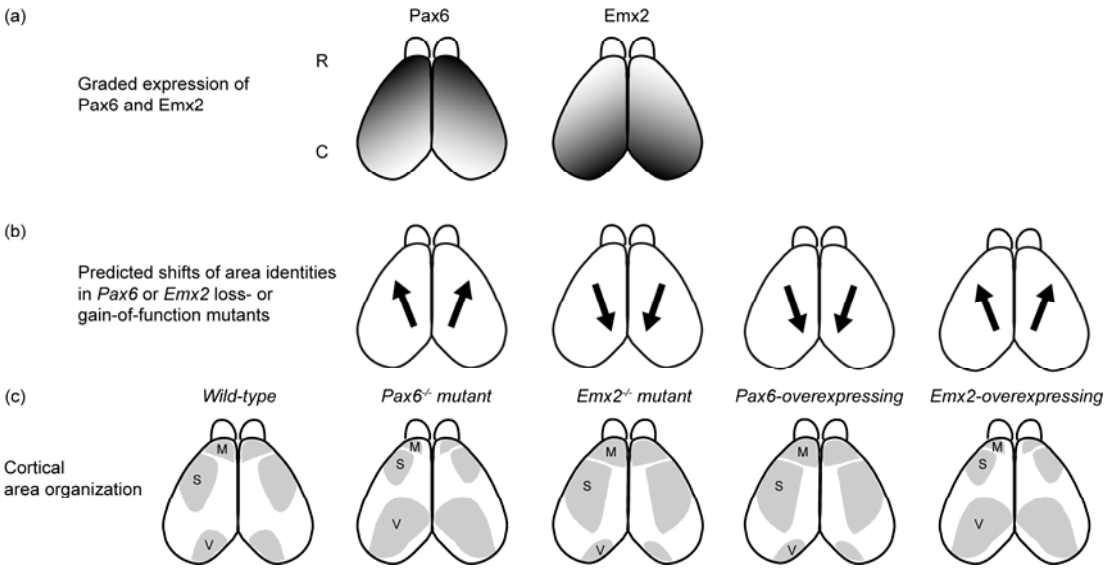

Figure 6. Schematic of a dorsal view of the mouse neocortex showing the graded expression patterns of Pax6 and Emx2 and the expected/observed areal shift in loss-of function and gain-of-function mutants. (a) In the wild-type cortex, Pax6 is expressed in a high rostro-lateral to low caudo-medial gradient, whereas Emx2 expression exhibits the opposite gradient. (b) If these genes confer areal identities to cortical cells, in the absence of *Pax6*, rostro-lateral areas, such as motor cortex, should expand, and caudo-medial areas, such as visual cortex, should contract. Loss of *Emx2* function would be expected to have the opposite effect. Overexpression of *Pax6* would be expected to result in a caudal shift of rostral areas at the expense of caudal areas, while the reverse phenotype would be predicted in the *Emx2*-overexpressing mice. (c) Cortical area organization in wild-type mice and areal phenotypes of mice lacking or overexpressing *Pax6* or *Emx2*. Analysis of area-specific gene expression patterns and thalamocortical projections support the above hypotheses except for the *Pax6*-overexpressing mutant mice. The latter mutants do not exhibit any caudal shift in the border between the somatosensory and visual cortical areas; a small but significant reduction of the somatosensory area relative to the total cortical area has been reported in these mutants (Manuel et al. 2007). R: rostral; C: caudal; M: motor area; S: somatosensory area; V: visual area.

1.8 Transcription factor gradients: interpreting the spatial and temporal roles of Pax6 levels in the developing cortex

Findings from analyses of cortical arealization in Pax6 loss- and gain-of-function mutant mice imply that the relationship between transcription factor levels and regulation of complex developmental processes is most likely not linear. Graded expression of transcription factors throughout the cortex is established by morphogens released from patterning centres around the borders of the cortical field. Such a complex system of gradients involving several transcription factors and signalling molecules is likely to function as a network for controlling specific aspects of cortical development and not as an on-off switch system. However, different expression levels of a given transcription factor in cortical progenitors, combined with distinct expression levels of other transcription factors within the same progenitors could lead to different developmental outcomes. This is exemplified by the neural diversity between (i) different cortical areas, and (ii) deep and superficial cortical layers, suggesting that levels of transcription factor expression in cortical progenitors might become important to coordinate important aspects of cortical development by exerting different effects at distinct developmental time windows. For instance, Pax6 expression is graded in cortical progenitors not only spatially but also temporally throughout development, with highest levels present at the onset of corticogenesis. The expression gradient of Pax6 correlates with the neurogenetic gradient since neurogenesis in rostrolateral cortical regions precedes that in caudomedial ones. Whether altering Pax6 expression levels either up or down has different effects at different stages of corticogenesis is an interesting hypothesis. Furthermore, do Pax6 levels affect different developmental aspects at different thresholds? For instance, eye development is sensitive to both elevated and decreased levels of Pax6. Does Pax6 affect cortical development in an analogous dosage-dependent manner, or does it modulate development in a context-dependent manner? Such unanswered questions represent the driving force for research work in the present thesis.

The expression pattern of Pax6 in the cortical neuroepithelium might reflect its role as a multifunctional player during cortical development, i.e. by coordinating a

number of developmental processes such as cortical progenitor proliferation, production of distinct layer-specific neuronal populations and neuronal migration to laminar positions. Chapter 3 describes experiments showing that increased Pax6 dosage reduces the proliferation of late cortical progenitors and results in the formation of thinner superficial layers in the postnatal cortex. The underlying mechanism of these defects is examined in Chapter 4, where Pax6 overexpression is found to lengthen the cell cycle and increase the Q exit of late cortical progenitors specifically, with no effect in the migration and cell fate specification of late-born neurons. These results indicate that cell cycle regulation and control of the balance between progenitor self-renewal and differentiation are highly sensitive to Pax6 dosage during late corticogenesis.

In light of the specific effects of Pax6 overexpression during superficial laminar development, a loss-of-function genetic approach is then employed in chapters 5 and 6. To directly investigate the function of Pax6 in late cortical development, a conditional knockout model that allows for spatial and temporal control of Pax6 deletion in cortical progenitors has been generated in the present study. The rationale behind this approach is that *Pax6*$^{-/-}$ mice exhibit many growth defects and cortical abnormalities from early developmental stages, hampering our understanding of the late primary roles of Pax6 during superficial layer formation. Furthermore, the early perinatal lethality of *Pax6* mutants restricts analyses at stages before neuronal migration to cortical layers is complete. Experiments in chapter 5 demonstrate that Pax6 is continuously required within cortical progenitors for suppression of ventral telencephalic fates within its domains of expression. These data extend previous findings indicating an important role for Pax6 in promoting dorsal identity in the developing telencephalon (Muzio et al. 2002b; Kroll and O'Leary 2005). In addition to ectopic ventral marker expression in the absence of *Pax6*, Tbr2-expressing progenitors (BPs) are severely reduced in the mutant cortex (Quinn et al. 2007). Consistent with the notion that BPs have limited self-renewing capacity and that they are continuously generated from Pax6-expressing progenitors, Pax6 is found to be required within cortical progenitors over the course of corticogenesis in order to specify BP identity.

Analyses of mutant mice lacking Pax6 from the earliest stages of corticogenesis have indicated that Pax6 function is important to regulate the rate of cortical progenitor proliferation and prevent progenitors from dividing in ectopic, non-surface positions (Gotz et al. 1998; Estivill-Torrus et al. 2002; Tuoc et al. 2009). Moreover, the failure of late-born neurons to exit their site of origin contributes to the formation of a hypocellular cortical plate and an enlarged germinal zone in *Pax6*$^{-/-}$ mice (Schmahl et al. 1993; Caric et al. 1997; Tarabykin et al. 2001; Schuurmans et al. 2004). However, the direct relationship between Pax6 loss and late cortical progenitor proliferation and neuronal migration remains to be explored. Experiments in chapter 6 provide evidence that Pax6 is a primary regulator of cortical progenitor proliferation, by demonstrating that late Pax6 ablation causes proliferation defects recapitulating those previously reported in *Pax6*$^{-/-}$ embryos. Moreover, neuronal migration studies led to a surprising finding: late-born neurons arising from Pax6-deficient progenitors are able to migrate to superficial layers once they exit the VZ; however, an enormous number of late-born neurons fail to leave their birthplace and accumulate in the germinal zone of the postnatal cortex through a both cell-autonomous and cell-non-autonomous mechanism. Defects arising after Pax6 loss in late cortical progenitors do not affect laminar fate; however, neurons of superficial layer identity are reduced in the mutant cortex. Collectively, findings here support a key role for Pax6 during superficial layer formation.

The impact of results from these gain- and loss-of-function strategies on the current knowledge of the role of Pax6 levels in cortical development are discussed in chapter 7.

CHAPTER 2

Materials and Methods

2.1 Animals and Genotyping

PAX77 mice carry five to seven copies of a 420-kb human genomic fragment incorporating the *PAX6* gene (Schedl et al. 1996). The mice were maintained on a CD1 background. PAX77 males were mated to CD1 females to generate littermates for experiments. The date of conception was assessed by the presence of a vaginal plug and recorded as embryonic day (E) 0.5. The first 24 hours after birth was defined as postnatal day (P) 0. To specifically inactivate *Pax6* in the developing cerebral cortex, *Pax6* floxed mice (*Pax6*$^{loxP/loxP}$) (Simpson et al. 2009) were crossed with a transgenic line that expressed the tamoxifen-inducible form of Cre recombinase (CreER^{T2}) under the control of the *Emx1* locus (Kessaris et al. 2006). The lines above were crossed with *Rosa26R-YFP* reporter mice (Srinivas et al. 2001) to generate triple transgenics in which the expression of the *Cre* transgene could be monitored. All transgenic lines were maintained by backcrossing with CD1 animals. To activate Cre activity, tamoxifen (T5648, Sigma) was dissolved by sonication, at a concentration of 50mg/ml in corn oil (Sigma, C8267), and administered by gavage into the stomach of pregnant mothers bearing embryos. Induction in embryos was performed using a single 10mg dose of tamoxifen at embryonic day (E) 10.5 or a single 12.5mg tamoxifen dose at E13.5. Embryonic or postnatal brains were harvested at the times specified after tamoxifen treatment. For postnatal analysis, a caesarean section was performed on pregnant mothers in the afternoon on E18.5 and pups were fostered. Control animals were *Pax6*$^{loxP/+}$; *Emx1-CreER*^{T2} and mutant animals were *Pax6*$^{loxP/loxP}$; *Emx1-CreER*^{T2}. In all cases, littermates were analysed. All of the experimental procedures were performed in accordance with institutional guidelines and UK Home Office regulations.

Mice were genotyped by performing Polymerase Chain Reaction (PCR) on genomic DNA from digested mouse tissue, reactions used standard conditions. For genotyping of mice carrying the *PAX77* transgene, two separate sets of primers were used in order to amplify a 283-bp region of transgenic human *PAX6* and a 399-bp region of mouse *Pax6* (primers for amplification of human *PAX6*: forward 5′-CCGTGTGCCTCAACCGTA-3′, reverse 5′-CACGGTTTACTGGGTCTGG-3′; primers for amplification of mouse *Pax6*: forward 5′-

GAGGGTTTCCTGGATCTGG-3′, reverse 5′-CGCAAATACACCTTTGCTCA-3′). Mice carrying the conditional mutant *Pax6^{loxP}* allele, in which *loxP* sites flank exons 5, 5a and 6 that encode the paired domain and are crucial for Pax6 function, were genotyped using primers (forward 5'-AAATGGGGG TGAAGTGTGAG-3', reverse 5'-TGCATGTTGCCTGAAAGAAG-3') targeted to the single distal *loxP* site (for targeting strategy and position of primers see Simpson et al. 2009, Fig1.A, D). Cre recombinase-expressing transgenic mice were genotyped using primers to the *Cre* cassette (forward 5'-CATTTGGGCCAGCTAAACAT-3', reverse 5'-ATTCTCCCACCG TCAGTACG-3'). DNA from *Cre$^{+/-}$* mice produced a 300-bp band. *Rosa26R-YFP* reporter transgenic mice were genotyped using primers to the *Rosa26R* locus (forward 5'-AAAGTCGCTCTG AGTTGTTAT-3'). DNA from mice carrying the *Rosa26R* allele produced a 300-bp band. DNA bands were separated by gel electrophoresis (at 85-90V for 1 h) and visualized under 320nm UV light.

2.2 Tissue preparation

To obtain embryos, pregnant females were deeply anesthetised by isoflurane inhalation and embryos were removed from the amniotic sac. Pups were deeply anesthetised with sodium pentobarbitone (50mg, intraperitoneally) and perfused transcardially with phosphate-buffered saline (PBS) followed by fixation with 4% paraformaldehyde (PFA) in PBS. Tails from pups or trunks from embryos were collected for genotyping. Brains from embryos and pups were fixed overnight in 4% PFA in PBS at 4°C. For paraffin sections, brains were dehydrated through increasing concentrations of ethanol before embedding in paraffin wax. Brains were sectioned on a microtome at 10 μm in the coronal plane and sections were mounted onto poly-L-lysine coated slides. For frozen sections, postnatal brains were cryoprotected in a series of sucrose gradients up to 30% sucrose in PBS at 4°C before being embedded in OCT (optimal cutting temperature) compound. Embryonic brains were cryoprotected in 15% sucrose in PBS at 4°C overnight before being embedded in a mixture of 15% sucrose in PBS/7.5% gelatine (Sigma). All samples were frozen on dry ice and stored at -20°C (80-°C for long-term storage). Frozen samples were serially sectioned on a Leica cryostat at 14μm (embryonic brains) or at 20 μm

(postnatal brains) in the coronal plane and sections were mounted onto Superfrost Plus slides (Fisher Scientific), air-dried at room temperature (RT) for 30-60 min and stored at -20°C until use.

2.3 Chimeric embryos

Chimeras were generated in John West's lab (University of Edinburgh) by embryo aggregation (West and Flockhart, 1994). Embryos differed at the *Gpi1* locus (encoding glucose phosphate isomerase) and one of each pair carried the β-globin *TgN (Hbb-b1)* transgene (abbreviated to *Tg*), identifiable by DNA in situ hybridization (Keighren and West, 1993; Lo, 1986; Lo et al., 1987). Outbred CD1A females (homozygous $Gpi1^{a/a}$ CD1 strain mice) were induced to ovulate and mated to PAX77 males on a CD1A background to produce PAX77 and wild-type embryos, all of which were $Gpi1^{a/a};Tg^{-/-}$. (C57BL/6 × CBA/Ca)F1 females ($Gpi1^{b/b}; Tg^{-/-}$) were induced to ovulate and mated to 'BTC' strain males ($Gpi1^{b/b};Tg^{+/+}$ on a mixed [C57BL/6 × CBA/Ca] background) to produce embryos, all of which were wild-type, $Gpi1^{b/b}; Tg^{+/-}$. Chimeras were transferred to pseudopregnant $Gpi1^{c/c}$ ('CF1' hybrid strain) females. E16.5 fetuses were dissected into cold PBS, the limbs and tails of the fetuses were removed and analyzed by GPI1 electrophoresis (West and Flockhart, 1994). Heads were fixed and processed for analysis by in situ hybridization and other body tissues were digested to obtain DNA for PCR genotyping to distinguish PAX77↔wild-type and wild-type↔wild-type chimeras. 3-5 non-consecutive coronal sections from each chimeric brain were examined for each hemisphere and each region along the anterior-posterior axis. Percentages of Tg^- cells were determined by counting numbers of hybridization signals and nuclei in 100 μm-wide boxes. The contribution of $Gpi1^{a/a}$ cells to chimeras used here was 42% to 86%.

To determine proportions of Tg- and Tg+ cells in M-phase in PAX77↔wild-type chimeras, β-globin DNA in situ hybridization was followed by immunostaining with anti-phosphorylated histone H3. Nickel was added to the diaminobenzidine visualization solution to obtain a grey precipitate. Cells were counted in 100 μm-wide sampling boxes in the VZ of the rostral cortex of each E16.5 chimeric or wild-

type embryo. Each count was repeated on 4-5 non-adjacent sections. The contribution of *Gpi1*$^{a/a}$ cells to the chimeras used here was 42-57%.

2.4 Bromodeoxyuridine/Iododeoxyuridine incorporation studies

Timed-pregnant females bearing wild-type and PAX77 embryos were given thymidine analogues (0.2ml of 10mg/ml, dissolved in 0.9% NaCl) by intraperitoneal injection. The thymidine analogues, 5-bromo-2'-deoxyuridine (BrdU) and 5-iodo-2'-deoxyuridine (IdU) (Sigma-Aldrich), are incorporated into cells during S-phase of the cell cycle. For *short-pulse* BrdU experiments, pregnant females were sacrificed 1 h after injection with BrdU. For *cell cycle analysis*, pregnant mothers received a single injection of IdU and, after 1.5 h, BrdU was injected; mice were sacrificed 30 min after the BrdU injection (Martynoga et al. 2005). To estimate the *leaving (Q) fraction* (Takahashi et al. 1994; Tarui et al. 2005), IdU was administered to E15.5 pregnant females at 9.00 a.m., followed by a BrdU injection at 10.30 a.m. (1.5 h later). The BrdU injection was followed by a series of 7 additional BrdU injections given at 3-hour intervals. Pregnant females were sacrificed 30 min after the last BrdU injection. For *analysis of migration*, pregnant females were given a single injection of BrdU at E15.5 or E17.5 and offspring were perfused at postnatal day (P) 7. In all cases, brains were removed, sectioned and processed for immunohistochemistry.

2.5 Immunohistochemistry

Following deparafinization in xylene, wax brain sections were rehydrated through descending ethanol series, followed by PBS wash. Cryosections were air dried for 30 min at RT and washed with PBS for 30 min. To block endogenous peroxidase on sections processed for diaminobenzidine (DAB) immunohistochemistry, sections were treated with 0.3% H_2O_2 in methanol for 15 min at RT before proceeding to the next step. For antigen retrieval, sections were microwave-heated in a solution of 0.01M sodium citrate, pH6.0; wax sections were heated for 20 min (4x 5 min at high

power) whereas cryosections were heated for 15 min (1x 5 min low power, 2x 5 min at simmer). Cryosections were heat-treated only when necessary for optimal detection of nuclear staining. To denature DNA for BrdU detection on non-heated cryosections, sections were immersed in 2N HCl for 30min at 37°C, neutralized with 0.1M Na borate buffer, pH8.5 for 15 min and washed with PBS. Sections were washed with PBS, 0.1% Triton X-100 before applying blocking solution (20% goat or donkey serum [Sigma] in PBS, 0.1% Triton X-100) for 30 min at RT. Sections were then incubated overnight at 4°C with primary antibodies diluted in blocking solution. Primary antibodies used were mouse anti-BrdU/IdU (BD Biosciences, 1:50 for immunofluorescence, 1:100 for DAB), rat anti-BrdU (Abcam ab6326, 1:50), mouse anti-proliferating cell nuclear antigen (PCNA) (Dako, 1:100), mouse anti-phosphorylated histone H3 (pH3) (for DAB: Sigma, 1:500; for immunofluorescence: Abcam ab1791, 1:200), mouse anti-Pax6 (DSHB, 1:50 for immunofluorescence, 1:200 for DAB), mouse anti-Mash1 (BD Biosciences, 1:100), mouse anti-Satb2 (Abcam ab51502, 1:25), mouse anti-β-III-tubulin (Sigma, 1:100), rabbit anti-Gsh2 (gift from Kenneth Campbell, 1:1500), rabbit anti-Olig2 (Millipore, 1:500), rabbit anti-Tbr1 (gift from Robert Henver, 1:100), rabbit anti-Tbr2 (Abcam ab23345, 1:100), rat anti-Ctip2 (Abcam ab18465, 1:250), goat anti-Cux1 (Santa Cruz, 1:50), goat anti-GFP (Abcam ab6673, 1:100 for microwaved sections, 1:500 for straight immunofluorescence), rabbit anti-GFP (Abcam ab290, for straight immunofluorescence only, 1:500). After optimization, antibodies that could be used without antigen retrieval on cryosections include: anti-Ctip2, anti-Satb2, anti-pH3, anti-Tbr1, rabbit anti-GFP. Following incubation with primary antibodies, the tissue was washed in PBS, 0.1% Triton X-100 and appropriate secondary antibodies were applied for 1 h at RT. For bright-field staining, biotinylated goat anti-mouse, goat anti-rabbit or donkey anti-mouse antibodies (all from Dako, 1:200) were used, followed by a standard avidin-biotin-DAB visualisation procedure (Vector Labs) before sections were coverslipped in DPX. For fluorescent staining, secondary antibodies used were goat anti-mouse Alexa Fluor 488, goat anti-rat Alexa Fluor 568, goat anti-rabbit Alexa Fluor 488, goat anti-rabbit Alexa Fluor 568, donkey anti-goat Alexa Fluor 488, donkey anti-goat Alexa Fluor 568, donkey anti-mouse Alexa Fluor 568, donkey anti-rabbit Alexa Fluor 568, donkey anti-rat Alexa Fluor 488 (all

from Molecular Probes, diluted at 1:200). For Pax6 immunofluorescence, biotinylated goat anti-mouse antibody (Dako, 1:100) was used before Alexa Fluor 488-conjugated streptavidin (Molecular Probes, 1:100). Nuclear counterstaining was performed with TOPRO-3 (1:1000 in dH_2O, Molecular Probes) for immunofluorescence, or 0.25% cresyl violet (in dH_2O) for light microscopy. Sections were coverslipped in Vectashield (Vector Labs) and stored in dark at 4°C. Fluorescent images were captured using a Leica NTS confocal microscope, whereas a Leica digital camera was used for light microscopy images. Pax6/YFP double immunohistochemistry was performed sequentially following protocols above; Pax6 staining was detected with DAB, sections were blocked and then incubated with goat anti-GFP, YFP immunoreactivity was revealed with donkey anti-goat 488, sections were coverslipped in Vectashield and photographed in a Leica digital camera. Bright-field and immunofluorescence images were overlaid in Adobe Photoshop and adjusted for lightness and contrast.

2.6 Flow cytometry

Cortical tissue was collected from E16.5 PAX77 and wild-type embryos separately at rostral and central neocortical levels. Eight individuals of each genotype collected from 3 separate litters were used for the analysis. Cells were dissociated using papain following manufacturer's instructions (Papain Dissociation System, Worthington Biochemichals, UK) and fixed in ice-cold 70% ethanol at a concentration of $1x10^6$ cells per ml. Dissociated cells were stained for β-tubulin isotype III (1:800) and primary antibody binding was detected using directly conjugated AlexaFluor® 488 (goat anti-mouse IgG, 1:800). To stain cellular DNA, cells were then incubated with propidium iodide (PI) at 50 μg/ml with RNAse A at 125 μg/ml. Cells were analysed on a Beckman-Coulter XL flow cytometer. 10,000-20,000 cells were analysed per sample.

2.7 Analysis

2.7.1 Cortical surface measurements

P9 brains were fixed overnight in 4% PFA at 4°C. Cerebral hemispheres were separated, flattened between glass slides with spacers and postfixed with the same fixative for 5 days. Flattened hemispheres were rinsed with PBS and slides were stored in 70% ethanol at 4°C before hemispheres were removed from slides and photographed with a Nikon microscope. Images were imported into Image Tool and the border around the cortex of wild-type and PAX77 hemispheres was drawn to measure the cortical surface.

2.7.2 Cortical layer thickness

Sections from 3 wild-type and 3 PAX77 P7 pups were stained with cresyl violet. For each brain, the thickness of cortical layers was measured using the Image Tool software (University of Texas Health Science Centre at San Antonio, San Antonio, TX, USA) on 16-28 non-adjacent sections at equivalent rostral, central and caudal levels.

2.7.3 Cortical progenitor numbers in S- or M-phase of the cell cycle

Cortical progenitors in S- or M-phase were assessed by BrdU or pH3 immunoreactivity, respectively. For BrdU analyses in PAX77 or *Pax6*$^{loxP/loxP}$; *Emx1-CreER*^{T2} embryos and appropriate controls, positive nuclei were counted in 100 μm-wide sampling boxes and counts were repeated on three to five non-consecutive sections for each cortical region per brain. In E15.5 PAX77 embryos and respective controls, counterstain of BrdU-reacted sections with cresyl violet enabled visualization of cytoarchitecture, i.e. radial alignment of VZ nuclei compared to scattered BrdU-positive nuclei in the SVZ, and therefore radial stripes were subdivided into a domain corresponding to the VZ and a more superficial domain and numbers of BrdU-positive cells were scored. PH3-positive cells localized in the ventricular surface were designated as apically dividing progenitors, whereas

positive nuclei at abventricular positions were designated as progenitors in basal mitoses. PH3-labelled cells were counted in 100 μm-wide sampling boxes in PAX77 embryos and respective controls; counts were repeated on ten to nineteen non-consecutive sections for each cortical region per brain. In *Pax6*$^{loxP/loxP}$; *Emx1-CreER*^{T2} embryos and respective controls, PH3-labelled cells were counted in 200 μm-wide sampling boxes and counts were repeated on four to five non-adjacent sections for each cortical region per brain. In all cases, BrdU and pH3 analyses were performed the middle of the rostral, central and caudal levels of the neocortex.

2.7.3 Cell cycle times

Age-matched wild-type and PAX77 sections were reacted to reveal IdU/BrdU labelling. To detect IdU, a mouse-anti-BrdU antibody, which cross-reacts with IdU, was used. The BrdU signal was distinguished from the IdU signal by using a rat-anti-BrdU-specific antibody. Sections were photographed at x40 magnification on a Leica NTS confocal microscope and then imported into Adobe Photoshop for counting. The analysis at E15.5 was performed in the middle of the rostral, central and caudal neocortex, whereas at E12.5 four locations were analysed, namely the middle of the rostral neocortex, a medial and a lateral region of the central cortex, and the middle of the caudal cortex (see Fig. 3.1C). This method identifies IdU-only and IdU/BrdU double-labelled cells. IdU-only labelled cells are those in S-phase at the start of the experiment that exit S-phase by the time of the BrdU injection, and are therefore designated as the leaving fraction (L_{cells}). BrdU/IdU double-labelled cells are those still in S-phase (S_{cells}) at the time of the BrdU injection. Proportions of L_{cells} and S_{cells} were calculated in the VZ and the lengths of the S-phase and the cell cycle were calculated by using the equations shown in Fig. 1A (Martynoga et al., 2005). To estimate the proportion of proliferating cells (P_{cells}), proportions of PCNA-positive cells were counted in the VZ of the same regions of cortex used for BrdU/IdU cell counts. Cell cycle times were also determined in a non-Pax6-expressing region of the lateral ganglionic eminence (LGE) at E15.5 following methods described above.

2.7.4 Q fraction

Following the protocol described above and summarized in Fig. 2A in chapter 4, sections at the rostral, central and caudal level of the cortex were processed for IdU/BrdU immunohistochemistry, photographed at x20 magnification on a Leica NTS confocal microscope and then imported into Adobe Photoshop for analysis. The principle of the analysis follows that described in Tarui et al. (2005). This paradigm is based on labelling a cohort of cells in S-phase over an experimentally defined period and following this cohort as it undergoes G_2, M and G_1 phases and reaches the point where a decision of whether to exit or re-enter cell cycle is made. As in the analysis of cell cycle times, a cohort of cells undergoing S-phase at the start of the experiment was labelled by IdU injection. Cells exiting S-phase in the 1.5-hr interval between the IdU injection and the first BrdU injection would have been labelled with IdU only (L_{cells}) and their fate would be followed. It should be noted that if a single S-phase tracer was to be injected, i.e. IdU only, the interval would determine the cell-cycle phase of traced cells at the end of the experiment: a short interval, i.e. 30 min to 1.5 h, would label progenitors in S-phase, a longer interval would be chosen if labelled cells were to be identified in G2-M phase at the end of the experiment, and an even longer interval should be used if labelled cells were to be in G1 phase at the time of sacrifice. Therefore, the interval of the S-phase tracer depends upon the aim of a given experiment and requires estimation of the length of each cell-cycle stage at the same developmental stage from previous experiments. For the experimental design here, findings from calculation of cell cycle times (Fig. 1, chapter 4) were used to calculate the total interval of IdU and BrdU injections. A short, 1.5 h, interval for IdU injection was used: this is both sufficient to label a cohort of S-phase cells at the start of the experiment and a prerequisite given that this interval should be the same as that used for calculation of cell cycle times in Fig. 1 (Chapter 4). To identify L_{cells} that re-enter S-phase instead of exiting cell cycle, the total duration of subsequent exposure to BrdU should be longer than Tc – Ts, or otherwise longer than the combined length of G_2, M and G_1 phases of the cell cycle. Again, based on cell cycle time calculations (Fig. 1, chapter 4) it was determined that subsequent exposure to BrdU for a total of 21 h was sufficient to follow L_{cells} that re-enter S-phase, which would have become double-labelled with BrdU. Pregnant females were

sacrificed 30 min after the last BrdU injection, since this period has been shown to be required for circulation of S-phase tracers in the bloodstream and labelling the DNA of S-phase cells at detectable levels (Nowakowski et al. 1989). Cells entering S-phase become detectably labelled for about 5-6 h post-BrdU injection (Hayes and Nowakowski 2000) and therefore sequential injections of BrdU every 3 h used here is considered approporiate for ensuring continuous availability of the S-phase tracer in the bloodstream. The leaving fraction was estimated by dividing the number of L_{cells} that had not re-entered S-phase at the end of the long exposure to BrdU (identified because they still contained only IdU; now designated Q_{cells}) by the number of L_{cells} multiplied by two. The number of L_{cells} from the cell cycle analysis was doubled because these cells would have undergone mitosis, thereby doubling the size of the L_{cell} cohort, before either exiting or re-entering the cell cycle.

2.7.5 BrdU birthdating

Anatomically-matched sections from P7 wild-type and PAX77 cortex were reacted to reveal BrdU label and camera lucida drawings were made of the laminar positions of heavily- and lightly-labelled BrdU-positive cells in rostral, central and caudal cortex, following methods described previously (Gillies and Price 1993; Caric et al. 1997). Heavy labelling was defined where a cell had more than half of its nucleus stained with BrdU. Drawings were repeated on three to five non-consecutive sections for each cortical region per brain. BrdU-positive cells were counted within 500-µm-wide strips through the depth of the cortex (sectioned coronally). These radial strips covered a cortical depth of 500 µm from the pial surface inward and were divided into 10 bins of equal depth (50 µm). Histograms were obtained of the average numbers of heavily and lightly BrdU-labelled at each depth from the pia.

For double-labelling of BrdU-positive cells with appropriate laminar markers, e.g. Tbr1 or Cux1, coronal sections from P7 wild-type and PAX77 cortex or *Pax6*$^{loxP/+}$; *Emx1-CreER*^{T2} and *Pax6*$^{loxP/loxP}$; *Emx1-CreER*^{T2} cortex at the rostral level were reacted. The proportions of double-labelled cells over the total number of BrdU-positive cells were calculated in 200-µm-wide strips spanning the depth of the deep layers (for BrdU/Tbr1 immunostaining) or the superficial layers (for BrdU/Cux1

immunostaining) of the cortex. For BrdU/Tbr1 analysis, only heavily-labelled BrdU-positive cells were counted. Counts were repeated on three to five non-consecutive sections per brain.

2.7.6 Statistical analysis

Analysis was performed on data collected from brains of at least 3 embryos/mice of each genotype. Statistical comparisons were made by Student's *t*-test (for single variables) and one-way ANOVA (for more than two-group comparisons) (Sigmastat). Asterisks above histograms indicate $P < 0.05$.

CHAPTER 3

Controlled Overexpression of Pax6 in vivo Causes Cell-autonomous Defects of Late Cortical Progenitors and Reduces the Thickness of Superficial Cortical Layers

*Published in Martine Manuel, Petrina A. Georgala et al. (2007). "Controlled overexpression of Pax6 in vivo negatively autoregulates the *Pax6* locus and causes cell autonomous defects of late cortical progenitor proliferation but has little effect on cortical arealization". Development. 134 (3):545-555.

3.1 Introduction

The complexity of brain structure and function is established through the generation of numerous and frequently subtle differences among progenitor cells and the neurons they produce. Molecular differences between cells in the embryonic nervous system are detectable from its inception and arise as cells are exposed to different levels of morphogens released by surrounding signalling centres. These morphogens determine the levels of expression of key transcription factors that pattern the nervous system, creating domains that express characteristic combinations of transcription factors specifying their morphologies and functions (Kerszberg 1999; Neumann and Cohen 1997; Tabata and Takei 2004; Yucel and Small 2006). The potential of a limited set of transcription factors to direct the generation of an enormous diversity of neuronal phenotypes might be enhanced greatly if different levels of transcription factors cause different developmental outcomes. If levels of expression are important, then enhanced expression above optimal levels should affect the development of cortical neurons. Here, this prediction was tested for the transcription factor Pax6.

In normal mice, corticogenesis occurs between E11.5 and E17.5 by a process of progenitor proliferation in the ventricular zone (VZ) followed by migration of neural precursors to the overlying cortical plate. Throughout corticogenesis, Pax6 is expressed mainly in progenitors residing in the VZ, known as apical progenitors (APs) (Gotz et al. 1998; Englund et al. 2005). Pax6 expression follows a rostrolateral (high) to caudomedial (low) gradient, similar to that of corticogenesis (Bayer and Altman 1991). Mice homozygous for a loss-of-function mutation of *Pax6* die at birth with serious brain abnormalities, including an abnormally thin cortical plate and an expanded proliferative zone due to failure of late-born neurons to migrate to laminar positions (Schmahl et al. 1993; Stoykova et al. 1996; Caric et al. 1997; Stoykova et al. 2000; Tarabykin et al. 2001). Previous studies identified a reduced progenitor population and defective differentiation as primary defects resulting from loss of Pax6 (Heins et al. 2002; Quinn et al. 2006).

To date, the role of Pax6 in cortical development has been examined mainly through loss-of-function studies in mutant mice. Whether the level at which it is expressed in

the brain is important is not clear, although its expression in a gradient in the cortex suggests it might be. Levels of Pax6 expression in the eye are critical, with both reduced and increased gene dosage causing defects in development (Schedl et al. 1996). Here, the speculation that increased levels of Pax6 might affect cortical progenitor proliferation and lamination was tested by using the PAX77 mouse line produced by Schedl et al. (1996). In addition to their two endogenous *Pax6* alleles, mice hemizygous for the *PAX77* transgene carry approximately six additional copies of the human *PAX6* locus, including its upstream and downstream regulatory regions (the mouse and human Pax6 proteins are identical). In PAX77 mice, Pax6 protein levels are increased about 1.5- to 3-fold, an increase that is not as great as the number of gene copies and has been explained through demonstration of negative feedback in the regulation of Pax6 (Manuel et al. 2007). The normal graded expression of Pax6 is conserved in the cortex of PAX77 mice (Manuel et al. 2007). The *PAX77* transgene is functional, as demonstrated by its ability to rescue the eye and brain defects in mice carrying loss-of-function mutations of *Pax6* (Schedl et al. 1996). In this chapter, results show that increased *PAX6* dosage reduces the thickness of superficial cortical layers specifically and impairs the proliferation of late cortical progenitors in a cell-autonomous fashion. These findings suggest that Pax6 levels have potent effects during late stages of corticogenesis, the time of superficial layer neuron generation.

3.2 Results

3.2.1 Pax6 overexpression decreases the thickness of superficial cortical layers

Gross examination of postnatal PAX77 brains failed to show any obvious differences in brain size compared to wild-type littermates. To further address this issue, the cortical surface area was measured on flattened cortices of PAX77 and wild-type postnatal brains (Fig. 1). The cortical surface area was significantly reduced in the PAX77 mice compared to controls (54.355 ± 0.629 mm^2 in wild-type, 48.67 ± 0.55 mm^2 in PAX77; Student's *t*-test $P < 0.001$, $n = 8$). To test whether Pax6 overexpression affects cortical lamination, the thickness of deep (V and VI) and superficial (II-IV combined) layers and of the marginal zone (future layer I) was measured at the rostral, central and caudal cortex of PAX77 and wild-type brains at P7 (Fig. 2). The thickness of superficial layers II-IV was significantly decreased in the rostral and central PAX77 cortex compared to wild-types (Student's *t*-test $P < 0.01$, $n = 3$ brains of each genotype) (Fig. 2C, D). The thickness of deep cortical layers and that of layer I were not significantly altered in the PAX77 cortex. Since the formation of superficial cortical layers occurs during late stages of corticogenesis, these results suggest that Pax6 overexpression might affect specifically late cortical development.

3.2.2 Pax6 overexpression alters cortical progenitor proliferation at late stages of corticogenesis

Previous studies showed that Pax6 is important in regulating cortical progenitor proliferation and promoting neurogenesis (Estivill-Torrus et al. 2002; Heins et al. 2002). Neurons destined for cortical layers IV-II are generated between E14.5 and E17.5, leading to the hypothesis that the thinner superficial layers in the PAX77 cortex might arise due to late cortical progenitor proliferation defects. The proliferative zone of the neocortex contains two populations of progenitors: apical progenitors (APs) undergo mitosis at the ventricular surface and express high levels

Figure 1

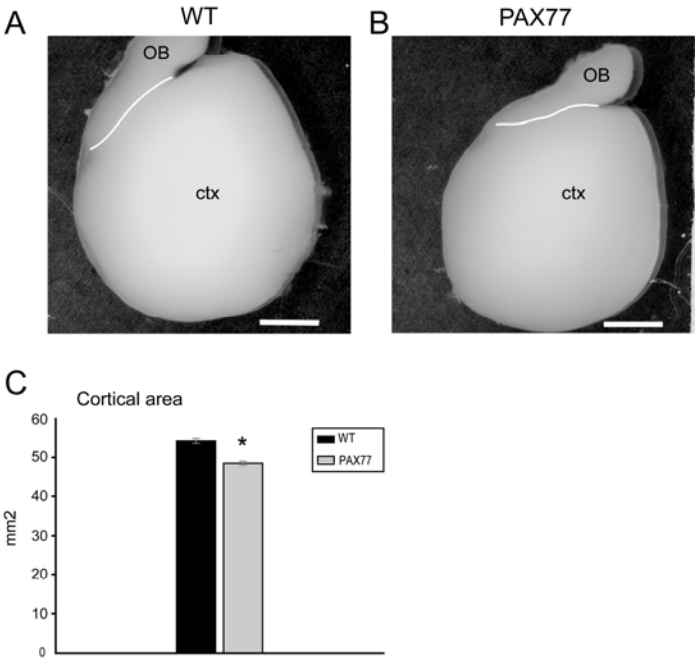

Figure 1. Pax6 overexpression leads to reduced cortical surface. (A, B) Dorsal views of wild-type and PAX77 flattened cortices at P9. The border between the cortex and the olfactory bulb is outlined on the images. (C) Cortical surface area was significantly (*) reduced in PAX77 mice compared to wild-type. Ctx, cortex; OB, olfactory bulb. Scale bar: 3mm.

Figure 2

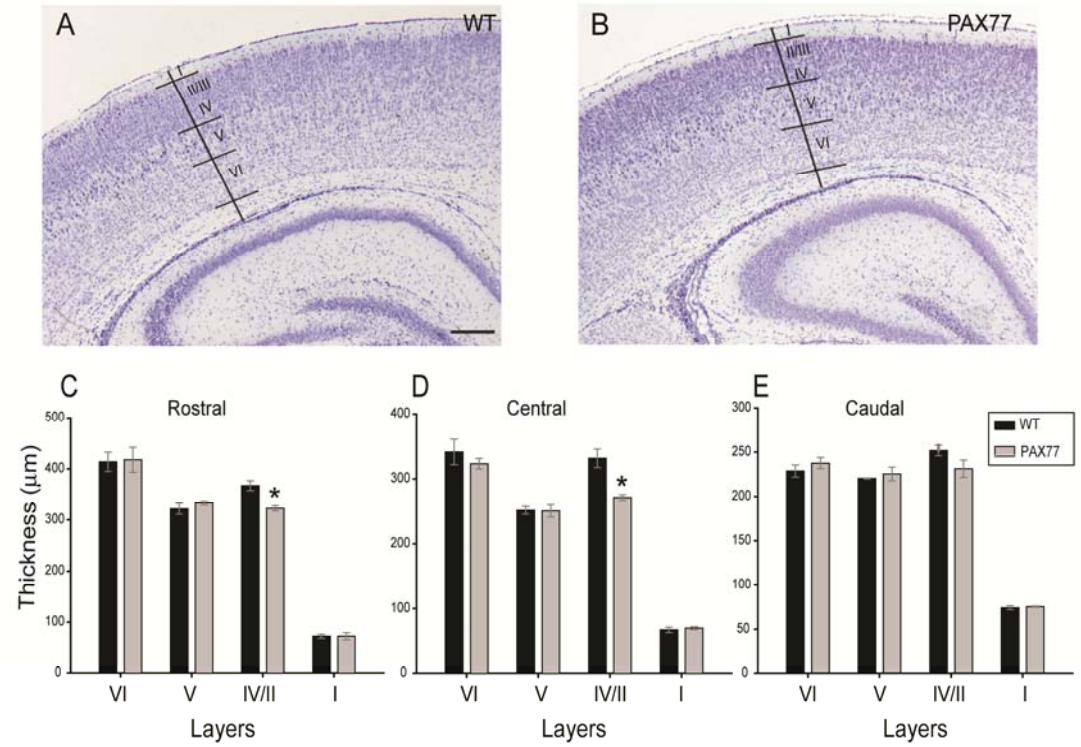

Figure 2. Pax6 overexpression affects the formation of superficial cortical layers. (A-B) Coronal sections through the cortex of (A) a wild-type and (B) a PAX77 mouse at P7, stained with cresyl violet. Borders between adjacent cortical layers were identified based on differences in cytoarchitecture and packing density. (C-E) Thickness of cortical layers I, II-IV (combined), V and VI in (C) rostral, (D) central and (E) caudal cortex of wild-type and PAX77 mice at P7. The thickness of layers II-IV was significantly (*) decreased in the rostral and central cortex of PAX77 mice compared to wild-types. Scale bar: 300 µm.

of Pax6; basal progenitors (BPs) are derived from APs and divide in the SVZ and basal VZ. Pax6 is downregulated during the transition from AP to BP (Englund et al., 2005). To examine progenitor proliferation in the PAX77 embryos, BrdU was used to label cortical progenitors in S-phase of the cell cycle (Fig. 3D-E, G-H) while phosphorylated histone H3 was used as a marker of mitotic progenitors (Fig. 3J, K). I determined the proportion of cells in S-phase (p^{Scells}) in the VZ along the cortex of PAX77 and wild-type embryos at E12.5, early in corticogenesis, and was unable to detect any significant difference between the genotypes (Fig. 3A-F). Then the p^{Scells} and the density of cells undergoing mitosis (d^{Mcells}) were determined along the cortex of wild-type and *PAX77*$^{+}$ embryos at E15.5, a late stage of corticogenesis. A significant reduction of p^{Scells} (Fig. 3G-I) and d^{Mcells} (Fig. 3J-L) among APs was detected in the rostral and central cortex of PAX77 embryos compared to wild-types (Student's *t*-test $P < 0.05$, $n = 3$ of each genotype). No significant difference was detected in the caudal cortex. Thus, Pax6 overexpression alters the proliferation of rostral and central APs at late stages of corticogenesis, while early progenitors seem unaffected in the PAX77 cortex. There was no significant alteration of p^{Scells} and d^{Mcells} among BPs in the rostral, central and caudal cortex of PAX77 embryos compared to wild-types. These results suggest that Pax6 overexpression affects specifically the proliferation of late cortical progenitors that normally express high levels of Pax6.

3.2.3 Effects of Pax6 overexpression on late cortical progenitors are cell autonomous

In PAX77 mice, Pax6 levels are increased at all its sites of expression and so a late-onset cortical defect might arise as a secondary consequence of defects elsewhere (e.g. PAX77 mice are microphthalmic and may have other as yet undetected extra-cortical abnormalities). I tested whether the defects detected in mutants reflect a requirement for a correct level of Pax6 within cortical progenitors themselves rather than in their environment. To discriminate between these two possibilities chimeric embryos (generated by John West's lab, University of Edinburgh) were analysed, in which mutant cells have the potential to interact with wild-type cells and any defects

Figure 3

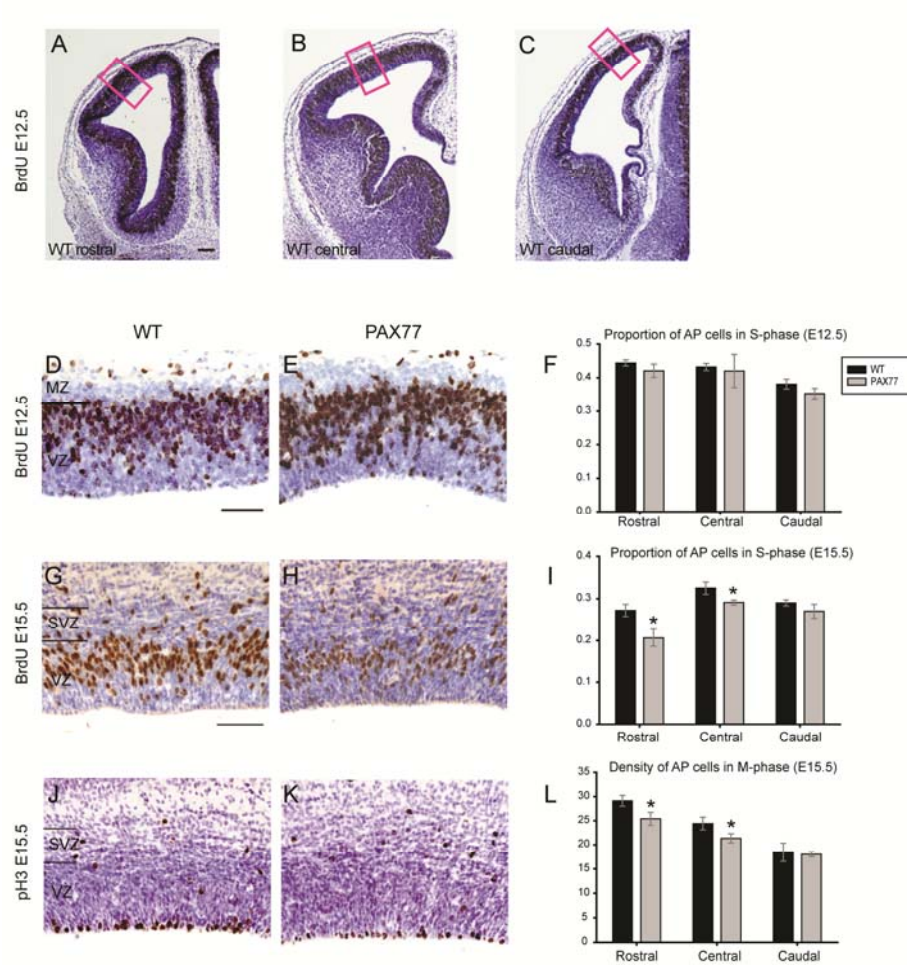

Figure 3. Pax6 overexpression affects late cortical progenitor proliferation. (A-C) Coronal sections at (A) rostral, (B) central and (C) caudal levels of the cortex (1 hemisphere shown) of an E12.5 wild-type embryo labeled with anti-BrdU (brown). Cell counts were made in 100 µm wide sampling boxes. (D, E) Examples of anti-BrdU labeling (brown) of coronal sections of the cortex of (D) a wild-type and (E) a PAX77 embryo at E12.5. (F) The proportion of AP cells in S-phase along the cortex of PAX77 embryos at E12.5 is not different from the wild-types. (G, H) Example of anti-BrdU labeling (brown) of coronal sections of the cortex of (G) a wild-type and (H) a PAX77 embryo at E15.5. Note that BrdU labelling intensity varied in both wild-type and PAX77 cortices; both heavily- and less heavily-stained BrdU-positive nuclei were counted in cortical sections through brains of both genotypes. (I) The proportion of AP cells in S-phase in the rostral and central cortex of PAX77 embryos at E15.5 is significantly decreased compared to the wild-types. (J, K) Example of anti-phosphorylated histone H3 labeling (brown) of coronal sections of the cortex of (J) a wild-type and (K) a PAX77 embryo at E15.5. (L) The density of AP cells in M-phase in the rostral and central cortex of PAX77 embryos at E15.5 is significantly decreased compared to the wild-types. All sections shown are counterstained with cresyl violet. MZ, marginal zone; VZ, ventricular zone; SVZ, subventricular zone. Scale bars: (A-E) 50 µm, (G, H, J, K) 70 µm.

that they retain are more likely to be cell autonomous. Embryos derived from a wild-type × PAX77 cross were aggregated to wild-type embryos, carrying the Tg transgene as a marker, to produce control chimeras [wild-type;Tg^-↔wild-type;Tg^+] or mutant chimeras [PAX77;Tg^-↔wild-type;Tg^+]. Cells derived from the wild-type embryo could be identified, after DNA in situ hybridization against *Tg* (described in Talamillo et al. 2003), by the presence of a brown spot in the nucleus (Fig. 4A, B). The global percentage of cells derived from each of the two embryos used to generate each chimera was estimated by quantitative analysis of GPI1 isozyme composition of the limbs (West and Flockhart, 1994), with the percentage of the GPI1A isozyme representing the contribution of cells derived from the wild-type × PAX77 cross.

3 control and 4 mutant chimeras were analyzed at E16.5 and the percentage of Tg^- cells in the proliferative zones (VZ and SVZ), the intermediate zone (IZ) and the cortical plate (CP) was determined at rostral, central and caudal positions of each chimeric cortex. For each chimera, the observed contribution of Tg^- cells to each cortical region (obsTg^-) was compared to the expected contribution of Tg^- cells (expTg^-) given by the percentage of GPI1A for that chimera. The mean ratio obsTg^- / expTg^- in the different cortical regions of the control chimeras was always slightly greater than 1 (between 1.08 and 1.23, Fig. 4C-E), reflecting the fact that the brown spot identifying Tg^+ cells was not always present in the plane of section analyzed and therefore the number of Tg^- cells was slightly overestimated. This applied equally to control and mutant chimeras. Analyses showed that the Tg^- cells in the mutant chimeras were significantly under-represented in the proliferative zones of the rostral (Student's *t*-test $P < 0.01$), central ($P < 0.05$) and caudal ($P < 0.05$) cortex compared to the control chimeras (Fig. 4C). The Tg^- cells in the mutant chimeras were also significantly under-represented in the intermediate zone of the rostral cortex (Student's *t*-test $P < 0.05$) compared to control chimeras (Fig. 4D). There was no difference in the contribution of Tg^- cells to the cortical plate between mutant and control chimeras (Fig. 4E), indicating that Pax6 overexpression does not affect the production of postmitotic cells at earlier developmental stages. Overall, these results suggest that, late in corticogenesis, cortical progenitors must express normal levels of Pax6 to contribute normally to the proliferative zones of the cortex.

Figure 4

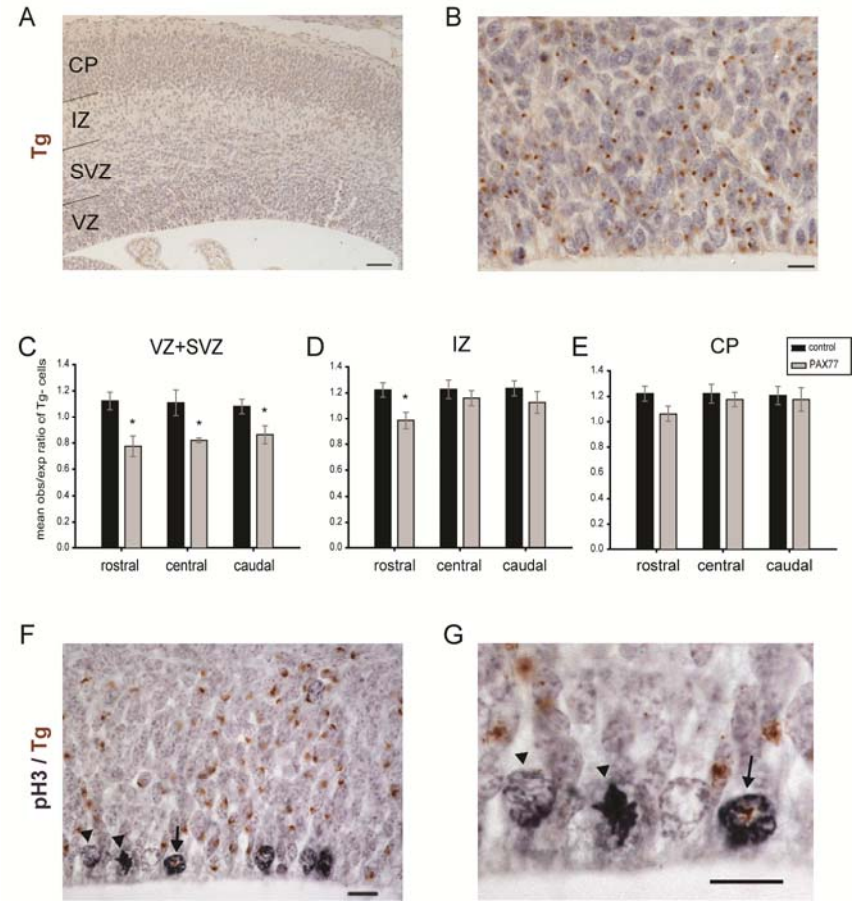

Figure 4. PAX77 cells are under-represented in the cortical proliferative layers of PAX77;Tg-↔wild-type;Tg+ chimeric embryos at E16.5. (A,B,F,G) Coronal sections through the cortex of a PAX77;Tg^-↔wild-type;Tg^+ chimera at E16.5. (A,B) Tg^+ cells (marked with brown dots) and Tg^- cells were counted in the proliferative layers (VZ and SVZ) the intermediate zone (IZ) and the cortical plate (CP). (C-E) Ratios of observed/expected contributions of Tg^- (i.e. PAX77) cells in (C) VZ and SVZ, (D) IZ and (E) CP. (C) PAX77;Tg^- cells are significantly (*) under-represented in the proliferative layers along the chimeric cortex and (D) in the intermediate zone of the rostral chimeric cortex. (F,G) Example of Tg^+(arrow) and Tg^- (arrowhead) apical progenitors in M-Phase labelled with anti-phosphorylated histone H3 (grey). Note that DNA in situ hybridization against *Tg* was performed prior to pH3 immunostaining which could mask the brown dot (arrow) in wild-type cells double-labelled with pH3. This would lead to an underestimation of numbers of wild-type cells in M-phase in chimeric embryos and therefore an overestimation of PAX77 cells in M-phase, meaning that the observed reduction of M-phase mutant cells compared to wild-types might be effectively further. Scale bars: (A) 50 μm; (B, F, G) 10 μm.

To test whether the under-representation of Pax6 overexpressing cells in the cortical proliferative zones of chimeras was due to a cell autonomous proliferation defect, phosphorylated histone H3 was used as a marker of mitotic cells (Fig. 4F, G). I compared the average proportion of Tg^+ and Tg^- cells in M-phase (p^{MTg+} and p^{MTg-} respectively) in the VZ of the rostral cortex of mutant chimeras to the average proportion of cells in M-Phase (p^{Mcells}) in the corresponding region of wild-type embryos. The average proportion of mutant cells in M-phase (p^{MTg-}) in chimeras (0.0123 ± 0.0044 s.e.m., n = 3) was significantly lower than p^{Mcells} in wild-type embryos (Student's t-test $P < 0.03$), indicating that correct levels of Pax6 are required cell-autonomously to enable late cortical progenitors to proliferate normally. The p^{MTg+} in mutant chimeras (0.0243 ± 0.003 s.e.m., n = 3) was not significantly different from p^{Mcells} in wild-type embryos (0.0242 ± 0.003 s.e.m., n = 3), indicating that the presence of Pax6 overexpressing cells does not affect the proliferation of wild-type cortical progenitors in mutant chimeras.

3.3 Discussion

3.3.1 Upregulation of Pax6 protein levels in PAX77 mice affects cortical development in a region-specific and time-dependent manner

PAX77 mice contain five to seven copies of the human *PAX6* locus, in addition to their two endogenous copies of *Pax6* (Schedl et al. 1996). Therefore, the presence of seven to nine copies of the gene in PAX77 mice, as opposed to two in wild-types, would be predicted to cause a 3.5- to 4.5-fold increase in Pax6 protein levels under normal conditions. However, quantitative analyses by Western blots have indicated that Pax6 protein levels are increased in the brain of PAX77 embryos by 1.5- to 3-fold compared to wild-types (Manuel et al. 2007), whereas in the developing eye a similar, 2.24-fold, increase has been reported in PAX77 mice (Dora et al. 2008). Elevation of Pax6 levels in PAX77 mice has also been demonstrated at the single-cell level by measurements of the fluorescent intensity on sections through PAX77 eye tissues (corneas and lens epithelia) immunoreacted for Pax6 (Dora et al. 2008; Chanas et al. 2009). The less than expected increase in Pax6 levels compared to gene copy numbers in PAX77 mice most likely reflects the negative autoregulation of Pax6, as demonstrated by both reduced GFP expression from the YAC transgene reporting on levels of *Pax6* activation and reduced levels of *Pax6* mRNA in PAX77 brains (Manuel et al. 2007). Although in PAX77 mice both Pax6 and Pax6(5a) isoforms are overexpressed and the canonical Pax6 predominates over Pax6(5a) as in wild-types, the isoform ratio differs from that in wild-types due to a higher increase in the Pax6(5a) isoform caused by the PAX77 transgene compared to the canonical Pax6 (Manuel et al. 2007; Dora et al. 2008).

Pax6 overexpression in PAX77 brains is restricted to regions that normally express Pax6 in wild-type brains without any ectopic sites of expression in transgenic mice. Importantly, the rostro-lateral^{high} to caudo-medial^{low} gradient of Pax6 expression is conserved in the PAX77 cortex. The graded expression of Pax6 throughout the rostral-caudal axis has been measured in E12.5 PAX77 and wild-type cortices by measuring the fluorescent intensity in rostral and caudal regions of sagittal brain sections immunolabelled for Pax6 (Manuel et al. 2007). This analysis indicated that the ratio of relative Pax6 levels between rostral and caudal regions is approximately

3 in the wild-type cortex, whereas in the PAX77 cortex this ratio equals to about 4, indicating an increased steepness of the cortical Pax6 gradient in PAX77 embryos compared to wild-type (Manuel et al. 2007). Interestingly, Pax6 levels were elevated at caudal levels of the PAX77 cortex with respect to wild-types and resembled those normally seen at the rostral pole of the wild-type cortex (Manuel et al. 2007), indicating a non-autonomous defect in caudal areas due to the maintained gradient throughout the rostral-caudal axis or a cell-autonomous effect due to the requirement other factors in low-Pax6-expressing regions. This could explain findings here that cortical development is more susceptible to Pax6 overexpression rostrally rather than caudally. Maintaining Pax6 within physiological levels could limit the effect of Pax6 overexpression in the caudal PAX77 cortex, whereas driving Pax6 expression at rostral and central cortical regions to exceed levels that are normally found during development could alter the developmental potential of cortical cells found in these regions. Indeed, data presented here suggest that Pax6 overexpression induces different responses to cortical cells along the rostral-caudal axis, with a gradual effect that is most severe in regions where Pax6 is normally highly expressed (i.e. rostrally) and least evident at caudal levels, where Pax6 levels are normally lowest. This could also explain findings that Pax6 overexpression affects cortical development in PAX77 mice specifically at late stages of corticogenesis. Sustaining Pax6 at elevated levels during late corticogenesis when Pax6 is normally reduced at both the mRNA and protein level compared to early corticogenesis (Tuoc and Stoykova 2008) appears to have profound effects in the PAX77 developing cortex. Failure to detect significant defects in the PAX77 cortex at early stages could simply reflect the fact that the about 2-fold increase in Pax6 levels is not sufficient to significantly affect the development of early cortical progenitors. Since Pax6 expression is strongly reduced throughout corticogenesis, it would be predicted that the differential Pax6 expression between PAX77 and wild-type cortices would be more enhanced compared to early stages and therefore explain observations here that Pax6 overexpression affects specifically late cortical progenitors. With regard to effects of Pax6 overexpression specifically in rostral and central cortical regions, where Pax6 is normally highly expressed, it is possible that in caudal areas the presence of factors other than Pax6 is both necessary and sufficient for the development of cortical

progenitors. Regionalization is unaffected in the PAX77 cortex and, importantly, the caudal-high to rostral-low cortical gradient of *Emx2* is maintained in the mutant (Manuel et al. 2007). Emx2 promotes cortical progenitor proliferation by favouring symmetric divisions leading to progenitor pool expansion, and also instructs the production of multiple cell lineage (Heins et al. 2001).

3.3.2 Cell-autonomous effect of Pax6 overexpression on late cortical progenitor proliferation

The present study shows that Pax6 overexpression in vivo affects specifically the proliferation of late cortical progenitors. This effect is strongest in rostral and central parts of the cortex, where levels of Pax6 are normally highest. At E15.5, there are significant reductions in the proportions of progenitor cells in S-phase and their densities in M-phase rostrally and centrally; reductions are slightly greater rostrally. In E16.5 chimeras, there are significant reductions in the numbers of mutant cells in rostral and central proliferative layers; again, the reduction is slightly larger rostrally. In addition, the proportion of mutant cortical progenitors in M-phase in the chimeric rostral cortex is lower than normal. Consistent with these findings, superficial cortical layers II-IV, which arise mainly from E15.5 onwards (Gillies and Price 1993), are significantly thinner in rostral and central cortex of postnatal mice overexpressing Pax6. These in vivo findings complement a previous study reporting that overexpression of Pax6 in vitro by viral transduction of dissociated cortical cells at E14.5 results in early cell cycle exit (Heins et al. 2002), since enhanced cell cycle exit of cortical progenitors during mid corticogenesis would lead to reduced progenitor numbers available for superficial layer neuron production at late stages of corticogenesis.

In the E15.5 caudal cortex, where Pax6 levels are lowest, there are no differences in the proportions of progenitor cells in S-phase and their densities in M-phase between PAX77 and wild-type mice. In the caudal cortex of E16.5 chimeras, however, numbers of mutant cells in the proliferative layers are significantly reduced, although the extent of the reduction is smaller than in central and rostral regions. A possible explanation for these regional differences is that the rostral cortex is more advanced

than caudal cortex at each embryonic age (Bayer and Altman 1991) and so the emergence of defects in the caudal proliferative layers is delayed.

Defects emerging earliest in the rostral proliferative zone can explain why the under-representation of mutant cell numbers is restricted to specifically the rostral intermediate zone of E16.5 chimeras (Fig. 4D). These defects have not translated into reductions in mutant cell numbers in the cortical plate by E16.5 (although there is a hint that a defect might be emerging in rostral cortical plate: Fig. 4E). They are, however, translated into defects of superficial layer thickness by P7, although significant reductions were only observed rostrally and centrally. Since P7 is after the time that migration of postmitotic neurons into the cortex is complete both rostrally and caudally, the most likely explanation for the lack of significant thinning in the caudal PAX77 cortex is that proliferation is affected less severely in this region, where Pax6 is normally expressed at its lowest levels. Overall, these findings indicate that levels of Pax6 within cortical progenitors become important in the regulation of their proliferation and hence the production of cortical layers.

Cell-autonomous proliferation defects were indicated by the under-representation of mitotic Pax6-overexpressing progenitors in chimeric embryos. Notably, PAX77 cells intermixed normally with wild-type cells in mutant chimeric cortices, unlike abnormalities reported in eye and nasal tissues of PAX77 chimeric mice with regard to reduced mixing of the two genetically distinct cell populations (Chanas et al. 2009). These tissue-specific differences could imply that increased levels of Pax6 influence cell adhesion molecules in a context-dependent manner. The effect of Pax6 overexpression on cell segregation reported by Chanas et al. (2009) differs from that seen in *Pax6*$^{-/-}$ ↔ wild-type chimeras where *Pax6*$^{-/-}$ cells are unable to contribute to the formation of the lens epithelium of the developing eye and move to the periphery instead (Collinson et al. 2001). Although under-represented, *Pax6*$^{-/-}$ cells have the capacity to contribute to the *Pax6*$^{-/-}$ ↔ wild-type chimeric cortex; however, mutant cells are excluded from wild-type cells as revealed by the formation of *Pax6*$^{-/-}$ cell clusters in mutant chimeras (Talamillo et al. 2003; Quinn et al. 2007). Together, these studies have suggested that Pax6 function is critically required to regulate cell surface properties and thus enable cell-cell communication, and have been

complemented nicely by demonstration that *Pax6*$^{-/-}$ cortical cells segregate from surrounding wild-type cells in vitro (Stoykova et al. 1997). A link between Pax6 and cell-adhesion molecules has been further supported by in vitro work showing that Pax6 activates L1 in neural tissues (Meech et al. 1999).

CHAPTER 4

The Generation of Superficial Cortical Layers Is Regulated by Levels of the Transcription Factor Pax6

*Published as Petrina A. Georgala, Martine Manuel and David J. Price. (2010). *Cereb Cortex.* doi: 10.1093/cercor/bhq061 [Epub ahead of print].

4.1 Introduction

The mammalian cerebral cortex is organised radially into six layers, each composed of neurons with characteristic morphologies, patterns of connectivity and gene expression. Lamina formation in the developing cortex requires precise generation and migration of cortical neurons. Progenitors in the ventricular zone (VZ) and subventricular zone (SVZ) of the mouse dorsal telencephalon undergo 11 cell cycles over a 6-day period to generate neurons destined for the cortical plate (CP) (Takahashi et al. 1995a). The cell cycle length of VZ progenitors increases with time as cortical neurogenesis proceeds, whereas it remains unchanged in SVZ progenitor cells (Takahashi et al. 1995b). After cell cycle withdrawal, newborn neurons migrate to the CP successively such that layers II-VI are formed in a deep-first/superficial-last sequence (Angevine and Sidman 1961; Rakic 1974). The final laminar position and subtype of cortical projection neurons is highly dependent on the time progenitors undergo final mitosis and exit the cell cycle (McConnell and Kaznowski 1991; Takahashi et al. 1999).

Throughout corticogenesis, progenitor cell divisions generate cells that must decide whether to re-enter the cell cycle or exit the cell cycle and differentiate into neurons with defined laminar fates. A number of transcription factors and cell cycle regulators have been implicated as intrinsic regulators of the decision to proliferate or differentiate. Increasing or decreasing the levels of these proteins disrupts the balance between the numbers of progenitor cells and differentiated cells and can lead to changes in the surface area and thickness of specific layers of the mature cortex (Caviness and Takahashi 1995; Rakic 1995; Kornack and Rakic 1998; Chenn and Walsh 2002, 2003; Caviness et al. 2003).

Previous studies have indicated that Pax6 is cell-autonomously required to control the balance between cell-cycle exit (Q exit) and re-entry of APs, and its loss of function results in an abnormal increase of Q cells from the onset of corticogenesis (Quinn et al. 2007). These early defects in *Pax6*$^{-/-}$ embryos result in premature depletion of the progenitor pool and contribute to the formation of an abnormally thin mutant cortex that specifically lacks expression of superficial layer markers (Schmahl et al. 1993; Caric et al. 1997; Tarabykin et al. 2001; Schuurmans et al.

2004). Although Pax6 influences the expression of various cyclins and Cdks (Sansom et al. 2009) recent studies failed to show differences in cell-cycle times of *Pax6*$^{-/-}$ cortical progenitors during early corticogenesis (Quinn et al. 2007). With regard to late corticogenesis, results from the Price group have suggested that *Pax6* deletion lengthens the cell cycle of late cortical progenitors (Estivill-Torrus et al. 2002). Interestingly, Pax6 positively regulates genes that promote either proliferative or differentiating divisions and therefore influences the balance between self-renewal and neurogenesis in a rather complicated, dosage-dependent manner (Sansom et al. 2009).

In chapter 3 it was reported that Pax6 overexpression acts cell-autonomously to impair the production of late-born cortical cells in rostral regions, where Pax6 is normally highly expressed. Here, the underlying mechanisms of these defects are being investigated by examining cell cycle kinetics, cell cycle exit, neuronal differentiation and radial migration in PAX77 mice. Cell-cycle length and cell cycle exit were increased at late stages of corticogenesis in APs residing in rostral cortical areas of PAX77 mice. Radial migration of late-born neurons as well as laminar fate specification was unaffected in the PAX77 cortex. Taken together, these data suggest that correct levels of Pax6 are critical primarily for cell cycle regulation and control of the proportion of cells that re-enter the cell cycle instead of leaving it to differentiate.

4.2 Results

4.2.1 Pax6 overexpression affects cortical cell production by regulating cell cycle length in late corticogenesis

To investigate the cause of the proliferation defects detected in the PAX77 cortex, cell cycle parameters in the VZ of PAX77 and wild-type cortex were analyzed by using the method illustrated in Fig. 1A-C (Martynoga et al. 2005; Quinn et al. 2007; see Methods). Since Pax6 is expressed in a gradient throughout the cortex, the analysis was performed at different levels across the rostral-caudal and medial-lateral axes (Fig. 1C). To calculate cell cycle lengths, proportions of proliferating cells (P_{cells}) in the VZ needed to be estimated. Since it has been shown previously that all VZ cells proliferate at E12.5 (Caviness et al. 1995; Estivill-Torrus et al. 2002; Martynoga et al. 2005), P_{cells} was estimated by counting all VZ cells at E12.5. To determine the proportion of P_{cells} at E15.5, PCNA immunohistochemistry was performed in PAX77 and wild-type cortex and the proportions of PCNA-positive cells were calculated at rostral, central and caudal levels of the cortex (Fig. 2): values were around 90% in all cases.

In E12.5 wild-type embryos, there was a tendency for cell cycle and S-phase to lengthen slightly (by about 2 h and 1.5 h respectively) from rostral to caudal cortex (Fig. 1D, E). These rostral-to-caudal trends were less obvious in E12.5 PAX77 embryos; in mutant rostral cortex, the cell cycle and S phase were about 1 h longer than in wild-types whereas in mutant caudal cortex they were similar to wild-type values (Fig. 1D, E). None of the differences at E12.5 were statistically significant. At E15.5, however, there were similar trends and differences were significant. In wild-type embryos, average cell cycle times lengthened progressively by about 7 h from rostral to caudal cortex (Fig. 1F) and these regional differences were significant (ANOVA $P < 0.01$, $n = 3$). In PAX77 embryos, neither cell cycle nor S-phase length varied regionally (Fig. 1F, G); ANOVA failed to show significant differences. Average cell cycle time was significantly longer in PAX77 cortex than in wild-type cortex in rostral regions (Student's *t*-test $P < 0.05$, $n = 3$), but not in central and caudal regions (Fig. 1F).

FIGURE 1

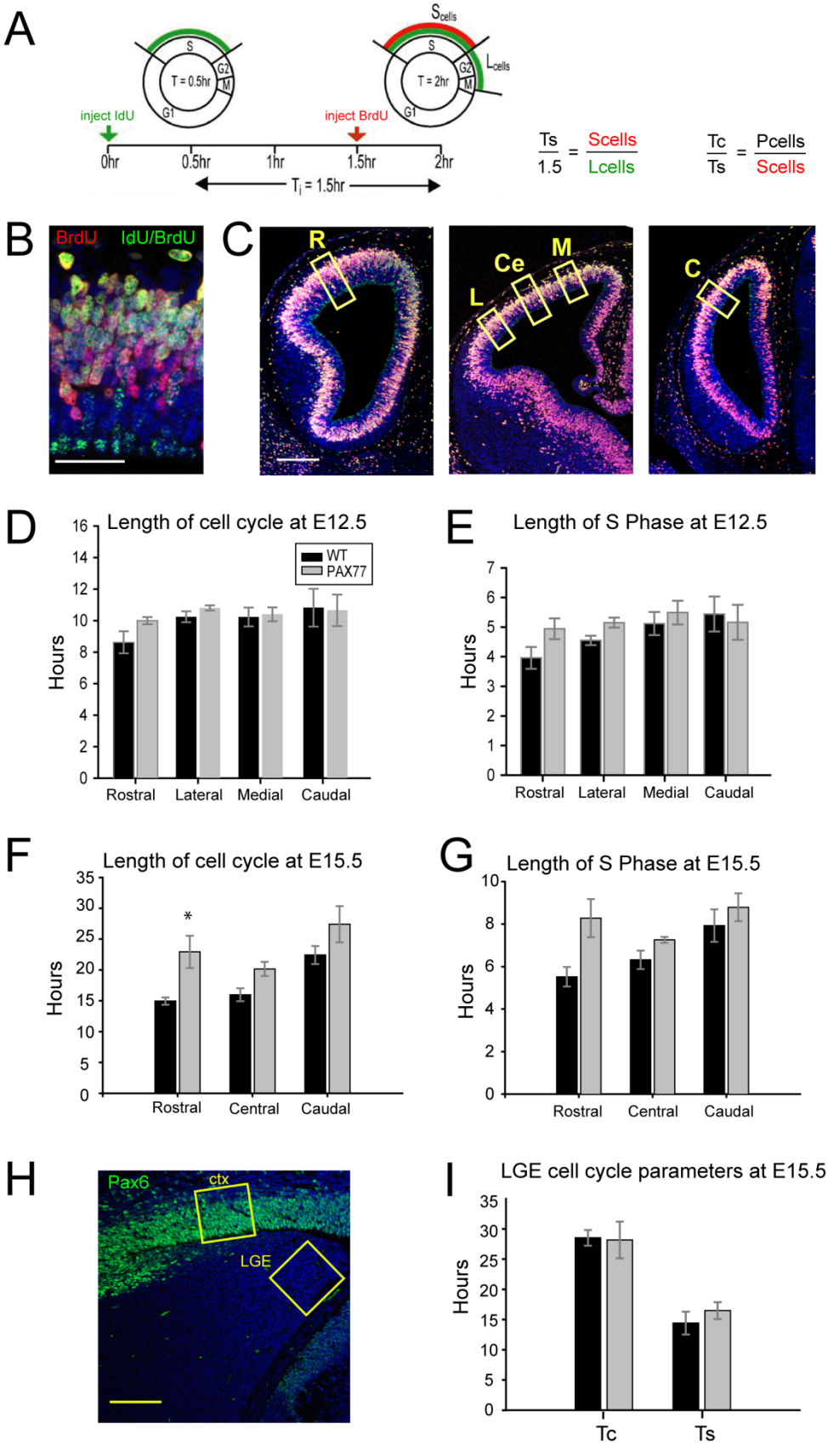
A
S
G2
M
G1
T = 0.5hr
T = 2hr
Scells
Lcells
inject IdU
inject BrdU
0hr
0.5hr
1hr
1.5hr
2hr
Ti = 1.5hr
Ts / 1.5 = Scells / Lcells
Tc / Ts = Pcells / Scells
B
BrdU
IdU/BrdU
C
R
Ce
M
L
C
D
Length of cell cycle at E12.5
WT
PAX77
Hours
Rostral
Lateral
Medial
Caudal
E
Length of S Phase at E12.5
Hours
Rostral
Lateral
Medial
Caudal
F
Length of cell cycle at E15.5
*
Hours
Rostral
Central
Caudal
G
Length of S Phase at E15.5
Hours
Rostral
Central
Caudal
H
Pax6
ctx
LGE
I
LGE cell cycle parameters at E15.5
Hours
Tc
Ts

Figure 1. Pax6 overexpression increases cell cycle length of apical progenitors at late stages of corticogenesis. (A) Schematic diagram of the timing of administration of thymidine analogues in order to label S-phase cells. The ratios shown were used to calculate cell cycle and S-phase length in wild-type and PAX77 embryos (T_s = length of S-phase; T_c = length of cell cycle; P_{cells} = all proliferating cells). (B) Coronal section through the cortex of an E12.5 wild-type embryo immunostained with antibodies specific for both BrdU and IdU (green) and BrdU alone (red) to identify S_{cells} (red and green double-labelled cells) and L_{cells} (green-only cells). (C) Coronal sections at rostral, central and caudal levels of the cortex of an E12.5 wild-type embryo immunostained with IdU/BrdU. Cell counts were made in 100 μm-wide sampling boxes in the ventricular zone of the cerebral wall. At E12.5, cells were counted in the rostral (R) cortex, lateral (L) and medial (M) regions at the central level, and in the caudal (C) cortex. At E15.5, cell counts were made at the rostral (R), central (Ce) and caudal (C) levels of the cortex. (D, E) Quantitative analysis showing (D) length of cell cycle (T_c) and (E) length of S-phase (T_s) in E12.5 wild-type and PAX77 embryos. At all the cortical levels examined, T_c and T_s were not significantly altered in the PAX77 cortex compared to wild-type. (F, G) Histograms showing (F) T_c and (G) T_s in the E15.5 wild-type and PAX77 cortex. Cell cycle was significantly longer in the rostral PAX77 cortex compared to wild-type. (H) Example of Pax6 immunofluorescence at the central level of an E15.5 PAX77 brain. Sampling boxes (100 μm-wide) indicate the regions where cell cycle kinetics were analysed at E15.5. T_c and T_s were estimated in the Pax6-positive cortex (ctx) and a Pax6-negative region of the lateral ganglionic eminence (LGE). (I) In Pax6-negative LGE, cell cycle times were not different between wild-type and PAX77 cortex at E15.5. All sections shown were counterstained with TO-PRO-3. Scale bars: 50 μm in B, 200 μm in C, 100 μm in H. Data represent the mean ± s.e.m. values.

FIGURE 2

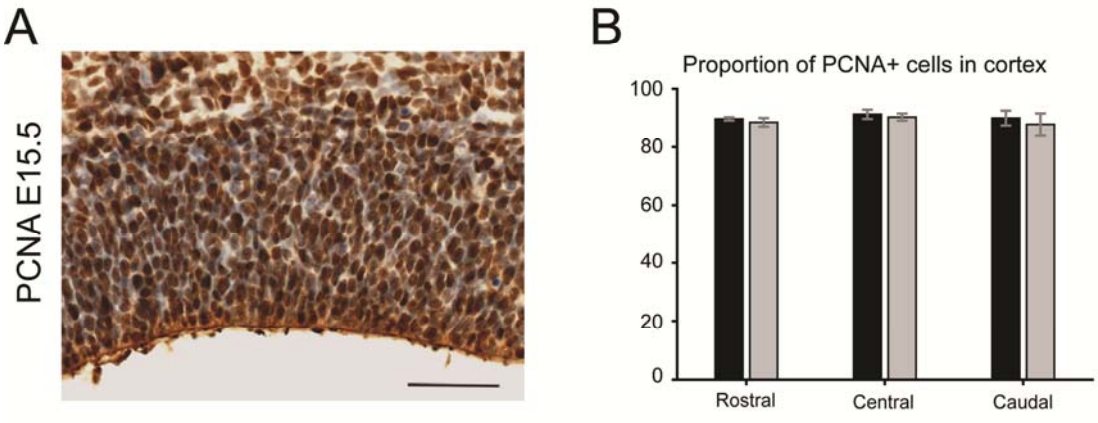

Figure 2. Proportions of proliferating cells in the cortical VZ of wild-type mice and PAX77 at E15.5. (A) Example of PCNA immunohistochemistry on a coronal section through the PAX77 cortex. (B) The proportions of PCNA-positive cells in the VZ of rostral, central and caudal cortical regions were not different between PAX77 and wild-types at E15.5. Scale bar: 100 μm.

Cell-cycle parameters were also compared between E15.5 wild-type and PAX77 embryos in a region of the developing telencephalon that does not express Pax6 at this age, the lateral ganglionic eminence (LGE) (Fig. 1H), to verify that the abnormal cell cycle parameters are not general effects on forebrain development. Analyses failed to show differences in cell cycle parameters in this region between PAX77 and wild-type embryos (Fig. 1I). These findings suggest that at late stages of corticogenesis the cell cycle parameters of apical progenitors in rostral cortical regions, where expression levels of Pax6 are normally highest, are modulated by the level of Pax6.

4.2.2 Pax6 overexpression causes increased cell cycle exit at late stages of corticogenesis

To determine whether Pax6 overexpression causes a shift in the proportion of dividing cells that leave the cell cycle instead of remaining as progenitors, cell cycle exit was examined at E15.5 by determining the leaving (Q) fraction. This was accomplished by using an IdU/BrdU labelling protocol (Fig. 3A; see Methods). The approach depends on counts of numbers of IdU-positive cells: examples of these cells are shown with green arrows in Fig. 3B. The Q fraction was significantly increased in the PAX77 cortex at rostral (Student's *t*-test $P < 0.01$; $n = 5$) and central levels (Student's *t*-test $P < 0.05$; $n = 5$), but was not altered at caudal levels compared to wild-types (Fig. 3C). These results indicate that at late stages of corticogenesis increased levels of Pax6 lead to increased proportions of proliferating cells exiting the cell cycle.

Increased rate of cell cycle exit before E16.5 would be expected to produce a corresponding increase in the proportion of neurons in the mutant cortex by E16.5. To investigate this, the early neuronal marker β-III-tubulin was employed and the proportion of positive postmitotic neurons was assessed by flow cytometry. Samples of mutant and control cortices covering rostral and central levels were dissociated at E16.5 and cells were stained with β-III-tubulin before analysis (Fig. 4A-C). A significant increase in the proportion of β-III-tubulin -positive neurons was detected

FIGURE 3

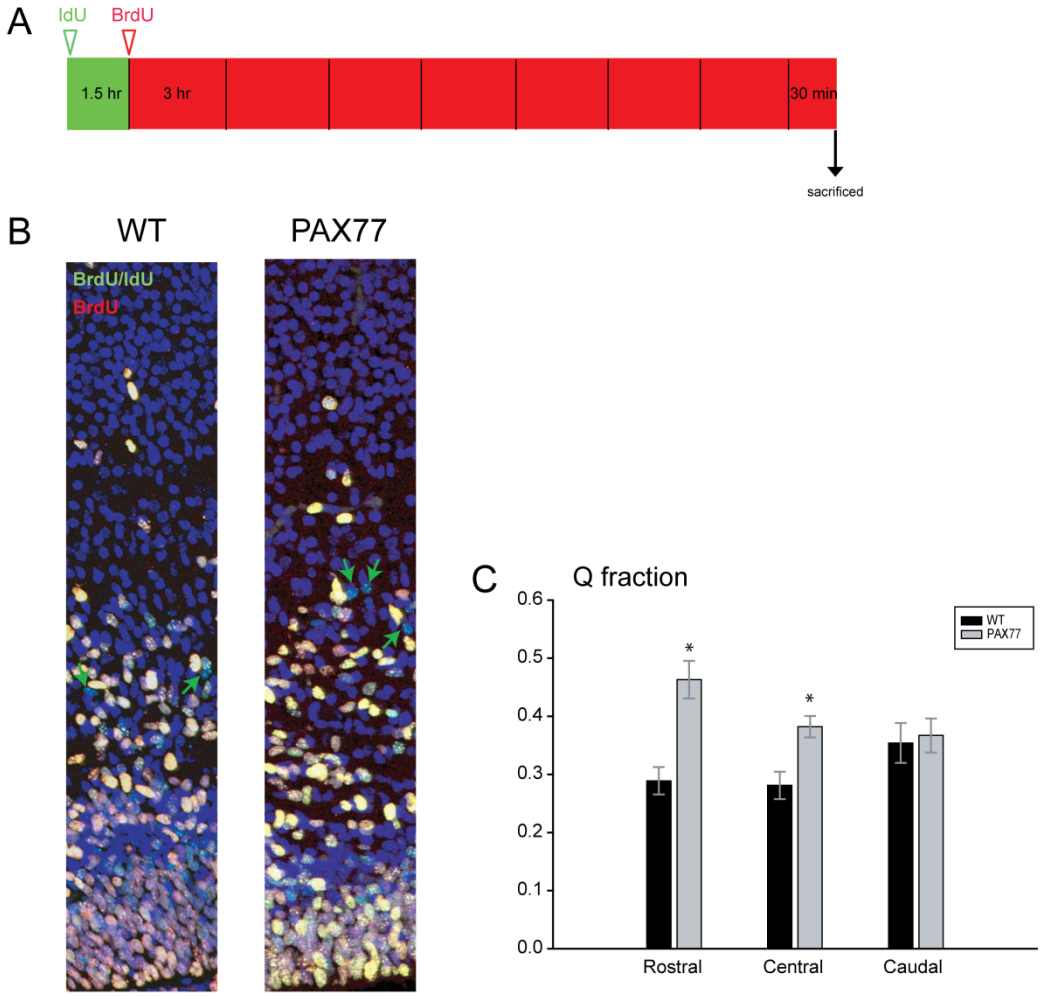

Figure 3. Pax6 overexpression increases the fraction of late cortical progenitors leaving the cell cycle. (A) Diagrammatic representation of the timing of administration of thymidine analogues in order to label S-phase cells and calculate the leaving (Q) fraction. (B) 100 µm-wide sections at a rostral cortical level immunostained with IdU and BrdU. The IdU-only cells (green arrows show examples), representing the Q cells, were counted in the cerebral wall of wild-type and PAX77 embryos. (C) The Q fraction was significantly (*) increased in the rostral and central PAX77 cortex compared to wild-type (data represent the mean ± s.e.m. values). Nuclei were counterstained with TO-PRO-3.

FIGURE 4

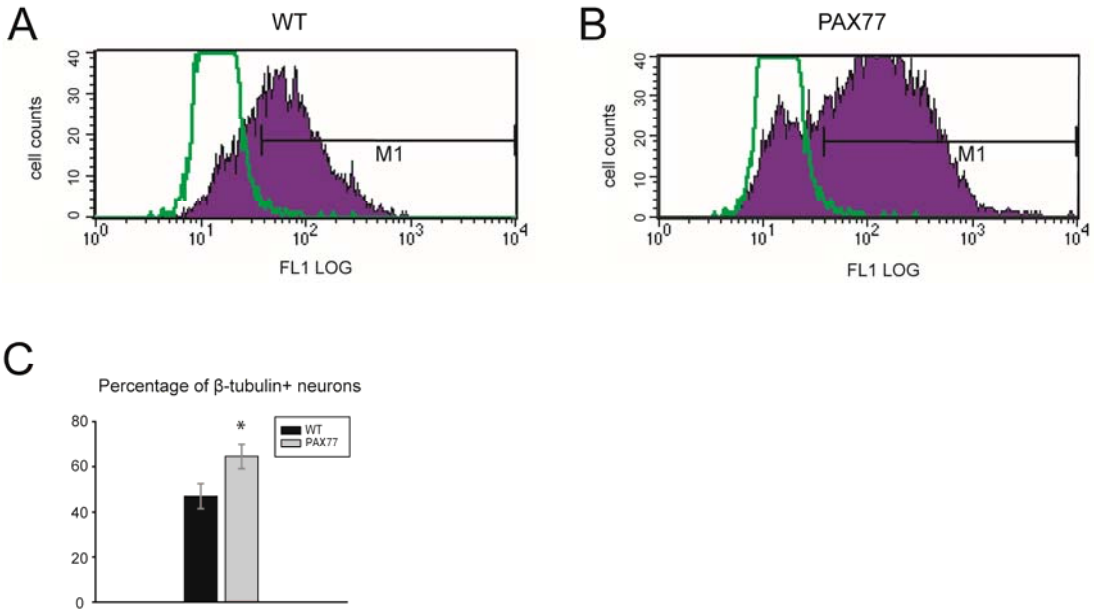

Figure 4. Increased proportion of neurons in the PAX77 cortex at E16.5. (A, B) Expression of β-III-tubulin quantified with flow cytometry in dissociated (A) wild-type and (B) PAX77 E16.5 cortical cells. Gating (M1) was established by a control reaction in cells stained with PI and secondary antibody only (no primary antibody). Grey line in histograms represents the plot obtained from control reaction; cells whose fluorescence (FL1LOG) fell within M1 considered to be positive for β-III-tubulin. Plots shown are from a single representative experiment for each genotype. (C) Histogram showing the mean proportions of cells (± s.e.m.s) classified as β-III-tubulin-positive in wild-type and PAX77 cortex. The percentage of β-III-tubulin-expressing cells was significantly higher in PAX77 cortex than in wild-type cortex.

in the PAX77 cortex compared to the wild-type cortex (Fig. 4D; Student's *t*-test $P < 0.05$; $n = 8$).

These findings on cell cycle exit, together with those on cell cycle times, provide an explanation for the reduced production of cortical cells in PAX77 embryos reported in the previous chapter: at E15.5, Pax6 overexpression slows the cell cycle and increases the proportions of cells exiting the cell cycle, thereby reducing the size of the proliferative pool.

4.2.3 Pax6 overexpression reduces the radial extent of the superficial layers

To explore laminar formation in PAX77 mice, I analysed the expression of cell type-specific markers known to be required for the specification of distinct subsets of neurons. Double immunohistochemistry for Satb2, which is expressed largely by superficial layer neurons but also by some deep layer neurons and is required for the specification of callosal neurons (Alcamo et al. 2008; Britanova et al. 2008), and Tbr1, known to be involved in the specification of deep layer neurons (Hevner et al. 2001), was performed in rostral PAX77 and wild-type cortices at E16.5 (Fig. 5A, B). As expected, Satb2-positive neurons were detected in both superficial and deep positions of the CP, while Tbr1 was expressed at high levels in the subplate and layer 6 neurons (Fig. 5A, B). For our quantitative analysis, the CP was divided into 2 domains: a superficial Satb2-positive/Tbr1-negative domain, and an inferior Satb2-positive/Tbr1-positive domain. The proportion of Satb2-positive cells was determined in the superficial CP; the proportions of Tbr1-positive and of Satb2-positive neurons were calculated in the lower CP (proportions are the numbers of positive cells divided by the total number of all cells in the counting area). Interestingly, in the PAX77 cortex there was a significant increase in the proportion of Tbr1-positive cells in the lower CP (Student's *t*-test $P < 0.05$; $n = 3$) accompanied by a significant decrease in the proportion of Satb2-positive cells (Student's *t*-test $P < 0.05$; $n = 3$) (Fig. 5D). The proportion of Satb2-positive neurons in the superficial CP was not significantly changed in the PAX77 cortex (Fig. 5C).

FIGURE 5

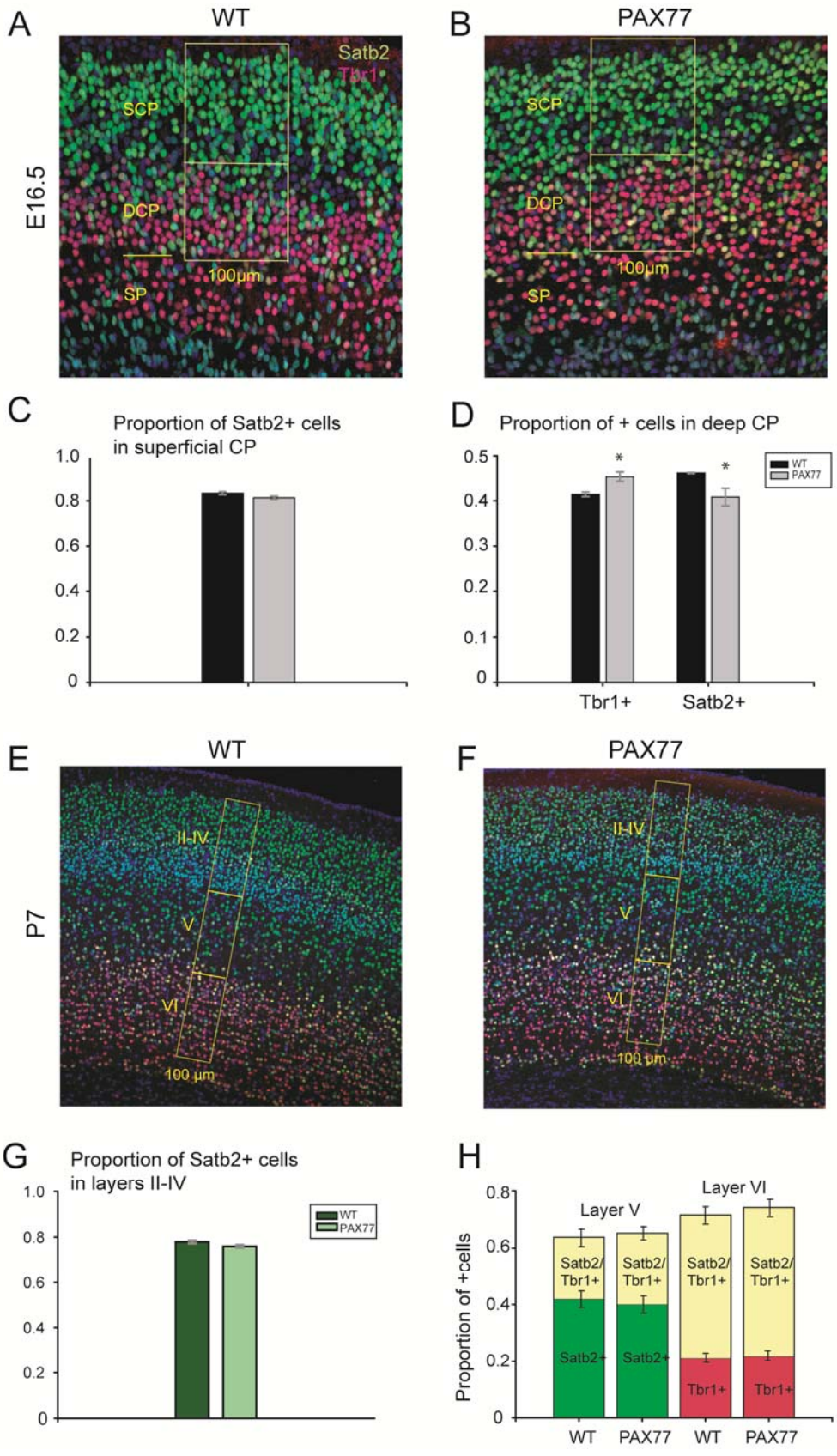
A
WT
Satb2
Tbr1
SCP
DCP
SP
100µm
E16.5
B
PAX77
SCP
DCP
SP
100µm
C
Proportion of Satb2+ cells
in superficial CP
1.0
0.8
0.6
0.4
0.2
0
D
Proportion of + cells in deep CP
0.5
0.4
0.3
0.2
0.1
0
*
*
WT
PAX77
Tbr1+
Satb2+
E
WT
II-IV
V
VI
100 µm
P7
F
PAX77
II-IV
V
VI
100 µm
G
Proportion of Satb2+ cells
in layers II-IV
1.0
0.8
0.6
0.4
0.2
0
WT
PAX77
H
Layer V
Layer VI
Proportion of +cells
0.8
0.6
0.4
0.2
0
Satb2/
Tbr1+
Satb2+
Tbr1+
WT
PAX77
WT
PAX77

Figure 5. Neurons in the PAX77 cortex are correctly specified according to their laminar position. (A, B) Immunohistochemistry for Satb2 (green) and Tbr1 (red) on coronal sections of E16.5 wild-type and PAX77 cortex at a rostral level. Cells were counted in the 100-µm-wide sampling box placed in the cortical plate (CP) of wild-type and PAX77 cortex. For quantitative analysis, the CP was divided into a superficial Satb2-positive/Tbr1-negative domain and a lower Satb2/Tbr1-positive domain by drawing a line at the border delineated by the band of Tbr1-positive cells in the upper part of the deep CP. (C, D) Quantification of the proportions of Satb2-positive neurons in the superficial CP and Satb2-positive and Tbr1-positive neurons in the deep CP of the E16.5 wild-type and PAX77 cortex. The proportion of Satb2-positive neurons in the superficial CP was not significantly altered in PAX77 embryos compared to wild-type. The proportion of Tbr1-positive neurons was significantly increased and the proportion of Satb2-positive neurons was significantly decreased in the deep CP of PAX77 mice compared to wild-types. (E, F) Examples of Satb2/Tbr1 labelling in coronal sections through the rostral cortex of P7 wild-type and PAX77 mice: cells were counted in the 100-µm-wide sampling boxes. Sampling boxes are the same size in E and F; the gap in the superficial domain of the sampling box in F highlights the reduced thickness of the PAX77 cortex compared to wild-type. In both wild-type and PAX77 cortex, Satb2-positive neurons were primarily detected in layers II-IV and also layer V, while Tbr1-positive neurons were mainly located in layer VI but were also detected in layer V where they appear as Tbr1/Satb2 double-labelled. (G) The proportion of Satb2-positive neurons was not significantly altered in the superficial layers (II-IV) of PAX77 cortex compared to wild-type. (H) Histograms show the proportions of Satb2-positive and Satb2-positive/Tbr1-positive neurons in layer V, as well as the proportions of Tbr1-positive and Tbr1-positive/Satb2-positive neurons in layer VI, of P7 wild-type and PAX77 cortex. No difference in the radial distribution of these neuronal populations in the lower cortical layers V and VI was detected between PAX77 and wild-type mice. DCP, deep cortical plate; SCP, superficial cortical plate; SP, subplate.

The altered proportions of Tbr1-positive cells and Satb2-positive cells in the deep CP of E16.5 PAX77 mice suggested that an alteration in the specification of deep layer neurons might be developing and, to test this, Tbr1/Satb2 double immunohistochemistry was performed at P7 (Fig. 5E, F). Coronal sections from PAX77 and wild-type cortex at a rostral level were reacted and Tbr1-positive, Satb2-positive and Tbr1/Satb2 double-labelled neurons were counted according to their laminar position. The proportion of Satb2-positive neurons in the superficial layers II-IV was not significantly altered in the PAX77 cortex (Fig. 5G). Neither the proportions of Satb2-positive and Satb2-positive/Tbr1-positive neurons in layer V, nor the proportions of Tbr1-positive and Tbr1-positive/Satb2-positive neurons in layer VI, were significantly different in the PAX77 cortex compared to wild-type (Fig. 5H). These results indicate that cortical neurons are correctly specified in correct proportions in PAX77 mice and express appropriate markers depending on their laminar position.

It was previously reported that the thickness of superficial layers (II-IV combined) is significantly reduced in the PAX77 compared to wild-type cortex at P7 (Chapter 3). In line with this, I found here that, at P7, the total number of Satb2-positive neurons in the 100μm-wide strips was significantly decreased in the superficial cortical layers of the PAX77 mice (183 ± 6 in wild-type, 153 ± 8 in PAX77; Student's *t*-test $P < 0.05$; $n = 3$), whereas cell numbers in layers V and VI were not significantly different between mutants and wild-types. This result indicates that the defects of cell cycle parameters in PAX77 embryos, which reduce the size of the proliferative pool by E15.5, feed through into reductions in superficial layer cell numbers postnatally.

The most likely explanation for the reduced proportion of Satb2-positive cells in the deep CP of E16.5 PAX77 embryos (Fig. 5D) is a reduction in the size of the population of late-generated Satb2-positive cells. Since superficial layers are only just starting to form at E16.5, many Satb2-positive neurons that will eventually contribute to the superficial layers might still be intermingled with deep layer Tbr1-expressing cells at E16.5. The presence of reduced numbers of Satb2-positive cells in the deep CP at E16.5 would result in a corresponding increase in the proportions of Tbr1-positive deep layer cells, as was seen at E16.5 (Fig. 5D). These would be

transient changes and would disappear postnatally once all Satb2-expressing cells reach their final destinations, leaving both superficial and deep layers with normal *proportions* of Satb2- and Tbr1-expressing cells, although superficial layers would have reduced *absolute numbers* of Satb2-expressing cells (summarized in Fig. 8).

4.2.4 Radial migration and layer-specification of cortical neurons appear normal in postnatal mice overexpressing *Pax6*

To address whether radial migration defects might contribute to the formation of thinner superficial layers in the PAX77 cortex, BrdU-birthdating experiments were performed. Pregnant females were injected with a single dose of BrdU at E15.5 or E17.5, and the laminar distribution of BrdU-positive cells was examined at P7, when neuronal migration is largely completed. Although densely- and lightly-labelled cells (Del Rio and Soriano 1989; Gillies and Price 1993) were counted separately, the radial distributions and numbers of both cell populations were similar in PAX77 and wild-type littermates, and so data from the two sets were combined for presentation here.

Most cells born from E15.5 onward were observed in superficial positions corresponding to cortical layers IV and III (Fig. 6A), while cells born from E17.5 onward occupied an area corresponding to layers III and II (Fig. 6E). The radial distributions of E15.5- or E17.5-labelled cells were very similar in the PAX77 and wild-type P7 cortex (Fig. 6B-D, F-H). These findings indicate that migration defects do not make a significant contribution to cortical abnormalities in PAX77 mice.

To investigate directly whether cortical neurons acquire their correct laminar fate according to their birth-date, BrdU was injected at E12.5 or E15.5 and birth-dated cells were double-labelled with layer-specific markers at P7. BrdU-positive neurons born at E12.5 were double-labelled with Tbr1 (Fig.7A, B); BrdU-positive neurons born at E15.5 were double-labelled with Cux1 (Fig. 7D, E) which normally identifies pyramidal neurons of superficial layers IV-II of the cortex (Nieto et al. 2004). Coronal sections from PAX77 and wild-type cortex at a rostral level were reacted and BrdU/Tbr1 double-labelled neurons were counted in layers VI and V separately

FIGURE 6

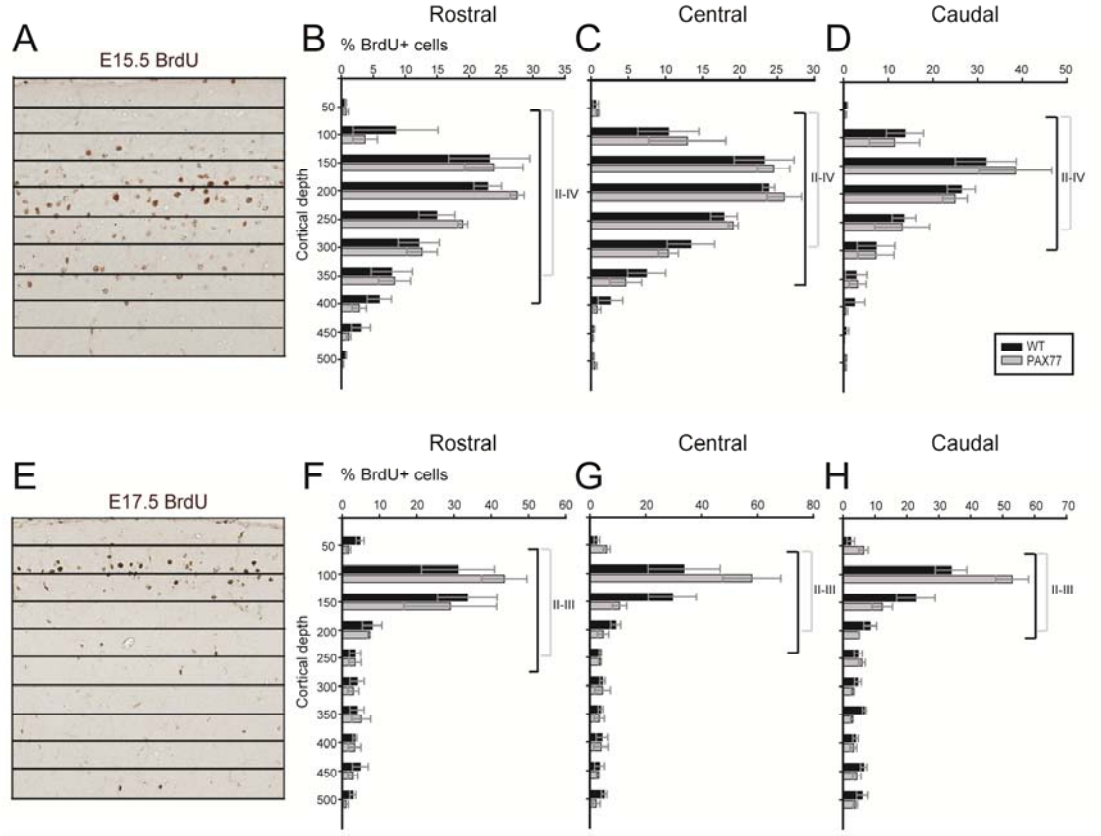

Figure 6. BrdU birthdating reveals that laminar positioning of late-born neurons is unaffected in the PAX77 cortex. (A, E) Coronal sections through the P7 rostral PAX77 cortex labelled with BrdU at the indicated age. BrdU-positive nuclei were quantified in each 50 μm-deep bin. (B-D, F-H) Graphical representations of data from birthdating studies show the mean percentages (± s.e.m.s) of BrdU-positive neurons in each bin at three rostro-caudal levels. Layer thickness is marked on the graphs for all cortical regions analysed (black for wild-type, grey for PAX77). Labelling at E15.5 revealed accumulation of BrdU-positive nuclei in layers II-IV in both wild-type and PAX77 cortices. A BrdU pulse at E17.5 primarily marked the genesis of layer II neurons in both wild-type and PAX77. No differences in the radial distribution of late-born neurons were detected between PAX77 and wild-type cortex.

(Fig. 7A, B). The proportions of BrdU/Tbr1 double-labelled neurons over total BrdU-positive neurons were not significantly altered in either layer VI or layer V of the PAX77 cortex (Fig. 7C), indicating that early-born neurons are correctly specified in the mutant cortex. The proportions of BrdU/Cux1 double-labelled neurons in layers IV-II were also not significantly different in the PAX77 cortex compared to wild-type (Fig. 7F). These results further confirm that Pax6 overexpression does not affect the specification of deep or superficial layer neurons born at early or late stages of corticogenesis, respectively.

FIGURE 7

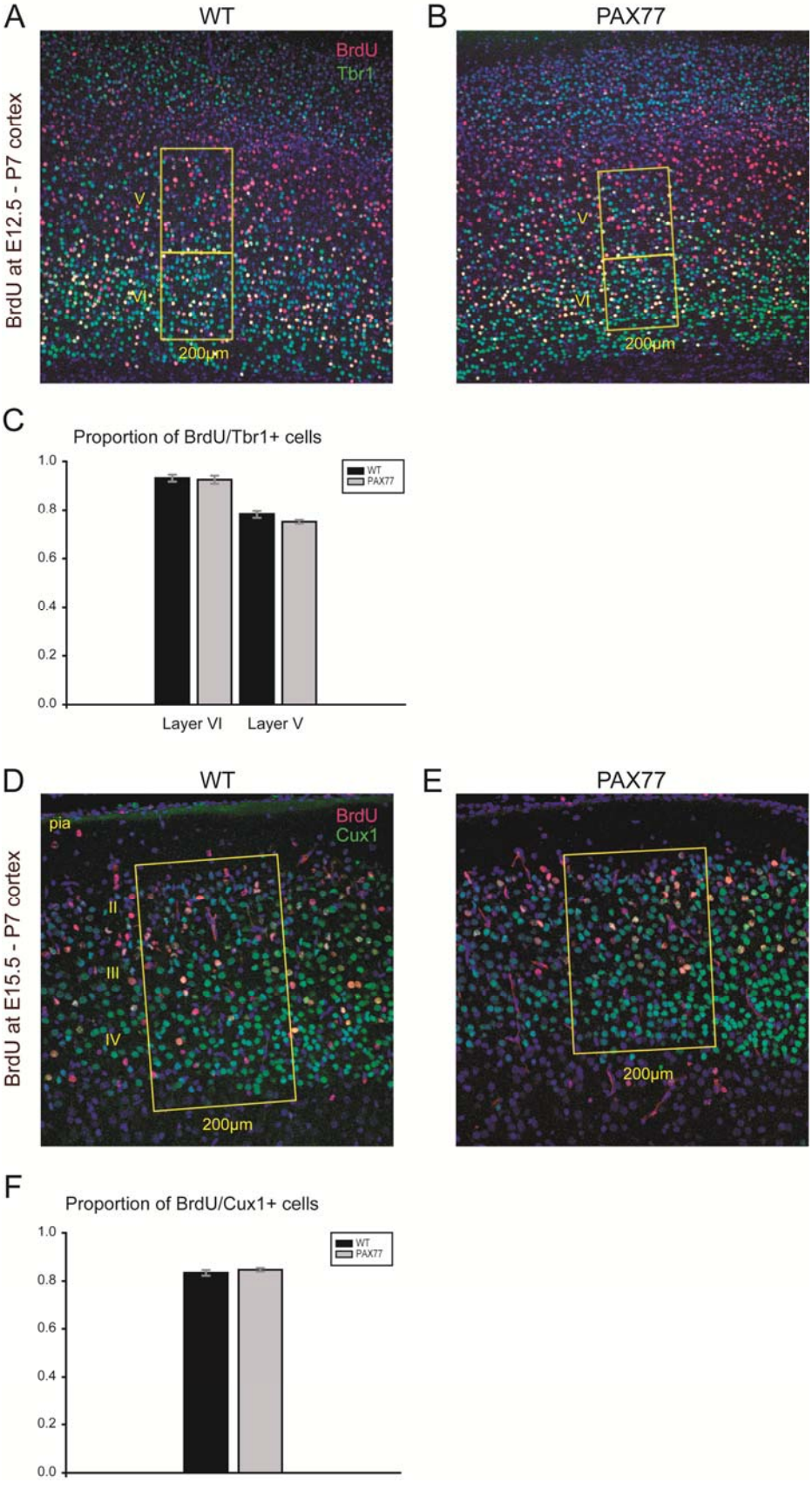
A
WT
B
PAX77
BrdU
Tbr1
BrdU at E12.5 - P7 cortex
V
VI
200µm
C
Proportion of BrdU/Tbr1+ cells
WT
PAX77
1.0
0.8
0.6
0.4
0.2
0.0
Layer VI
Layer V
D
WT
E
PAX77
pia
BrdU
Cux1
BrdU at E15.5 - P7 cortex
II
III
IV
200µm
F
Proportion of BrdU/Cux1+ cells
WT
PAX77
1.0
0.8
0.6
0.4
0.2
0.0

Figure 7. Cortical neurons in the PAX77 cortex are correctly specified according to their birthdate. (A, B) Double immunostaining for BrdU (red) and Tbr1 (green) on coronal sections through the cortex of P7 wild-type and PAX77 mice given BrdU at E12.5. The numbers of heavily-labelled BrdU cells and BrdU(heavily-labelled)/Tbr1 double-labelled cells were counted in 200-μm-wide radial stripes in layers VI and V of wild-type and PAX77 cortices. (C) The proportions of BrdU labelled cells that were Tbr1 double-labelled were not significantly altered in either layer VI or V of the PAX77 cortex compared to wild-type. (D, E) High-power views of the superficial layers of the rostral cortex double-immunostained for Cux1 (green), a marker of superficial layer (IV-II) neurons, and BrdU (red) in P7 wild-type and PAX77 mice injected with BrdU at E15.5. The numbers of BrdU-positive and BrdU/Cux1 double-labelled cells were counted in 200-μm-wide radial stripes spanning through the superficial layers of wild-type and PAX77 cortices. (F) The proportions of BrdU/Cux1 double-labelled neurons were not significantly different in the superficial layers of the PAX77 cortex compared to wild-type.

FIGURE 8

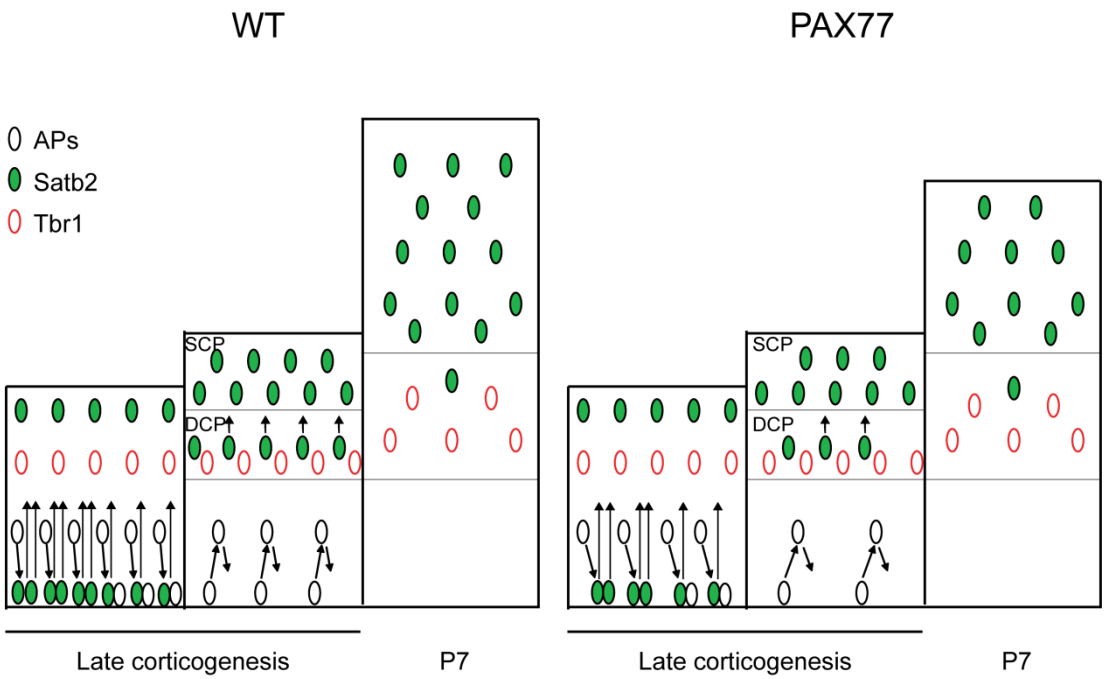

Figure 8. Model of cortical lamination in mice overexpressing Pax6. At late stages of corticogenesis, progenitors in the proliferative zone generate superficial layer fate carried by Satb2-positive cells. These cells migrate through the deep CP, where earlier-born Tbr1-positive cells reside, to reach their final superficial laminar positions. In the PAX77 cortex, the number of deep layer Tbr1-positive cells is normal but, at late stages of corticogenesis, the progenitor pool is depleted due to lengthened cell cycle times and increased fractions of cells exiting the cell cycle. There is, therefore, a reduced production of late-born Satb2-positive cells and less Satb2-positive cells transit though the deep layers to the superficial layers of the CP in PAX77 mice. Postnatally, superficial layers are thinned in the PAX77 cortex compared to wild-type due to a reduction in the number of Satb2-positive cells. DCP, deep cortical plate; SCP, superficial cortical plate.

4.3 Discussion

In chapter 3 it was shown that, at late stages of corticogenesis, overexpression of Pax6 acts cell autonomously to reduce the production of cortical cells, resulting in the formation of thinner superficial layers in the postnatal cortex. In this study, the possible mechanisms by which Pax6 controls the production of late-born neurons and superficial layers of the cortex were examined. Pax6 overexpression was found to lengthen the cell cycle of cortical VZ progenitors and promote cell cycle exit at late stages of corticogenesis. Both of these abnormalities would reduce the size of the progenitor pool as corticogenesis proceeds, and therefore reduce cortical cell production. Consistent with this, it is reported here that Pax6 overexpression resulted in reduced numbers of superficial layer neurons, without affecting the laminar specification of this depleted population (summarized in Fig. 8). These findings indicate that correct levels of Pax6 are required by cortical progenitors at late stages of corticogenesis to maintain their cell cycle times and moderate their exit from the cell cycle, thereby regulating the size of the progenitor pool.

4.3.1 Disregulation of Pax6 levels influences cortical progenitor proliferation

During cortical neurogenesis, cell divisions in the cortical VZ generate additional progenitors as well as postmitotic neurons. The total number of mitotic cycles progenitors undergo is limited throughout corticogenesis and is determined in part by cell cycle length and in part by the fraction of cells leaving the cell cycle to differentiate. The balance between these two processes is a critical determinant of the final neuronal number and therefore of the size of the cortex (Takahashi et al. 1994).

In apical progenitors, which normally express high levels of Pax6 (Gotz et al. 1998; Englund et al. 2005), both cell cycle length and proportions of cells exiting the cell cycle increase as corticogenesis advances (Takahashi et al. 1994; Estivill-Torrus et al. 2002; present study). Here, I also observed regional differences in the lengths of the cell cycles, which lengthened progressively from rostral to caudal cortex at E15.5, indicating that cell cycle parameters are regulated both temporally and spatially during corticogenesis in wild-type embryos. Pax6 is also differentially

regulated spatially and temporally: its levels are higher in rostral than in caudal apical progenitors and its levels decline as corticogenesis progresses (Stoykova and Gruss 1994; Manuel et al. 2007). A rostral (high) to caudal (low) gradient of Pax6 expression is maintained in PAX77 embryos, with levels of expression increased proportionately along the gradient (i.e. with the largest absolute increases in Pax6 levels occurring rostrally: Manuel et al. 2007). Results here show that the consequence of this increase is to abolish the rostral-caudal difference in cell cycle lengths by increasing lengths rostrally. It appears, therefore, that the relationship between Pax6 expression level and cell cycle length across the cortex is not linear. It is possible that for normal cell cycling, Pax6 levels must be within a band and if its upper limit is exceeded cell cycles lengthen.

Loss of Pax6 also leads to a reduced number of apically dividing cortical progenitors (Estivill-Torrus et al. 2002; Tamai et al. 2007). Detailed analyses of cell-cycle kinetics have suggested that, although absence of Pax6 does not lengthen cell cycle times at early stages of corticogenesis, it does lengthen them at E15.5 (Estivill-Torrus et al. 2002; Quinn et al. 2007). Furthermore, recent analyses showed that *Pax6*$^{-/-}$ mutant cells exit the cell cycle in abnormally large numbers, suggesting a primary cell-autonomous role for Pax6 in control of cell cycle exit (Quinn et al. 2007). Both gain and loss of Pax6 have similar effects on cortical progenitors, indicating that not just the presence of Pax6 but also maintenance of correct Pax6 levels is critical for spatially and temporally appropriate cell cycle parameters. This finding is reminiscent of the effects of both lowering and raising Pax6 levels on eye development, both of which generate small eyes (Schedl et al. 1996).

Results here provide an explanation for previous observations that the number of late apical progenitors in S-phase and M-phase is reduced in the PAX77 cortex (Chapter 3) and are in line with in vitro work where forced Pax6 expression, which is likely to cause very large increases in Pax6 levels, inhibits progenitor proliferation (Heins et al. 2002; Hack et al. 2004; Cartier et al. 2006). Recent analyses have suggested that Pax6 has the ability to both promote and inhibit cortical progenitor proliferation by regulating the expression of cell cycle regulators (Sansom et al. 2009). Its cell cycle commitment functions are, however, counterbalanced by its positive regulation of

genes that promote cell cycle exit (Sansom et al. 2009). Taking these findings together with results reported here suggests that when Pax6 is overexpressed its ability to drive progenitors to exit the cell cycle is dominant over its function in cell-cycle commitment.

Lengthening of the cell cycle and increased cell cycle exit during superficial layer formation would be expected to reduce the number of subsequent mitotic divisions and therefore the production of neurons destined for more superficial positions, and, indeed, results presented here confirm this prediction. Reduction in the size of the progenitor pool as a result of disruption of normal levels of Pax6, either up or down, provides an explanation for the underproduction of superficial cortical layer neurons in both *Pax6*$^{-/-}$ mutant and Pax6 overexpressing mice (Tarabykin et al. 2001; Quinn et al. 2007; Manuel et al. 2007; Sansom et al. 2009; Tuoc et al. 2009; present study). Although the final laminar phenotype is far more severe in *Pax6*$^{-/-}$ mice, it is intriguing that both loss- and gain-of-function of Pax6 lead to thinning of superficial layers. An attractive hypothesis is that Pax6 regulates a dynamic transcriptional network that influences both stem cell maintainance and neurogenesis in a level dependent manner. Recent identification of Pax6-bound genes and altered gene expression in the cortex of *Pax6*$^{-/-}$ mice and transgenic mice overexpressing Pax6 support such a model (Sansom et al. 2009). These studies have shown that increasing Pax6 levels in the developing cortex drives progenitors toward cell cycle exit and precocious neurogenesis through the induction of proneural gene expression and basal progenitor genesis, given that transcription factors such as Ngn2, Neurod1 and Tbr2 show positive dependency on Pax6 expression. Ineterestingly, Pax6 also appears to positively regulate cell cycle regulators, such as Cdks, as well as Notch effectors, be it direct or indirect (Sansom et al. 2009). The current model suggests that cortical development is sensitive to disruption of Pax6 levels either up or down. In a wild-type cortex, Pax6 has a potent neurogenic activity that is normally counterbalanced by its role in maintaining stem cell self-renewal. Loss of Pax6 leads premature cell cycle exit and precocious neurogenesis due to reduced cell cycle commitment of mutant progenitors. This highlights the fact that the final laminar phenotype in *Pax6*$^{-/-}$ mutant and Pax6 overexpressing mice is achieved through distinct biological mechanisms.

4.3.2 Roles of Pax6 in neurogenesis and laminar specification of cortical neurons

Cell cycle exit and neuronal differentiation are tightly regulated during cortical development. Loss of Pax6 function increases the proportions of neurons in the developing cortex at early stages of corticogenesis (Estivill-Torrus et al. 2002; Quinn et al. 2007), as well as in other parts of the CNS such as the eye and the spinal cord (Philips et al. 2005; Bel-Vialar et al. 2007). The increased proportions of neurons in the *Pax6*$^{-/-}$ mutant cortex or retina during early development seem best explained by an increased cell cycle exit (Philips et al. 2005; Quinn et al. 2007; Tuoc et al. 2009). Findings here, that increased levels of Pax6 in vivo enhance cell cycle exit and lead to increased proportions of neurons at late stages of corticogenesis, are in accord with previous in vitro studies showing that Pax6 overexpression promotes neuronal differentiation under culture conditions (Heins et al. 2002; Hack et al. 2004; Haubst et al. 2004). Recent analyses have also suggested that increasing Pax6 levels in vivo results in advanced neurogenesis in the developing cortex (Sansom et al. 2009)

Cell cycle exit is also closely associated with laminar positioning and laminar fate of cortical neurons. Laminar fates of cortical neurons are determined when they are early postmitotic cortical precursors and become progressively restricted as development advances (McConnell and Kaznowski 1991; Frantz and McConnell 1996; Desai and McConnell 2000; Britanova et al. 2008). Some previous studies have suggested that Pax6 might be involved in regulating the laminar properties of cortical neurons (Schuurmans et al. 2004; Osumi et al. 2008). Findings here that cell cycle parameters are disrupted in the PAX77 cortex motivated me to investigate whether laminar fate is altered in these mice. They provide a good model to explore the role of altered Pax6 levels on laminar specification since, unlike *Pax6*$^{-/-}$ mutants, they do not die perinatally, before laminar formation is complete, their cortical cells are not fundamentally respecified to ventral telencephalic fates (Kroll and O'Leary 2005; Quinn et al. 2007; Manuel et al. 2007) and late-generated neurons do not fail to migrate appropriately (Caric et al. 1997; Fukuda et al. 2000). BrdU-birthdating experiments demonstrated that late-born neurons are properly positioned in the superficial layers of the PAX77 cortex. However, analyses showed that cortical neurons acquire their correct laminar identities at correct proportions in both deep

and superficial cortical layers in the postnatal PAX77 cortex, indicating that increased levels of Pax6 do not affect laminar phenotypes.

How do Pax6 levels regulate the development of superficial layer neurons? Increased Pax6 levels control specific aspects of laminar development related more to cell-cycle commitment and cell-cycle length regulation of late cortical progenitors than to cell fate determination. In contrast, loss of Pax6 function depletes the progenitor pool from the earliest stages of corticogenesis and contributes to the formation of an abnormal cortical environment where late-born neurons cannot migrate to appropriate superficial laminar positions (Caric et al. 1997; Fukuda et al. 2000; Quinn et al. 2007). Collectively, these data indicate that both gain- and loss-of-function of Pax6 affect the formation of superficial layers of the cortex, but the final laminar phenotype seems to be achieved through different mechanisms. Precise levels of Pax6 are required primarily to regulate cell cycle properties, thereby ensuring the production of appropriate numbers of superficial layer neurons.

CHAPTER 5

Spatially and Temporally Specific Elimination of Pax6 Function in Conditional Knockout Mice Reveals Important Roles for Pax6 in Suppressing Ventral Fates and Promoting Dorsal Cell Identities in the Developing Telencephalon

5.1 Introduction

The embryonic dorsal telencephalon is the progenitor site for production of cortical projection neurons, while GABAergic interneurons are generated ventrally (Marin and Rubenstein 2001; Gorski et al. 2002). Spatial and temporal regulation of gene expression in the embryonic telencephalon is central for cellular diversity. Progenitor-restricted expression of transcription factors in the embryonic cortex has suggested a close relationship between progenitors and their descendant neuronal phenotypes. Pax6 is expressed in apical progenitors from the earliest stages of corticogenesis, while Tbr2 is expressed in basal progenitors arising at around E12 (Englund et al. 2005; for review, see Hevner 2006). During corticogenesis, asymmetric division of apical progenitors results in the production of one cortical precursor, whereas basal progenitors serve mostly as direct neurogenic progenitors by undergoing symmetric division to produce two postmitotic neurons (Chenn and McConnell 1995; Gotz et al. 1998; Haubensak et al. 2004; Miyata et al. 2004; Noctor et al. 2004). Sequential migration of postmitotic neurons out of the proliferative zone leads ultimately to the formation of a six-layered cerebral cortex, with neurons localized within defined layers sharing similar morphologies, molecular features and connectivity (O'Leary and Koester 1993; McConnell 1995; O'Leary and Nakagawa 2002).

Unravelling the molecular mechanisms that underlie layer-specific neuron production through dissection of the specific temporal and spatial roles of progenitor cell subtypes is of particular interest. Sequential expression of Pax6, Ngn2 and Tbr2 in cortical progenitors has been suggested as a crucial transcription factor cascade for production of projection neurons (reviewed in Hevner 2006). Recently, genetic fate mapping and conditional mutagenesis of crucial molecular determinants specifying basal progenitor fate have revealed important roles for basal progenitors in contributing neurons particularly to superficial layers of the cortex (Arnold et al. 2008; Sessa et al. 2008; Kowalczyk et al. 2009; Pinto et al. 2009). Analyses of null mutant mice deficient for *Pax6* or *Ngn2* have suggested that superficial-layer neuron generation is Pax6-dependent, whereas deep-layer neuron generation is controlled by Ngn2 (Schuurmans et al. 2004). However, the early perinatal lethality of these null

mutants, as well as the fact that the gene of interest is inactivated from the earliest stages of its normal expression, hampers our understanding of the primary roles of such important transcriptional regulators in controlling formation of specific laminae. This highlights the need for the generation of new genetic tools that allow for spatial and temporal control of gene inactivation in order to delineate the molecular mechanisms that potentially underlie the development of specific layer neuron subtypes.

Pax6$^{-/-}$ embryos exhibit severe abnormalities of cortical development, including progressive ventralization of the mutant cortex leading to a striatum-like molecular profile and excess of GABAergic interneurons in the mutant cortex (Kroll and O'Leary 2005). Whether Pax6 is necessary for the initial establishment of telencephalic patterning or it is still required at later developmental stages to maintain dorsal identity, by promoting pallial gene expression and antagonizing transcriptional cascades typical of the subpallium, remains a question. Furthermore, Pax6 loss from the onset of corticogenesis leads to increased cell cycle exit of early cortical progenitors, thus depleting the mutant progenitor pool available for superficial layer neuron generation later on (Quinn et al. 2007). Moreover, late-born neurons fail to adopt laminar positions and accumulate in the proliferative zone of the *Pax6* deficient cortex, leading to the formation of an abnormally thin cortex mostly attributable to an almost complete loss of superficial layer neurons (Caric et al. 1997; Tarabykin et al. 2001; Tuoc et al. 2009). Whether the final laminar phenotype in *Pax6* loss-of-function mutants is the consequence of early defects in the mutant cortex or Pax6 is also required during late corticogenesis to regulate superficial laminar formation is not clear. Basal progenitors are severely misspecified in the *Pax6*$^{-/-}$ cortex (Tarabykin et al. 2001; Nieto et al. 2004; Quinn et al. 2007), raising the question of whether this is a secondary defect in the mutant cortex or Pax6 is directly required in late cortical progenitors to regulate basal progenitor specification and ultimately superficial laminar fate.

In order to determine the primary later functions of a transcriptional regulator such as Pax6 that masters cortical development from the earliest stages, as well as to demarcate the temporal windows in which Pax6 controls specific processes crucial

for cortical development, spatially and temporally controlled gene inactivation is required. Here, the primary requirements of Pax6 during mid and late corticogenesis were addressed by using a genetic approach that allows for inducible deletion of *Pax6* exclusively in cortical progenitors. Temporal and spatial control of *Pax6* mutagenesis was achieved using a floxed *Pax6* allele (Simpson et al. 2009) and a driver line carrying the inducible form of the site-specific Cre recombinase (*Cre-ER^{T2}*) under control of the *Emx1* locus (Kessaris et al. 2006). Use of the *Rosa26R-YFP* reporter line (Srinivas et al. 2001) confirmed successful recombination and faithful expression of the *Cre* transgene subsequent to tamoxifen administration. By using this triple allelic combination and by transiently activating *Cre-ER*, Pax6 was selectively abolished in cortical progenitors during mid or late corticogenesis. Pax6 conditional knock-out (cKO) mice were viable with no obvious behavioural abnormalities at early postnatal ages. Pax6 ablation during mid-corticogenesis consistently resulted in a notable reduction of the cortical surface, a phenotype reproducing that previously described in *Pax6* deficient mice (Schmahl et al. 1993; Caric et al. 1997; Tarabykin et al. 2001; Tuoc et al. 2009) and confirming an efficient cKO by using this strategy. Analyses of cKO mutants lacking Pax6 from mid or late stages of corticogenesis recapitulated previous findings in *Pax6$^{-/-}$* mice (Muzio et al. 2002; Kroll and O'Leary 2005; Quinn et al. 2007) and revealed a novel requirement of Pax6 function during mid and late corticogenesis for continuous suppression of ventral cell fates and maintenance of an appropriate dorsal cell fate in cortical progenitors. Collectively, the new transgenic mouse line generated in this study represents a valuable tool for delineating the specific primary roles of Pax6 in defined temporal windows throughout cortical development.

5.2 Results

5.2.1 Tamoxifen administration in *Pax6$^{loxP/loxP}$; Emx1-CreER* mice at E10.5 leads to Pax6 ablation at E13.5 and reduced cortical tissue postnatally

Tamoxifen-induced recombination peaks at 24-48 h post-injection in *Emx1-CreER^{T2}* embryos (Kessaris et al. 2006). To determine the recombination efficiency induced by tamoxifen and the consequent loss of Pax6, tamoxifen was administered into pregnant females at E10.5 and embryos were analysed at E12.5 (48 h post-tamoxifen administration). Surprisingly, Pax6 protein was still detected with an apparently normal pattern in the E12.5 *Pax6$^{loxP/loxP}$*; *Emx1-CreER*$^{E10.5tamox}$ cortex (Fig. 1B) compared to control (Fig. 1A). To monitor for successful *Cre*-mediated recombination, sections of the same brains were immuno-reacted for YFP; YFP was intensely expressed in the vast majority of cells in the cortex (Fig. 1C), showing that failure to inactivate Pax6 in the E12.5 *Pax6$^{loxP/loxP}$*; *Emx1-CreER*$^{E10.5tamox}$ cortex is not due to incomplete recombination and further verifying that the Cre/loxP-mediated deletion is restricted to dorsal telencephalic regions in this model system. These observations indicate that Pax6 protein persists in the cortex of E12.5 *Pax6$^{loxP/loxP}$*; *Emx1-CreER*$^{E10.5tamox}$ mice, after *Cre*-mediated recombination has occurred.

Then, Pax6 expression was tested in the cortex of *Pax6$^{loxP/loxP}$*; *Emx1-CreER*$^{E10.5tamox}$ mice at E13.5 (72-hours post-tamoxifen administration). There was a clear loss of Pax6 protein from dorsal telencephalic progenitors that express Emx1 (cells around the pallial-subpallial boundary are spared) in the E13.5 *Pax6$^{loxP/loxP}$*; *Emx1-CreER*$^{E10.5tamox}$ mutant cortex (Fig. 1D, E). As expected, in other brain regions where Pax6 is normally expressed but Emx1 is not (e.g. thalamus), Pax6 expression in mutants was comparable to controls (Fig. 1D, E). Therefore, Pax6 is lost from *Pax6$^{loxP/loxP}$*; *Emx1-CreER*$^{E10.5tamox}$ mutant embryos between E12.5 and E13.5, before the onset of superficial layer generation from E14.5 onwards.

The effect of Pax6 loss in *Pax6$^{loxP/loxP}$*; *Emx1-CreER*$^{E10.5tamox}$ mutant cortex was examined postnatally. Mutant brains showed a markedly reduced size of the cerebral

FIGURE 1

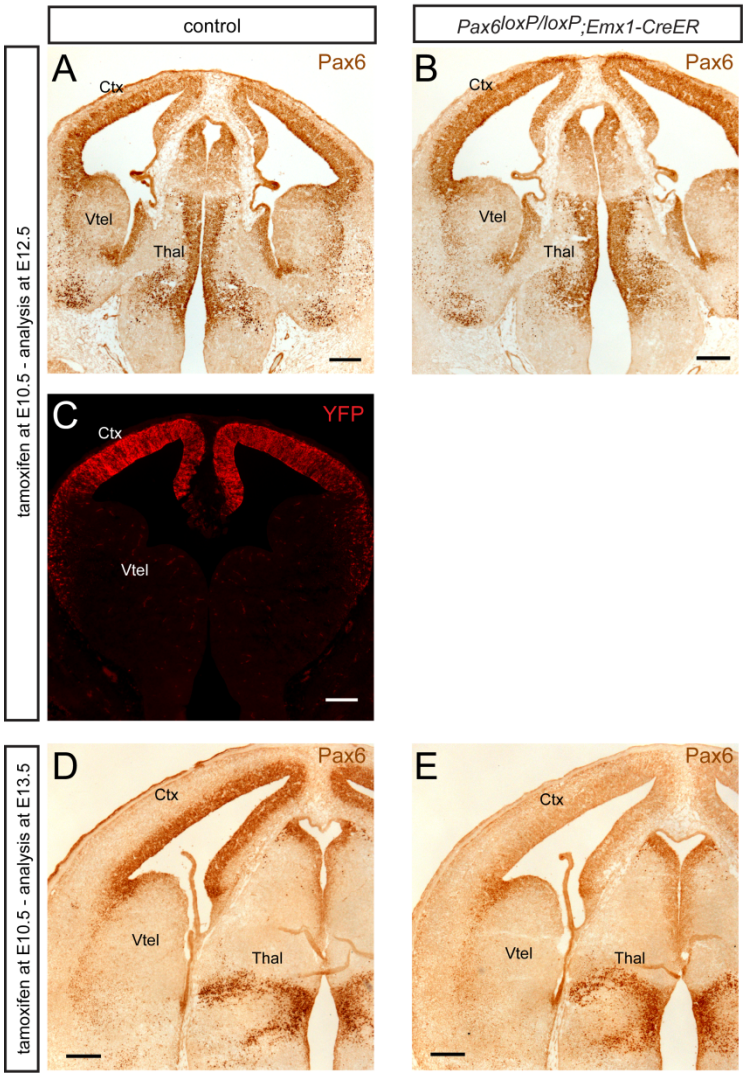

Figure 1. E10.5 tamoxifen administration leads to Pax6 loss at E13.5 but not at E12.5 in the cortex of *Pax6*$^{loxP/loxP}$; *Emx1-CreER* $^{E10.5tamox}$ **embryos.** (A, B) Coronal sections of E12.5 (A) control (*Pax6*$^{loxP/+}$; *Emx1-CreER* $^{E10.5tamox}$) and (B) mutant (*Pax6*$^{loxP/loxP}$; *Emx1-CreER* $^{E10.5tamox}$) cortices immunolabelled for Pax6. Pax6 protein is present in the cortex of *Pax6*$^{loxP/loxP}$; *Emx1-CreER* $^{E10.5tamox}$ embryos 48-hrs post-tamoxifen administration. (C) Coronal section through the telencephalon of E12.5 control brain immunostained for YFP. YFP expression indicates that the presence of Pax6 protein in (B) the mutant cortex 48-hours post-tamoxifen injection is not due to unsuccessful recombination. Note the restricted expression of YFP into the dorsal telencephalon. (D, E) Coronal sections of E13.5 (D) control and (E) mutant cortices immunolabelled for Pax6 72-hrs post-tamoxifen administration. Note the loss of Pax6 in the mutant cortex compared to control. As expected, Pax6 was detected in regions of the mutant brain where the *Cre* transgene driven by *Emx1* should not expressed, i.e. the ventral telencephalon and thalamus. Ctx, cortex; Thal, thalamus; Vtel, ventral telencephalon. Scale bars represent 200 μm (D, E).

FIGURE 2

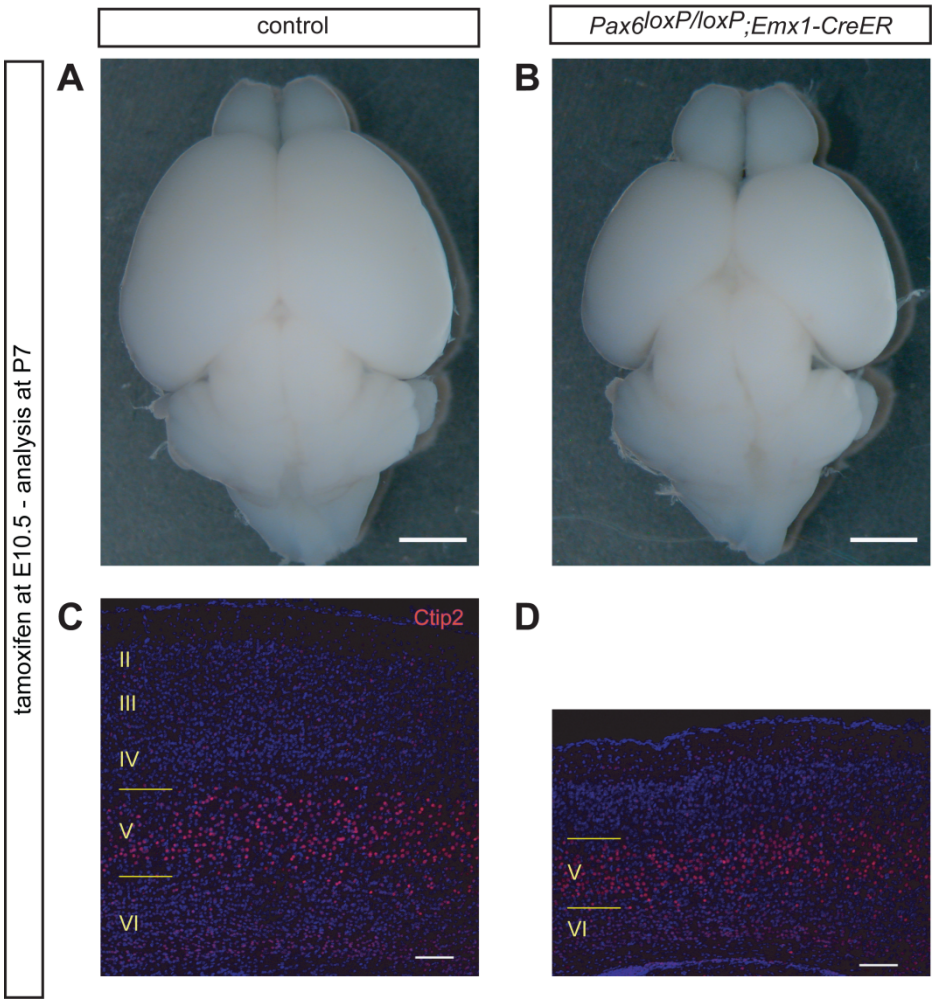

Figure 2. Cortex-specific Pax6 ablation at mid-stages of corticogenesis leads to reduced cortical tissue. (A, B) Dorsal views of P7 brains show a marked reduction of cortical size in *Pax6*$^{loxP/loxP}$*; Emx1-CreER* $^{E10.5tamox}$ mutant brain compared to control$^{E10.5tamox}$. (C, D) Coronal sections of P7 (C) control and (D) mutant cortices at central level labelled for Ctip2, which is expressed at high levels in corticospinal neurons of layer V. The lines in (C, D) indicate the borders between layers VI-V and V-IV. The thickness of Ctip2-negative superficial layers (IV-II) of the cortex was strikingly reduced in the mutant (D) compared to control (C). Scale bars represent 2mm (A, B) and 100µm (C, D).

cortex at P7 compared to control (Fig. 2A, B). Histological examination revealed a severe reduction in cortical thickness. Layer-specific immunostaining of P7 cortices with Ctip2, which is known to be required for specification of corticospinal motor neurons located in layer V (Arlotta et al. 2005), showed strongly reduced thickness of Ctip2-negative superficial layers in the mutant cortex (Fig. 2C, D). These morphological brain abnormalities resemble those reported recently from Tuoc et al. (2009), where *Pax6* was conditionally knocked-out from the earliest stages of corticogenesis using a conventional *Emx1-Cre*.

5.2.2 Tamoxifen administration in *Pax6$^{loxP/loxP}$; Emx1-CreER* mice at E13.5 leads to disruption of Pax6 function in late cortical progenitors

In order to inactivate Pax6 specifically during late corticogenesis, tamoxifen was administered to *Pax6$^{loxP/loxP}$*; *Emx1-CreER* mice at E13.5 and the loss of Pax6 expression was examined by Pax6 immunohistochemistry. At E15.5, 48 h post-tamoxifen administration, a marked reduction in Pax6 protein was observed in the mutant cortex compared with control (Fig. 3A, B). Consistent with observations in the E13.5 *Pax6$^{loxP/loxP}$*; *Emx1-CreER*$^{E10.5tamox}$ mutant cortex, normal levels of Pax6 expression were observed in cortical regions where the *Cre* transgene is not expressed, i.e. the dorsal lateral ganglionic eminence. However, substantial numbers of Pax6-positive cells were detected in the E15.5 mutant cortex, suggesting two alternative possibilities: (1) recombination efficiency might not be the highest possible in these control and mutant littermates, or (2) the Pax6 protein is stable enough such that it is detectable for some time after *Cre*-mediated recombination has occurred in the cortex of mice treated with tamoxifen. YFP immunostaining on these brains indicated that high proportions of cortical cells were expressed YFP (Fig. 4B, B'), therefore not supporting the first possibility of low recombination efficiency in these E15.5 littermates. Intriguingly, high magnification views of cortical sections double-immunostained with Pax6 and YFP showed that a number of Pax6-expressing cells were also positive for YFP, indicating that individual cells had recombined loxP sites but still contained Pax6 protein (Fig 4A-C, A'-C'). These observations further support the second explanation of an enhanced stability of the

FIGURE 3

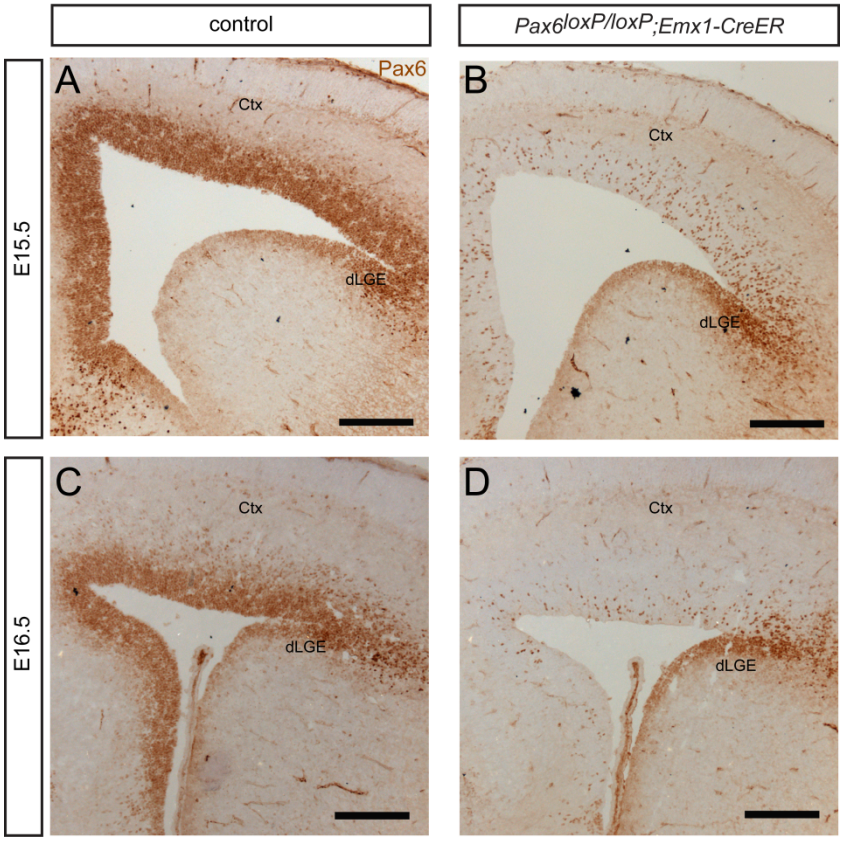

Figure 3. Tamoxifen administration into *Pax6$^{loxP/loxP}$; Emx1-CreER* mice at E13.5 results in Pax6 loss at E15.5 but the effect is more obvious at E16.5. (A-D) Coronal sections through the rostral cortex of (A, C) control and (B, D) mutant mice immunolabeled for Pax6. Mice were injected with tamoxifen at E13.5 and analyses were performed at (A, B) E15.5 or (C, D) E16.5, 48 h or 72 h post-tamoxifen administration, respectively. Note the Pax6 loss in the mutant cortex (B, D) compared to respective controls (A, C). More Pax6-positive cells were detected in the mutant cortex at E15.5 (B) compared to the E16.5 mutant cortex (D). As expected, Pax6 expression was normal in compartments of the mutant brain where the *Cre* transgene driven by *Emx1* should not be expressed, i.e. the dLGE. Ctx, cortex; dLGE, dorsal lateral ganglionic eminence. Scale bars, 200µm.

FIGURE 4

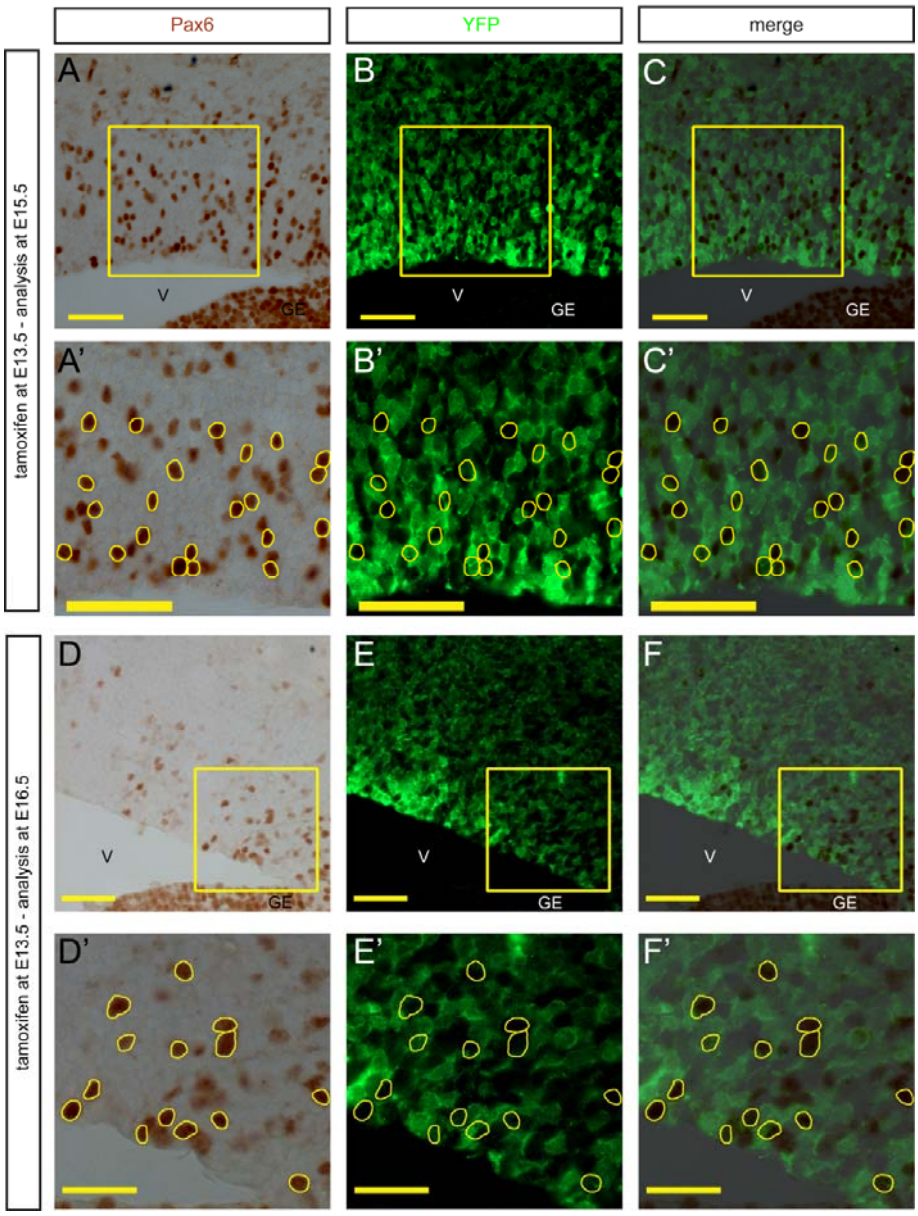

Figure 4. High-level Pax6 expression is excluded from YFP-positive cells in the cortex of *Pax6$^{loxP/loxP}$; Emx1-CreER; R26-YFP* mice injected with tamoxifen at E13.5. The extent of colocalization of Pax6 (brown) and YFP (green) in *Pax6$^{loxP/loxP}$*; *Emx1-CreER; R26-YFP* $^{E13.5tamox}$ mice was assessed by antibody staining at (A-C, A'-C') E15.5 and (D-F, D'-F') E16.5. Boxed areas in A-C and D-F are shown in high magnification in A'-C' and D'-F', respectively. Circled cells in A'-C' and D'-F' indicate examples of Pax6-positive cells, as in A' and D'. (A'-C') Note that at E15.5, 48 h post-tamoxifen administration, relative levels of Pax6 expression are lower in YFP-expressing cells compared to non-YFP-expressing cells in the mutant cortex. (D'-F') At E16.5, 72 h post-tamoxifen administration, most YFP-positive cells had lost Pax6 expression in the mutant cortex. YFP colocalized with Pax6 in few cells that expressed low levels of Pax6. GE, ganglionic eminence; v, ventricle. Medial to the left. Scale bars, 50µm.

Pax6 protein after gene excision, in agreement with previous findings demonstrating the long (12 h) half-life of Pax6 (Turque et al. 1994). To further investigate the persistence of Pax6 expression in the cortex of *Pax6*$^{loxP/loxP}$; *Emx1-CreER*$^{E13.5tamox}$ mice, immunohistochemical analysis was performed at E16.5. Notably, Pax6 expression was further reduced 72 h post-tamoxifen administration (Fig. 3 C, D). High magnification analysis of cortical sections immunoreacted for Pax6 and YFP indicated that a minority of Pax6-expressing cells were double-labelled with YFP; these double-labelled cells exhibited mostly low levels of Pax6 expression, suggesting that Cre-recombination results in progressive elimination of Pax6 (Fig. 4D-F, D'-F').

These analyses indicate that although YFP reports faithfully on Cre recombination driven by *Emx1*, it does not reliably detect cells that have lost Pax6 protein post-tamoxifen administration. Recombination peaks at 24-48 h post-tamoxifen injection in *Emx1-CreER* embryos (Kessaris et al. 2006). Results here show that although E10.5 tamoxifen administration in *Pax6*$^{loxP/loxP}$; *Emx1-CreER* embryos induces Cre-mediated recombination 48 h later, as revealed by YFP expression, it does not affect Pax6 protein expression in YFP-expressing cells. However, it does lead to Pax6 ablation at E13.5, 72 h post-tamoxifen injection. Interestingly, E13.5 tamoxifen administration down-regulates Pax6 expression in YFP-expressing cells 48 h later, an effect that is more obvious 72 h post-tamoxifen injection. This time difference between the early and late tamoxifen-induced Pax6 protein loss could be explained by 1) previous observations that Pax6 levels vary in cortical progenitors throughout development, with highest mRNA and protein levels present at early stages (Tuoc and Stoykova 2008), and 2) a possible longer half-life of the protein at early stages compared to late. It is therefore likely that degredation of protein levels in early cortical progenitors might require a more extended time period after Cre-mediated recombination occurs in *Pax6*$^{loxP/loxP}$; *Emx1-CreER* embryos compared to late stages. Although tamoxifen-induced Pax6 loss in conditional mutants has not been tested at the mRNA level, it would not be surprising if the same time-dependent effect occurs with regard to mRNA downregulation post-tamoxifen induction.

5.2.3 Pax6 elimination in cortical progenitors during mid- or late-corticogenesis leads to ectopic expression of ventral markers into the cKO cortex

The expression domains of transcription factors are central in fate decisions of telencephalic progenitors. Several transcription factors are expressed in the proliferative zones of either the dorsal or ventral telencephalon (dTel or vTel) in a complimentary manner and their expression is required for proper establishment of the developing telencephalon. Previous studies of *Pax6*$^{-/-}$ mice have indicated that *Pax6* acts as a "master gene" in leading telencephalic progenitors to adopt a dorsal versus ventral fate and promote key aspects of the cortical morphogenetic programme, including the proper generation of glutamatergic neurons and concurrent suppression of a GABAergic interneuron fate (Stoykova et al. 2000; Toresson et al. 2000; Yun et al. 2001; Muzio et al. 2002b; Kroll and O'Leary 2005). An unanswered question is whether Pax6 is required for the initial specification of dTel identity or it is also crucial at later stages for the maintenance of dorsal character and continuous suppression of ventral identity in the mouse telencephalon. Previous analyses focused on *Pax6* loss-of-function mutants where *Pax6* is absent from the earliest stages of telencephalic development. The more pronounced abnormal molecular phenotype of the *Pax6*$^{-/-}$ dTel described previously during mid- and late-stages of telencephalic development might merely arise due to early patterning defects in the *Pax6*$^{-/-}$ mutants.

To test whether *Pax6* ablation at mid- or late-stages of corticogenesis affects telencephalic patterning, expression patterns of two sets of genes normally restricted to the dTel or vTel were analysed in E15.5 *Pax6*$^{loxP/loxP}$; *Emx1-CreER*$^{E10.5tamox}$ and E16.5 *Pax6*$^{loxP/loxP}$; *Emx1-CreER*$^{E13.5tamox}$ mice. The ventral marker Mash1 is highly expressed in progenitors of the ganglionic eminence (GE), whereas expression levels are low to non-detectable in the ventricular zone (VZ) of the dTel (Parras et al. 2007) (Fig. 5A, E). At E15.5, Mash1 expression demarcates the boundary between the vTel and the dorsal ganglionic eminence (dLGE) (Fig. 5A). In E15.5 *Pax6*$^{loxP/loxP}$; *Emx1-CreER*$^{T2\ E10.5tamox}$ brains, Mash1 was dramatically upregulated in the VZ of the cortex, such that expression levels were similar to those exhibited ventrally (Fig. 5A'). At E16.5, the boundary of high Mash1 expression in the dLGE was evident in both control and *Pax6*$^{loxP/loxP}$; *Emx1-CreER*$^{T2\ E13.5tamox}$ mutant brains (Fig. 5E, E').

However, Mash1 expression was severely upregulated in the VZ of the *Pax6*$^{loxP/loxP}$; *Emx1-CreER*^{T2} $^{E13.5tamox}$ mutant pallium (Fig. 5E'). Gsh2 expression is normally confined to progenitors of the GE forming a sharp boundary in the dLGE (Fig. 5B, F). Pax6 removal at either mid or late-stages of corticogenesis resulted in robust expression of Gsh2 in the VZ of the mutant cortex (Fig. 5B', F').

Then, I examined the localization of the transcription factor Olig2, which identifies oligodendrocyte progenitor cells and their descendants in the cortex, namely oligodendrocytes and astrocytes (Tekki-Kessaris et al. 2001; Parras et al. 2007; Petryniak et al. 2007). Olig2-positive cells are initially confined in the VZ of the MGE and they gradually scatter throughout the telencephalon such that high numbers of Olig2-positive cells reach the pallium by E17.5 (Takebayashi et al. 2000; Nery et al. 2002; Miyoshi et al. 2007; Ono et al. 2008). Consistent with this ventral-to-dorsal progression of Olig2 expression, in E15.5 control brains very few Olig2-positive cells had reached the pallium (Fig. 5C), whereas at E16.5 a substantial number of Olig2-positive cells were distributed throughout the control cortex except for the medial pallium (Fig. 5H). In E15.5 *Pax6*$^{loxP/loxP}$; *Emx1-CreER*^{T2} $^{E10.5tamox}$ mutant brains, an ectopic domain of high Olig2 expression was evident in the dTel VZ, reminiscent of that present in progenitors of the GE (Fig. 5C', C). Moreover, great numbers of Olig2-positive cells dispersed in abventricular positions of the mutant cortex compared to control (Fig. 5C', C). A similar pattern of ectopic Olig2

FIGURE 5

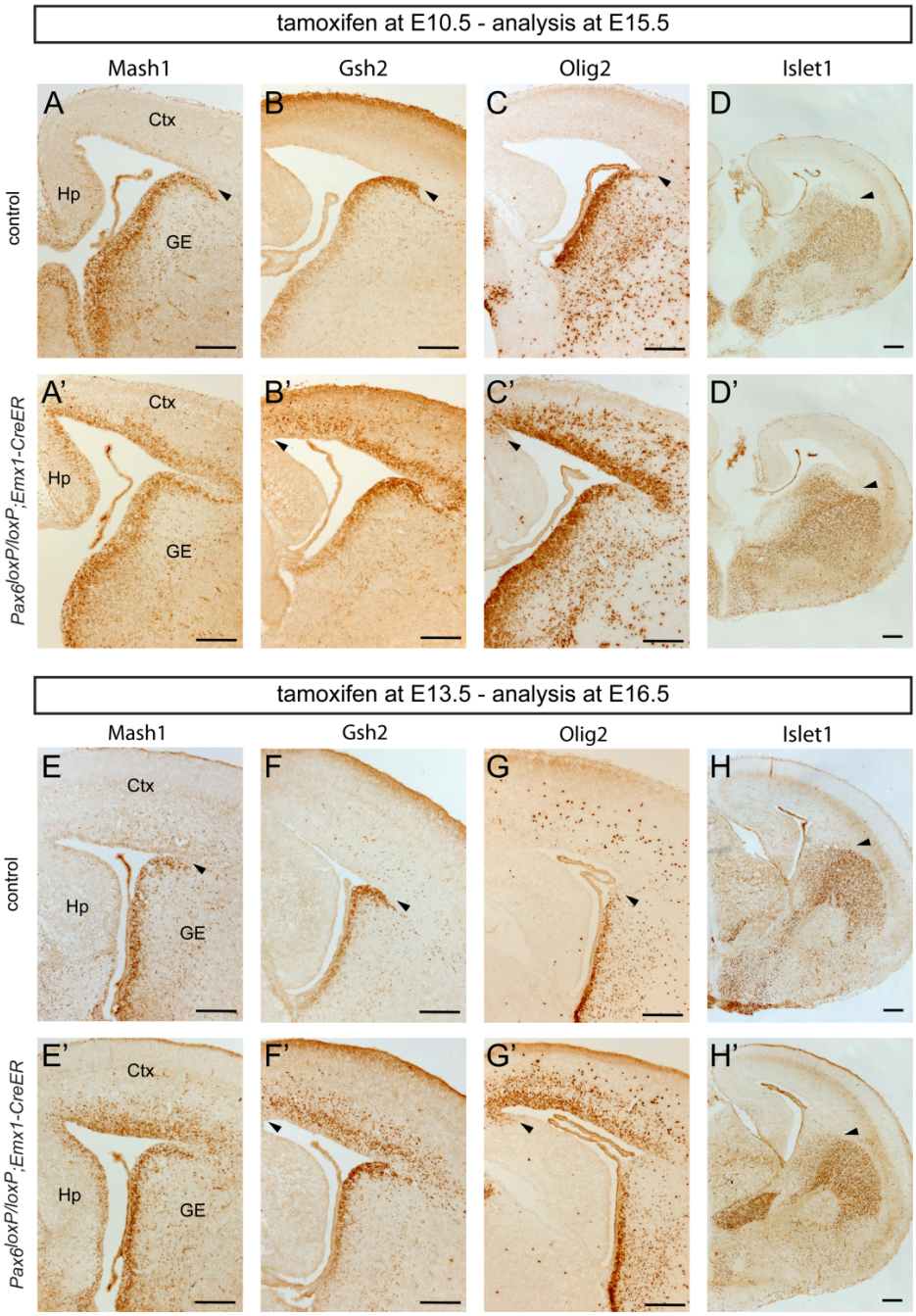

Figure 5. Pax6 inactivation during mid- or late-corticogenesis leads to ectopic expression of ventral markers into the mutant cortex. (A, A', E, E') Mash1, (B, B', F, F') Gsh2, (C, C', G, G') Olig2 and (D, D', H, H') Islet1 protein expression in coronal sections through the telencephalon of E15.5 (A-D) control $^{E10.5tamox}$ and (A'-D') *Pax6$^{loxP/loxP}$;Emx1-CreER* $^{E10.5tamox}$ mutant mice, and E16.5 (E-H) control $^{E13.5tamox}$ and (E'-H') *Pax6$^{loxP/loxP}$; Emx1-CreER* $^{E13.5tamox}$ mutant mice. Arrowheads point to the dorsal boundary of the expression domains. Islet1 expression in both (D') E15.5 and (H') E16.5 mutants was indistinguishable from respective controls. Ctx, cortex; Hp, hippocampus; GE, ganglionic eminence. Coronal sections, medial to the left. Scale bars, 200µm.

expression was observed in E16.5 *Pax6*$^{loxP/loxP}$; *Emx1-CreER*^{T2} $^{E13.5tamox}$ mutant cortex compared to respective controls (Fig. 5G', G), although the density of Olig2-positive cells in the mutant dTel VZ was not as high as that detected in the E15.5 *Pax6*$^{loxP/loxP}$; *Emx1-CreER*^{T2} $^{E10.5tamox}$ mutant cortex (Fig. 5C'). The distribution of Olig2-positive cells in both E15.5 *Pax6*$^{loxP/loxP}$; *Emx1-CreER*^{T2} $^{E10.5tamox}$ and E16.5 *Pax6*$^{loxP/loxP}$; *Emx1-CreER*^{T2} $^{E13.5tamox}$ mutant dTel VZ was comparable to that of ectopic Gsh2-positive cells. The subpallial marker Islet1 marks differentiating projection neurons in the striatum (Toresson et al. 2000; Toresson and Campbell 2001), normally detectable in the ventral LGE (Stenman et al., 2003) (Fig. 5E, I), was not affected in E15.5 *Pax6*$^{loxP/loxP}$; *Emx1-CreER*^{T2} $^{E10.5tamox}$ or E16.5 *Pax6*$^{loxP/loxP}$; *Emx1-CreER*^{T2} $^{E13.5tamox}$ mutant brains compared to controls (Fig. 5E', I').

These marker analyses indicate that inactivation of *Pax6 s*pecifically at mid or late stages of corticogenesis results in expression of ventral markers in essentially the entire dTel VZ, except for the medial pallium. Therefore, in cortical regions where Pax6 is normally expressed at high levels, progenitors are extremely sensitive to Pax6 loss even after they have acquired a dorsal character, suggesting that Pax6 is constantly required within cortical progenitors to maintain their correct fate and restrict them from adopting ventral identity.

5.2.4 Pax6 inactivation during mid- or late-stage corticogenesis affects basal progenitor fate

The ectopic expression of ventral markers into the cortex of both *Pax6*$^{loxP/loxP}$; *Emx1-CreER*^{T2} $^{E10.5tamox}$ and *Pax6*$^{loxP/loxP}$; *Emx1-CreER*^{T2} $^{E13.5tamox}$ mice may affect the dorsal fate specification of these mutant progenitors. To directly test this possibility, Tbr2 was employed as a dTel marker, which is also specifically expressed in the basal progenitors of the developing cortex (Englund et al. 2005; Hevner et al. 2006). A large loss of Tbr2 expression was detected in the cortex of *Pax6*$^{loxP/loxP}$; *Emx1-CreER*^{T2} $^{E10.5tamox}$ mutant mice at E15.5 compared to control, especially in the lateral cortex where Pax6 levels are normally high (Fig. 6A-B, A'-B'). Expression levels were unaffected in the mutant medial pallium, where Pax6 is normally expressed at low levels, and they also marked the pallial-subpallial boundary in the mutant (Fig.

6A-B, A'-B'). Interestingly, Pax6 ablation in late cortical progenitors also affected Tbr2 expression in the mutant cortex, particularly in the subventricular zone (SVZ) (Fig. 6C-E, C'-E'). Quantitative analysis revealed a significant decrease in the number of Tbr2-positive cells in the E16.5 *Pax6*$^{loxP/loxP}$; *Emx1-CreER*^{T2} E13.5tamox mutant cortex compared to control (321.8 ± 10.47 in control, 234.77 ± 12.13 in mutant; Student's *t*-test $P = 0.006$; $n = 3$ per genotype). Collectively, although Pax6 inactivation during mid- or late-stages of corticogenesis leads to dramatic elevation of ventral markers into the proliferative zone of the mutant pallium, mutant progenitors still express dorsal markers, though in reduced numbers compared to controls. These findings suggest that Pax6 is continuously required within cortical progenitors to regulate basal progenitor fate.

FIGURE 6

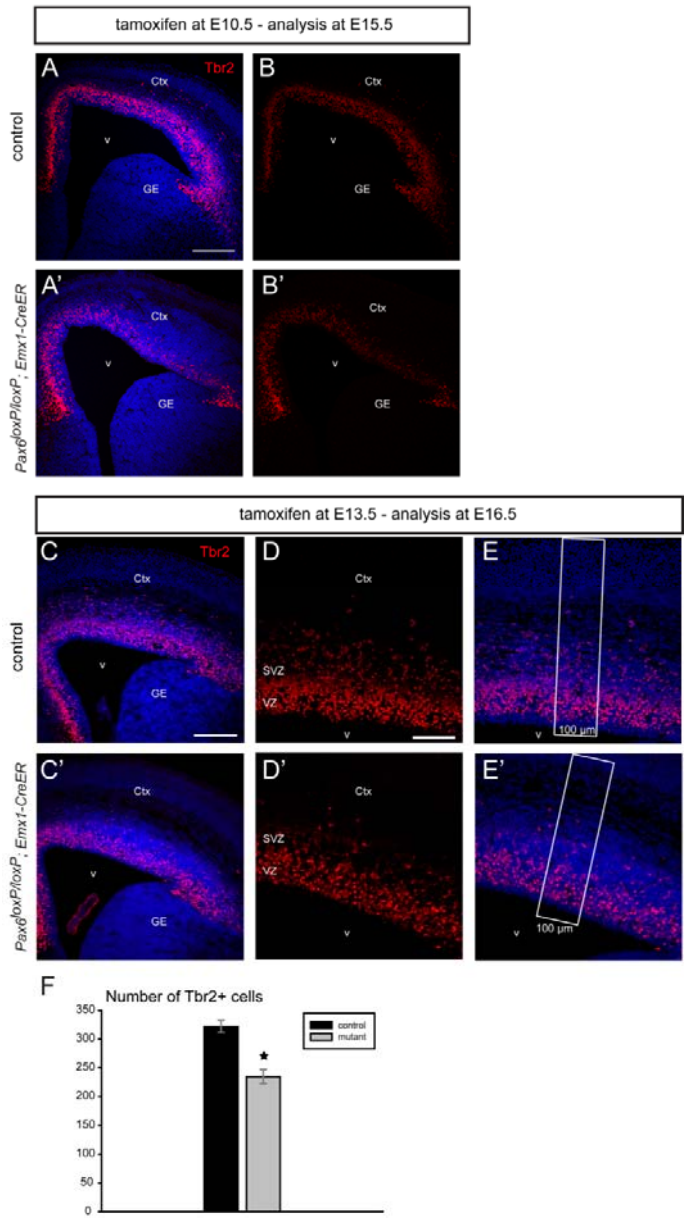

Figure 6. Basal progenitor identity is affected in the cortex of mice lacking Pax6 from mid- or late-stage corticogenesis. (A-B, A'-B') Tbr2 staining on coronal sections through the telencephalon of E15.5 control$^{E10.5tamox}$ and *Pax6$^{loxP/loxP}$;Emx1-CreER*$^{E10.5tamox}$ mice at a rostral level, showing that the amount of Tbr2-expressing cells is extremely decreased in the mutant cortex compared to control. Note that Tbr2 expression is unaffected in the mutant medial pallium and that it also demarcates the pallial-subpallial boundary of the mutant brain. (C-E, C'-E') Coronal sections through the E16.5 control $^{E13.5tamox}$ and *Pax6$^{loxP/loxP}$ Emx1-CreER* $^{E13.5tamox}$ rostral cortex immunolabeled for Tbr2. Tbr2-positive cells were quantified in 100-µm-wide radial stripes, as shown in E, E'. (F) The number of Tbr2-positive cells was significantly reduced in the E16.5 mutant cortex compared to control. Medial to the left. Sections were counterstained with TOPRO-3. Ctx, cortex; GE, ganglionic eminence; VZ, ventricular zone; SVZ, subventricular zone. Scale bars represent (A, C) 200µm, (D) 100 µm.

5.3 Discussion

5.3.1 Pax6 continuously restricts subpallial fates into the ventral telencephalon

The orchestrated production of projection neuron and interneuron subtypes in the dorsal and ventral embryonic telencephalon, respectively, is central for the formation of a mature, functional cerebral cortex. This multistep process requires differential activation of transcription factor genes in dorsal and ventral domains of the embryonic telencephalon. Previous work on *Pax6*$^{-/-}$ mice has suggested that Pax6 is required within cortical progenitors to promote dorsal gene expression and concurrently suppress ventral cell fates, either directly or indirectly (Stoykova et al. 2000; Toresson et al. 2000; Yun et al. 2001; Muzio et al. 2002; Kroll and O'Leary 2005). Here, conditional Pax6 inactivation in mid- or late-cortical progenitors resulted in severe upregulation of ventral telencephalic markers in the mutant cortex, a molecular profile resembling that previously described in *Pax6*$^{-/-}$ mice. Interestingly, ventral markers were ectopically expressed in the *Pax6* cKO cortical field except for the medial pallium, where levels of Pax6 expression are normally low. This could indicate compensation from Emx2 function that is more prominent in the medial pallium compared to lateral cortical regions (Muzio et al. 2000b). The striatum-like molecular profile of the *Pax6* cKO cortex was evident at different levels of the mutant cortex across the rostral-caudal axis, indicating that Pax6 deficiency affects dorsal-ventral specification in the same fashion even in regions where its expression levels are normally not the highest. The initial establishment of a proper dorsal identity in the *Pax6* cKO cortex was not sufficient for its late maintenance, demonstrating that Pax6 has a prominent, dynamic role for antagonizing ventral cell identities in its expression domains. Together, these new findings reflect the central role of Pax6 throughout corticogenesis for continuously repressing a transcriptional code responsible for specifying subpallial cell fate.

Cells of ventral identity were presumably locally born by progenitors in the dTel VZ of the *Pax6* cKO cortex. In this study, regional identity was analyzed in *Pax6* cKO embryos that permanently labelled *Emx1*-lineage cortical cells covered essentially the entire pallium, suggesting that locally generated pallial progenitors undergo re-specification and up-regulate ventral markers after loss of Pax6. These observations

are in agreement with *Emx1-Cre* fate mapping studies in *Pax6*$^{-/-}$ mutants showing that ectopic neurons of ventral identity are generated in the mutant pallium rather than migrating from the GE (Kroll and O'Leary 2005). It would be interesting to test whether cells ectopically expressing ventral markers in the *Pax6* cKO cortex are also mitotically active. Although pallial markers are downregulated in the *Pax6*$^{-/-}$ cortex, they are still expressed in the mutant cortex (Toresson et al. 2000; Yun et al. 2001; Muzio et al. 2002; Kroll and O'Leary 2005). In line with these data, Pax6 inactivation at either mid- or late stages of corticogenesis significantly reduced, but did not abolish, Tbr2 expression in the mutant cortical field. Interestingly, the signal density of Tbr2 and ventral markers in the VZ of the *Pax6* cKO cortex suggests that the majority of these ectopic ventral cells might co-express dorsal markers, a molecular profile similar to that previously described in *Pax6*$^{-/-}$*; Emx2*$^{-/-}$ double-knockout mutants (Muzio et al., 2002b). Direct demonstration of dorsal and ventral marker co-expression in individual pallial progenitors of the *Pax6* cKO cortex would directly demonstrate that progenitors in the mutant pallium undergo extensive pallial-to-subpallial re-specification.

The great majority of Olig2-lineage cells normally differentiate into GABAergic interneurons in the cortex (Miyoshi et al., 2008; Ono et al., 2008). Moreover, ectopic Mash1 expression is sufficient to re-direct the fate of cortical progenitors and drive production of GABAergic interneurons (Parras et al. 2002; Roybon et al. 2010). Kroll and O'Leary (2005) showed a severe increase in the number of GABAergic interneurons in the *Pax6*$^{-/-}$ cortex. Whether the functional outcome of the pallial activation of genes normally restricted to the subpallium is an abnormal increase in the number of GABAergic interneurons in the *Pax6* cKO cortex, needs further investigation.

The pallial-subpallial boundary (PSPB) is formed at the molecular interface of high Pax6 expression in the ventral pallium and Gsh2 expression in the dorsal LGE (Toresson et al. 2000; Corbin et al. 2003; Carney et al. 2006). Previous studies have suggested a mutual repression between Pax6 and Gsh2 that is central to PSPB formation (Mastick et al. 1997; Corbin et al. 2000; Yun et al. 2001; Carney et al. 2009). At E11.5, Pax6 and Gsh2 expression overlaps in a subset of cells in the PSPB,

whereas later on co-expression declines such that, by E15.5, Pax6 and Gsh2 expression is largely refined into different domains (Corbin et al. 2003). Pax6 inactivation even in a small subset of cells normally co-expressing Pax6 and Gsh2 (by using a conventional *Gsh2*-Cre) results in a striking expansion of Gsh2 expression in the mutant cortex (Cocas L., Georgala PA. et al. manuscript submitted to *J Neuroscience*). This further highlights the key requirement for Pax6 function in order to antagonize expression of ventral markers in the dorsal telencephalon.

5.3.2 Pax6 function is required for basal progenitor fate specification

Cortical projection neurons arise from asymmetric divisions of Pax6-expressing apical progenitors and symmetric divisions of basal progenitors of the embryonic cortex (Chenn and McConnell 1995; Gotz et al. 1998; Haubensak et al. 2004; Miyata et al. 2004; Noctor et al. 2004). While expression of a number of transcription factors has been identified in the SVZ where basal progenitors reside, Tbr2 acts as the key molecular determinant of this progenitor cell type (Tarabykin et al. 2001; Nieto et al. 2004; Englund et al. 2005; Arnold et al. 2008; Sessa et al. 2008). Basal progenitors originate from Pax6-expressing apical progenitors, with a peak between E12 and E16, and Tbr2 expression exhibits a rostro-lateral^{high} to caudo-medial^{low} gradient, similar to that of Pax6 (Bulfone et al. 1999). Pax6 directly promotes basal progenitor production (Sansom et al. 2009), while analyses of *Pax6*$^{-/-}$↔*Pax6*$^{+/+}$ chimeric embryos have suggested a cell-autonomous role for Pax6 for normal expression of Tbr2 (Quinn et al. 2007). Pax6 loss from the onset of corticogenesis results in abolishment of SVZ gene expression in the mutant cortex, suggesting a severe misspecification of basal progenitor cells in the mutant cortex (Tarabykin et al. 2001; Nieto et al. 2004; Zimmer et al. 2004; Englund et al. 2005). Here, removal of Pax6 in cortical progenitors at either mid- or late stages of corticogenesis resulted in a remarkable decrease of Tbr2-expressing cells, especially in regions where Pax6 is normally expressed at high levels. Interestingly, the remaining Tbr2-expressing cells in the *Pax6* cKO cortex were located in a mutant cortical domain exhibiting severe ventralization, further suggesting that basal progenitors are misspecified in the cKO

cortex. Together, these findings demonstrate that basal progenitor fate is continuously Pax6-dependent throughout the entire course of corticogenesis.

Pax6 regulates basal progenitor fate specification by acting upstream of a number of transcription factors that function as important molecular determinants of basal progenitor fate, including *Ngn2* (Scardigli et al. 2003; Miyata et al. 2004; Britz et al. 2006), *AP2*γ (Holm et al. 2007; Pinto et al. 2009) and *Tbr2* (Englund et al. 2005; Sansom et al. 2009). While Pax6 and Tbr2 are specifically expressed in apical and basal progenitors, respectively, Ngn2 and AP2γ identify a subset of apical progenitors with prospective basal progenitor fates (Englund et al. 2005; Britz et al. 2006; Hevner et al. 2006; Pinto et al. 2008; Kowalczyk et al. 2009). Studies in *Pax6*$^{-/-}$ mice have suggested that other factors cooperate with Pax6 to induce Ngn2 expression (Stoykova et al. 2000). In contrast to AP2γ, which appears to have a temporal role in basal progenitor specification restricted in mid-corticogenesis (Pinto et al. 2009), results here indicate that basal progenitor specification is extremely sensitive to Pax6 loss throughout the entire time course of corticogenesis. Collectively, these findings demonstrate that Pax6 functions at a higher hierarchical level as an activator of basal progenitor fate compared to other transcriptional regulators. Furthermore, they exemplify the precise requirements for correct levels of transcription factors in cortical progenitors in order to generate appropriate numbers and types of cortical projection neurons throughout development and different regions of the cortex. Since Pax6 and AP2γ have a stronger effect in opposing regions of the cortex with respect to its rostral-caudal axis (Pinto et al. 2008; present study), Pax6 loss in caudal regions from mid-corticogenesis would be anticipated to cause a less severe phenotype in basal progenitor specification in these regions due to compensation from AP2γ function. In this context, given that basal progenitors generate two postmitotic neurons (Haubensak et al. 2004) Pax6 inactivation is expected to lead to a more severe laminar phenotype rostrally compared to caudal cortical regions.

CHAPTER 6

Requirements for Pax6 Function during the Formation of Superficial Cortical Layers

6.1 Introduction

The formation of the cerebral cortex is a multistep process that requires tight regulation of progenitor cell proliferation, cell fate determination and ordered neuronal migration. Pax6 is expressed in apical progenitors throughout the entire time of corticogenesis, and therefore its function is likely involved in several processes during cortical development. Apical progenitors represent the self-renewing cortical progenitors that exhibit a unique cell cycle-dependent nuclear movement along the apical-basal axis, a process called interkinetic nuclear migration; basal progenitors represent the non-surface-dividing neurogenic progenitors (for review, see Fishell and Kriegstein 2003).

Loss of Pax6 from the earliest stages of corticogenesis disrupts interkinetic nuclear migration and results in exuberant mitoses of cortical progenitors in ectopic, basal positions (Haubst et al. 2004; Quinn et al. 2007; Tamai et al. 2007; Tuoc et al. 2009). Furthermore, increased cell cycle exit of *Pax6*$^{-/-}$ progenitors at early stages leads to premature neurogenesis and depletion of the progenitor pool in the mutant cortex (Estivill-Torrus et al. 2002; Quinn et al. 2007). The reduced cortical surface area in *Pax6* loss-of-function mutants is primarily caused due to depletion of superficial layers, evidence that has implicated Pax6 in regulating superficial laminar fate (Tarabykin et al. 2001; Schuurmans et al. 2004; Osumi et al. 2008; Tuoc et al. 2009). However, defects in superficial laminar formation in the *Pax6*-deficient cortex might arise due to an early depletion of the progenitor pool or migration abnormalities of late-born neurons, which instead of adopting superficial laminar positions accumulate in the proliferative zone (Fukuda et al. 2000; Tarabykin et al. 2001; Schuurmans et al. 2004). Tuoc et al. (2009) recently reported a cortex-specific *Pax6* cKO mouse model which, for the first time, provided the opportunity to analyse cortical development in *Pax6* mutants postnatally. These studies demonstrated proliferation defects of late cortical progenitors and an almost complete loss of superficial layer neurons in the *Pax6* deficient cortex. However, similar to *Pax6*$^{-/-}$ mice, this type of analysis precludes definite conclusions of a direct effect of Pax6 on late corticogenesis, since use of a conventional *Emx1-Cre* leads to gene inactivation in cortical progenitors from the earliest stages of cortical development.

To gain information on the roles of Pax6 in late cortical development, Pax6 was selectively ablated in cortical progenitors during stages of superficial layer neuron production. Other than the temporal control of *Pax6* deletion in the *Pax6* conditional knockout (cKO) mouse model analysed here, an attractive aspect of the strategy utilized in this study is that it also provides a unique opportunity to create a cortical environment composed of wild-type and *Pax6*$^{-/-}$ mutant cells, resembling that of a chimera. In chimeras, a mixture of mutant and wild-type cells inhabit the same space in a developing organism and therefore intrinsic and extrinsic effects of gene function can be distinguished. In principle, the inability to rescue a particular defective developmental aspect of mutant cells in the presence of wild-type cells suggests cell-autonomous defects, whereas induction of abnormalities in wild-type cells surrounded by mutant cells indicates a cell-non-autonomous requirement of the studied gene in the particular defective process. Previous studies using *Pax6*$^{-/-}$ ↔*Pax6*$^{+/+}$ chimeric embryos have revealed important cell-autonomous and cell-non-autonomous roles for Pax6 in both cortical and eye development (Quinn et al. 1996; Collinson et al. 2000, 2001; Talamillo et al. 2003; Quinn et al 2007). In this study, transient activation of *Emx1-CreER* results in Cre-mediated recombination in a number of *Emx1*-lineage cortical cells that is tamoxifen dose-dependent. Genetic fate mapping of individual cells that have undergone Cre-mediated recombination with the *R26-YFP* reporter enables distinction between *Pax6*$^{-/-}$ and wild-type cortical cells in the same animal. Here, taking advantage of this model, mosaic removal of *Pax6* function in late cortical progenitors suggests that late Pax6 function is required for the generation of a normal cortical environment where late-born neurons can migrate to laminar positions. Moreover, analyses in the context of cKO mice lacking Pax6 from either mid- or late-stage corticogenesis suggest that Pax6 is a key regulator of cortical progenitor proliferation throughout corticogenesis. Proliferation or neuronal migration defects, even in regions of the cKO cortex where Pax6 is not normally expressed at its highest levels, provide strong evidence that for a direct, key requirement for Pax6 function for controlling crucial developmental aspects during superficial laminar formation.

6.2 Results

6.2.1 Late removal of Pax6 affects distinct phases of cortical neuron migration

To assess whether late Pax6 function is required for superficial layer formation, late-born cortical neurons in *Pax6*$^{loxP/loxP}$; *Emx1-CreER*; *R26-YFP* $^{E13.5tamox}$ mutant and *Pax6*$^{loxP/+}$; *Emx1-CreER*; *R26-YFP* $^{E13.5tamox}$ control mice were birthdated with BrdU at E15.5 and their laminar positioning was examined at P7, by which time cortical neuron migration is complete. Analyses were performed at the rostral (Fig. 1), central (Fig. 2) and caudal level (Fig. 3) of the cortex, since Pax6 is expressed in a gradient throughout the cortex. To determine whether likely effects of late Pax6 ablation on neuronal migration arise through a cell-autonomous or/and a cell-non-autonomous mechanism, cortices were double-labelled with BrdU and YFP. Numbers of BrdU/YFP double-labelled and BrdU-positive/YFP-negative cells were quantified in 250-µm-wide radial stripes divided into equally-spaced bins (Fig. 1-3). The proportions of BrdU/YFP double-labelled and BrdU-positive/YFP-negative cells scored in each bin over the total number of BrdU/YFP double-labelled and BrdU-positive/YFP-negative cells counted across cortical laminae were determined in control and mutant mice.

Quantitative analyses of BrdU/YFP double-labelled cells over total numbers of BrdU-positive cells in control and mutant cortices revealed high *Cre*-mediated recombination efficiency in these littermates (rostral: 0.724 ± 0.064 in control, 0.614 ± 0.062 in mutant; central: 0.831 ± 0.017 in control, 0.768 ± 0.046 in mutant; caudal: 0.822 ± 0.021 in control, 0.828 ± 0.013 in mutant). The higher recombination efficiency observed in the caudal cortex compared to rostral levels could be explained due to the graded expression of endogenous *Emx1* in a caudo-medial^{high} to rostro-lateral^{low} fashion throughout the cortex (Briata et al. 1996; Mallamaci et al. 1998). Furthermore, although Emx1 is expressed in virtually all cortical progenitors, its expression in the postnatal cortex is not ubiquitous in every single cortical cell; substantial numbers of GABAergic neurons and glial cells populate the postnatal cortex such that around 85% of cortical neurons are Emx1-positive (Chan et al. 1999; Guo et al. 2000; Chan et al. 2001). These observations indicate a high effectiveness of *Cre*-mediated recombination in the P7 control and mutant cortices analyzed here.

In the rostral mutant cortex, the total number of BrdU-positive cells was slightly reduced across all laminae (113.33 ± 3.024 in control, 91.889 ± 9.633 in mutant) while the total number of BrdU/YFP double-labelled cells was further reduced compared to control (81.78 ± 6.516 in control, 57.11 ± 10.272 in mutant). These differences were not statistically significant between the two genotypes (Student's *t*-test). Proportions of both BrdU/YFP double-labelled and BrdU-positive/YFP-negative neurons exhibited a peak distribution in superficial positions of the mutant cortex, similar to control (Fig. 1E, F). Proportions of BrdU/YFP double-labelled cells were slightly decreased in the superficial mutant cortex while they were considerably increased in deep laminar positions compared to control (Fig. 1E). Interestingly, these birthdating studies revealed a striking accumulation of late-born cells in a deep aspect of the mutant cortex; severely increased numbers of BrdU-positive cells, most of which were also labelled with YFP, accumulated below the white matter (formerly the intermediate zone) leading to the formation of an abnormally enlarged germinal zone in the mutant (Fig. 1B', D'). These findings suggest that, in rostral cortical regions, loss of Pax6 function during the time of superficial layer neuron production influences the ability of late-born neurons to leave their birthplace and migrate to appropriate superficial laminar positions. Intriguingly, such migration defects observed in the mutant cortex were not accompanied by a significant under-representation of late-born neurons in cortical layers.

Qualitative analyses at the central level showed that the proportions of BrdU-positive/YFP-negative cells in superficial laminar positions were very comparable between the two genotypes (Fig. 2D), whereas the peak distribution of BrdU/YFP double-labelled cells was slightly more superficial in the mutant cortex compared to control (Fig. 2C). With regard to the presence of BrdU- positive cells in deep laminar positions, distributions of both BrdU/YFP double-labelled and BrdU-positive/YFP-negative cells were minimal in both control and mutant cortex (Fig. 2C, D). Interestingly, an abnormal band of BrdU-positive cells was detected in a deep position (below the white matter) of the lateral mutant cortex (Fig. 2A', B'), presumably indicating that a number of late-born neurons also fail to migrate away from their birthplace in the central mutant cortex.

FIGURE 1

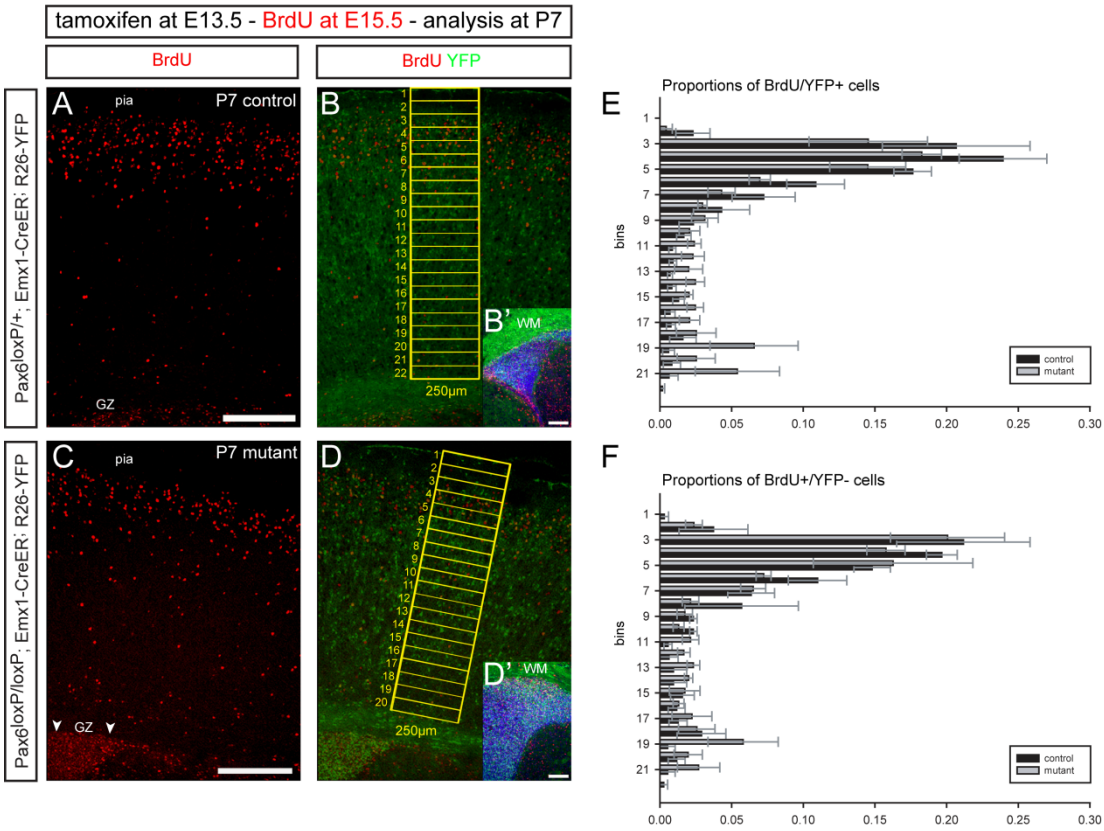

Figure 1. Loss of Pax6 function during late corticogenesis leads to enlargement of the germinal neuroepithelium in the postnatal cortex but does not affect significantly the radial distribution of late-born neurons in the rostral mutant cortex. (A-D) Coronal sections through the rostral cortex of P7 control and mutant mice injected with tamoxifen at E13.5 and BrdU at E15.5. Sections were immunolabeled for BrdU and YFP; medial to the left. The number of BrdU-positive cells was visibly reduced in superficial positions of the mutant cortex compared to control. Notably, large numbers of BrdU-positive cells were observed in the GZ of the mutant cortex. (B, D) The cortical depth was divided into equally spaced 50µm-deep bins, and the number of BrdU/YFP double-labelled and BrdU-positive/YFP-negative cells was scored in each bin. (B', D') High magnification views of the control and mutant GZ shown in B and D, respectively; sections in B' and D' were also counterstained with TOPRO-3 to better visualize cell densities. Note the increase in the size of the mutant GZ with respect to control; the enlarged GZ in the mutant contained high numbers of BrdU/YFP double-labelled cells, but BrdU-positive/YFP-negative cells were also observed. (E, F) Bin distributions of (E) BrdU/YFP double-labelled cells and (F) BrdU-positive/YFP-negative cells (± s.e.m.) in the P7 control and mutant rostral cortex. GZ, germinal zone; WM, white matter. Scale bar, 250 µm.

FIGURE 2

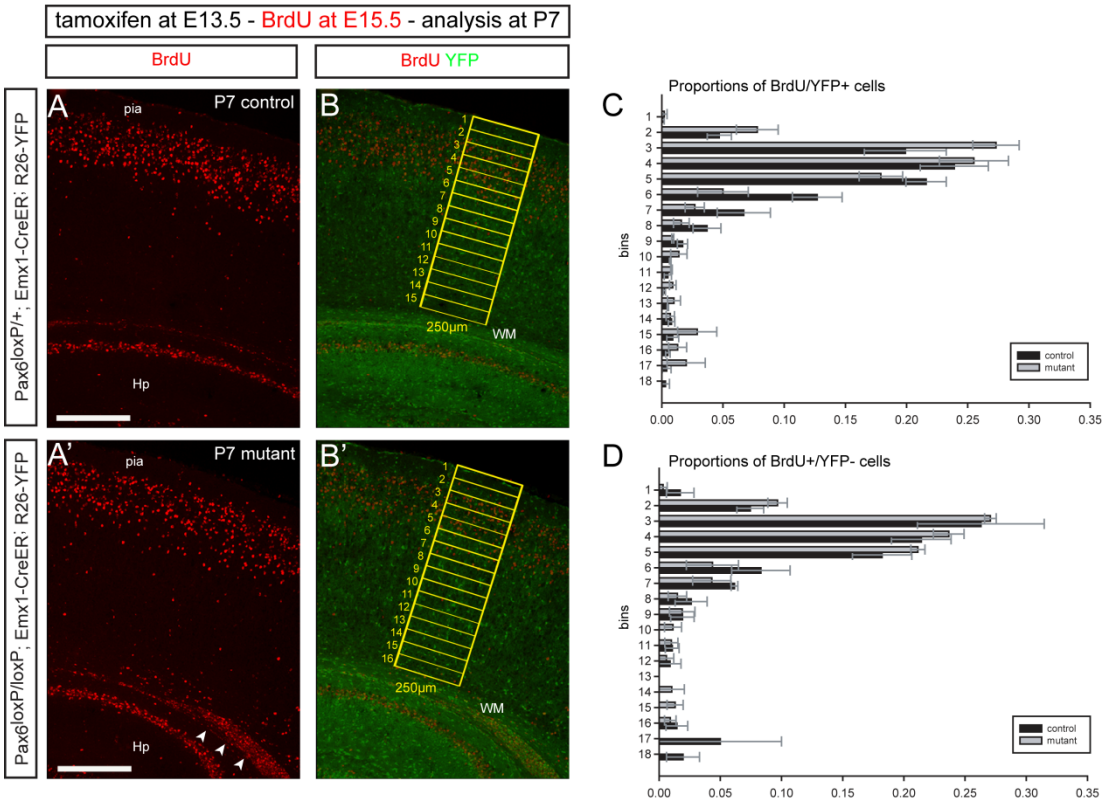

Figure 2. Pax6 deletion during late corticogenesis leads to migration abnormalities of late-born neurons in the central cortex but the final laminar distribution of late-born neurons is unaffected in the mutant cortex. (A-B, A'-B') Coronal sections through the central cortex of P7 control and mutant mice injected with tamoxifen at E13.5 and BrdU at E15.5. Sections were immunoreacted for BrdU and YFP. Medial to the left. (A, A') Late-born BrdU-positive cells formed a denser band in the superficial layers of the control cortex compared to control. Arrowheads indicate the abnormal positioning of BrdU-positive cells in deep locations of the mutant cortex. (B, B') Cortices were divided into equally spaced 50µm-deep bins, and the numbers of BrdU/YFP double-labelled and BrdU-positive/YFP-negative cells were quantified in each bin. (C, D) Graphical representations from birthdating studies in the central cortex showing the proportions of BrdU/YFP double-labelled and BrdU-positive/YFP-negative neurons (± s.e.m.) in each bin. Hp, hippocampus; WM, white matter. Scale bar represents 250 µm.

Caudally, the peak distribution of BrdU-positive/YFP-negative cells was observed in a more superficial domain of the mutant cortex compared to control (Fig. 3D). Such differences between the two genotypes were also evident in the distribution of BrdU/YFP double-labelled cells (Fig. 3C). Again, BrdU-positive cells abnormally accummulated in the deep part of the mutant cortex (Fig. 3A', A). Thus, despite the fact that Pax6 is normally expressed at lower levels in the caudal cortex compared to rostral, loss of Pax6 function during late corticogenesis seems to have a significant effect in the capacity of late-born neurons to migrate out of their site of origin in the caudal cortex.

It could be hypothesized that placement of mutant *Pax6* cells in a cortical environment which resembles more that of a wild-type cortex might be able to rescue the migration defects observed in late-born neurons of the cKO cortex. To test this, similar BrdU birthdating studies were performed in $Pax6^{loxP/loxP}$ mice exhibiting a low *Emx1-Cre* recombination efficiency after tamoxifen administration at E13.5 (Fig. 4). Quantifications of total BrdU-positive and BrdU-YFP double-labelled cells in the rostral cortex of these P7 mice showed that the induction in these control and mutant littermates was around 15%. Strikingly, the presence of even low numbers of *Pax6* mutant cells in the cKO cortex resulted in an abnormal displacement of E15.5-born neurons in deep positions below the white matter, leading to a noticeable enlargement of the germinal neuroepithelium (Fig. 4A'-C'). These findings support further a cell-autonomous requirement for Pax6 during late corticogenesis for proper migration of late-born neurons to cortical layers, while the presence of a substantial number of BrdU-positive/YFP-negative cells in the germinal neuroepithelium of the cKO cortex exhibiting low *Emx1-Cre* recombination (Fig. 4C') also indicate non-cell-autonomous migration defects in the mutant cortex.

In summary, these results demonstrate that Pax6 deficiency in late cortical progenitors leads to increased accumulation of late-born neurons in the mutant germinal zone, likely through both cell-autonomous and cell-non-autonomous mechanisms. The inability to rescue the migration defects even in the context of a *Pax6* cKO cortex exhibiting low recombination efficiency suggests a fundamental requirement for Pax6 in late cortical progenitors to regulate migration of descendant

FIGURE 3

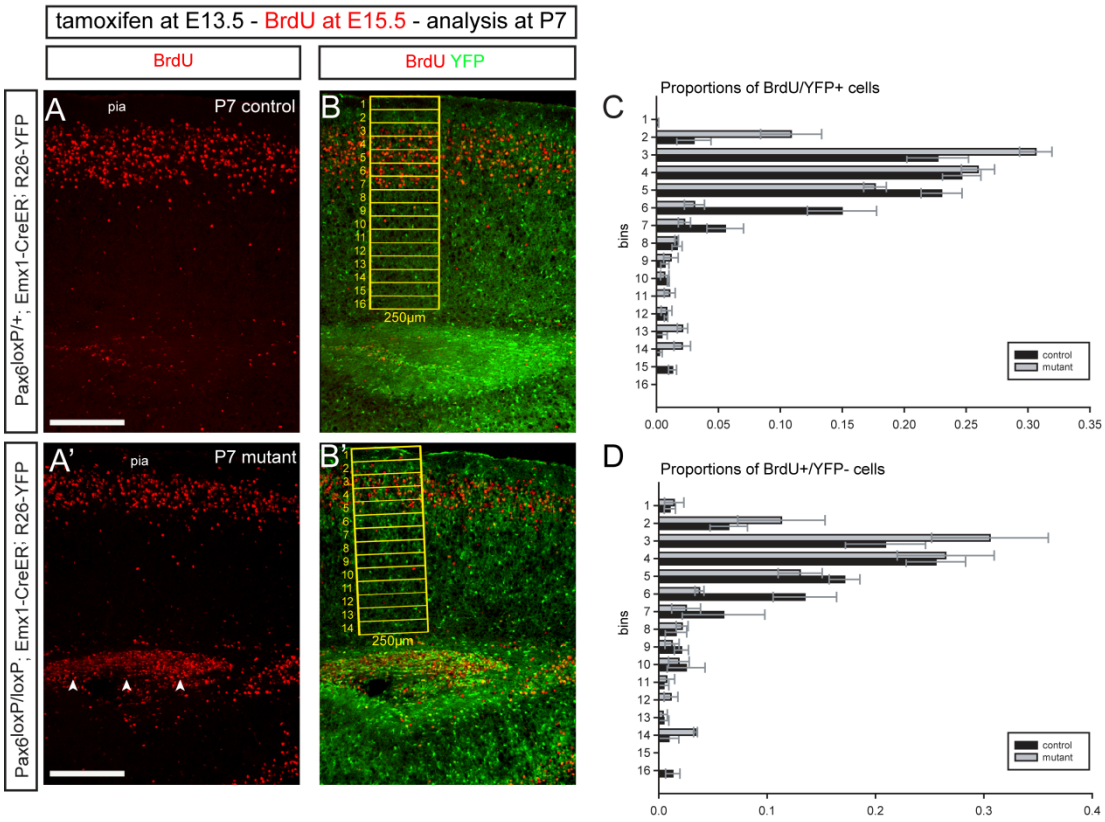

Figure 3. Pax6 inactivation during late corticogenesis affects the migration of late-born neurons in the caudal cortex but the final laminar distribution of late-born neurons is not significantly altered in the mutant cortex. (A-B, A'-B') Coronal sections through the caudal cortex of P7 control and mutant mice injected with tamoxifen at E13.5 and BrdU at E15.5. Cortices were immunostained with anti-BrdU and anti-YFP. Medial to the right. (A, A') BrdU-labelled cells formed a thinner band in the superficial layers of the mutant caudal cortex compared to control. Migration abnormalities of late-born cortical neurons were also detected in the caudal mutant cortex; great numbers of BrdU-positive cells accumulated in deep positions of the mutant cortex (arrowheads in A'). (B, B') Note the high YFP expression in both control and mutant cortex, indicating high Cre-mediated recombination efficiency. The cortical mantle was divided into equally spaced 50µm-deep-bins covering the whole depth of cortical layers. BrdU/YFP double-labelled and BrdU-positive/YFP-negative cells were quantified in each bin. (C, D) Graphical representations from birthdating studies in the caudal cortex showing the proportions of BrdU/YFP double-labelled and BrdU-positive/YFP-negative neurons (± s.e.m.) in each bin. Scale bar represents 250 µm.

FIGURE 4

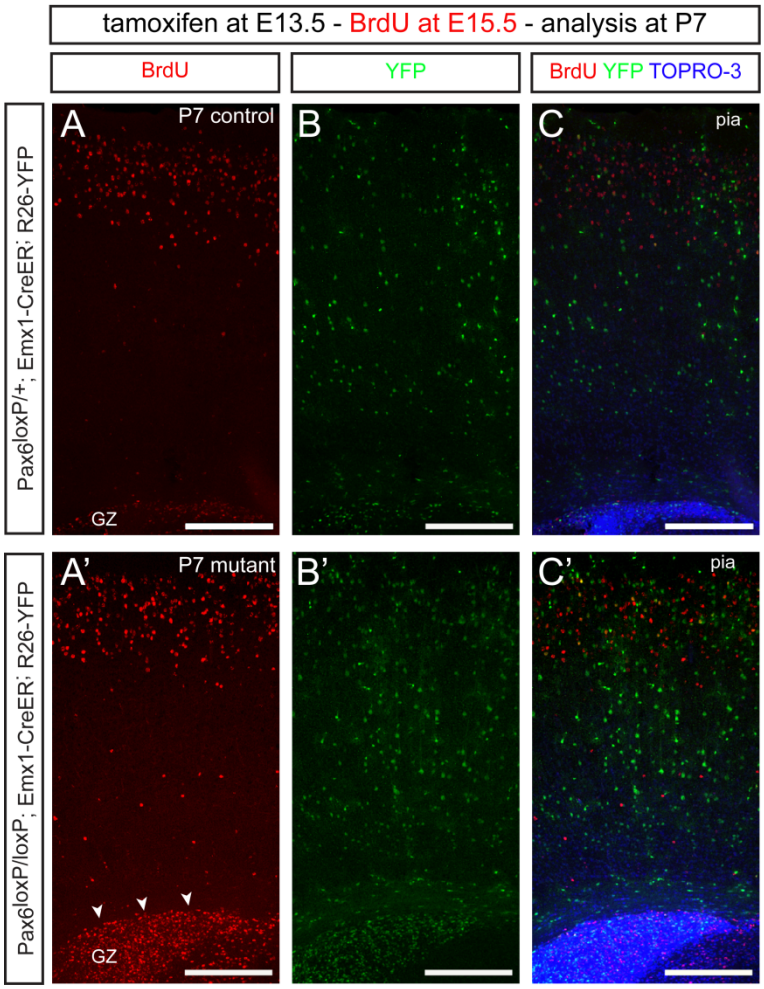

Figure 4. Low *Emx1-CreER* recombination in *Pax6*$^{loxP/loxP}$ mice during late corticogenesis is sufficient to lead to the formation of an expanded germinal neuroepithelium in the P7 mutant cortex. Immunohistochemistry for BrdU (red) and YFP (green) in coronal sections through the rostral cortex of P7 (A-C) control and (A'-C') mutant mice injected with tamoxifen at E13.5 and BrdU at E15.5. (A, A') Increased numbers of BrdU-positive cells were detected in the germinal zone of the mutant cortex (arrowheads in A') compared to control. (B-C, B'-C') Note the few YFP-positive cells in the cortex of both control and mice, indicating low recombination efficiency in these littermates. The expanded germinal zone in the mutant contained increased numbers of YFP-positive cells. Medial to the left. GZ, germinal zone. Scale bars, 250µm.

late-born cortical neurons to appropriate laminar positions. In addition, a marked increase in the numbers of late-born neurons was consistently noticed at all levels of the cKO cortex throughout the rostral-caudal axis, most likely reflecting an enhanced progenitor proliferation after late loss of Pax6.

6.2.2 Pax6 inactivation during late stages of corticogenesis affects superficial laminar formation

Although the birthdating studies showed a normal peak distribution of late-born neurons in superficial positions of the P7 mutant cortex, the possibility of late conditional Pax6 deletion in directly affecting superficial cortical layer formation cannot be excluded. To directly test this hypothesis, late-born cortical neurons in *Pax6*$^{loxP/loxP}$*; Emx1-CreER; R26-YFP* $^{E13.5tamox}$ mice were birth-dated by injecting BrdU at E15.5 and BrdU-positive neurons were double-labelled with Cux1 at P7 (Fig. 5A, B). The proportions of BrdU/Cux1 double-labelled cells over the total number of BrdU-labelled cells were slightly decreased in the mutant cortex compared with control (0.771 ± 0.014 in control, 0.703 ± 0.011 in mutant), but these minor differences were found to be statistically significant (Student's *t*-test P = 0.017, n = 3 per genotype) (Fig. 5C). It should be noted that this analysis was performed in the P7 cortex of *Pax6*$^{loxP/loxP}$*; Emx1-CreER; R26-YFP* $^{E13.5tamox}$ mice where nearly 60% of BrdU-positive cells were double-labelled with YFP in the rostral mutant cortex; therefore, given that the analysis was not conducted in the context of a complete *Pax6* knockout cortex, the relatively minor but significant decrease in the proportions of BrdU/Cux1 double-labelled cells in the mutant cortex might indicate a more pronounced role for Pax6 in directly regulating the specification of superficial layer neurons.

A reduced width of the Cux1-positive domain was observed in the P7 mutant cortex compared to control (Fig. 5A, B). Indeed, the total number of Cux1-positive cells was significantly reduced in the mutant cortex (299.05 ± 18.52 in control, 231.11 ± 7.18 in mutant; Student's *t*-test P = 0.027, n = 3 per genotype). To examine the radial distribution of Cux1-labelled cells, the Cux1-positive domain was subdivided into

FIGURE 5

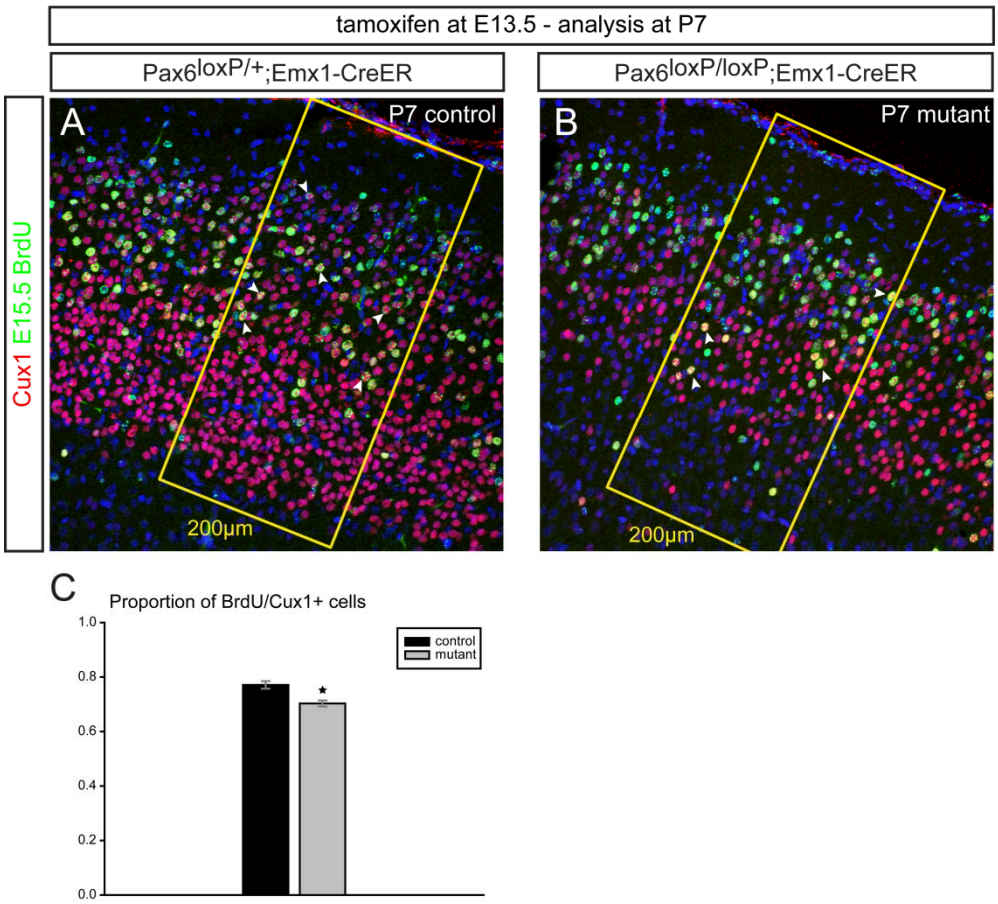

Figure 5. Late Pax6 function is required for specifying superficial laminar identity into late-born neurons at correct proportions. (A, B) High-magnification images of superficial cortical layers at the rostral level of P7 control (*Pax6$^{loxP/+}$; Emx1-CreER* $^{E13.5tamox}$) and mutant (*Pax6$^{loxP/loxP}$; Emx1-CreER* $^{E13.5tamox}$) mice injected with tamoxifen at E13.5 followed by BrdU administration at E15.5. Coronal sections double-immunostained with BrdU (green) and Cux1 (red). Arrowheads point to BrdU-positive neurons co-expressing Cux1. The numbers of BrdU-positive and BrdU/Cux1 double-labelled cells were counted in 200-µm-wide radial stripes through the cortex of control and mutant mice. (C) Quantitative analysis shows that the proportions of BrdU-positive cells that were double-labelled with Cux1were slightly reduced in the mutant cortex with respect to control, but this difference was found to be statistically significant (Student's *t*-test $P = 0.017$, $n = 3$ per genotype).

bins of equal 50-µm depth and the proportions of immunolabeled cells scored into each bin over total numbers of Cux1-expressing cells were determined in P7 control and mutant cortices (Fig. 6A-C). Qualitative analysis showed that the proportions of Cux1-labelled cells were increased in superficial positions of the mutant cortex, whereas they were decreased in lower laminar positions corresponding to layer IV.

The radial distribution of E15.5-born neurons in superficial layers of P7 control and mutant cortex was also examined in the same sections as those used for the BrdU/Cux1 analysis in Fig. 5 (Fig. 6D, E). Increased proportions of BrdU-labelled cells were detected in the most superficial domain of the mutant cortex, accompanied by a decreased contribution to deeper positions of the superficial mutant cortex compared to control (Fig. 6F). The total number of BrdU-labelled cells in superficial layers of the mutant cortex was decreased (82.08 ± 7.21 in control, 67.31 ± 1.65 in mutant) but not significantly altered compared to control (Student's *t*-test).

Collectively, these findings indicate that, at late stages of corticogenesis, *Pax6*-deficient progenitors do produce superficial layer neurons that exhibit an apparently normal molecular phenotype. However, late Pax6 function is required for specifying late-born superficial neuron identity at correct proportions, at least at rostral levels of the cortex.

6.2.3 Pax6 loss during mid-corticogenesis leads to reduced numbers and disturbed specification of late-born neurons in superficial cortical layers

Injection of tamoxifen at E10.5 was used to examine further the production of superficial layers in the conditional *Pax6* mutant cortex. Late-born neurons in *Pax6*$^{loxP/loxP}$*; Emx1-CreER; R26-YFP* $^{E10.5tamox}$ mice were birthdated by injecting BrdU at E15.5, and BrdU-positive cells were double-labelled with Cux1 at P7 (Fig. 7A, B). Quantifications of BrdU/YFP double-labelled and BrdU-positive/YFP-negative cells in the rostral cortex indicated high recombination efficiency in control and mutant littermates; the proportion of BrdU/YFP double-labelled cells over total numbers of BrdU-positive cells was around 80%. The number of E15.5-born neurons was significantly reduced in the superficial layers of the P7 mutant cortex (69.15 ±

FIGURE 6

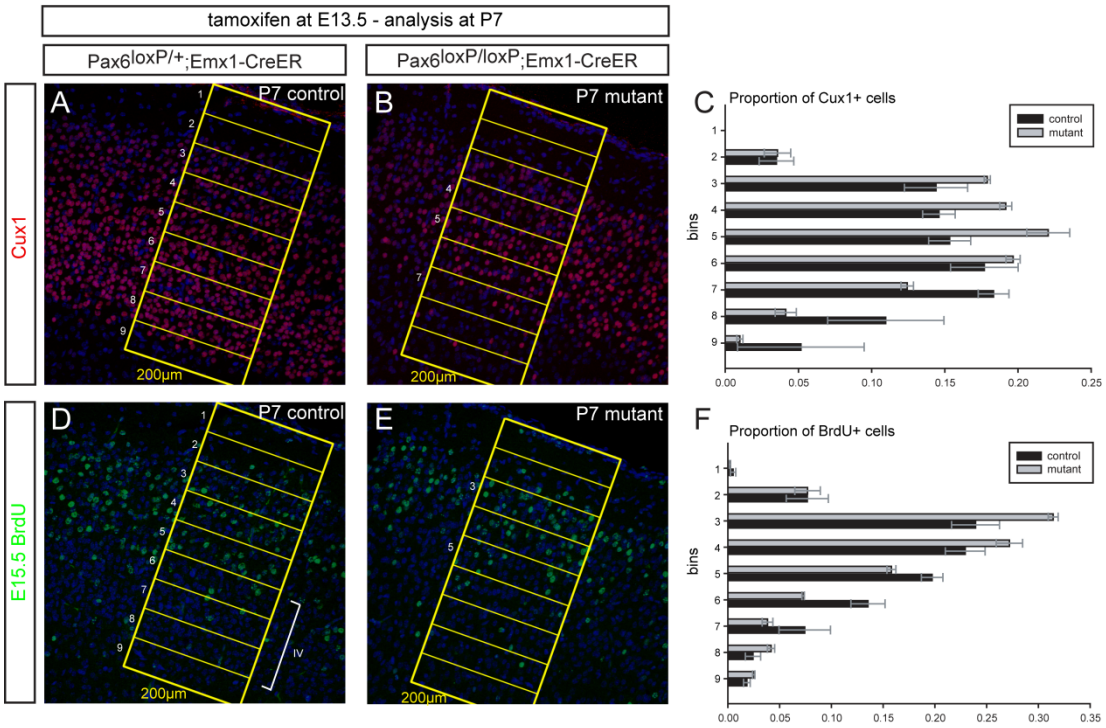

Figure 6. Radial distributions of Cux1-positive and E15.5-born cells in superficial layers of mice lacking Pax6 during late corticogenesis. Coronal sections through the rostral cortex of P7 control and mutant mice immunolabeled with (A, B) anti-Cux1 and (D, E) anti-BrdU. The radial thickness of the superficial aspect of the cortex was divided into equally spaced 50-µm-deep bins and the number of Cux1-expressing or BrdU-labelled neurons was assigned into each bin. (A, B) The width of the Cux1-positive domain was visibly thinner in the mutant cortex compared to control. (C) In the mutant cortex, proportions of Cux1-labelled neurons were increased in superficial positions (bin4: 0.146 ± 0.011 in control, 0.192 ± 0.004 in mutant; bin 5: 0.153 ± 0.014 in control, 0.221 ± 0.015 in mutant) compared to more inferior ones (bin 7: 0.183 ± 0.011 in control, 0.124 ± 0.004 in mutant). Note that the decreased proportions of Cux1-positive cells in bin 7 of the mutant cortex corresponds to layer IV in the control, better visualized in D showing views of the same cortical section as in A. (D, E) Patterns of BrdU labelling in P7 control and mutant mice after injection of BrdU at E15.5. (F) Proportions of BrdU-labelled neurons were increased in superficial positions of the mutant cortex (bin 3: 0.239 ± 0.023 in control, 0.314 ± 0.005 in mutant), accompanied by a decrease in more inferior ones (bin 5: 0.197 ± 0.01 in control, 0.158 ± 0.004 in mutant). The altered distribution of BrdU-labelled cells in bin 5 of the mutant cortex corresponds to the bottom of layer III in the control in D.

6.67 s.e.m. in control, 14.45 ± 2.43 in mutant; Student's *t*-test $P < 0.002$; $n = 3$ of each genotype). In controls, nearly 80% of BrdU labelled cells were double-labelled for Cux1; in mutants there was a large significant reduction to about 30% in the proportion of BrdU labelled cells that were Cux1 double-labelled (Fig. 7C). These findings indicate that both generation and specification of superficial layer neurons are severely affected by loss of Pax6 from mid-stages of corticogenesis.

6.2.4 Pax6 ablation during late corticogenesis does not affect cell fate specification of neurons localized in deep cortical layers

According to the "inside-out" pattern of cortical layering, the generation of deep layer neurons should precede the time of Pax6 loss in the *Pax6*$^{loxP/loxP}$*; Emx1-CreER; R26-YFP* $^{E13.5tamox}$ cortex. Although Pax6 ablation in these mutants would not be expected to affect deep layer formation, the morphological features of deep layer neurons should be examined. The cellular identity of layer VI and V neurons was assessed in the P7 mutant cortex by immunostaining sections at the central level with Tbr1 or Ctip2 (Fig. 8). To also test whether the few late-born neurons located in deep layers of the mutant cortex (as reported in 6.2.1) switch fate and acquire a deep-layer identity, cortical sections of mice injected with BrdU at E15.5 were double- labelled for BrdU. High-level Ctip2-expressing neurons in layer V (Fig. 8B, D) and Tbr1-expressing neurons in layer VI were present in the mutant cortex (Fig. 8F, H), supporting the interpretation that deep layer neurons are born normally and are correctly specified according to their laminar position when Pax6 is inactivated during late corticogenesis. The characteristic morphology of large pyramidal neurons in layer V was preserved in the mutant cortex (Fig. 8B, D). However, an expansion of layers V and VI was observed in the mutant cortex compared to control, accompanied by a reduction in the thickness of mutant superficial layers IV/II and especially that of layer IV (Fig. 8 A-B, E-F). Notably, BrdU-labelled cells located in deep layers of the mutant cortex did not co-express Ctip2 or Tbr1 (Fig. 8 D, H), indicating that neurons born from E15.5 onwards are not misspecified to deep layer neurons even if they occupy laminar positions where neurons of a deep laminar fate are normally found.

FIGURE 7

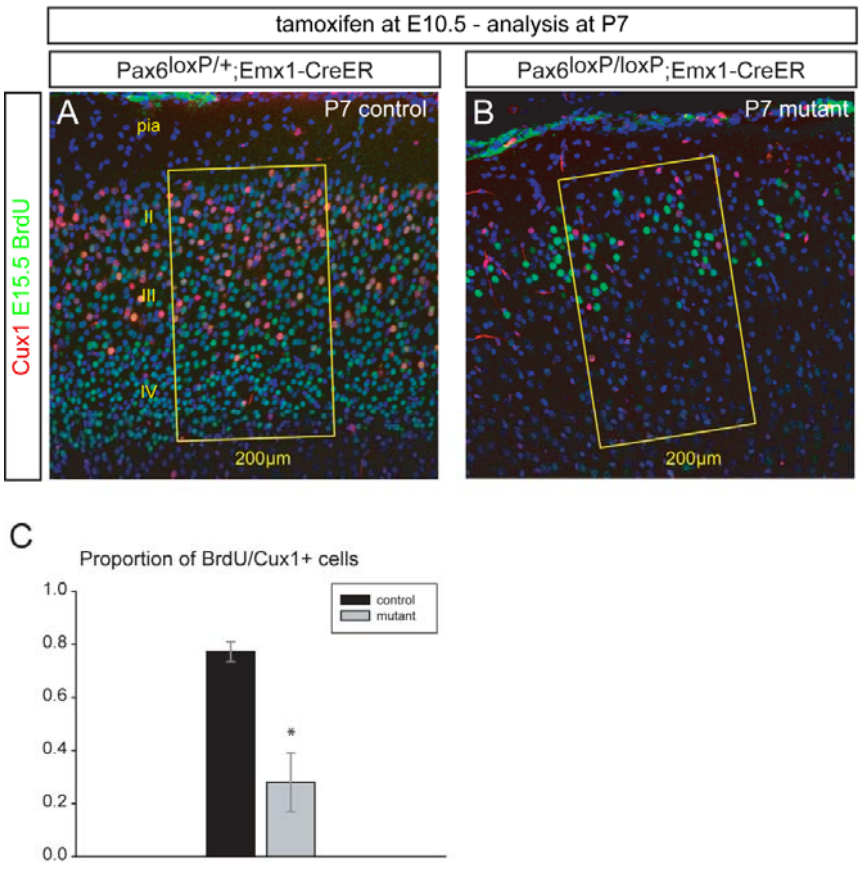

Figure 7. Late-born neurons are severely reduced in number and are not correctly specified in superficial cortical layers of conditional knock-out mice lacking Pax6 from mid-corticogenesis. (A, B) High-power views of superficial cortical layers (IV-II) of P7 control (*Pax6*$^{loxP/+}$; *Emx1-CreER*^{T2}) and mutant (*Pax6*$^{loxP/loxP}$; *Emx1-CreER*^{T2}) mice injected with tamoxifen at E10.5 followed by BrdU administration at E15.5; images show double-immunostaining for BrdU (red) and Cux1 (green). Note the severe reduction in the number of both BrdU-labelled cells and Cux1-labelled cells in the superficial layers of the mutant cortex. The numbers of BrdU-positive and BrdU/Cux1 double-labelled cells were counted in 200-µm-wide radial stripes through the cortex of control and mutant mice. (C) The proportions of BrdU-positive cells that were Cux1/BrdU double-labelled were significantly reduced in the mutant cortex compared to control (Student's *t*-test $p<0.01$; n=3 of each genotype).

FIGURE 8

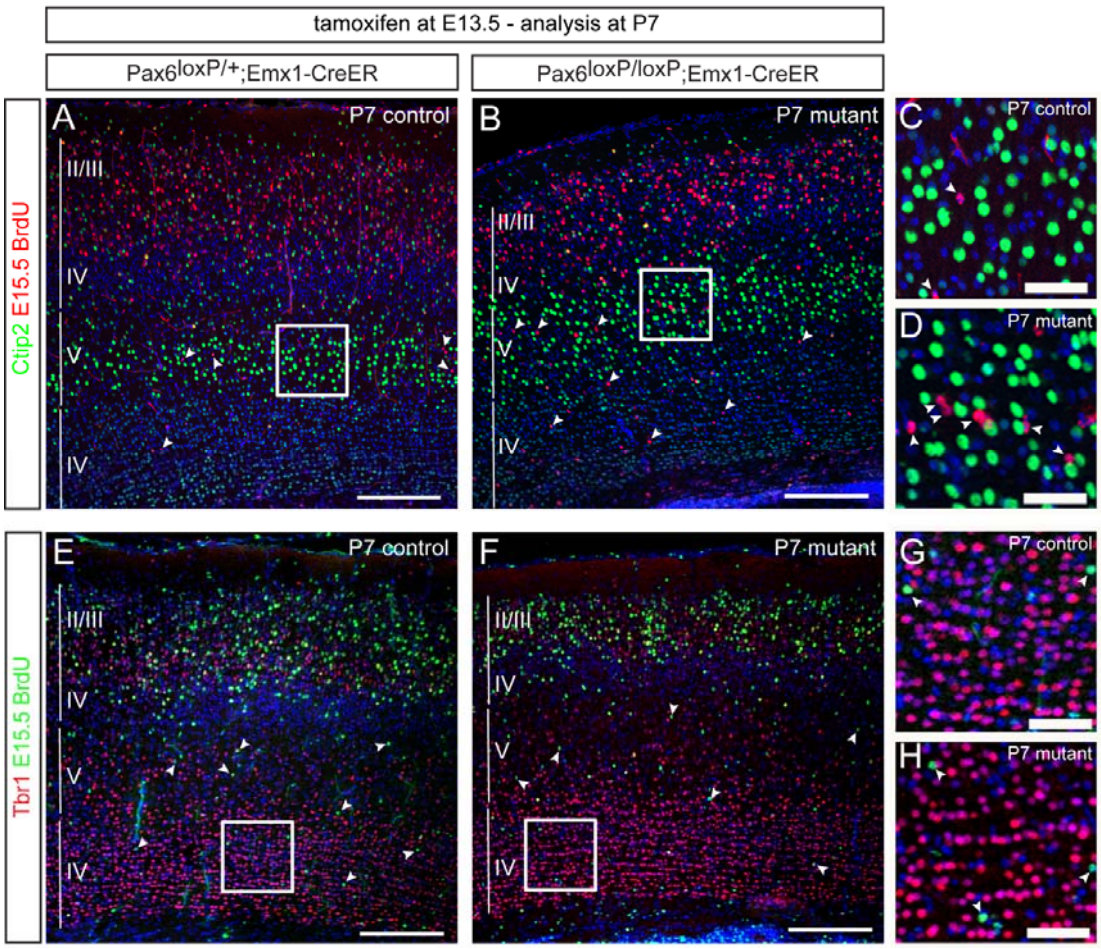

Figure 8. Deep layer neurons are correctly specified in the postnatal cortex of mice lacking Pax6 during late corticogenesis. Deep cortical layers in P7 control and mutant brains were visualized by using (A, B) Ctip2, which is expressed at high levels in corticospinal neurons of layer V, and (C, D) Tbr1, which is highly expressed in neurons of layer VI. A decrease in the thickness of layer IV was detected in the mutant cortex (B, D) with respect to control (A, C). Arrowheads point to late-born neurons BrdU-positive neurons distributed in deep layers VI and V of the control and mutant cortex. Examples of boxed regions are shown at a higher magnification to the right. Consistent with previous observations, slightly increased numbers of BrdU-positive cells were detected in deep laminar positions of the P7 mutant cortex (B, D) with respect to control (A, C). Late-born BrdU-positive cells distributed in deep layers of the mutant cortex did not co-express Ctip2 (B) or Tbr1 (D), indicating that they are not misspecified to deep layer neurons. Scale bars, 200µm (A-B, E-F), 50 µm (C-D, G-H).

6.2.5 Late Pax6 inactivation leads to increased accumulation of late-born neurons in the P0 cortex through both a cell-autonomous and cell-non-autonomous mechanism

To further investigate neuronal migration in the cortex of *Pax6$^{loxP/loxP}$; Emx1-CreER* $^{E13.5tamox}$ mice, neurons were birthdated via injection of BrdU at E16.5 and their positioning in control and mutant cortices was assessed at P0. Coronal sections through the rostral, central and caudal cortex of *Pax6$^{loxP/+}$; Emx1-CreER; R26-YFP* $^{E13.5tamox}$ control and *Pax6$^{loxP/loxP}$; Emx1-CreER; R26-YFP* $^{E13.5tamox}$ mutant mice were double-immunolabeled with BrdU and YFP (Fig. 9, 10 and 11 A-C, A'-C'). A severe expansion of the mutant VZ compared to control was observed at all levels. To quantify this defect, and to also assess whether abnormalities are caused through a cell-autonomous and/or a cell-non-autonomous mechanism, numbers of BrdU/YFP double-labelled and BrdU-positive/YFP-negative cells were counted in 200-µm-wide radial stripes covering the depth of the ventricular zone (VZ), intermediate zone (IZ) and cortical plate (CP) of the mutant and control cortex (Fig. 9, 10, 11C-C'). Analyses of the proportions of BrdU/YFP double-labelled cells or BrdU-positive/YFP-negative cells in each cortical region (VZ, IZ or CP) over the total number of BrdU/YFP double-labelled cells or BrdU-positive/YFP-negative cells in all three regions revealed significant differences between control and mutant cortex (Fig. 9, 10, 11D-E). At all levels throughout the rostral-caudal axis, ANOVA showed significantly different distributions of BrdU/YFP double-labelled cells and BrdU-positive/YFP-negative cells in the P0 mutant cortex compared to controls ($P < 0.001$, $n = 3$ per genotype). A 2-fold increase in the proportion of BrdU/YFP double-labelled cells located in the VZ was found in the mutant cortex compared to control (rostral: 0.487 ± 0.015 in control, 0.852 ± 0.018 in mutant, Student's *t*-test $P < 0.001$, $n = 3$ per genotype; central: 0.408 ± 0.038 in control, 0.723 ± 0.054 in mutant, Student's *t*-test $P = 0.009$, $n = 3$ per genotype; caudal: 0.438 ± 0.045 in control, 0.754 ± 0.005 in mutant, Student's *t*-test $P = 0.002$, $n = 3$ per genotype). These differences in the VZ were accompanied by significant reductions in the proportions of BrdU/YFP double-labelled cells located in the mutant CP with respect to control (rostral: 0.249 ± 0.024 in control, 0.083 ± 0.015 in mutant, Student's *t*-test $P = 0.004$, $n = 3$ per genotype; central: 0.364 ± 0.016 in control, 0.167 ± 0.026 in mutant,

FIGURE 9

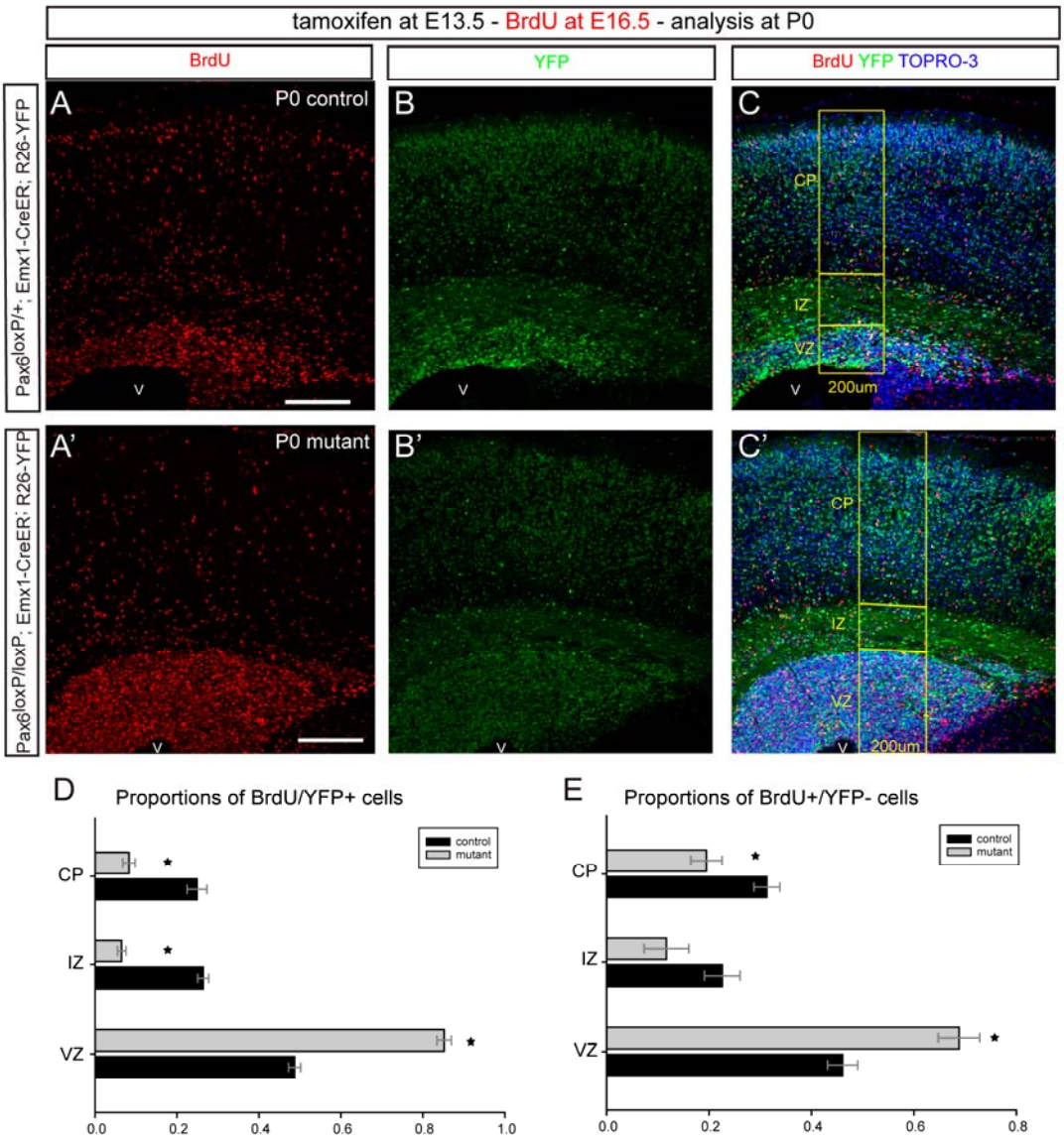

Figure 9. Pax6 inactivation in late cortical progenitors results in cell-automomous and cell-non-autonomous migration abnormalities of late-born neurons in the rostral P0 mutant cortex. (A-C, A'-C') Coronal sections through the rostral cortex of P0 (A-C) control and (A'-C') mutant mice injected with tamoxifen at E13.5 and BrdU at E16.5. Medial to the left. Cortices were immunostained for BrdU and YFP and counterstained with TOPRO-3. Increased numbers of BrdU-labelled neurons were detected in the mutant cortex. The VZ of the rostral mutant cortex was densely packed with BrdU-positive cells leading to a severe expansion of the mutant VZ compared to control. Numbers of BrdU/YFP double-labelled and BrdU-positive/YFP-negative cells were counted in radial stripes spanning the whole depth of cortices, as shown in C, C'. (C, D) Graphical representations of data from BrdU birthdating showing that the proportions of late-born BrdU/YFP double-labelled and BrdU-positive/YFP-negative cells were differentially distributed in the mutant cortex versus control. IZ, intermediate zone; CP, cortical plate; VZ, ventricular zone; v, ventricle. Scale bars: 200 µm.

FIGURE 10

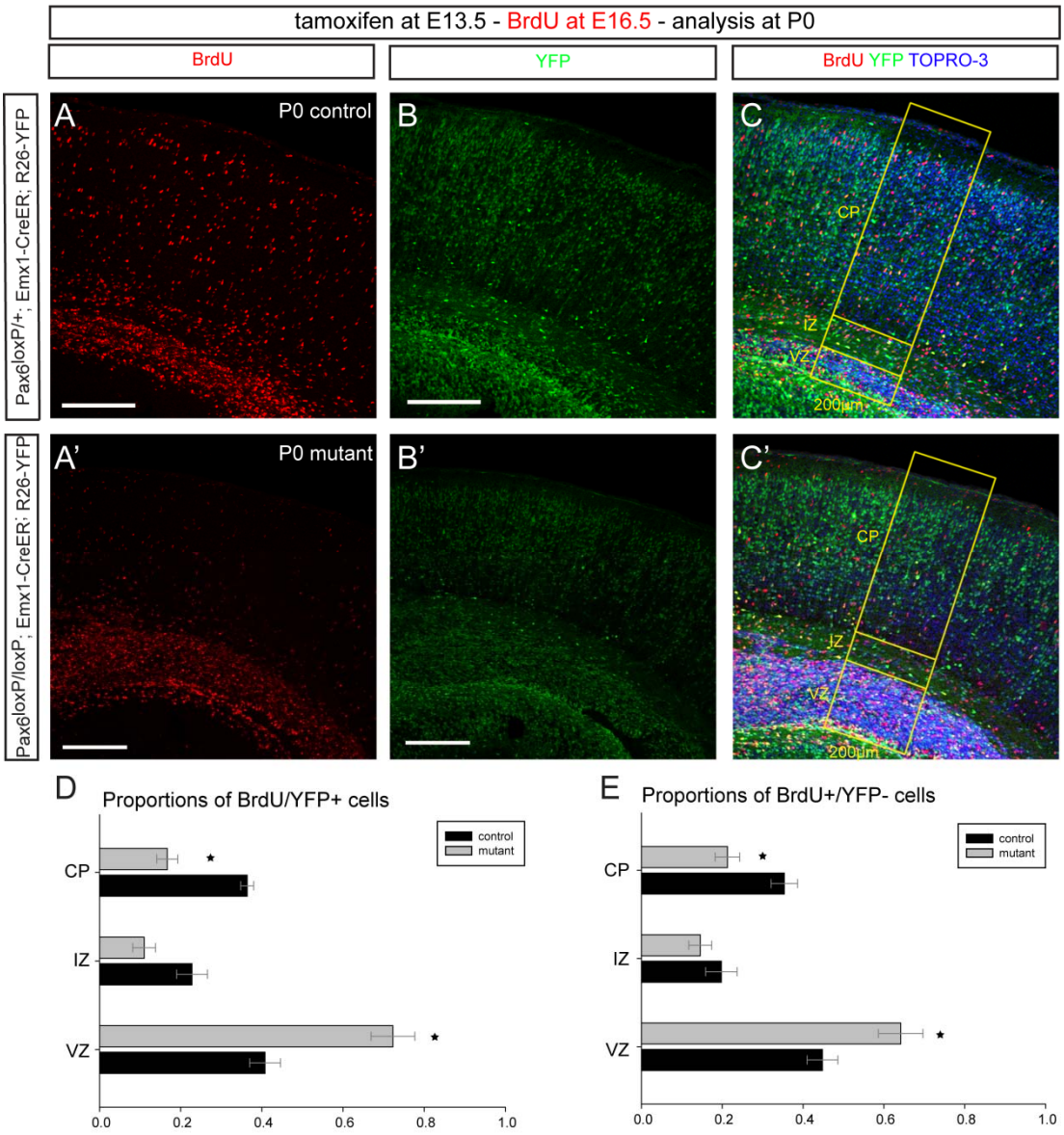

Figure 10. Cell-autonomous and cell-non-autonomous migration defects in the central P0 cortex of mice lacking Pax6 during late corticogenesis. (A-C, A'-C') Coronal sections through the central cortex of P0 (A-C) control and (A'-C') mutant mice injected with tamoxifen at E13.5 and BrdU at E16.5. Medial to the left. Sections were immunostained for BrdU and YFP and counterstained with TOPRO-3. A notable increase in the number of BrdU-labelled cells was detected in deep positions of the mutant cortex, while BrdU-labelled cells were under-represented in the mutant cortical plate (CP) with respect to control. Cortices were divided into 3 bins corresponding to the ventricular zone (VZ), intermediate zone (IZ) and CP. BrdU/YFP double-labelled and BrdU-positive/YFP-negative cells in each bin were counted in control and mutant. (D, E) Graphical representations of data from BrdU birthdating showing that the radial distribution of proportions of both BrdU/YFP double-labelled and BrdU-positive/YFP-negative cells in the VZ and CP were significantly different (*) between the two genotypes. Scale bars: 200 µm.

Student's *t*-test $P = 0.003$, $n = 3$ per genotype; caudal: 0.343 ± 0.065 in control, 0.15 ± 0.002 in mutant, Student's *t*-test $P = 0.041$, $n = 3$ per genotype). Proportions of BrdU/YFP double-labelled cells were also significantly reduced in the IZ of the rostral and caudal mutant cortex compared to control (rostral: 0.264 ± 0.013 in control, 0.065 ± 0.011 in mutant, Student's *t*-test $P < 0.001$, $n = 3$ per genotype; caudal: 0.219 ± 0.033 in control, 0.096 ± 0.006 in mutant, Student's *t*-test $P = 0.021$, $n = 3$ of each genotype). Throughout the rostral-caudal mutant cortex, absolute numbers of BrdU/YFP double-labelled cells in the CP were not significantly different compared to control (Student's *t*-test), indicating that the significantly altered distribution of BrdU/YFP double-labelled cells in the mutant cortex is due to a severe increase in the number BrdU/YFP double-labelled cells located in the mutant VZ.

Interestingly, the radial distribution of BrdU-positive/YFP-negative cells in the P0 cortex was also affected by late Pax6 loss. The proportions of BrdU-positive/YFP-negative cells were significantly increased in the mutant VZ (rostral: 0.461 ± 0.029 in control, 0.688 ± 0.041 in mutant, Student's *t*-test $P = 0.011$, $n = 3$ per genotype; central: 0.448 ± 0.038 in control, 0.642 ± 0.055, Student's *t*-test $P = 0.045$, $n = 3$ per genotype; caudal: 0.458 ± 0.021 in control, 0.695 ± 0.05 in mutant, Student's *t*-test $P = 0.012$, $n = 3$ per genotype). These changes were accompanied by significantly reduced proportions of BrdU-positive/YFP-negative cells in the CP of the rostral and central mutant cortex (rostral: 0.313 ± 0.026 in control, 0.195 ± 0.03 in mutant, Student's *t*-test $P = 0.041$, $n = 3$ per genotype; central: 0.354 ± 0.033 in control, 0.213 ± 0.03 in mutant, Student's *t*-test $P = 0.034$, $n = 3$ per genotype), while in the CP of the caudal cortex differences between the two genotypes were not statistically significant (0.319 ± 0.052 in control, 0.185 ± 0.017 in mutant, Student's *t*-test $P = 0.073$, $n = 3$ per genotype). These results indicate that Pax6 inactivation during superficial layer neuron generation causes cell-autonomous and cell-non-autonomous defects in the radial distribution of late-born neurons in the P0 cortex.

The radial thickness of the VZ, IZ, CP and layer I was also measured in the P0 control and mutant cortices. As expected, the thickness of the mutant VZ was significantly increased compared to control at all levels throughout the cortex

FIGURE 11

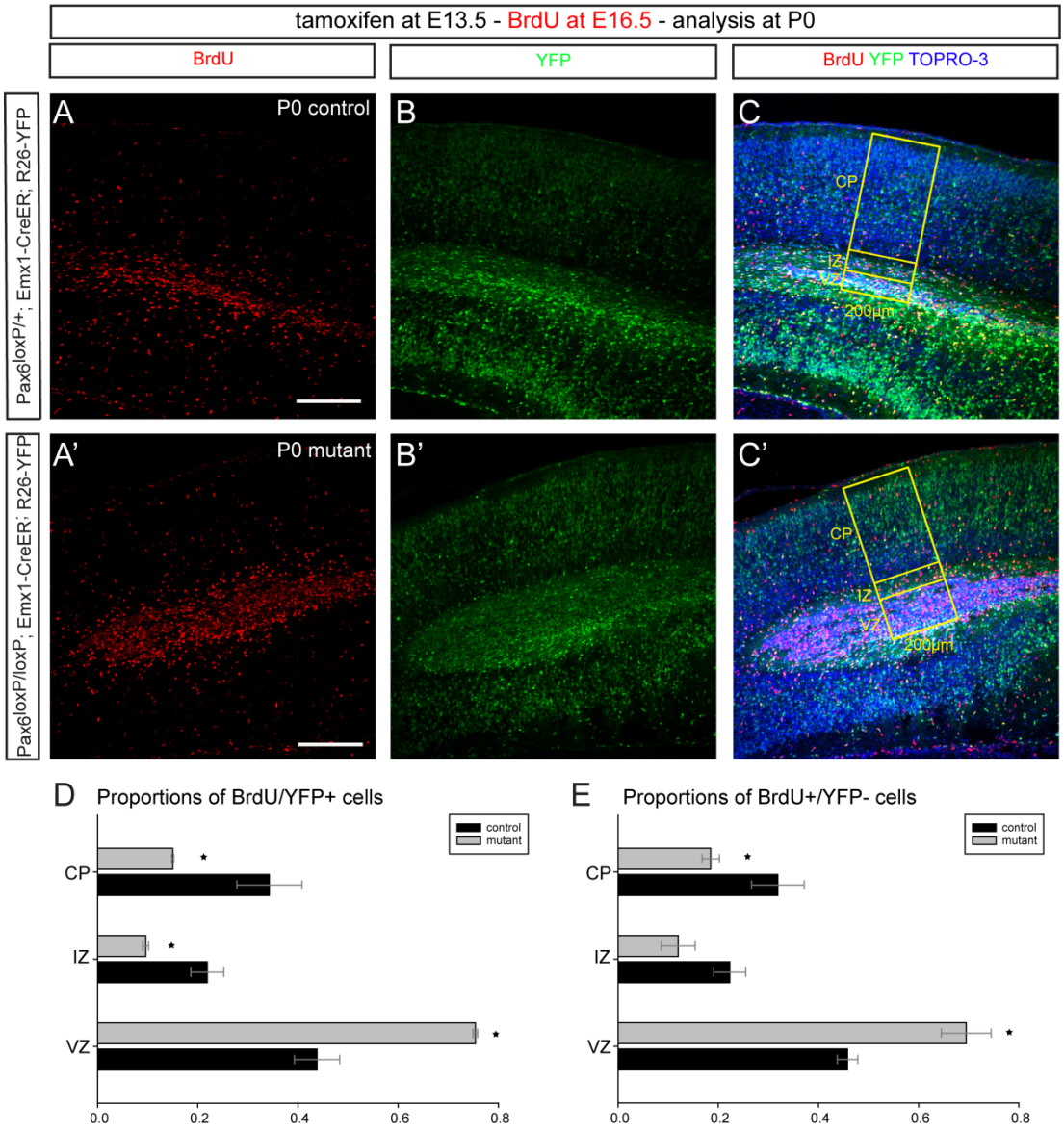

Figure 11. Late Pax6 inactivation impairs the migration capacity of late-born cortical neurons in the caudal P0 cortex both cell-autonomously and cell-non-autonomously. (A-C, A'-C') Coronal sections through the caudal cortex of P0 (A-C) control and (A'-C') mutant mice injected with tamoxifen at E13.5 and BrdU at E16.5. Medial to the left. Sections were immunostained for BrdU and YFP and counterstained with TOPRO-3. Increased numbers of late-born BrdU-labelled cortical neurons were specifically detected in deep positions of the mutant cortex, corresponding to the mutant VZ. Numbers of BrdU/YFP double-labelled and BrdU-positive/YFP-negative cells were counted in radial stripes spanning the whole depth of control and mutant cortices, as shown in C, C'. (C, D) Graphical representations of data from BrdU birthdating showing that the proportions of late-born BrdU/YFP double-labelled and BrdU-positive/YFP-negative cells were significantly different (*) in regions across the mutant cortex compared with control. IZ, intermediate zone; CP, cortical plate; VZ, ventricular zone; v, ventricle. Scale bars: 200 µm.

(rostral: 3.76 ± 0.336 cm in control, 8.53 ± 1.043 cm in mutant, Student's *t*-test P = 0.012; central: 2.28 ± 0.182 cm in control, 4.92 ± 0.848 cm in mutant, Student's *t*-test P = 0.038; caudal: 1.5 ± 0.104 cm in control, 3.05 ± 0.182 cm in mutant, Student's *t*-test P = 0.002; n = 3 per genotype) (Fig. 12A-C). A slight decrease in the thickness of the mutant CP was detected in the caudal cortex compared to control, although this difference was statistically significant (12.99 ± 0.147 cm in control, 11.81 ± 0.062 in mutant, Student's *t*-test P = 0.002; n = 3 per genotype).

Findings here suggest that late loss of Pax6 function affects neuronal migration both cell-autonomously and cell-non-autonomously; abnormally increased numbers of late-born neurons were inappropriately localized in their birthplace instead of migrating outwards to cortical layers in the P0 mutant cortex. During late stages of corticogenesis, radial glial cells (RGCs) provide the structural framework for neuronal migration to appropriate laminar positions in the cortex. To assess whether migration abnormalities of late-born neurons in the mutant cortex arise due to defects in the architecture of the radial glial scaffold, the morphology of YFP-labelled cells was examined in high magnification images of the P0 control and mutant cortex (Fig. 13C-D, C'-D'). YFP-labelled neurons were morphologically arranged in the same radial orientation across the thickness of both mutant and control cortex, while in the underlying subplate (SP) and IZ the density of YFP-labelled processes was very high in both genotypes. Visualization of callosal commissural (CC) neurons indicated that the morphology of YFP-labelled CC neurons in the mutant cortex was similar to control (Fig. 13A-B, A'-B'). These findings indicate that the gross morphology of pyramidal neurons throughout the cortex is not affected by Pax6 loss in late cortical progenitors, and further suggest that the organization of the radial glial scaffold does not make a significant contribution to migration defects observed in the postnatal *Pax6*$^{loxP/loxP}$; *Emx1-CreER*; *R26-YFP* $^{E13.5tamox}$ mutant cortex.

FIGURE 12

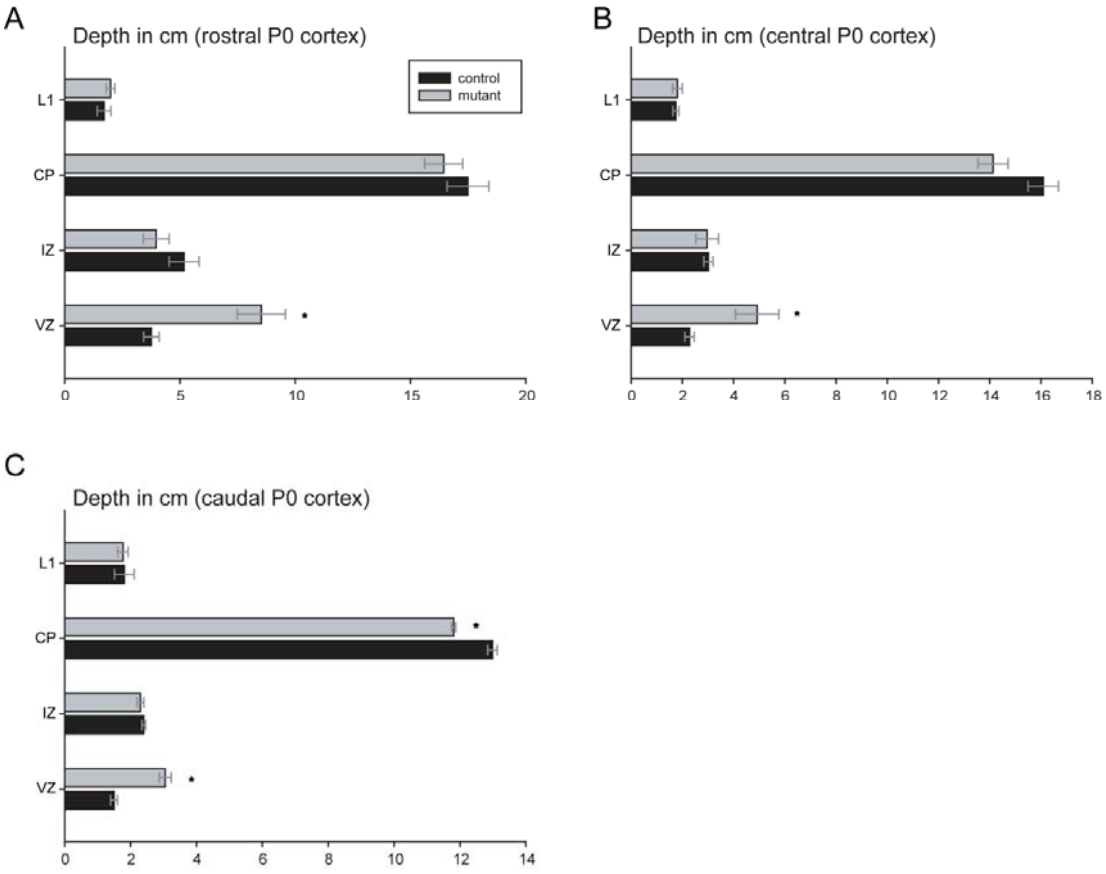

Figure 12. Late Pax6 inactivation leads to increased VZ thickness in the P0 mutant cortex at all cortical levels throughout the rostral-caudal axis. The depth of *Pax6*$^{loxP/+}$*; Emx1-CreER* $^{E13.5tamox}$ control and *Pax6*$^{loxP/loxP}$*; Emx1-CreER* $^{E13.5tamox}$ mutant P0 cortices was divided radially into 4 bins corresponding, from inside-out, to ventricular zone (VZ), intermediate zone (IZ), cortical plate (CP) and layer 1 (L1). (A-C) Graphical representations of depth measurements (± s.e.m.) in the (A) rostral, (B) central and (C) caudal cortex of control and mutant mice. The depth of the mutant VZ was significantly increased with respect to controls at all rostral-caudal levels analyzed. The thickness of the mutant CP was found to be significantly decreased in the mutant caudal cortex compared to control.

6.2.6 Conditional inactivation of Pax6 during late corticogenesis impairs cortical progenitor proliferation

To conclusively determine whether late inactivation of Pax6 induces cortical progenitor proliferation, the number of S-phase progenitors in *Pax6*$^{loxP/loxP}$; *Emx1-CreER*; *R26-YFP* $^{E13.5tamox}$ mice was first assessed at E15.5, a developmental stage at which Pax6 protein expression was found to be reduced in the mutant cortex. Tamoxifen was injected into E13.5 pregnant females and BrdU was injected 48 h post-tamoxifen administration; cortices were analysed 1 h after the BrdU pulse. E15.5 control and mutant cortices were double-labelled with BrdU and YFP (Fig. 14A-C, A'-C') in order to discriminate between S-phase cells that had undergone Cre recombination and those that had escaped recombination; the cell population co-expressing BrdU and YFP in the mutant cortex would include S-phase progenitors that would normally express Pax6 but have lost Pax6 expression due to Cre recombination, whereas the BrdU-positive/YFP-negative cell population would include Pax6-expressing progenitors in the mutant cortex. The vast majority of cells in the cortex of control and mutant mice were expressing YFP (Fig. 14B, B'). Quantification of BrdU/YFP double- labelled and BrdU-positive/YFP-negative cells in the control and mutant cortex at rostral, central and caudal levels revealed that nearly 85% of BrdU-labelled cells were doubled-labelled for YFP in controls, while in mutants nearly 80% of BrdU-positive cells co-expressed YFP. Neither the numbers of BrdU/YFP double-labelled cells (Fig. 14D) nor the numbers of BrdU-positive/YFP-negative cells (rostral: 21.39 ± 7.08 in control, 45.55 ± 14.98 mutant; central: 13.22 ± 2.82 in control, 20.33 ± 3.79 in mutant; caudal: 11.33 ± 1.64 in control, 20.11 ± 4.95 in mutant) were significantly different between E15.5 control and mutant cortex. However, the total number of BrdU-labelled cells was significantly increased in the rostral mutant cortex compared with control (136.64 ± 4.76 in control, 166.61 ± 4.04 in mutant, Student's *t*-test $P = 0.009$; $n = 3$ of each genotype). Such differences in the total number of BrdU-labelled cells between the two genotypes were less obvious in central (116 ± 7.76 in control, 133.66 ± 5.23 in mutant) and caudal (95.78 ± 1.5 in control, 108.78 ± 3.85 in mutant) levels, although differences between control and mutant cortex were found to be significant caudally (Student's *t*-test $P = 0.035$; $n = 3$ of each genotype). These findings indicate an

FIGURE 13

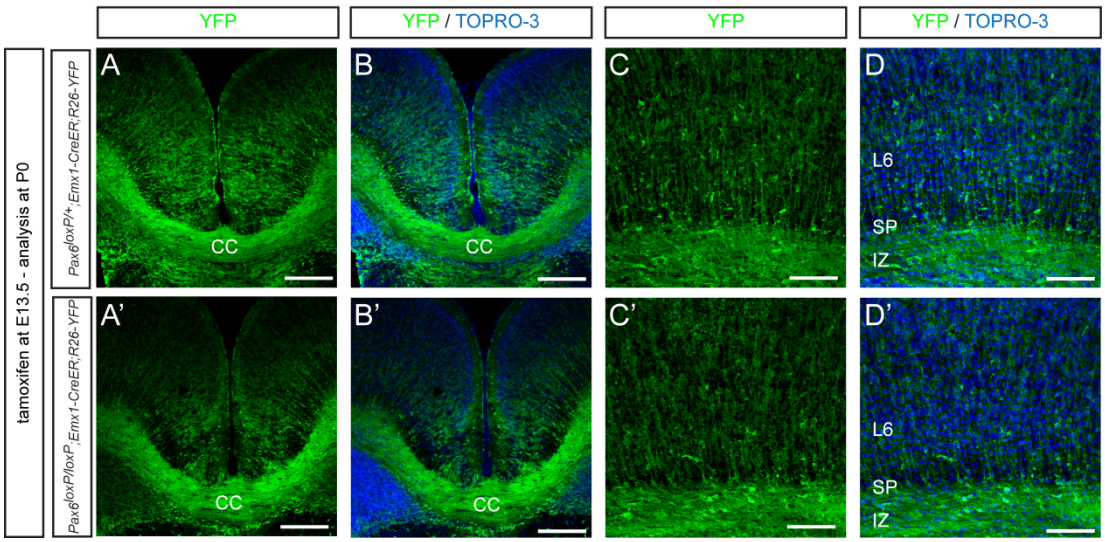

Figure 13. Morphology of YFP-labelled neurons in the P0 cortex of control and *Pax6*$^{loxP/loxP}$; *Emx1-CreER; R26-YFP* $^{E13.5tamox}$ mutant mice. (A-D, A'-D') Coronal sections through the rostral cortex of (A-D) control and (A'-D') mutant mice immunostained for YFP. The radial alignment of YFP-labelled neurons across the cortical thickness appeared normal in mutant mice. The corpus callosum (CC) formed normally in these mutants. (C-D, C'-D') High magnification images of (D) control and (D') mutant cortex showed that the morphology of YFP-labelled processes is indistinguishable between the two genotypes. CC, corpus callosum; IZ, intermediate zone; L6, layer 6; SP, subplate. Scale bars: 200µm (A-B, A'-B'), 100 µm (C-D, C'-D').

immediate tendency of increased progenitor proliferation in regions of the E15.5 *Pax6*$^{loxP/loxP}$; *Emx1-CreER*; *R26-YFP* $^{E13.5tamox}$ cortex, and imply that a more severe proliferation defect might be developing due to Pax6 loss in late cortical progenitors.

To investigate whether progenitor proliferation in the *Pax6*$^{loxP/loxP}$; *Emx1-CreER*; *R26-YFP* $^{E13.5tamox}$ mutant cortex is affected at later developmental stages, BrdU/YFP immunohistochemistry was performed in E16.5 embryos, 72 h post-tamoxifen injection (Fig. 14E-G, E'-G'). Notably, the number of BrdU/YFP double-labelled cells was significantly increased in the mutant cortex compared to control at all rostral-caudal levels (Fig. 14H), while the number of BrdU-positive/YFP-negative cells was significantly different between mutant and control only in the rostral and central cortex (rostral: 16.11 ± 0.4 in control, 37.67 ± 6.11 in mutant, Student's *t*-test $P = 0.024$, $n = 3$ of each genotype; central: 11 ± 1.35 in control, 24.78 ± 3.17 in mutant, Student's *t*-test $P = 0.016$, $n = 3$ of each genotype; caudal: 11.67 ± 2.52 in control, 17.78 ± 2.39 in mutant). These results indicate that loss of Pax6 during late corticogenesis increases the proliferation of cortical progenitors cell-autonomously at all levels throughout the rostral-caudal axis. Interestingly, late Pax6 inactivation also stimulates cortical progenitor proliferation through a cell-non-autonomous mechanism in regions where it is normally highly expressed. These proliferation defects are more profound in the mutant cortex with some delay with regard to the time of Pax6 inactivation.

To provide further evidence for a direct role of Pax6 in late cortical progenitor proliferation, immunohistochemistry for phosphohistone H3 (pH3) was employed to evaluate the number of progenitors in cell mitosis. Immunolabeling with PH3 allows discrimination between cells undergoing mitosis in apical or basal locations, corresponding to apical or basal progenitors, respectively. Analysis was performed on the same control and mutant brains used for the BrdU/YFP experiments above. Control and mutant cortices at the rostral, central and caudal levels were immunoreacted with PH3 at E15.5 (48 h post-tamoxifen injection) (Fig. 15A, B) and E16.5 (72 h post-tamoxifen injection) (Fig. 15D, E). Since the vast majority of progenitors were YFP-positive in both control and mutant cortices, as shown in Fig.

FIGURE 14

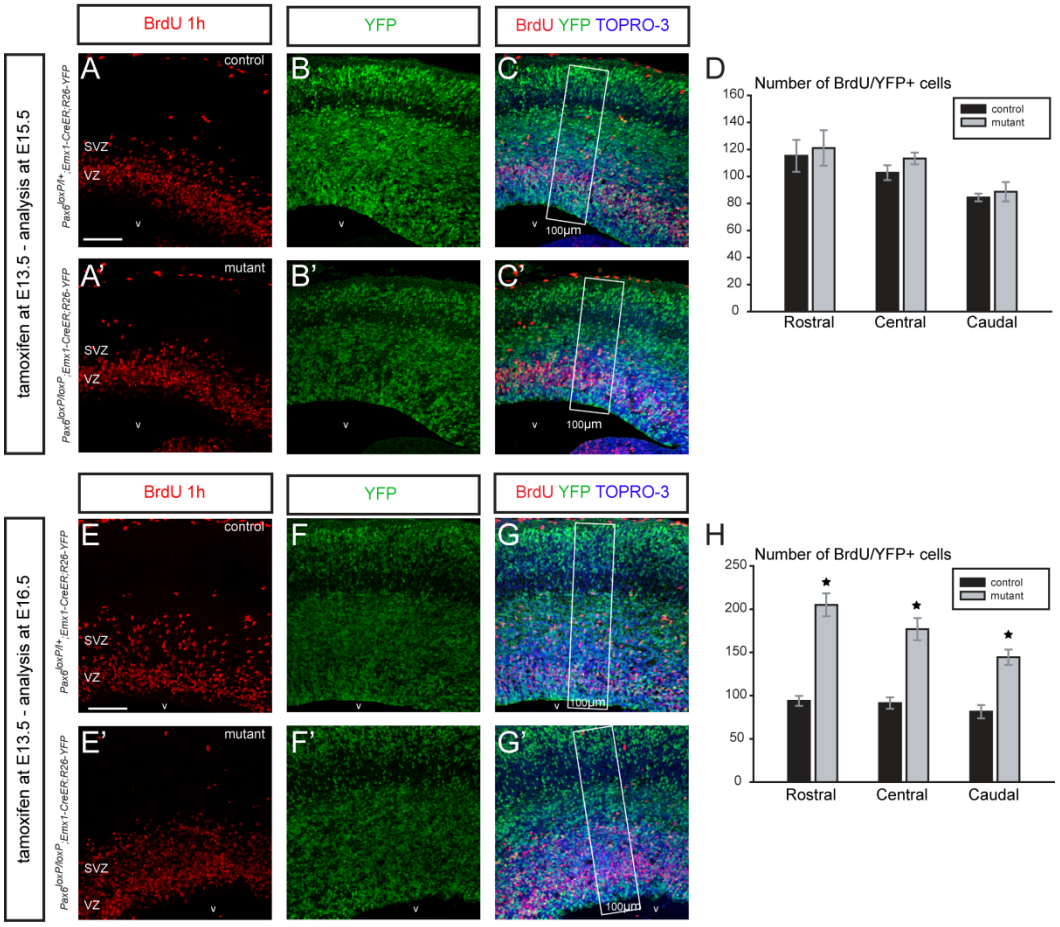

Figure 14. BrdU incorporation reveals increased proliferation of mutant progenitors in the cortex of *Pax6$^{loxP/loxP}$; Emx1-CreER; R26-YFP* $^{E13.5tamox}$ mice at E16.5 but not at E15.5. (A-C, A'-C', E-G, E'-G') Coronal sections of (A-C, A'-C') E15.5 and (E-G, E'-G') E16.5 (A-C, E-G) control and (A'-C', E'-G') mutant rostral cortices double-immunostained for BrdU/YFP following a 1 h BrdU pulse labelling. Sections were counterstained with TOPRO-3. A strong induction in BrdU incorporation was visible in the E16.5 mutant cortex compared with control, especially in the region of the mutant SVZ (E, E'). The numbers of BrdU/YFP double-labelled cells and BrdU-positive/YFP-negative cells were counted in 100-µm-wide radial stripes as shown in C-C', G-G'. (D) Quantitative analysis of BrdU/YFP double-positive nuclei at E15.5 indicated that proliferation was not significantly affected in the *Pax6$^{loxP/loxP}$; Emx1-CreER* $^{E13.5tamox}$ mutant cortex 48 h post-tamoxifen injection. (H) The number of BrdU/YFP double-positive nuclei was significantly increased in the mutant cortex at E16.5, 72 h post-tamoxifen injection. This increase was evident in all levels throughout the mutant cortex with respect to control. Note that the numbers of BrdU/YFP double-positive nuclei in the control did not vary throughout the rostral-caudal axis, whereas in the mutant cortex a higher increase was detected in rostral compared to caudal levels. VZ, ventricular zone; v, ventricle; SVZ, subventricular zone. Scale bars, 100µm.

14B-B', F-F' and discussed above, sections were labelled with PH3 only, assuming that most of PH3-positive progenitors in the mutant cortex would have either lost Pax6 expression (apical progenitors) or have originated from apical progenitors that had lost Pax6 after Cre recombination (basal progenitors).

The number of mitotic cells on the apical surface was not significantly changed between the mutant and control cortex at E15.5 (Fig. 15C). The number of basally dividing cells was not significantly altered in the mutant cortex compared to control at the rostral (4.12 ± 1.87 in control, 8.75 ± 0.38 in mutant; Student's *t*-test P = 0.072; n = 3 of each genotype) and central cortex (4.69 ± 0.86 in control, 9.33 ± 1.84 in mutant; Student's *t*-test P = 0.084; n = 3 of each genotype) (Fig. 15D). Differences were statistically significant at the caudal level (2.22 ± 0.37 in control, 5.02 ± 0.45 in mutant; Student's *t*-test P = 0.008; n = 3 of each genotype), although the total number of mitotic cells (apically and basally, combined) was not significantly different between control (13.39 ± 1.56) and mutant (13.81 ± 1.25) cortex at the caudal level (Student's *t*-test). These results suggest that there is a trend towards an increase in basal mitosis in the E15.5 mutant cortex; failure to detect significant differences in the total number of mitotic cells between mutant and control at the caudal level implies that overall mitosis is not significantly affected in the cortex of *Pax6*$^{loxP/+}$*; Emx1-CreER; R26-YFP* $^{\text{E13.5tamox}}$ mutants at E15.5.

At E16.5, however, a significant increase in the number of basal mitoses was detected in the rostral and central mutant cortex compared to control (rostral: 9.36 ± 0.31 in control, 18.44 ± 1.37 in mutant, Student's *t*-test P = 0.003, n = 3 of each genotype; central: 13.73 ± 0.82 in control, 20.25 ± 1.72 in mutant, Student's *t*-test P = 0.027, n = 3 of each genotype), while basal mitosis at the caudal level was not significantly different between the two genotypes (Fig. 15H). The total number of mitotic cells was significantly increased in the mutant cortex at the rostral (22.72 ± 1.69 in control; 30.09 ± 1.91 in mutant; Student's *t*-test P = 0.04, n = 3 of each genotype) and central level (24.58 ± 1.14 in control; 30.53 ± 1.63 in mutant; Student's *t*-test P = 0.04, n = 3 of each genotype). The numbers of apically dividing cells in the mutant cortex remained similar to those of controls (Fig. 15G).

FIGURE 15

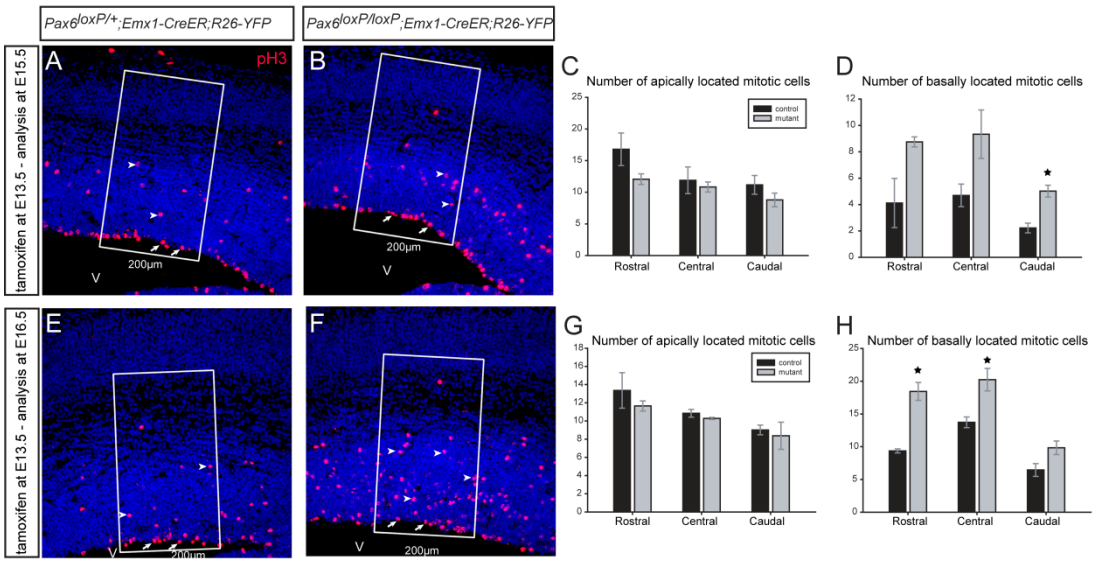

Figure 15. Pax6 inactivation in late cortical progenitors affects cell division. (A-B, E-F) Coronal sections through the rostral cortex of (A, B) E15.5 and (E, F) E16.5 (A, E) *Pax6*$^{loxP/+}$*; Emx1-CreER*$^{E13.5tamox}$ control and (B, F) *Pax6*$^{loxP/loxP}$*; Emx1-CreER*$^{E13.5tamox}$ mutant mice immunoreacted for pH3. Mitotic (pH3-positive) cells were counted in apical (indicated by arrows) and basal locations (arrowheads) in 200-µm-wide radial stripes. A strong induction in basal mitoses was visible in the E16.5 mutant cortex with respect to control. (C, D) The number of apical mitoses was not significantly altered in the E15.5 mutant cortex compared with control, while a significant (*) increase in basal mitosis was detected in the caudal mutant cortex. (G, H) Basally located mitotic cells were significantly increased at rostral and central levels of the mutant cortex compared with control, while they were not significantly affected in the caudal mutant cortex. V, ventricle. Sections were counterstained with TOPRO-3. Medial to the left.

These data demonstrate that loss of Pax6 in late cortical progenitors leads to increased progenitor proliferation, especially in cortical regions where levels of Pax6 expression are normally high. Furthermore, late Pax6 inactivation increases the number of basal mitosis without affecting the numbers of progenitors dividing at apical positions. These findings fit well with previous data showing that embryos lacking Pax6 from the earliest stages of corticogenesis exhibit increased numbers of cortical progenitors that divide in ectopic, basal positions (Haubst et al., 2004; Quinn et al., 2007; Tuoc et al., 2009).

6.2.7 Pax6 ablation during mid-stages of corticogenesis affects cortical progenitor proliferation

To further investigate the effect of Pax6 loss on cortical progenitor proliferation, injection of tamoxifen at E10.5 was used. Proliferation was examined at E13.5, the earliest time of Pax6 loss in *Pax6$^{loxP/loxP}$; Emx1-CreER; R26-YFP* $^{E10.5tamox}$ mutant mice. Pregnant females were injected with BrdU at E13.5, 72 h post-tamoxifen administration, and BrdU incorporation was tested 1 h later. Sections through the rostral, central and caudal cortex of control and mutant mice were double-immunostained for BrdU and YFP (Fig. 16A-C, A'-C'). Quantification of BrdU/YFP double-labelled and BrdU-positive/YFP-negative cells revealed that nearly 95% of BrdU-positive cells were co-expressing YFP in both control and mutant cortex. Pax6 inactivation at E13.5 resulted in significantly increased numbers of BrdU/YFP double-positive cells in the rostral mutant cortex compared with control (134.89 ± 3.27 in control, 188.33 ± 7.81 in mutant; Student's *t*-test $P = 0.003$, $n = 3$ of each genotype) (Fig. 16D). The proliferation of non-YFP-expressing progenitors was unaffected in the mutant cortex; equal numbers of BrdU-positive/YFP-negative cells were observed in the control and mutant cortex at all levels.

To examine whether Pax6 ablation at E13.5 has a more profound effect on cortical progenitor proliferation at later developmental stages, BrdU/YFP experiments were performed in *Pax6$^{loxP/loxP}$; Emx1-CreER; R26-YFP* $^{E10.5tamox}$ mutant and control cortices at E15.5 (Fig. 16E-G, E'-G'). A high induction was also observed in these littermates; nearly 95% of BrdU-labelled cells were co-expressing YFP in both

control and mutant cortex. Progenitor proliferation was severely affected in the YFP-positive cell population of the mutant cortex, while there was no change in the number of BrdU-positive/YFP-negative cells between the two genotypes at all cortical levels. Significantly increased numbers of BrdU/YFP double-labelled cells were detected in the mutant cortex compared to control (rostral: 94.67 ± 4.99 in control, 183.89 ± 12.19 in mutant, Student's *t*-test $P = 0.002$, $n = 3$ per genotype; central: 89 ± 3.84 in control, 152.78 ± 2.28 in mutant, Student's *t*-test $P < 0.001$, $n = 3$ per genotype ; caudal: 77 ± 2 in control, 97.33 ± 5 in mutant, Student's *t*-test $P = 0.02$, $n = 3$ per genotype) (Fig. 16H). Although such differences were significant at all levels, a rostral-to-caudal trend in the effect of Pax6 loss was again observed, with differences between the two genotypes being greater at the rostral level and becoming more subtle caudally.

The number of cells undergoing division at apical or basal locations was also examined by employing PH3 immunohistochemistry on sections of the same E13.5 and E15.5 mutant and control brains as used for the BrdU/YFP analyses (Fig 17A-B, E-F). The number of apical mitoses was not affected in the E13.5 mutant cortex at the rostral and caudal level, while in the central mutant cortex a slight but significant decrease in the number of apically located PH3-positive cells was detected (19.73 ± 0.37 in control; 18.02 ± 0.24 in mutant; Student's *t*-test $P = 0.018$, $n = 3$ of each genotype) (Fig. 17C). The number of PH3-positive cells at basal locations was significantly increased in the E13.5 mutant cortex at the rostral field (15.12 ± 2.32 in control, 28 ± 3.71 in mutant; Student's *t*-test $P = 0.04$, $n = 3$ per genotype), although it was unaffected at central and caudal levels (Fig. 17D). The increase in basal mitoses in the rostral mutant cortex, as well as the increase in apical mitoses in the central mutant cortex, was not sufficient to cause an overall significant increase in the total number of mitoses in the mutant cortex at the rostral or central level compared with control (rostral: 37.37 ± 2.46 in control, 47.83 ± 6.11 in mutant; central: 31.18 ± 1.93 in control, 30.93 ± 1.29 in mutant). In the E15.5 *Pax6*$^{loxP/loxP}$*; Emx1-CreER; R26-YFP* $^{E10.5tamox}$ mutant cortex, the number of basal mitoses was severely increased compared to control (rostral: 4.45 ± 1.42 in control, 26.67 ± 0.58 in mutant, Student's *t*-test $P < 0.001$, $n = 3$ per genotype; central: 3.5 ± 0.63 in

FIGURE 16

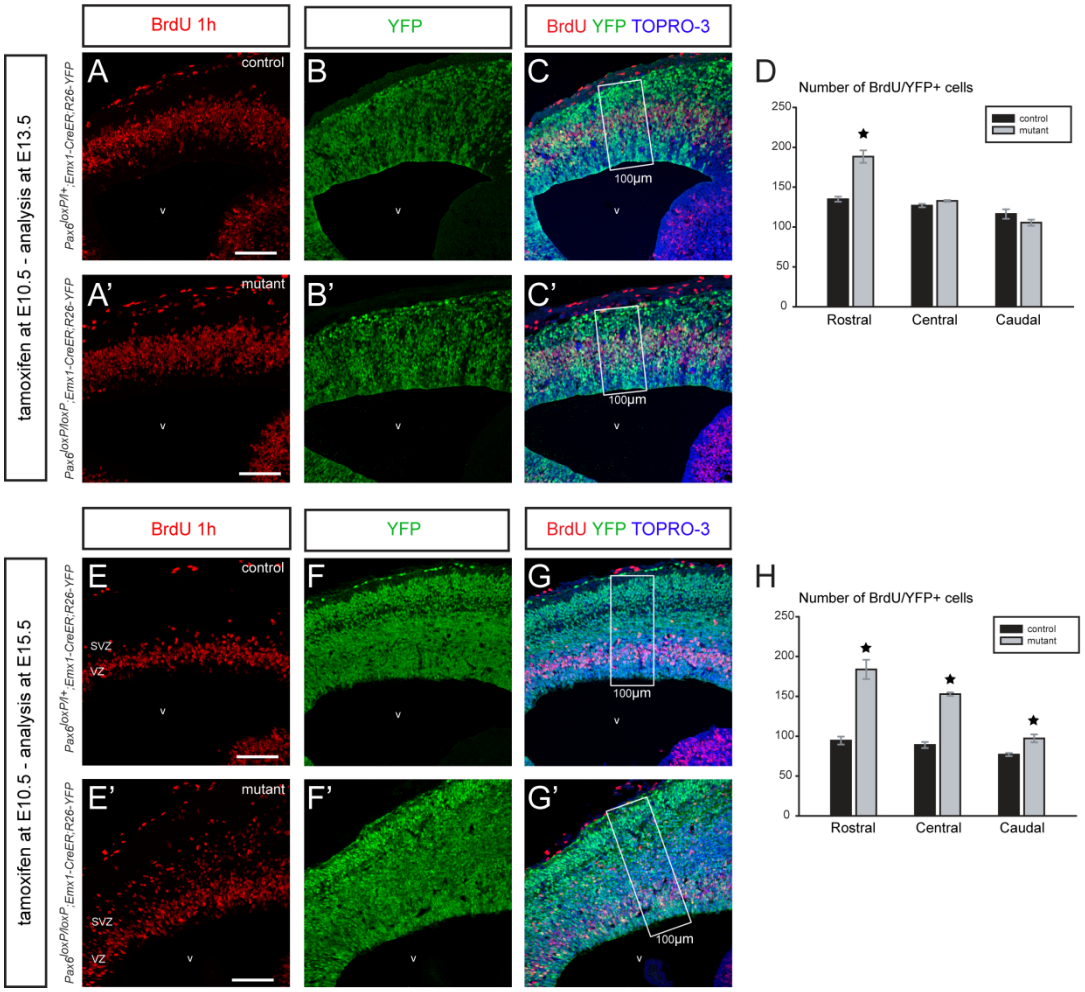

Figure 16. Pax6 inactivation during mid-corticogenesis induces cortical progenitor proliferation as revealed by increased BrdU incorporation in mutant progenitors. (A-C, A'-C', E-G, E'-G') Coronal sections of (A-C, A'-C') E13.5 and (E-G, E'-G') E15.5 (A-C, E-G) control and (A'-C', E'-G') mutant rostral cortices immunoreacted for BrdU and YFP following a 1 h BrdU pulse labelling. Sections were counterstained with TOPRO-3. A strong increase in BrdU incorporation was visible in the E15.5 mutant cortex compared with control, particularly in the region of the mutant SVZ (E, E'). The numbers of BrdU/YFP double-labelled cells and BrdU-positive/YFP-negative cells were counted in 100-µm-wide radial stripes shown in C-C', G-G'. (D) At E13.5, the number of BrdU/YFP double-labelled cells was significantly (*) increased in the rostral mutant cortex compared with control. At the central and caudal level, regions where Pax6 is normally expressed at lower levels, numbers were unaltered in the mutant cortex with respect to control. (H) The numbers of BrdU/YFP double-labelled cells were significantly increased at all levels of the mutant cortex compared to control. Note the gradual decrease in numbers of mutant S-phase progenitors from rostral to caudal cortex, indicating a stronger effect of Pax6 loss in cortical regions where it is normally highly expressed. SVZ, subventricular zone; VZ, ventricular zone. V, ventricle. Scale bars: 100µm.

control, 20.08 ± 2.33 in mutant, Student's *t*-test $P = 0.002$, $n = 3$ per genotype; caudal: 2.37 ± 0.41 in control, 9.43 ± 0.32 in mutant, Student's *t*-test $P < 0.001$, $n = 3$ per genotype) (Fig. 17H). The number of apically dividing cells was unaffected in the E15.5 mutant cortex compared with control (Fig. 17G). The strong increase in the number of basal mitoses led to a significant increase in the total number of mitotic figures in the mutant cortex with respect to control (rostral: Student's *t*-test $P < 0.001$, $n = 3$ of each genotype; central: Student's *t*-test $P = 0.018$, $n = 3$ of each genotype; caudal: Student's *t*-test $P = 0.049$, $n = 3$ of each genotype).

These findings suggest that loss of Pax6 at E13.5 has an immediate effect on the proliferation of cortical progenitors only in rostral cortical regions, where Pax6 is normally highly expressed. Later on, this effect is more profound and also extends to cortical regions where Pax6 expression levels are lower, i.e. caudally. Taken together, Pax6 ablation at either mid- or late-corticogenesis increases the number of basal mitoses as well as the number of S-phase cortical progenitors, indicating that Pax6 is a key regulator of cortical progenitor proliferation throughout the time course of cortical development.

FIGURE 17

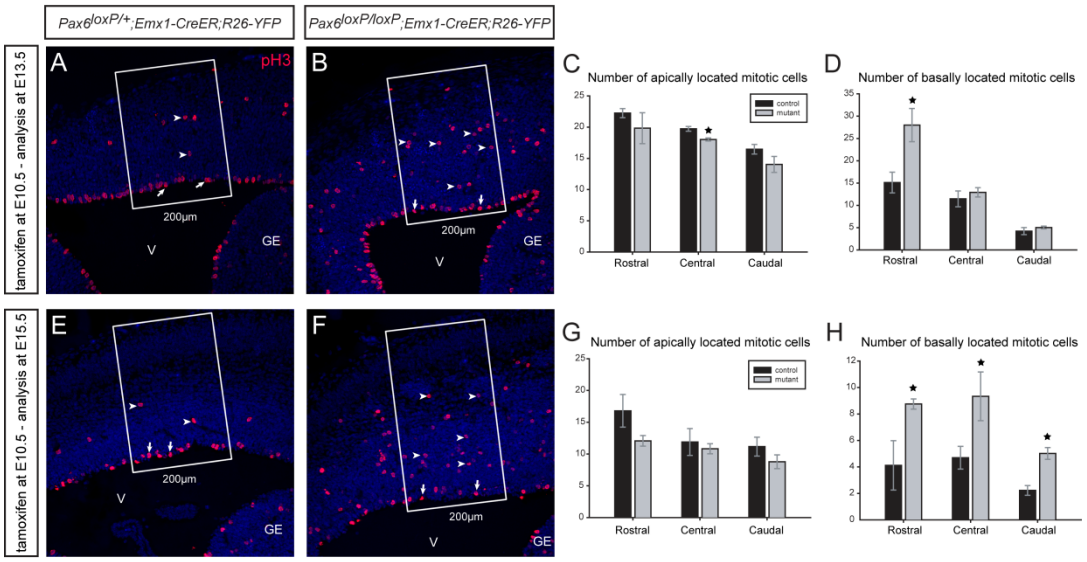

Figure 17. Loss of Pax6 function at mid-stages of corticogenesis affects progenitor cell division. (A-B, E-F) Coronal sections of (A, B) E13.5 and (E, F) E15.5 (A, E) control and (B, F) mutant telencephalons at the rostral level immunolabelled for phosphorylated histone H3. Mitotic (pH3-positive) cells were counted in apical (indicated by arrows) and basal locations (arrowheads) in 200-µm-wide radial stripes. (C, D) Quantitative analysis of pH3-positive cells showed that the number of apical mitosis was not significantly altered in the E13.5 mutant cortex compared to control at rostral and caudal levels, while a significant (*) decrease was detected in the central mutant cortex with respect to control. A significant increase in the number of basally located pH3-positive cells was detected in the E13.5 mutant cortex at rostral levels compared to control, while basal mitoses at central and caudal levels was unaffected in the mutant. (G, H) The numbers of apically dividing cells were not significantly different between E15.5 mutant and control cortices. However, the numbers of mitotic cells in basal positions were significantly increased in the E15.5 mutant cortex with respect to control at all levels. GE, ganglionic eminence; v, ventricle. Sections were counterstained with TOPRO-3. Medial to the left.

6.3 Discussion

6.3.1 Conditional Pax6 inactivation induces cortical progenitor proliferation mostly through a cell-autonomous mechanism

The formation of a functional cerebral cortex requires that the appropriate types of neurons are present at the right place, in correct numbers. Cortical projection neurons are born locally from dorsal telencephalic progenitor cells in a sequential manner, and newly postmitotic cells simultaneously leaving the cell cycle differentiate into neurons of a defined laminar fate (McConnell 1995). Thus, the cerebral cortex forms sequentially in an "inside-out" fashion (Rakic 1974). It is now well-established that cortical progenitors can be subdivided into two main groups which differ, among other aspects, in molecular expression profiles and the exact location they undergo cell division. Apical progenitors, located in the VZ, express Pax6 and divide at apical positions adjacent to the lateral ventricle (Gotz et al. 1998; Englund et al. 2005). Basal progenitors, located in the overlying SVZ, express *Tbr2* and the recently identified transcription factor *AP2γ* (Englund et al. 2005; Arnold et al. 2008; Sessa et al. 2008; Pinto et al. 2009) and divide at basal, abventricular positions.

Loss- and gain-of-function analyses have implicated Pax6 as an intrinsic regulator of progenitor proliferation. Cortical progenitor proliferation is induced in *Pax6* loss-of-function mutants, while it is reduced after Pax6 overexpression (Gotz et al. 1998; Warren et al. 1999; Heins et al. 2002; Hack et al. 2004; Haubst et al. 2004; Berger et al. 2007; Manuel et al. 2007; Quinn et al. 2007; Georgala et al. 2010). The specific role of Pax6 function during mid and late stages of corticogenesis was directly investigated here by conditional mutagenesis. These new findings indicate that cortical progenitors are extremely sensitive to Pax6 loss throughout the time course of corticogenesis. Either mid or late inactivation of Pax6 resulted in significantly increased numbers of S-phase cortical progenitors at all rostral-caudal levels. Of note, Pax6 ablation from E15.5 resulted in a severe increase in the number of S-phase progenitors in the mutant VZ and particularly in the mutant SVZ at E16.5, comparable to that previously described in E16.5 *Pax6* null mice (Gotz et al. 1998). The increased numbers of S-phase progenitors in *Pax6* cKO mutants suggest two alternative possibilities, or a combination of both. Pax6 loss in late cortical

progenitors might result in: (1) shortening of cell cycle times that would lead to increased numbers of mutant progenitors incorporating BrdU after a short 1 h pulse employed in this study, or/and (2) reduced cell-cycle exit, and concurrently increased cell cycle commitment, that would lead to increased numbers of mutant progenitors. Intriguingly, previous studies have suggested that Pax6 loss increases cell-cycle length of cortical progenitors at E15.5 (Estivill-Torrus et al. 2002; Quinn et al. 2007). However, these observations might indicate secondary abnormalities due to severe early developmental defects in *Pax6* loss-of-function mutants. In this context, Pax6 loss from the onset of corticogenesis leads to progressive ventralization and induced production of normally ventrally-derived GABAergic neurons in the mutant cortex (Kroll and O'Leary 2005). Lengthening of the cell cycle, previously reported in the *Pax6*$^{-/-}$ cortex, could be an outcome of an increased number of GABAergic neurons populating the mutant cortex. Analyses in chapter 3 support this hypothesis by demonstrating that cell-cycle times in the ventral telencephalon are normally doubled compared to those in cortical progenitors. Whether Pax6 loss in late cortical progenitors affects cell-cycle properties deserves further research. This could be addressed via the BrdU/IdU labelling method described in chapter 3. With regard to the second possibility, of increased cell-cycle commitment of mutant progenitors that could explain the observed increase in BrdU-incorporation in the *Pax6* cKO cortex, this seems more unlikely. Loss of Pax6 protein in the mouse model studied here is just occurring at E15.5, 48 h post-tamoxifen administration, and BrdU incorporation studies at E15.5 failed to reveal significant differences between control and mutant cortex. Therefore, analyses of BrdU incorporation carried out in E16.5 *Pax6* cKOs would not allow enough time for detection of severely increased progenitor cell numbers, given that progenitors would normally progress through only one cell cycle from E15.5 to E16.5. These assumptions are based on results presented in chapter 3, where cell- cycle length was found to last between 20-25 h in the E15.5 wild-type cortex. However, the possibility of increased cell-cycle commitment could be tested directly in the E16.5 *Pax6* cKO cortex by immunostaining cortices with the proliferating cell nuclear antigen (PCNA) and assessing the proportions of proliferating cells after late loss of Pax6.

BrdU incorporation studies here demonstrated that Pax6 loss from mid or late stages of corticogenesis affects preferentially the proliferation of mutant cells throughout the rostral-caudal levels of the cKO cortex, supporting a cell-autonomous requirement for Pax6 function. However, the proliferation of cells that had not recombined Cre was also affected in regions of the E16.5 *Pax6*$^{loxP/loxP}$*; Emx1-CreER* $^{E13.5tamox}$ cortex where Pax6 in normally expressed at high levels, suggesting a cell-non-autonomous role for Pax6 in these regions. Basal mitoses were severely increased after loss of Pax6 in either mid or late cortical progenitors, although correctly specified basal progenitors were found to be decreased in the *Pax6* cKO cortex. It appears therefore that Pax6 inactivation from mid or late cortical progenitors induces ectopic cell division, similar to that previously described in *Pax6* null or cKO mutants lacking Pax6 from the earliest stages of corticogenesis (Haubst et al. 2004; Quinn et al. 2007; Tuoc et al. 2009). These defects likely reveal that Pax6 function is constantly required throughout corticogenesis to maintain normal interkinetic nuclear migration of apical progenitors, an assumption that fits well with results from Tamai et al. (2007) reporting on disrupted interkinetic nuclear migration in *Pax6*$^{-/-}$ mutants. Given that Pax6 is specifically expressed in progenitors within the cortex, it is not surprising that its loss of function has an effect on progenitor proliferation throughout corticogenesis. It is remarkable though that its inactivation at either early, mid or late cortical progenitors results in the same phenotype at all rostral-caudal levels, with an induction of proliferation and increased numbers of progenitors dividing at ectopic locations during the time of superficial layer neuron generation. Moreover, a cell-autonomous requirement for Pax6 is indicated here even in caudal cortical regions, while in regions of normally high expression Pax6 loss can also cause non-autonomous proliferation defects.

It is important to note that profound proliferation defects at all levels of the *Pax6* cKO cortex were detected with some delay with respect to the time of Pax6 down-regulation. At times immediately after Pax6 downregulation, proliferation defects in the mutant cortex were just arising and were mostly associated with regions where Pax6 is normally expressed at high levels. These findings demonstrate the gradual effect of Pax6 deficiency in cortical progenitor proliferation. Progenitor proliferation drives neuronal production that can lead ultimately to an enlarged cortical surface

area (Caviness et al. 1995; Rakic, 1995; Chen and Walsh 2002, 2003). Interestingly, increased progenitor proliferation due to Pax6 loss in late cortical progenitors, during the time of superficial layer neuron generation, did not result in increased numbers of late-born neurons occupying mutant superficial layers due to migration defects. Birthdating studies of E16.5-born neurons in the P0 cKO cortex clearly demonstrated a severe increase in the production of late-born neurons, further supporting cell-autonomous and non-autonomous proliferation defects arising after Pax6 loss in late cortical progenitors.

Together, these findings further support the role of Pax6 as an intrinsic regulator of cortical progenitor proliferation. Sansom et al. (2009) have demonstrated that Pax6 has the ability to both promote and inhibit cortical progenitor proliferation by regulating the expression of cell cycle regulators. Increasing or decreasing levels of Pax6 upsets this balance, with Pax6 ablation leading to increased progenitor proliferation in the *Pax6*$^{-/-}$ cortex and overexpression resulting in reduced cell production. However, dysregulation of Pax6 levels either way leads to reduced cortical growth, with abnormalities being more severe in the *Pax6*$^{-/-}$ cortex. The phenotype in the *Pax6*$^{-/-}$ cortex is likely attributable to premature cell-cycle exit leading to a severe depletion of the mutant progenitor pool during superficial layer neuron production (Estivill-Torrus et al. 2002; Quinn et al. 2007). In this context, specific late-inactivation of Pax6 employed in this study allowed for maintenance of the progenitor pool and direct assessment of the role of Pax6 function during late corticogenesis. Results presented here demonstrate that Pax6 ablation leads to a severe induction in cell proliferation even in cortical regions and at times that its levels are not the highest. The outcome of increased late cortical progenitor proliferation in the *Pax6* cKO cortex was an increased production of late-born neurons, in contrast to mice lacking Pax6 from the onset of corticogenesis. Collectively, these data provide direct evidence for a key role for Pax6 in controlling progenitor proliferation throughout corticogenesis, and demonstrate that loss of Pax6 function has the ability to impair cortical progenitor proliferation both in a cell-autonomous and non-autonomous fashion.

6.3.2 Pax6 controls migration of late-born cortical neurons by both a cell-autonomous and non-autonomous mechanism

Cortical precursors born in the proliferative layers of the embryonic dorsal telencephalon migrate radially to the developing cortical plate in a characteristic order, such that they migrate past earlier-born neurons to adopt more superficial positions. Thus, the cerebral cortex forms sequentially in an "inside-out" manner (Rakic 1974). Results here indicate that Pax6 inactivation exclusively in late cortical progenitors specifically affects the exit of late-born neurons from their birthplace, resembling migration abnormalities previously described in *Pax6*$^{-/-}$ embryos (Schmahl et al. 1993; Caric et al. 1997; Tarabykin et al. 2001; Talamillo et al. 2003). Interestingly, the autonomously affected mutant cells of the cKO cortex were capable of inducing migration deficiency in surrounding wild-type, late-born neurons. Migration defects of *Pax6*$^{-/-}$-derived neurons were not rescued even after mixing mutant cortical cells with an excess of wild-type cells in the cKO cortex, strongly supporting a key requirement for Pax6 function in regulating neuronal migration. Thus, it appears that late Pax6 function is required both within progenitors themselves as well as their environment for migration of late-born neurons away from their site of production. These findings fit well with previous studies of chimeric embryos suggesting that Pax6 is intrinsically required for normal migration of late-born neurons away from the SVZ/IZ boundary of the embryonic cortex (Talamillo et al. 2003). Interestingly, these analyses have shown that *Pax6*$^{-/-}$ mutant cells accumulating in the proliferative region express neuronal markers. The present study extends previous findings above and directly demonstrates that late-born neurons generated from *Pax6*$^{-/-}$ progenitors, once they exit the proliferative region, they have the intrinsic ability to migrate radially and adopt superficial laminar positions in the postnatal cortex. Furthermore, results here showed that neuronal migration defects in the *Pax6* cKO were compensated for by an induction in late cortical progenitor proliferation, thus leading ultimately to similar numbers of late-born neurons adopting superficial positions in the mutant cortex. Together, findings from the present and previous studies suggest that Pax6 may facilitate neuronal migration by providing genetic input during the waiting period of migratory cells in the SVZ/IZ region and contributing to the progress of neuronal migration to next

phase that involves initiation of migration towards the cortical plate (Kriegstein and Noctor 2004).

A non-autonomous requirement for Pax6 function in neuronal migration has been previously suggested from Caric et al. (1997) by demonstrating that migration abnormalities of late-born *Pax6*$^{-/-}$ neurons are rescued after transplantation into wild-type cortex. The non-autonomous migration defects documented in the *Pax6* cKO cortex could arise from defective cell-cell interaction. For instance, radial migration of late-born cortical neurons is largely dependent on guidance from radial glial cells. Although Pax6 is cell-autonomously required for normal radial glia morphology (Gotz et al. 1998), the morphological phenotype of radial glial cells appeared normal in the *Pax6* cKO cortex, most likely due to normal Pax6 expression during early and mid corticogenesis in these mutants. However, defective signalling between abnormally differentiated radial glia and wild-type cortical cells during the latest stages of corticogenesis remains a possibility. Furthermore, non-autonomous migration defects in the germinal zone of the *Pax6* cKO cortex might well arise due to defective cell-cell signalling from misplaced mutant neurons that retain a ventral telencephalic character. Whether the enlarged germinal zone in the postnatal *Pax6* cKO cortex contains high numbers of GABAergic cells is a critical question that deserves further investigation. The presence of abnormally increased numbers of cortical cells in the embryonic *Pax6* cKO cortex exhibiting a molecular profile characteristic of that in the ventral telencephalon suggests that late Pax6 loss might ultimately lead to enhanced numbers of differentiated GABAergic cells in the postnatal mutant cortex. This would further suggest defective cell-cell interactions between cells of dorsal and ventral character inhabiting the same region in the *Pax6* cKO cortex.

6.3.3 Conditional Pax6 deletion from mid or late stages of corticogenesis affects superficial laminar fate of late-born neurons

Laminar fates of cortical neurons are determined when they are early postmitotic cortical precursors and become progressively restricted as development advances (McConnell and Kaznowski 1991; Frantz and McConnell 1996; Desai and

McConnell 2000; Britanova et al. 2008). The specific expression of Pax6 in progenitors throughout corticogenesis makes this molecule an excellent candidate for specifying neuronal identities. Thus, given the crucial role of Pax6 in regulating progenitor proliferation and specifying cortical identity, it is important to determine whether Pax6 function is required to specify laminar-specific properties of cortical projection neurons. Previous studies have implicated *Pax6* in controlling superficial laminar fate, while *Ngn* function seems to be required for deep laminar identities (Tarabykin et al. 2001; Schuurmans et al. 2004; Osumi et al. 2008). However, unambiguous conclusions about laminar phenotypes cannot be drawn from embryonic analyses. The role of Pax6 in regulating laminar identity was addressed here by analyses of *Pax6* cKO mice which are viable postnatally.

Pax6 deletion during mid-stages of corticogenesis severely compromised superficial layer development. Both the numbers and specification of late-born neurons were markedly affected in the superficial layers of the mutant cortex, a laminar phenotype resembling that of cKOs lacking Pax6 from early corticogenesis (Tuoc et al. 2009). To directly examine whether Pax6 function is necessary during late corticogenesis for specifying superficial laminar fate, Pax6 was inactivated specifically in late cortical progenitors. Deep and superficial layer-specific markers were expressed in appropriate laminar positions throughout the *Pax6* cKO cortex. As expected, deep layer neurons, which are generated at times preceding Pax6 loss in the cKO cortex, exhibited correct molecular and cellular properties in the mutant, i.e. characteristic pyramidal morphology of corticospinal layer V neurons. Although superficial layer neurons had a correct superficial laminar identity in the *Pax6* cKO cortex, analysis showed that the absolute number of neurons with superficial fate was significantly reduced in the mutant. Despite this, BrdU birthdating at E15.5 indicated that total numbers of late-born neurons were not significantly affected in the mutant cortex. Importantly, proportions of late-born neurons with appropriate superficial laminar identity were reduced after late Pax6 inactivation. These findings indicate that Pax6 ablation exclusively in late cortical progenitors does not result in complete loss of superficial-layer marker expression. However, Pax6 is required in late corticogenesis to correctly specify the superficial laminar identity of late-born neurons in correct proportions.

Recently, another group reported that Pax6 ablation in late cortical progenitors, through crossing Pax6 conditional mice with a hGFAP-Cre expressed from E13.5, did not affect the number or the specification of superficial layer neurons (Tuoc et al. 2009). However, in this case superficial layer formation was not extensively studied and conclusions were based on observations that deep layer markers (Ctip2 and Tbr1) and the superficial layer marker Cux1 were expressed in the mutant cortex. Data presented in this study is in agreement with these observations of no gross abnormalities in mutant superficial layers after late Pax6 inactivation. However, careful analysis here indicated both the number of Cux1-expressing cells and the proportions of E15.5-born neurons double-labelled with Cux1 were significantly affected in the *Pax6* cKO cortex.

Within the superficial domain of the cortex, E15.5-birthdated neurons were mostly detected in laminar positions corresponding to layers II/III in both controls and *Pax6* cKOs lacking Pax6 specifically in late cortical progenitors. However, this analysis indicated that E15.5-birthdated neurons were distributed in more superficial positions of the *Pax6* cKO cortex. Many layer II/III neurons project to the contralateral hemisphere through the corpus callosum. Consistent with the failure to detect significant differences in the number of superficially located E15.5-born neurons between the two genotypes, together with observations that Cux1-expressing neurons were distributed in slightly more superficial positions of the mutant cortex, the size of the corpus callosum appeared normal in the mutants. Of note, layer IV was visibly reduced in the cKO cortex. Layer IV neurons are generated from E14.5 onwards, and therefore tamoxifen administration at E13.5 in $Pax6^{loxP/loxP}$*; Emx1-CreER* mice might affect the generation of layer IV neurons. This hypothesis could be tested directly by marking the genesis of layer IV neurons via BrdU birthdating in *Pax6* cKO mice. However, results presented here showed that downregulation of Pax6 48 h post-tamoxifen administration at E13.5 did not have a significant effect on progenitor proliferation, in contrast to severe defects detected in *Pax6* cKO mice 72 h post-tamoxifen administration.

Conditional Pax6 inactivation from mid-corticogenesis resulted in a more profound superficial laminar phenotype. In controls, 80% of E15.5-born/BrdU-positive cells

were expressing Cux1, while in the mutants percentages were reduced to 30%. Importantly, BrdU/YFP analysis in these P7 cortices revealed that 80% of BrdU-positive cells had recombined loxP sites. It is conceivable therefore that the remaining Cux1-expressing neurons in the *Pax6* cKO cortex might represent wild-type cells, further supporting the involvement of Pax6 in regulating superficial laminar fate. This could be directly examined by double-labelling mutant cortices with Cux1 and YFP and determining whether Cux1-positive neurons are negative for YFP. Pax6 ablation from either mid or late corticogenesis led to ventralization of the mutant cortex at E15.5, but did not result in the same laminar phenotype postnatally. Thus, the more severe superficial laminar defects detected in mutants lacking Pax6 from mid-corticogenesis are not secondary to the ventral-like phenotype in the mutant cortex. Furthermore, although the embryonic cKO cortex exhibited abundant upregulation of ventral markers, the vast majority of cortical cells were of an Emx1-lineage in both embryonic and postnatal mutant brains exhibiting high efficiency of *Cre*-mediated recombination. These findings suggest that the cortex of cKO mice is not over-populated by GABAergic interneurons of a ventral origin. Although it could be argued that dorsal cells of *Emx1*-lineage are fundamentally respecified into GABAergic neurons in the P7 *Pax6* cKO cortex, similar to the phenotype of *Pax6*$^{-/-}$ mice previously reported from Kroll and O'Leary (2005), the fact that layers of the P7 mutant cortex expressed layer markers typical of pyramidal layer neurons, makes this assumption unlikely. To directly prove that layers of P7 cKO cortices do not contain abundant numbers of GABAergic neurons, a pan- GABAergic interneuron marker as GAD67 needs to be employed in future analyses.

Together, findings presented here indicate that Pax6 is required for specifying superficial laminar fate, but its function seems to vary throughout corticogenesis. Pax6 deficiency from E13.5 has a severe effect on superficial laminar specification that is comparable with the previously reported phenotype of cKO mice lacking Pax6 from the onset of corticogenesis (Tuoc et al. 2009). Pax6 inactivation in late cortical progenitors also results in a superficial laminar phenotype. These abnormalities in *Pax6* cKO mice could be linked to the severe loss of Tbr2-expressing basal progenitors which normally arise at around E12 and contribute to the formation of superficial layer neurons (Tarabykin et al. 2001; Englund et al. 2005; Arnold et al.

2008; Sessa et al. 2008). Consistent with this hypothesis, basal progenitors were severely diminished in the E15.5 mutant cortex after Pax6 inactivation from mid-corticogenesis. Late inactivation of Pax6 also resulted in a remarkable decrease of correctly specified basal progenitor cells, but basal progenitor fate as well as the final superficial laminar phenotype in these conditional mutants was less affected compared to Pax6 loss at earlier stages. Thus, it seems likely that the coordinated action of Pax6 and Tbr2 is required for specification of superficial layer neurons in appropriate numbers. Concomitant reduction of both transcription factors might contribute to the development of a more severe superficial laminar phenotype.

CHAPTER 7

General Discussion

Experiments in the present thesis aimed to explore the spatial and temporal roles of Pax6 function in cortical development by employing gain- and loss-of-function strategies. Pax6 overexpression was found to impair the production of late-born cortical precursors cell-autonomously, leading to the formation of thinner superficial layers in the PAX77 mutant cortex. Increased levels of Pax6 were reported to lengthen the cell cycle of late cortical progenitors and promote cell cycle exit during late stages of corticogenesis. Consistent with an expected reduction of the progenitor pool due to reduced cell-cycle commitment of late progenitors in the PAX77 cortex, Pax6 overexpression led to reduced numbers of superficial layer neurons, without affecting their laminar specification. Such effects of Pax6 overexpression in cortical development were particularly evident in rostral cortical regions, where Pax6 is normally expressed at its highest levels. Results from overexpression studies here suggest that correct levels of Pax6 are required by progenitors at late stages of corticogenesis, specifically, to maintain their cell cycle times and moderate their exit from the cell cycle, thereby regulating the size of the progenitor pool.

Conditional ablation of Pax6 during late corticogenesis increased cortical progenitor proliferation, as well as ectopic, non-apical cell divisions, and resulted in overproduction of late-born neurons at all rostral-caudal levels throughout the mutant cortex. Importantly, Pax6 mutant progenitors lacking Pax6 from either mid or late stages of corticogenesis ectopically activated expression of markers normally confined to progenitors of the ventral telencephalon, which give rise to the adjacent striatum. Moreover, late Pax6 inactivation affected the capacity of late-born neurons to exit the proliferative compartment of the cortex both in a cell-autonomous and cell-non-autonomous manner, resulting in the formation of an expanded germinal zone in the postnatal mutant cortex. This phenotype closely mimics that of mutants lacking Pax6 from the onset of corticogenesis, described by previous studies (Schmahl et al. 1993; Caric et al. 1997; Fukuda et al. 2000; Tarabykin et al. 2001; Haubst et al. 2004; Schuurmans et al. 2004). The cause of the increased accumulation of late-born neurons in the *Pax6* cKO germinal zone will be addressed in future studies. It is likely that the observed ectopic activation of ventral telencephalic markers in the mutant cortex could lead to a switch in the differentiation programme of cortical precursors towards a GABAergic neuron

phenotype, similar to previously reported defects in *Pax6*$^{-/-}$ mutants (Kroll and O'Leary 2005). In contrast to *Pax6*$^{-/-}$ mice, late-born neurons were able to adopt appropriate superficial laminar positions in the cKO cortex analysed here and differentiate accordingly, although they expressed appropriate superficial laminar markers at reduced proportions. On the other hand, Pax6 ablation from mid-stages of corticogenesis dramatically reduced the number of superficially localized late-born cortical neurons, which were also not correctly specified in the mutant cortex. Collectively, these findings directly demonstrate that late Pax6 function is required to regulate crucial developmental aspects during superficial laminar formation.

Analyses here, together with previous findings, indicate that Pax6 plays a central role during corticogenesis by acting on the decision of cortical precursor cells of whether to exit or re-enter the cell cycle. Loss of Pax6 function from the earliest stages of corticogenesis causes premature cell cycle exit that leads to a depletion of the progenitor pool, and hence leads to reduced neuronal production in the mutant cortex (Quinn et al. 2007). The well-documented hypocellular cortical plate in the *Pax6*$^{-/-}$ cortex, mostly attributable to an under-representation of late-born, superficial-layer neurons, is in accordance with such an early reduction in the size of the mutant progenitor pool (Schmahl et al. 1993; Caric et al. 1997; Fukuda et al. 2000; Tarabykin et al. 2001; Haubst et al. 2004; Schuurmans et al. 2004). Reduced neuronal production in *Pax6*$^{-/-}$ mutants is accompanied by increased numbers of cortical progenitors, whereas Pax6 overexpression inhibits cortical progenitor proliferation (Gotz et al. 1998; Warren et al. 1999; Estivill-Torrus et al. 2002; Haubst et al. 2004; Berger et al. 2007; present study).

A better understanding of the effect of Pax6 levels in cortical progenitor proliferation and neuronal output throughout corticogenesis requires identification of downstream targets in Pax6-expressing apical progenitors. Recent work has started unravelling important pathways via which Pax6 exerts its function to control these processes. For instance, the Notch signalling pathway is known to influence cell fate specification during neural development. In particular, Notch function is central to the inhibition of neurogenesis and maintenance of a progenitor cell character and, interestingly, its activation promotes radial glial cell fate (Yoon et al. 2004; Yoon and Gaiano 2005).

In addition to the specific activation of Notch in VZ progenitors, the Par-complex proteins also localize in the apical domain of VZ progenitors and promote the proliferation of self-renewing progenitors through activation of Notch pathway components (Costa et al. 2008). The anti-neurogenic effects of Notch signalling arise by antagonizing the function of proneural genes, including Neurogenin1 (Ngn1), Ngn2 and Mash1 (Hatakeyama et al. 2004). Thus, Pax6 and Notch signalling seem to have antagonizing functions on cortical neurogenesis and cell-cycle commitment by differentially regulating the same sets of transcriptional regulators: Pax6 induces Ngn2 and Tbr2 function, whereas both of these key transcription factors are negatively regulated by downstream targets and effectors of Notch (Sansom et al. 2009). It is conceivable therefore that when levels of Notch effectors are low, Pax6 function has the capacity to drive apical progenitors towards neurogenesis and basal progenitor generation. Interestingly, the level of expression of Par proteins declines considerably over the course of corticogenesis, suggesting that Notch signalling has much stronger effects at early stages of corticogenesis (Costa et al. 2008). This model fits well with results here showing that increased Pax6 levels promote cell cycle exit and neuronal differentiation during late corticogenesis, presumably due to redundancy of Notch activity. Findings that such defects were most prominent in regions of the Pax6-overexpressing cortex where Pax6 is normally highly expressed, i.e. rostrally, further support this interpretation. With regard to basal progenitor generation, Pax6 loss from the onset of corticogenesis abolishes Tbr2 expression in the mutant cortex (Quinn et al. 2007). Here, Pax6 inactivation at mid stages of corticogenesis affected more severely the number of Tbr2-expressing cells in the mutant cortex compared to late loss of Pax6 function. Together, these data are also in agreement with the prevailing view that Notch activation exerts its maximum function at early stages of corticogenesis.

Disruption of Pax6 function exclusively in late cortical progenitors had an immediate, cell-autonomous effect on progenitor proliferation that led ultimately to the production of enormous numbers of late-born cortical neurons. These findings likely reflect that loss of Pax6 results in a dominant function of Notch activity and other cell cycle regulators that are negatively regulated by Pax6 under normal conditions. Indeed, Pax6 directly promotes expression of a number of cyclin-

dependent kinase (Cdk) inhibitors and other cell cycle regulators that inhibit G1 cell cycle progression and thus reduce self-renewal of neural stem cells (Duparc et al. 2007; Sansom et al. 2009). Intriguingly, Pax6 also positively regulates expression of Cdks and transcription factors which function in progenitor cells to promote self-renewal (Sansom et al. 2009). Such observations have indicated that Pax6 is a major component of a dynamic network that determines the balance between self-renewal and differentiation in neural stem cells. Based on gain- and loss-of-function approaches, previous studies have suggested that the ability of Pax6 to both promote and inhibit self-renewal in progenitor cells depends on its expression levels (Sansom et al. 2009). According to the recently proposed model, increasing Pax6 levels enhances the neurogenic function of Pax6 in a manner that dominates its role in progenitor self-renewal, whereas decreased levels seem to cause premature cell cycle exit and precocious neurogenesis due to reduced expression of key cell cycle regulators in cortical progenitors. While supported, among others, by findings that loss of Pax6 function reduces the neurogenic capacity of mutant progenitors and depletes the mutant progenitor pool available for late-born neuron production through increased cell cycle exit during early-stage corticogenesis (Heins et al. 2002; Quinn et al. 2007), such a model is likely oversimplified. Gain of Pax6 function here indicated that early-born, deep-layer neurons were not overproduced in mutant mice, thus implying that increased levels of Pax6 do not drive early cortical progenitors towards cell cycle exit. As discussed above, Pax6 overexpression significantly induced cell cycle exit of cortical progenitors during late corticogenesis, highlighting the fact that individual aspects of cortical development are temporarily regulated by Pax6 and thus are sensitive to Pax6 levels at different thresholds. This interpretation is further supported by findings that, at early stages of corticogenesis, cell cycle parameters were not affected in the PAX77 cortex, whereas Pax6 overexpression significantly increased cell cycle length of late cortical progenitors in rostral regions of the mutant cortex. Collectively, these data extend previous findings on the effects of Pax6 levels on cortical progenitor proliferation and neurogenesis and further suggest that the consequences of disruption of Pax6 levels differ on a developmental stage-dependent manner. Investigating the temporal control of core genetic networks

influencing corticogenesis through manipulation of temporal *Pax6* deletion, i.e. using the model employed in the present study, remains a primary goal for future work.

Elucidating the molecular and cellular networks in which Pax6 operates has important implications for the field of neurobiology as well as for future treatment of brain disorders. For example, the potent neurogenic role of Pax6 has tremendous clinical importance for the development of effective stem-cell based strategies that would enable cell replacement therapy. Pax6 overexpression is sufficient to reprogramme even postnatal cortical astrocytes towards functional neurons, whereas non-Pax6-expressing mouse striatal cells are resistant to Pax6-driven neurogenesis (Heins et al. 2002; Berninger et al. 2007). On the other hand, Pax6 overexpression in neural stem cells derived from the human cortex or striatum increases neurogenesis and concurrently inhibits the generation of astrocytes, whereas Pax6 ablation has the opposite effect (Kallur et al. 2008; Mo and Zecevic 2008). These data are in good agreement with the recent demonstration that, in contrast to the rodent brain, Pax6 is expressed both in the human fetal cortex and striatum (Mo and Zecevic 2008). Furthermore, findings that disruption of Pax6 levels has prominent effects on cortical progenitor proliferation are also of clinical significance. For instance, low levels of PAX6 expression are indicative of poor prognosis for patients with glioblastoma multiforme (GBM), the most common of primary malignant brain tumors (Zhou et al. 2003). Most importantly, PAX6 activation is sufficient to suppress GBM cell growth both in vitro and in vivo (Zhou et al. 2005). In agreement with this, a tumor suppressor role for PAX6 has also been demonstrated in tissues other than the brain (Shyr et al. 2010).

A trend towards increasing the proliferation capacity of neurogenic progenitor cells is considered to be central to the evolutionary expansion of the cerebral cortex. As exemplified by the cortical phenotype in *Pax6* loss-of-function mutants, neuronal production would be reduced if the progenitor pool is reduced in size due to premature cell cycle exit or low proliferation rate of self-renewing cortical progenitors. Furthermore, basal mitoses of cortical progenitors have increased in number during evolution. The recent characterization of basal progenitors, which have limited self-renew capacity and double the neuron number after a single round

of cell division, has proposed that this progenitor cell population contributes to increased neuronal production and thus might explain the increase in cortical size in primates (Kriegstein et al. 2006). However, such a scenario seems not to be fully supported by recent work. Other than the VZ, the germinal compartment of the primate cortex comprises an inner subventricular zone (ISVZ) and an outer SVZ (OSVZ) (Smart et al. 2002; Fish et al. 2008). On the basis of their cell biology and marker expression, the primate ISVZ progenitors resemble the rodent basal progenitors (Fish et al. 2008). The basally-dividing OSVZ progenitor population, a unique feature of the primate cortex, expands considerably prior to the peak of neuronal production and it appears that this novel proliferative layer is the major source of superficial layer neurons in primates (Smart et al. 2002; Lukaszewicz et al. 2005). OSVZ progenitors express Pax6 and exhibit radial glial characteristics, thus supporting the idea that evolution has favoured the generation of radial glial cells that function as neural stem cells (Lukaszewicz et al. 2005; Fish et al. 2008; Hansen et al. 2010). Furthermore, elegant live-cell imaging of developing human tissue has recently shown that the OSVZ progenitor population expands massively in a Notch signalling-dependent manner (Hansen et al. 2010). Following on from these observations, Pax6-expressing progenitors are central to a mechanism employed for the evolutionary expansion of the cerebral cortex.

BIBLIOGRAPHY

Alcamo EA, Chirivella L, Dautzenberg M, Dobreva G, Fariñas I, Grosschedl R, McConnell SK. 2008. Satb2 regulates callosal projection neuron identity in the developing cerebral cortex. Neuron. 57(3):364–377.

Anderson S, Eisenstat D, Shi L, Rubenstein JL. 1997. Interneuron migration from basal forebrain to neocortex: dependence on Dlx genes. Science. 278:474–476.

Anderson SA, Marin O, Horn C, Jennings K, Rubenstein JL. 2001. Distinct cortical migrations from the medial and lateral ganglionic eminences. Development. 128:353–363.

Angevine JB and Sidman RL. 1961. Autoradiographic study of cell migration during histogenesis of the cerebral cortex in the mouse. Nature. 192:766-768.

Anton ES, Kreidberg JA, Rakic P. 1999. Distinct functions of alpha3 and alpha(v) integrin receptors in neuronal migration and laminar organization of the cerebral cortex. Neuron 22:277–289.

Arlotta P, Molyneaux BJ, Chen J, Inoue J, Kominami R, Macklis JD. 2005. Neuronal subtype-specific genes that control corticospinal motor neuron development in vivo. Neuron 45(2):207-221.

Armentano M, Chou SJ, Tomassy GS, Leingärtner A, O'Leary DD, Studer M. 2007. COUP-TFI regulates the balance of cortical patterning between frontal/motor and sensory areas. Nat Neurosci. 10:1277–86.

Arnold SJ, Huang GJ, Cheung AF, Era T, Nishikawa S, Bikoff EK, Molnár Z, Robertson EJ, Groszer M. 2008. The T-box transcription factor Eomes/Tbr2 regulates neurogenesis in the cortical subventricular zone. Genes Dev. 22(18):2479-84.

Attardo A, Calegari F, Haubensak W, Wilsch-Bräuninger M, Huttner WB. 2008. Live imaging at the onset of cortical neurogenesis reveals differential appearance of

the neuronal phenotype in apical versus basal progenitor progeny. PLoS One. 3(6):e2388.

Bamiou DE, Musiek FE, Sisodiya SM, Free SL, Davies RA, Moore A, van Heyningen V, Luxon LM. 2004. Deficient Auditory Interhemispheric Transfer in Patients with *PAX6* Mutations. Ann Neurol 56:503-509.

Bannister AP. 2005. Inter- and intra-laminar connections of pyramidal cells in the neocortex. Neurosci. Res. 53:95–103.

Batista-Brito R and Fishell G. 2009. The developmental integration of cortical interneurons into a functional network. Curr Top Dev Biol. 87:81-118.

Bayer SA and Altman J. 1991. Development of the endopiriform nucleus and the claustrum in the rat brain. Neuroscience. 45:391-412.

Bel-Vialar S, Medevielle F, Pituello F. 2007. The on/off of Pax6 controls the tempo of neuronal differentiation in the developing spinal cord. Dev Biol. 305(2): 659-673.

Bentivoglio M, Tassi L, Pech E, Costa C, Fabene PF, Spreafico R. 2003. Cortical development and focal cortical dysplasia. Epileptic Disord. 5(Suppl 2):27–34.

Berger J, Berger S, Tuoc TC, D'Amelio M, Cecconi F, Gorski JA, Jones KR, Gruss P, Stoykova A. 2007. Conditional activation of Pax6 in the developing cortex of transgenic mice causes progenitor apoptosis. Development 134(7):1311-22.

Berninger B, Costa MR, Koch U, Schroeder T, Sutor B, Grothe B, Götz M. 2007. Functional properties of neurons derived from in vitro reprogrammed postnatal astroglia. J Neurosci. 27(32):8654-64.

Bielle F, Griveau A, Narboux-Nême N, Vigneau S, Sigrist M, Arber S, Wassef M, Pierani A. 2005. Multiple origins of Cajal-Retzius cells at the borders of the developing pallium. Nat Neurosci. 8(8):1002-12.

Bishop KM, Goudreau G, O'Leary DD. 2000. Regulation of area identity in the mammalian neocortex by Emx2 and Pax6. Science 288:344–334.

Bishop KM, Rubenstein JL, O'Leary DD. 2002. Distinct actions of Emx1, Emx2, and Pax6 in regulating the specification of areas in the developing neocortex. J Neurosci. 22:7627–7638.

Bopp D, Burri M, Baumgartner S, Frigerio G, Noll M. 1986. Conservation of a Large Protein Domain in the Segmentation Gene *paired* and in Functionally Related Genes of Drosophila. Cell 47:1033-1040.

Bopp D, Jamet E, Baumgartner S, Burri M, Noll M. 1989. Isolation of two tissue specific Drosophila paired box genes, Pox meso and Pox neuro. *EMBO J* 8:3447-3457.

Borrell V, Kaspar BK, Gage FH, Callaway EM. 2006. In vivo evidence for radial migration of neurons by long-distance somal translocation in the developing ferret visual cortex, *Cereb. Cortex.* 16:1571–1583.

Borello U and Pierani A. 2010. Patterning the cerebral cortex: travelling with morphogens. Curr Opin Genet Dev. 20(4):408-415.

Briata P, Di Blas E, Gulisano M, Mallamaci A, Iannone R, Boncinelli E, Corte G. 1996. EMX1 homeoprotein is expressed in cell nuclei of the developing cerebral cortex and in the axons of the olfactory sensory neurons. Mech Dev. 57(2):169-80.

Britanova O, Akopov S, Lukyanov S, Gruss P, Tarabykin V. 2005. Novel transcription factor Satb2 interacts with matrix attachment region DNA elements in a tissue-specific manner and demonstrates cell-type-dependent expression in the developing mouse CNS. Eur J Neurosci. 21(3):658-68.

Britanova O, de Juan Romero C, Cheung A, Kwan KY, Schwark M, Gyorgy A, Vogel T, Akopov S, Mitkovski M, Agoston D, Sestan N, Molnár Z, Tarabykin V. 2008. Satb2 is a postmitotic determinant for upper-layer neuron specification in the neocortex. *Neuron.* 57(3):378–392.

Britz O, Mattar P, Nguyen L, Langevin LM, Zimmer C, Alam S, Guillemot F, Schuurmans C. 2006. A role for proneural genes in the maturation of cortical progenitor cells. Cereb Cortex. 16 Suppl 1:i138-51.

Butt SJ, Fuccillo M, Nery S, Noctor S, Kriegstein A, Corbin JG, Fishell G. 2005. The temporal and spatial origins of cortical interneurons predict their physiological subtype. Neuron. 48:591–604.

Calegari F and Huttner WB. 2003. An inhibition of cyclin-dependent kinases that lengthens, but does not arrest, neuroepithelial cell cycle induces premature neurogenesis. J Cell Sci. 116(24):4947-55.

Calegari F, Haubensak W, Haffner C, Huttner WB. 2005. Selective lengthening of the cell cycle in the neurogenic subpopulation of neural progenitor cells during mouse brain development. J. Neurosci. 25:6533–6538.

Callaerts P, Halder G, Gehring WJ. 1997. PAX-6 in development and evolution. Annu Rev Neurosci 20:483-532.

Campbell K. 2003. Dorsal-ventral patterning in the mammalian telencephalon. Curr Opin Neurobiol. 13:50-56.

Caric D, Gooday D, Hill RE, McConnell SK, Price DJ. 1997. Determination of the migratory capacity of embryonic cortical cells lacking the transcription factor Pax-6. Development. 124:5087-5096.

Carney RS, Alfonso TB, Cohen D, Dai H, Nery S, Stoica B, Slotkin J, Bregman BS, Fishell G, Corbin JG. 2006. Cell migration along the lateral cortical stream to the developing basal telencephalic limbic system. J Neurosci. 26:11562-11574.

Cartier L, Laforge T, Feki A, Arnaudeau S, Dubois-Dauphin M, Krause KH. 2006. Pax6-induced alteration of cell fate: shape changes, expression of neuronal alpha tubulin, postmitotic phenotype, and cell migration. J Neurobiol. 66(5):421-436.

Caviness VS Jr. 1982 Neocortical histogenesis in normal and reeler mice: a developmental study based upon [3H]thymidine autoradiography. Brain Res. 256:293–302.

Caviness V and Takahashi T. 1995. Proliferative events in the cerebral ventricular zone. Brain Dev. 17(3):159-163.

Caviness V, Takahashi T, Nowakowski R. 1995. Numbers, time and neocortical neuronogenesis: a general developmental and evolutionary model. Trends Neurosci. 18:379–383.

Caviness VS, Goto T, Tarui T, Takahashi T, Bhide PG, Nowakowski RS. 2003. Cell output, cell cycle duration and neuronal specification: a model of integrated mechanisms of the neocortical proliferative process. Cereb Cortex. 13:592–598.

Caviness VS Jr, Nowakowski RS, Bhide PG. 2009. Neocortical neurogenesis: morphogenetic gradients and beyond. Trends Neurosci. 32(8):443-50.

Cecchi C. 2002. Emx2: a gene responsible for cortical development, regionalization and area specification. Gene. 291(1-2):1-9.

Chalepakis G, Stoykova A, Wijnholds J, Tremblay P, Gruss P. 1993. Pax: Gene Regulators in the Developing Nervous System. J Neurobiol 24:1367-1384.

Chan CH, Godinho LN, Thomaidou D, Tan SS, Gulisano M, Parnavelas JG. 2001. Emx1 is a marker for pyramidal neurons of the cerebral cortex. Cereb Cortex. 11(12):1191-8.

Chanas SA, Collinson JM, Ramaesh T, Dorà N, Kleinjan DA, Hill RE, West JD. 2009. Effects of elevated Pax6 expression and genetic background on mouse eye development. Invest Opthalmol Vis Sci. 50(9):4045-59.

Chapouton P, Gartner A, Gotz M. 1999. The role of Pax6 in restricting cell migration between developing cortex and basal ganglia. Development. 126:5569–5579.

Chenn A and McConnell SK. 1995. Cleavage orientation and the asymmetric inheritance of Notch1 immunoreactivity in mammalian neurogenesis. Cell. 82:631–641.

Chenn A and Walsh CA. 2002. Regulation of cerebral cortical size by control of cell cycle exit in neural precursors. Science. 297(5580):328.

Chenn A and Walsh CA. 2003. Increased neuronal production, enlarged forebrains and cytoarchitectural distortions in beta-catenin overexpressing transgenic mice. Cereb Cortex. 13(6):599-606.

Chen B, Schaevitz LR, McConnell SK. 2005a. Fezl regulates the differentiation and axon targeting of layer 5 subcortical projection neurons in cerebral cortex. Proc Natl Acad Sci USA. 102:17184–17189.

Chen JG, Rasin MR, Kwan KY, Sestan N. 2005b. Zfp312 is required for subcortical axonal projections and dendritic morphology of deep-layer pyramidal neurons of the cerebral cortex. Proc Natl Acad Sci U S A. 102(49):17792-7.

Chen B, Wang SS, Hattox AM, Rayburn H, Nelson SB, McConnell SK. 2008. The Fezf2-Ctip2 genetic pathway regulates the fate choice of subcortical projection neurons in the developing cerebral cortex. Proc Natl Acad Sci USA. 105:11382–11387.

Cocas L, Georgala PA, Mangin JM, Clegg J, Kessaris N, Haydar T, Gallo V, Price DJ, Corbin J. Pax6 is required at the telencephalic pallial-subpallial boundary for the generation of neuronal diversity in the post-natal limbic system. *J Neuroscience* (submitted).

Collinson JM, Hill RE, West JD. 2000. Different roles for Pax6 in the optic vesicle and facial epithelium mediate early morphogenesis of the murine eye. Development. 127(5):945-56.

Collinson JM, Quinn JC, Buchanan MA, Kaufman MH, Wedden SE, West JD, Hill RE. 2001. Primary defects in the lens underlie complex anterior segment abnormalities of the Pax6 heterozygous eye. Roc Natl Acad Sci U S A. 98(17):9688-93.

Collinson JM, Quinn JC, Hill RE, West JD. 2003. The roles of Pax6 in the cornea, retina, and olfactory epithelium of the developing mouse embryo. Dev Biol. 255(2):303-12.

Corbin JG, Gaiano N, Machold RP, Langston A, Fishell G. 2000. The Gsh2 homeodomain gene controls multiple aspects of telencephalic development. Development. 127(23):5007-20.

Corbin JG, Rutlin M, Gaiano N, Fishell G. 2003. Combinatorial function of the homeodomain proteins Nkx2.1 and Gsh2 in ventral telencephalic patterning. Development. 130:4895-4906.

Costa MR, Wen G, Lepier A, Schroeder T, Götz M. 2008. Par-complex proteins promote proliferative progenitor divisions in the developing mouse cerebral cortex. Development. 135(1):11-22.

Costa MR, Götz M, Berninger B. 2010. What determines neurogenic competence in glia? Brain Res Rev. 63(1-2):47-59

del Río JA and Soriano E. 1989. Immunocytochemical detection of 5'-bromodeoxyuridine incorporation in the central nervous system of the mouse. Brain Res Dev Brain Res. 49(2):311-317.

del Río JA, Martínez A, Fonseca M, Auladell C, Soriano E. 1995. Glutamate-like immunoreactivity and fate of Cajal-Retzius cells in the murine cortex as identified with calretinin antibody. Cereb Cortex. 5(1):13-21.

Di Cristo G. 2007. Development of cortical GABAergic circuits and its implications for neurodevelopmental disorders. Clin Genet. 72(1):1-8.

Denaxa M, Chan CH, Schachner M, Parnavelas JG, Karagogeos D. 2001. The adhesion molecule TAG-1 mediates the migration of cortical interneurons from the ganglionic eminence along the corticofugal fiber system. Development. 128:4635–4644.

Denaxa M, Kyriakopoulou K, Theodorakis K, Trichas G, Vidaki M, Takeda Y, Watanabe K, Karagogeos D. 2005. The adhesion molecule TAG-1 is required for proper migration of the superficial migratory stream in the medulla but not of cortical interneurons. Dev Biol. 288:87–99.

Desai AR and McConnell SK. 2000. Progressive restriction in fate potential by neural progenitors during cerebral cortical development. Development. 127:2863–2872.

Deutsch U, Dressler GR, Gruss P. 1988. *Pax 1*, A Member of a Paired Box Homologous Murine Gene Family, Is Expressed in Segmented Structures during Development. Cell 53:617-625.

Di Cristo G. 2007. Development of cortical GABAergic circuits and its implications for neurodevelopmental disorders. Clin Genet. 72(1):1-8.

Dorà N, Ou J, Kucerova R, Parisi I, West JD, Collinson JM. 2008. PAX6 dosage effects on corneal development, growth, and wound healing. Dev Dyn. 237(5):1295-306.

Dulabon L, Olson EC, Taglienti MG, Eisenhuth S, McGrath B, Walsh CA, Kreidberg JA, Anton ES. 2000. Reelin binds alpha3beta1 integrin and inhibits neuronal migration. Neuron. 27:33–44.

Duparc RH, Abdouh M, David J, Lépine M, Tétreault N, Bernier G. 2007. Pax6 controls the proliferation rate of neuroepithelial progenitors from the mouse optic vesicle. Dev Biol. 301(2):374-87.

Englund C, Fink A, Lau C, Pham D, Daza RA, Bulfone A, Kowalczyk T, Hevner RF. 2005. Pax6, Tbr2, and Tbr1 are expressed sequentially by radial glia, intermediate progenitor cells, and postmitotic neurons in developing neocortex. J Neurosci. 25:247–251.

Estivill-Torrus G, Pearson H, van Heyningen V, Price DJ, Rashbass P. 2002. Pax6 is required to regulate the cell cycle and the rate of progression from symmetrical to asymmetrical division in mammalian cortical progenitors. Development. 129(2):455-466.

Fukamauchi F, Aihara O, Wang YJ, Akasaka K, Takeda Y, Horie M, Kawano H, Sudo K, Asano M, Watanabe K, Iwakura Y. 2001. TAG-1-deficient mice have

marked elevation of adenosine A1 receptors in the hippocampus. Biochem Biophys Res Commun. 281:220–226.

Fish JL, Dehay C, Kennedy H, Huttner WB. 2008. Making bigger brains-the evolution of neural-progenitor-cell division. J Cell Sci. 121(Pt 17):2783-93.

Fishell G and Kriegstein AR. 2003. Neurons from radial glia: the consequences of asymmetric inheritance. Curr Opin Neurobiol. 13(1):34-41.

Fishell G and Hanashima C. 2008. Pyramidal neurons grow up and change their mind. Neuron. 57:333–338.

Flames N, Long JE, Garratt AN, Fischer TM, Gassmann M, Birchmeier C, Lai C, Rubenstein JL, Marin O. 2004. Short- and long-range attraction of cortical GABAergic interneurons by neuregulin-1. Neuron. 44:251–61.

Flames N and Marín O. 2005. Developmental mechanisms underlying the generation of cortical interneuron diversity. Neuron. 46(3):377-81.

Fogarty M, Grist M, Gelman D, Marin O, Pachnis V, Kessaris N. 2007. Spatial genetic patterning of the embryonic neuroepithelium generates GABAergic interneuron diversity in the adult cortex. J Neurosci. 27:10935–46.

Frantz GD and McConnell SK. 1996. Restriction of late cerebral cortical progenitors to an upper-layer fate. Neuron. 17(1):55-61.

Fuerstenberg S, Broadus J, Doe CQ. 1998. Asymmetry and cell fate in the Drosophila embryonic CNS. Int J Dev Biol. 42(3):379-383.

Fujita S. 1964. Analysis of neuron differentiation in the central nervous system by tritiated thymidine autoradiography. J. Comp. Neurol. 122:311 -327.

Fukuchi-Shimogori T and Grove EA. 2001. Neocortex patterning by the secreted signaling molecule FGF8. Science 294:1071 -1074.

Fukuchi-Shimogori T and Grove EA. 2003. Emx2 patterns the neocortex by regulating FGF positional signaling, *Nat Neurosci* 6. 825–831.

Fukuda T, Kawano H, Osumi N, Eto K, Kawamura K. 2000. Histogenesis of the cerebral cortex in rat fetuses with a mutation in the Pax-6 gene. Dev Brain Res. 120:65–75.

Furuta Y, Piston DW, Hogan BL. 1997. Bone morphogenetic proteins (BMPs) as regulators of dorsal forebrain development. Development. 124:2203 -2212.

Garel S, Huffman KJ, Rubenstein JLR. 2003. Molecular regionalization of the neocortex is disrupted in Fgf8 hypomorphic mutants. Development 130:1903–1914.

Gaspard N, Bouschet T, Hourez R, Dimidschstein J, Naeije G, van den Ameele J, Espuny-Camacho I, Herpoel A, Passante L, Schiffmann SN, Gaillard A, Vanderhaegen P. 2008. An intrinsic mechanism of corticogenesis from embryonic stem cells. Nature 455:351–357.

Georgala PA, Manuel M, Price DJ. 2010. The Generation of Superficial Cortical Layers Is Regulated by Levels of the Transcription Factor Pax6. Cereb Cortex. [Epub ahead of print] doi: 10.1093/cercor/bhq061.

Gillies K and Price DJ. 1993. The fates of cells in the developing cerebral cortex of normal and methylazoxymethanol acetate-lesioned mice. Eur J Neurosci. 5:73-84.

Glaser T, Lane J, Housman D. 1990. A Mouse Model of the Aniridia-Wilms Tumor Deletion Syndrome. Science 250:823-827.

Glickstein SB, Monaghan JA, Koeller HB, Jones TK, Ross ME. 2009. Cyclin D2 is critical for intermediate progenitor cell proliferation in the embryonic cortex. J Neurosci. 29(30):9614-24.

Gopal PP and Golden JA. 2008. Pax6-/- mice have a cell nonautonomous defect in nonradial interneuron migration. Cereb Cortex. 18:752–762.

Gorski JA, Talley T, Qiu M, Puelles L, Rubenstein JL, Jones KR. 2002. Cortical excitatory neurons and glia, but not GABAergic neurons, are produced in the Emx1-expressing lineage. J Neurosci. 22(15):6309-14.

Götz M, Stoykova A, Gruss P. 1998. Pax6 controls radial glia differentiation in the cerebral cortex. Neuron. 21:1031-1044.

Götz M and Barde YA. 2005. Radial glial cells defined and major intermediates between embryonic stem cells and CNS neurons. Neuron. 46(3):369-372.

Götz M and Huttner WB. 2005. The cell biology of neurogenesis. Nature Rev. Mol. Cell Biol. 6:777–788.

Gressens P. 2006. Pathogenesis of migration disorders. Curr Opin Neurol. 19(2) :135-140.

Grindley JC, Davidson DR, Hill RE. 1995. The role of Pax-6 in eye and nasal development. Development 121:1433-1442.

Grove EA, Williams BP, Li DQ, Hajihosseini M, Friedrich A, Price J. 1993. Multiple restricted lineages in the embryonic rat cerebral cortex. Development. 117: 553–561.

Grove EA, Tole S, Limon J, Yip L, Ragsdale CW. 1998. The hem of the embryonic cerebral cortex is defined by the expression of multiple Wnt genes and is compromised in Gli3-deficient mice. Development 125:2315–2325.

Guillemot F. 2005. Cellular and molecular control of neurogenesis in the mammalian telencephalon. Curr. Opin. Cell Biol. 17:639–647.

Guillemot F. 2007. Cell fate specification in the mammalian telencephalon, Prog. Neurobiol. 8337–52.

Guo H, Hong S, Jin XL, Chen RS, Avasthi PP, Tu YT, Ivanco TL, Li Y. 2000. Specificity and efficiency of Cre-mediated recombination in Emx1-Cre knock-in mice. Biochem Biophys Res Commun. 273(2):661-5.

Hack MA, Sugimori M, Lundberg C, Nakafuku M, Götz M. 2004. Regionalization and fate specification in neurospheres: the role of Olig2 and Pax6. Moll Cell Neurosci. 25(4):664-678.

Hamasaki T, Leingärtner A, Ringstedt T, O'Leary DD. 2004. EMX2 regulates sizes and positioning of the primary sensory and motor areas in neocortex by direct specification of cortical progenitors. Neuron. 43(3):359-72.

Hanashima C, Li SC, Shen L, Lai E, Fishell G. 2004. Foxg1 suppresses early cortical cell fate. Science (New York, NY) 303:56-59.

Hanashima C, Fernandes M, Hebert JM, Fishell G. 2007. The role of Foxg1 and dorsal midline signaling in the generation of Cajal-Retzius subtypes. J Neurosci. 27(41):11103-11.

Hansen DV, Lui JH, Parker PR, Kriegstein AR. 2010. Neurogenic radial glia in the outer subventricular zone of human neocortex. Nature. 464(7288):554-561.

Hartfuss E, Galli R, Heins N, Götz M. 2001. Characterization of CNS precursor subtypes and radial glia. Dev Biol. 229: 15–30.

Hatakeyama J, Bessho Y, Katoh K, Ookawara S, Fujioka M, Guillemot F, Kageyama R. 2004. Hes genes regulate size, shape and histogenesis of the nervous system by control of the timing of neural stem cell differentiation. Development. 131(22):5539-50.

Hatten ME. 1999. Central nervous system neuronal migration. Annu Rev Neurosci. 22:511–539.

Haubensak W, Attardo A, Denk W, Huttner WB. 2004. Neurons arise in the basal neuroepithelium of the early mammalian telencephalon: a major site of neurogenesis. *Proc Natl Acad Sci U S A*. 101:3196–3201.

Haubst N, Berger J, Radjendirane V, Graw J, Favor J, Saunders GF, Stoykova A, Gotz M. 2004. Molecular dissection of Pax6 function: the specific roles of the paired domain and homeodomain in brain development. Development. 131:6131–6140.

Hebert JM and Fishell G. 2008. The genetics of early telencephalon patterning: some assembly required. *Nat Rev Neurosci*. 9:678-685.

Heins N, Malatesta P, Cecconi F, Nakafuku M, Tucker KL, Hack MA, Chapouton P, Barde YA, Gotz M. 2002. Glial cells generate neurons: the role of the transcription factor Pax6. Nat Neurosci. 5:308–315.

Hevner RF, Shi L, Justice N, Hsueh Y, Sheng M, Smiga S, Bulfone A, Goffinet AM, Campagnoni AT, Rubenstein JL. 2001. Tbr1 regulates differentiation of the preplate and layer 6. Neuron. 29:353–366.

Hevner RF, Miyashita-Lin E, Rubenstein JL. 2002. Cortical and thalamic axon pathfinding defects in Tbr1, Gbx2, and Pax6 mutant mice: evidence that cortical and thalamic axons interact and guide each other. J Comp Neurol. 447:8–17.

Hevner RF, Neogi T, Englund C, Daza RA, Fink A. 2003. Cajal-Retzius cells in the mouse: transcription factors, neurotransmitters, and birthdays suggest a pallial origin. Brain Res Dev Brain Res. 141(1-2):39-53.

Hevner RF, Daza RA, Englund C, Kohtz J, Fink A. 2004. Postnatal shifts of interneuron position in the neocortex of normal and reeler mice: evidence for inward radial migration. Neuroscience. 124:605–618.

Hevner RF. 2006. From radial glia to pyramidal-projection neuron: transcription factor cascades in cerebral cortex development. Mol Neurobiol. 33(2):33-50.

Hayes NL and Nowakowski RS. 2000. Exploiting the dynamics of S-phase tracers in developing brain: interkinetic nuclear migration for cells entering versus leaving the S-phase. Dev Neurosci. 22(1-2):44-55.

Hill RE, Favor J, Hogan, BL, Ton CC, Saunders GF, Hanson IM, Prosser J, Jordan T, Hastie ND, van Heyningen V. 1991. Mouse small eye results from mutations in a paired-like homeobox-containing gene. Nature. 354:522-525.

Hoch RV, Rubenstein JL, Pleasure S. 2009. Genes and signaling events that establish regional patterning of the mammalian forebrain. Semin Cell Dev Biol. 20(4):378-386.

Hogan BLM, Horsburgh G, Cohen J, Hetherington CM, Fischer G, Lyon MF. 1986. Small eye (Sey): a homozygous lethal mutation on chromosome 2 which affects the differentiation of both lens and nasal placodes in the mouse. J Embryol Exp Morph. 97:95-110.

Hogan BL, Hirst EM, Horsburgh G, Hetherington CM. 1988. Small eye (Sey): a mouse model for the genetic analysis of craniofacial abnormalities. Development 103. Suppl:115-119.

Holm PC, Mader MT, Haubst N, Wizenmann A, Sigvardsson M, Götz M. 2007. Loss- and gain-of-function analyses reveal targets of Pax6 in the developing mouse telencephalon. Mol Cell Neurosci. 34(1):99-119.

Huang Z. 2009. Molecular regulation of neuronal migration during neocortical development. Moll Cell Neurosci. 42(1):11-22.

Hynes RO. 2002. Integrins: bidirectional, allosteric signaling machines. Cell. 110(6):673-687.

Jones L, Lopez-Bendito G, Gruss P, Stoykova A, Molnar Z. 2002. Pax6 is required for the normal development of the forebrain axonal connections. Development. 129:5041–5052.

Jun S and Desplan C. 1996. Cooperative interactions between paired domain and homeodomain. Development 122:2639-2650.

Kallur T, Gisler R, Lindvall O, Kokaia Z. 2008. Pax6 promotes neurogenesis in human neural stem cells. Mol Cell Neurosci. 38(4):616-28.

Keighren M and West JD. 1993. Analysis of cell ploidy in histological sections of mouse tissues by DNA-DNA in situ hybridization with digoxigenin-labelled probes. Histochem J. 25:30-44.

Kerszberg M. 1999. Morphogen propagation and action: towards molecular models. Semin Cell Dev Biol. 10:297-302.

Kessaris N, Fogarty M, Iannarelli P, Grist M, Wegner M, Richardson WD. 2006. Competing waves of oligodendrocytes in the forebrain and postnatal elimination of an embryonic lineage. Nat Neurosci. 9(2):173-179.

Koester SE and O'Leary DD. 1993. Connectional distinction between callosal and subcortically projecting cortical neurons is determined prior to axon extension. Dev Biol. 160(1):1-14.

Kornack DR and Rakic P. 1998. Changes in cell-cycle kinetics during the development and evolution of primate neocortex. Proc Natl Acad Sci U S A. 95(3):1242-1246.

Kowalczyk T, Pontious A, Englund C, Daza RA, Bedogni F, Hodge R, Attardo A, Bell C, Huttner WB, Hevner RF. 2009. Intermediate neuronal progenitors (basal progenitors) produce pyramidal-projection neurons for all layers of cerebral cortex. Cereb Cortex. 19(10): 2439-50.

Kriegstein AR and Götz M. 2003. Radial glia diversity: a matter of cell fate. Glia 43 (1):37–43.

Kriegstein AR and Noctor SC. 2004. Patterns of neuronal migration in the embryonic cortex. Trends Neurosci. 27:392–399.

Kriegstein A, Noctor S, Marítnez-Cerdeño V. 2006. Patterns of neural stem and progenitor cell division may underlie evolutionary cortical expansion. Nat Rev Neurosci. 7:883–890.

Kroll TT and O'Leary DD. 2005. Ventralized dorsal telencephalic progenitors in Pax6 mutant mice generate GABA interneurons of a lateral ganglionic eminence fate. Proc Natl Acad Sci U S A. 102(20):7374-7379.

Lang D, Powell SK, Plummer RS, Young KP, Ruggeri BA. 2007. PAX genes: Roles in development, pathophysiology and cancer. Biochem Pharmacol 73:1-14.

Lange C, Huttner WB, Calegari F. Cdk4/cyclinD1 overexpression in neural stem cells shortens G1, delays neurogenesis, and promotes the generation and expansion

of basal progenitors. Cell Stem Cell. 5(3):320-331.

Lavdas AA, Mione MC, Parnavelas JG. 1996. Neuronal clones in the cerebral cortex show morphological and neurotransmitter heterogeneity during development. Cereb Cortex. 6(3):490-497.

Lavdas AA, Grigoriou M, Pachnis V, Parnavelas JG. 1999. The medial ganglionic eminence gives rise to a population of early neurons in the developing cerebral cortex. J. Neurosci. 19(18):7881–7888.

Leone DP, Srinivasan K, Chen B, Alcamo E, McConnell SK. 2008. The determination of projection neuron identity in the developing cerebral cortex. Curr Opin Neurobiol. 18:28–35.

Lewis DA, Hashimoto T, Morris HM. 2008. Cell and receptor type-specific alterations in markers of GABA neurotransmission in the prefrontal cortex of subjects with schizophrenia. Neurotox Res. 14(2-3):237-248.

Lo CW. 1986. Localization of low abundance DNA sequences in tissue sections by in situ hybridization. J Cell Sci. 81:143-62.

Lo CW, Coulling M, Kirby C. 1987. Tracking of mouse cell lineage using microinjected DNA sequences: analyses using genomic Southern blotting and tissue-section in situ hybridizations. Differentiation. 35:37-44.

Lukaszewicz A, Savatier P, Cortay V, Giroud P, Huissoud C, Berland M, Kennedy H, Dehay C. 2005. G1 phase regulation, area-specific cell cycle control, and cytoarchitectonics in the primate cortex. Neuron. 47(3):353-64.

Mallamaci A, Iannone R, Briata P, Pintonello L, Mercurio S, Boncinelli E, Corte G. 1998. EMX2 protein in the developing mouse brain and olfactory area. Mech Dev. 77(2):165-172.

Mallamaci A, Muzio L, Chan CH, Parnavelas J, Boncinelli E. 2000. Area identity shifts in the early cerebral cortex of Emx2-/- mutant mice. 3(7):679-86.

Malatesta P, Hack MA, Hartfuss E, Kettenmann H, Kirchhoff F, Götz M. 2003. Neuronal or glial progeny: regional differences in radial glia fate. Neuron. 37: 751–764.

Manuel M, Georgala PA, Carr CB, Chanas S, Kleinjan DA, Martynoga B, Mason JO, Molinek M, Pinson J, Pratt T, Quinn JC, Simpson TI, Tyas DA, van Heyningen V, West JD, Price DJ. 2007. Controlled overexpression of Pax6 in vivo negatively autoregulates the Pax6 locus, causing cell-autonomous defects of late cortical progenitor proliferation with little effect on cortical arealization. Development. 134:545-555.

Marin O and Rubenstein JL. 2001. A long, remarkable journey: tangential migration in the telencephalon. Nat. Rev. Neurosci. 2:780–790.

Martínez S and Puelles L. 2000. Neurogenetic compartments of the mouse diencephalon and some characteristic gene expression patterns. Results Probl Cell Differ. 30:91-106.

Martynoga B, Morrison H, Price DJ, Mason JO. 2005. Foxg1 is required for specification of ventral telencephalon and region-specific regulation of dorsal telencephalic precursor proliferation and apoptosis. Dev Biol. 283(1):113-127.

Mastick GS, Davis NM, Andrews GL, Easter SS Jr. 1997. Pax-6 functions in boundary formation and axon guidance in the embryonic mouse forebrain. Development 124:1985-1997.

McCarthy M, Turnbull DH, Walsh CA, Fishell G. 2001. Telencephalic neural progenitors appear to be restricted to regional and glial fates before the onset of neurogenesis. J Neurosci. 21: 6772–6781.

McConnell SK. 1988. Fates of visual cortical neurons in the ferret after isochronic and heterochronic transplantation. J Neurosci. 8:945–74.

McConnell SK and Kaznowski CE. 1991. Cell cycle dependence of laminar determination in developing neocortex. Science. 254:282-5.

McConnell SK. 1995. Constructing the cerebral cortex: neurogenesis and fate determination. Neuron. 15(11):6987-98.

Meech R, Kallunki P, Edelman GM, Jones FS. 1999. A binding site for homeodomain and Pax proteins is necessary for L1 cell adhesion molecule gene expression by Pax-6 and bone morphogenetic proteins. Proc Natl Acad Sci U S A. 96(5):2420-5.

Meyer G, Soria JM, Martínez-Galán JR, Martín-Clemente B, Fairén A. 1998. Different origins and developmental histories of transient neurons in the marginal zone of the fetal and neonatal rat cortex. J Comp Neurol. 397(4):493-518.

Mitchell BD and Macklis JD. 2005. Large-scale maintenance of dual projections by callosal and frontal cortical projection neurons in adult mice. J Comp Neurol. 482(1):17-32.

Miyama S, Takahashi T, Nowakowski RS, Caviness VS Jr. 1997. A gradient in the duration of the G1 phase in the murine neocortical proliferative epithelium. Cereb Cortex. 7(7):678-89.

Miyata T, Kawaguchi A, Okano H, Ogawa M. 2001. Asymmetric inheritance of radial glial fibers by cortical neurons. Neuron. 31:727–741.

Miyata T, Kawaguchi A, Saito K, Kawano M, Muto T, Ogawa M. 2004. Asymmetric production of surface-dividing and non-surface-dividing cortical progenitor cells. Development 131:3133-3145.

Miyata T and Ogawa M. 2007. Twisting of neocortical progenitor cells underlies a spring-like mechanism for daughter-cell migration. Curr. Biol. 17:146–151.

Miyoshi G, Butt SJ, Takebayashi H, Fishell G. 2007. Physiologically distinct temporal cohorts of cortical interneurons arise from telencephalic Olig2-expressing precursors. J Neurosci. 27:7786–7798.

Miyoshi G, Hjerling-Leffler J, Karayannis T, Sousa VH, Butt SJ, Battiste J, Johnson JE, Machold RP, Fishell G. 2010. Genetic fate mapping reveals that the caudal

ganglionic eminence produces a large and divese population of superficial cortical interneurons. J Neurosci 30: 1582–1594.

Mo Z and Zecevic N. 2008. Is Pax6 critical for neurogenesis in the human fetal brain? Cereb Cortex. 18(6):1455-65.

Molnár Z and Cheung AF. 2006. Towards the classification of subpopulations of layer V pyramidal projection neurons. Neurosci. Res. 55:105–115.

Molyneaux BJ, Arlotta P, Hirata T, Hibi M, Macklis JD. 2005. *Fezl* is required for the birth and specification of corticospinal motor neurons. Neuron. 47:817–831.

Molyneaux BJ, Arlotta P, Menezes JR, Macklis JD. 2007. Neuronal subtype specification in the cerebral cortex. Nat Rev Neurosci. 8:427–437.

Mountcastle VB. 1997. The columnar organization of the neocortex. Brain 120:701-722.

Muzio L, DiBenedetto B, Stoykova A, Boncinelli E, Gruss P, Mallamaci A. 2002a. Emx2 and Pax6 control regionalization of the pre-neuronogenic cortical primordium. Cereb Cortex. 12(2):129-139.

Muzio L, DiBenedetto B, Stoykova A, Boncinelli E, Gruss P, Mallamaci A. 2002b. Conversion of cerebral cortex into basal ganglia in Emx2(−/−) Pax6(Sey/Sey) double-mutant mice. Nat. Neurosci. 5:737–745.

Nadarajah B, Brunstrom JE, Grutzendler J, Wong RO, Pearlman AL. 2001. Two modes of radial migration in early development of the cerebral cortex. Nat. Neurosci. 4:143–150.

Nadarajah B, Alifragis P, Wong RO, Parnavelas JG. 2002. Ventricle-directed migration in the developing cerebral cortex. Nat Neurosci. 5:218–224.

Nadarajah B and Parnavelas JG. 2002. Modes of neuronal migration in the developing cerebral cortex. Nat Rev Neurosci 3:423–432.

Nery S, Fishell G, Corbin JG. 2002. The caudal ganglionic eminence is a source of distinct cortical and subcortical cell populations. Nat Neurosci (2002) 5:1279–1287.

Neumann C and Cohen S. 1997. Morphogens and pattern formation. Bioessays. 19:721-9.

Nguyen L, Besson A, Roberts JM, Guillemot F. 2006. Coupling cell cycle exit, neuronal differentiation and migration in cortical neurogenesis. Cell Cycle. 5:2314–2318.

Nieto M, Monuki ES, Tang H, Imitola J, Haubst N, Khoury SJ, Cunningham J, Gotz M, Walsh CA. 2004. Expression of Cux-1 and Cux-2 in the subventricular zone and upper layers II-IV of the cerebral cortex. J Comp Neurol. 479(2):168-180.

Noctor SC, Flint AC, Weissman TA, Dammerman RS, Kriegstein AR. 2001. Neurons derived from radial glial cells establish radial units in neo-cortex. Nature. 409:714–720.

Noctor SC, Flint AC, Weissman TA, Wong WS, Clinton BK, Kriegstein AR. 2002. Dividing precursor cells of the embryonic cortical ventricular zone have morphological and molecular characteristics of radial glia. J Neurosci. 22:3161–3173.

Noctor SC, Martínez-Cerdeño V, Ivic L, Kriegstein AR. 2004. Cortical neurons arise in symmetric and asymmetric division zones and migrate through specific phases. Nat Neurosci. 7:136–144.

Nowakowski RS, Lewin SB, Miller MW. 1989. Bromodeoxyuridine immunohistochemical determination of the lengths of the cell cycle and the DNA-synthetic phase for an anatomically defined population. J Neurocytol. 18(3):311-8.

Ohkubo Y, Chiang C, Rubenstein JL. 2002. Coordinate regulation and synergistic actions of BMP4, SHH and FGF8 in the rostral prosencephalon regulate morphogenesis of the telencephalic and optic vesicles. Neuroscience 111:1-17.

Ohshima T, Hirasawa M, Tabata H, Mutoh T, Adachi T, Suzuki H, Saruta K, Iwasato T, Itohara S, Hashimoto M, Nakajima K, Ogawa M, Kulkarni AB, Mikoshiba K. 2007. Cdk5 is required for multipolar-to-bipolar transition during radial neuronal migration and proper dendrite development of pyramidal neurons in the cerebral cortex. Development. 134:2273–2282.

O'Leary DD and Koester SE. 1993. Development of projection neuron types, axon pathways, and patterned connections of the mammalian cortex. Neuron. 10:991–1006.

O'Leary DD and Nakagawa Y. 2002. Patterning centers, regulatory genes and extrinsic mechanisms controlling arealization of the neocortex. Curr Opin Neurobiol. 121(1):14-25.

O'Leary DD and Sahara S. 2008. Genetic regulation of arealization of the neocortex. Curr Opin Neurobiol. 18(1):90-100.

Olson EC and Walsh CA. 2002. Smooth, rough and upside-down neocortical development. Curr Opin Genet Dev. 12(3):320-327.

Ono K, Takebayashi H, Ikeda K, Furusho M, Nishizawa T, Watanabe K, Ikenaka K. 2008. Regional- and temporal-dependent changes in the differentiation of Olig2 progenitors in the forebrain, and the impact on astrocyte development in the dorsal pallium. Dev Biol. 320(2):456-68.

O'Rourke NA, Dailey ME, Smith SJ, McConnell SK. 1992. Diverse migratory pathways in the developing cerebral cortex. Science. 258(5080):299-302.

Osumi N, Shinohara H, Numayama-Tsuruta K, Maekawa M. 2008. Concise review: Pax6 transcription factor contributes to both embryonic and adult neurogenesis as a multifunctional regulator. Stem Cells. 26(7):1663-1672.

Parnavelas JG, Barfield JA, Franke E, Luskin MB. 1991. Separate progenitor cells give rise to pyramidal and nonpyramidal neurons in the rat telencephalon. Cerebral Cortex. 1: 463–468.

Parras CM, Schuurmans C, Scardigli R, Kim J, Anderson DJ, Guillemot F. 2002. Divergent functions of the proneural genes Mash1 and Ngn2 in the specification of neuronal subtype identity. Genes Dev. 16(3):324-38.

Parras CM, Hunt C, Sugimori M, Nakafuku M, Rowitch D, Guillemot F. 2007. The proneural gene Mash1 specifies an early population of telencephalic oligodendrocytes. J Neurosci. 27(16):4233-42.

Petryniak MA, Potter GB, Rowitch DH, Rubenstein JL. 2007. Dlx1 and Dlx2 control neuronal versus oligodendroglial cell fate acquisition in the developing forebrain. Neuron. 55(3):417-33.

Philips GT, Stair CN, Young Lee H, Wroblewski E, Berberoglu MA, Brown NL, Mastick GS. 2005. Precocious retinal neurons: Pax6 controls timing of differentiation and determination of cell type. Dev Biol. 279:308–321.

Pilaz LJ, Patti D, Marcy G, Ollier E, Pfister S, Douglas RJ, Betizeau M, Gautier E, Cortay V, Doerflinger N, Kennedy H, Dehay C. 2009. Forced G1-phase reduction alters mode of division, neuron number, and laminar phenotype in the cerebral cortex. Proc Natl Acad Sci U S A. 106(51):21942-9.

Pinto L and Götz M. 2007. Radial glial cell heterogeneity--the source of diverse progeny in the CNS. Prog Neurobiol. 83(1):2-23.

Pinto L, Drechsel D, Schmid MT, Ninkovic J, Irmler M, Brill MS, Restani L, Gianfranceschi L, Cerri C, Weber SN, Tarabykin V, Baer K, Guillemot F, Beckers J, Zecevic N, Dehay C, Caleo M, Schorle H, Götz M. 2009. AP2gamma regulates basal progenitor fate in a region- and layer-specific manner in the developing cortex. Nat Neurosci. 12(10):1229-1237.

Pla R, Borrell V, Flames N, Marin O. 2006. Layer acquisition by cortical GABAergic interneurons is independent of Reelin signaling. J Neurosci. 26:6924–6934.

Pratt T., Vitalis T, Warren N, Edgar JM, Mason JO, Price DJ. 2000. A role for Pax6 in the normal development of dorsal thalamus and its cortical connections. Development, 127. 5167-5178.

Pratt T, Quinn JC, Simpson TI, West JD, Mason JO, Price DJ. 2002. Disruption of early events in thalamocortical tract formation in mice lacking the transcription factors Pax6 or Foxg1. J. Neurosci. 22:8523-8531.

Price DJ, Aslam S, Tasker L, Gillies K. 1997. Fates of the earliest generated cells in the developing murine neocortex. J Comp Neurol. 377(3):414-22.

Price J and Thurlow L. 1988. Cell lineage in the rat cerebral cortex: a study using retroviral-mediated gene transfer. Development. 104: 473–482.

Quinn JC, West JD, Hill RE. 1996. Multiple functions for Pax6 in mouse eye and nasal development. Genes Dev. 10(4):435-46.

Quinn JC, Molinek M, Martynoga BS, Zaki PA, Faedo A, Bulfone A, Henver RF, West JD, Price DJ. 2007. Pax6 controls cerebral cortical cell number by regulating exit from the cell cycle and specifies cortical cell identity by a cell autonomous mechanism. Dev Biol. 302:50–65.

Quiring R, Walldorf U, Kloter U, Gehring WJ. 1994. Homology of the *eyeless* Gene of *Drosophila* to the *Small eye* gene in Mice and *Aniridia* in Humans. Science 265:785-789.

Ragsdale CW and Grove EA. 2001. Patterning the mammalian cerebral cortex. Curr. Opin. Neurobiol. 11:50 -58.

Rakic P. 1971. Guidance of neurons migrating to the fetal monkey neocortex. Brain Res. 33(2):471-476.

Rakic P. 1972. Mode of cell migration to the superficial layers of fetal monkey neocortex. J Comp Neurol. 145: 61–83.

Rakic P. 1974. Neurons in rhesus monkey visual cortex: systematic relation between time of origin and eventual disposition. Science. 183:425-427.

Rakic P. 1988. Specification of cerebral cortical areas. Science. 241:170–6.

Rakic P. 1995. A small step for the cell, a giant leap for mankind: a hypothesis of neocortical expansion during evolution. Trends Neurosci. 18(9):383-388.

Rakic P, Hashimoto-Torii K, Sarkisian MR. 2007. Genetic determinants of neuronal migration in the cerebral cortex. Novartis Found Symp. 288:45-53.

Rakic P. 2009. Evolution of the neocortex: a perspective from developmental biology. Nat Rev Neurosci. 10(10):724-35.

Rice DS and Curran T. 2001. Role of the reelin signaling pathway in central nervous system development. Annu. Rev. Neurosci. 24:1005–39.

Roybon L, Mastracci TL, Ribeiro D, Sussel L, Brundin P, Li JY. 2010. GABAergic differentiation induced by Mash1 is compromised by the bHLH proteins Neurogenin2, NeuroD1, and NeuroD2. Cereb Cortex. 20(5):1234-44.

Salomoni P and Calegari F. 2010. Cell cycle control of mammalian neural stem cells: putting a speed limit on G1. Trends Cell Biol. 20(5):233-43.

Sansom SN, Griffiths DS, Faedo A, Kleinjan DJ, Ruan Y, Smith J, van Heyningen V, Rubenstein JL, Livesey FJ. 2009. The level of the transcription factor Pax6 is essential for controlling the balance between neural stem cell self-renewal and neurogenesis. PloS Genet. 5(6):e1000511.

Sansom SN and Livesey FJ. 2009. Gradients in the brain: the control of the development of form and function in the cerebral cortex. Cold Spring Harb Perspect Biol. 1(2):a002519.

Scardigli R, Bäumer N, Gruss P, Guillemot F, Le Roux I. 2003. Direct and concentration-dependent regulation of the proneural gene Neurogenin2 by Pax6. Development. 130(14):3269-81.

Schedl A, Ross A, Lee M, Engelkamp D, Rashbass P, van Heyningen V, Hastie ND. 1996. Influence of PAX6 gene dosage on development: overexpression causes severe eye abnormalities. Cell. 86(1):71-82.

Schlaggar BL and O'Leary DD. 1991. Potential of visual cortex to develop an array of functional units unique to somatosensory cortex. Science. 252(5012):1556-60.

Schmahl W, Knoedlseder M, Favor J, Davidson D. 1993. Defects of neuronal migration and the pathogenesis of cortical malformations are associated with Small eye (Sey) in the mouse, a point mutation at the Pax-6-locus. Acta Neuropathol. 86: 126-135.

Schuurmans C, Armant O, Nieto M, Stenman JM, Britz O, Klenin N, Brown C, Langevin LM, Seibt J, Tang H, Cunningham JM, Dyck R, Walsh C, Campbell K, Polleux F, Guillemot F. 2004. Sequential phases of cortical specification involve Neurogenin-dependent and -independent pathways. EMBO J. 23:2892-2902.

Sessa A, Mao CA, Hadjantonakis AK, Klein WH, V. Broccoli V. 2008. Tbr2 directs conversion of radial glia into basal precursors and guides neuronal amplification by indirect neurogenesis in the developing neocortex. Neuron 60:56–69.

Shimamura K and Rubenstein JL. 1997. Inductive interactions direct early regionalization of the mouse forebrain. Development. 124(14):2709-2718.

Shyr CR, Tsai MY, Yeh S, Kang HY, Chang YC, Wong PL, Huang CC, Huang KE, Chang C. 2010. Tumor suppressor PAX6 functions as androgen receptor co-repressor to inhibit prostate cancer growth. Prostate. 70(2):190-9.

Sidman RL, Miale IL, Feder N. 1959. Cell proliferation and migration in the primitive ependymal zone: an autoradiographic study of histogenesis in the nervous system. Exp Neurol. 1:322-333.

Simpson TI, Pratt T, Mason JO, Price DJ. 2009. Normal ventral telencephalic expression of Pax6 is required for normal development of thalamocortical axons in embryonic mice. Neural Dev. 4:19.

Sisodyia SM, Free SL, Williamson KA, Mitchell TN, Willis C, Stevens JM, Kendall BE, Shorvon SD, Hanson IM, Moore AT, van Heyningen V. 2001. *PAX6* haploinsufficiency causes cerebral malformation and olfactory dysfunction in humans. Nat Genet 28:214-216.

Smart IH. 1972. Proliferative characteristics of the ependymal layer during the early development of the mouse diencephalon, as revealed by recording the number, location, and plane of cleavage of mitotic figures. J Anat. 113(Pt 1):109-129.

Smart IH. 1973. Proliferative characteristics of the ependymal layer during the early development of the mouse neocortex: a pilot study based on recording the number, location and plane of cleavage of mitotic figures. J Anat. 116:67–91.

Smart IH and McSherry GM. 1982. Growth patterns in the lateral wall of the mouse telencephalon. II. Histological changes during and subsequent to the period of isocortical neuron production. J Anat. 134(Pt 3):415-42.

Smart IH, Dehay C, Giroud P, Berland M, Kennedy H. 2002. Unique morphological features of the proliferative zones and postmitotic compartments of the neural epithelium giving rise to striate and extrastriate cortex in the monkey. Cereb Cortex. 12(1):37-53.

Solecki DJ, Govek EE, Tomoda T, Hatten ME. 2006. Neuronal polarity in CNS development. Genes Dev. 20(19):2639-47.

Soriano E and Del Rio JA. 2005. The cells of Cajal–Retzius: still a mystery one century after. Neuron 46:389–394.

Srinivas S, Watanabe T, Lin CS, William CM, Tanabe Y, Jessell TM, Costantini F. 2001. Cre reporter strains produced by targeted insertion of *EYFP* and *ECFP* into the *ROSA26* locus. BMC Dev Biol. 1:4.

Stenman JM, Wang B, Campbell K. 2003. Tlx controls proliferation and patterning of lateral telencephalic progenitor domains. J Neurosci. 23:10568–10576.

Storm E, Rubenstein JLR, Martin GR. 2003. Negative regulation between two FGF signaling pathways as a mechanism for generating distinct phenotypes in response to different levels of FGF8. Proc. Natl. Acad. Sci. USA 100:1757-1762.

Stoykova A and Gruss P. 1994. Roles of Pax-genes in developing and adult brain as suggested by expression patterns. J. Neurosci. 14:1395-1412.

Stoykova A, Fritsch R, Walther C, Gruss P. 1996. Forebrain patterning defects in Small eye mutant mice. Development. 122:3453–3465.

Stoykova A, Gotz M, Gruss P, Price J. 1997. Pax6-dependent regulation of adhesive patterning, R-cadherin expression and boundary formation in developing forebrain. Development. 124:3765-3777.

Stoykova A, Treichel D, Hallonet M, Gruss P. 2000. Pax6 modulates the dorsoventral patterning of the mammalian telencephalon. J Neurosci. 20(21):8042-8050.

Subramanian L, Remedios R, Shetty A, Tole S. 2009. Signals from the edges: the cortical hem and antihem in telencephalic development. Semin Cell Dev Biol. 20(6):712-718.

Supèr H, Soriano E, Uylings HB. 1998. The functions of the preplate in development and evolution of the neocortex and hippocampus. Brain Res Brain Rev. 27(1):40-64.

Sussel L, Marin O, Kimura S, Rubenstein JL. 1999. Loss of Nkx2.1 homeobox gene function results in a ventral to dorsal molecular respecification within the basal telencephalon: evidence for a transformation of the pallidum into the striatum. Development. 126:3359–3370.

Tabata T and Takei Y. 2004. Morphogens, their identification and regulation. Development. 131:703-12.

Takahashi T, Nowakowski RS, Caviness V. Jr. 1993. Cell cycle parameters and patterns of nuclear movement in the neocortical proliferative zone of the fetal mouse. J Neurosci.13:820–833.

Takahashi T, Nowakowski RS, Caviness VS Jr. 1994. Mode of cell proliferation in the developing mouse neocortex. Proc Natl Acad Sci U S A. 91(1):375-379.

Takahashi T, Nowakowski R, Caviness VS Jr. 1995a. The cell cycle of the pseudostratified ventricular epithelium of the murine cerebral wall. J Neurosci. 15:6046-6057.

Takahashi T, Nowakowski R, Caviness VS Jr. 1995b. Early ontogeny of the secondary proliferative population of the embryonic murine cerebral wall. J Neurosci. 15(9):6058-68.

Takahashi T, Nowakowski RS, Caviness VS Jr. 1996. The leaving or Q fraction of the murine cerebral proliferative epthithelium: a general model of neocortical neuronogenesis. J. Neurosci 16:6183–6196.

Takahashi T, Goto T, Miyama S, Nowakowski RS, Caviness Jr VS. 1999. Sequence of Neuron Origin and Neocortical Laminar Fate: Relation to Cell Cycle of Origin in the Developing Murine Cerebral Wall. J Neurosci. 19(23):10357-10371.

Takeuchi A and O'Leary DD. 2006. Radial migration of superficial layer cortical neurons controlled by novel Ig cell adhesion molecule MDGA1. J. Neurosci. 26:4460–4464.

Talamillo A, Quinn JC, Collinson JM, Caric D, Price DJ, West JD, Hill RE. 2003. Pax6 regulates regional development and neuronal migration in the cerebral cortex, Dev Biol. 255:151–163.

Tamai H, Shinohara H, Miyata T, Saito K, Nishizawa Y, Nomura T, Osumi N. 2007. Pax6 transcription factor is required for the interkinetic nuclear movement of neuroepithelial cells. Genes Cells. 12(9):983-996.

Tamamaki N, Nakamura K, Okamoto K, Kaneko T. 2001. Radial glia is a progenitor of neocortical neurons in the developing cerebral cortex. Neurosci Res. 41: 51–60.

Tan SS, Kalloniatis M, Sturm K, Tam PP, Reese BE, Faulkner-Jones B. 1998. Separate progenitors for radial and tangential cell dispersion during development of the cerebral neocortex. Neuron. 21(2):295-304.

Tanaka D, Nakaya Y, Yanagawa Y, Obata K, Murakami F. 2003. Multimodal tangential migration of neocortical GABAergic neurons independent of GPI-anchored proteins. Development. 130:5803–5813

Tanaka DH, Maekawa K, Yanagawa Y, Obata K, Murakami F. 2006. Multidirectional and multizonal tangential migration of GABAergic interneurons in the developing cerebral cortex. Development. 133:2167–2176.

Tanaka DH, Yanagida M, Zhu Y, Mikami S, Nagasawa T, Miyazaki J, Yanagawa Y, Obata K, Murakami F. 2009. Random walk behavior of migrating cortical interneurons in the marginal zone: time-lapse analysis in flat-mount cortex. J Neurosci. 29(5):1300-11.

Tarabykin V, Stoykova A, Usman N, Gruss P. 2001. Cortical upper layer neurons derive from the subventricular zone as indicated by Svet1 gene expression. Development. 128:1983–1993.

Tarui T, Takahashi T, Nowakowski RS, Hayes NL, Bhide PG, Caviness VS. 2005. Overexpression of p27 Kip 1, probability of cell cycle exit, and laminar destination of neocortical neurons. Cereb Cortex. 15(9):1343-1355.

Tekki-Kessaris N, Woodruff R, Hall AC, Gaffield W, Kimura S, Stiles CD, Rowitch DH, Richardson WD. 2001. Hedgehog-dependent oligodendrocyte lineage specification in the telencephalon. Development. 128(13):2545-54.

Theil T, Aydin S, Koch S, Grotewold L, Rüther U. 2002. Wnt and Bmp signalling cooperatively regulate graded Emx2 expression in the dorsal telencephalon. Development. 129(13):3045-54.

Thomson AM and Bannister AP. 2003. Interlaminar connections in the neocortex. Cereb Cortex. 13(1):5-14.

Tissir F and Goffinet AM. 2003. Reelin and brain development. Nat. Rev. Neurosci. 4:496–505.

Ton CCT, Hirvonen H, Miwa H, Weil MM, Monaghan P, Jordan T, van Heyningen V, Hastie ND, Meijers-Heijboer H, Drechsler M, Royer-Pokora B, Collins F, Swaroop A, Strong LC, Saunders GF. 1991. Positional Cloning and Characterization of a Paired Box- and Homeobox-Containing Gene from the Aniridia Region. Cell 67:1059-1074.

Ton, CCT, Miwa H, Saunders GF. 1992. *Small eye* (*Sey*): Cloning and Characterization of the Murine Homolog of the Human Aniridia Gene. Genomics 13:251-156.

Toresson H, Potter SS, Campbell K. 2000. Genetic control of dorsal-ventral identity in the telencephalon: opposing roles for Pax6 and Gsh2. Development. 127:4361–4371.

Toresson H and Campbell K. 2001. A role for Gsh1 in the developing striatum and olfactory bulb of Gsh2 mutant mice. Development. 128(23):4769-80.

Tsai LH and Gleeson JG. 2005. Nucleokinesis in neuronal migration. Neuron. 46:383–388.

Tuoc TC and Stoykova A. 2008. Trim11 modulates the function of neurogenic transcription factor Pax6 through ubiquitin-proteosome system. Genes Dev. 22(14):1972-86.

Turque N, Plaza S, Radvanyi F, Carriere C, Saule S. 1994. Pax-QNR/Pax-6, a paired box- and homeobox-containing gene expressed in neurons, is also expressed in pancreatic endocrine cells. Mol Endocrinol. 8(7):929-38.

Tyas DA, Pearson H, Rashbass P, Price DJ. 2003. Pax6 Regulates Cell Adhesion during Cortical Development. Cereb Cortex 13:612-619.

Tuoc TC, Radyushkin K, Tonchev AB, Pinon MC, Ashery-Padan R, Molnar Z, Davidoff MS, Stoykova A. 2009. Selective cortical layering abnormalities and

behavioral deficits in cortex-specific Pax6 knock-out mice. J Neurosci. 29(26):8335-8349.

Valcanis H and Tan SS. 2003. Layer specification of transplanted interneurons in developing mouse neocortex. J Neurosci. 23:5113–5122.

van der Meer-de Jong R, Dickinson ME, Woychik RP, Stubbs L, Hetherington C, Hogan BLM. 1990. Location of the Gene Involving the Small Eye Mutation on Mouse Chromosome 2 Suggests Homology with Human Aniridia 2 (AN2). Genomics 7:270-275.

Walsh C and Cepko CL. 1988. Clonally related cortical cells show several migration patterns. Science. 241:1342–1345.

Walsh C and Cepko CL. 1992. Widespread dispersion of neuronal clones across functional regions of the cerebral cortex. Science. 255:434–440.

Walsh C and Cepko CL. 1993. Clonal dispersion in proliferative layers of developing cerebral cortex. Nature. 362(6421):632-5.

Walsh CA and Goffinet AM. 2000. Potential mechanisms of mutations that affect neuronal migration in man and mouse. Curr Opin Genet Dev. 10(3):270-4.

Walther C and Gruss P. 1991. Pax-6, a murine paired box gene, is expressed in the developing CNS. Development. 113:1435-1449.

Warren, N. and Price, D.J. (1997). Roles of Pax-6 in murine diencephalic development. Development. 124:1573-1582.

Warren N, Caric D, Pratt T, Clausen JA, Asavaritikrai P, Mason JO, Hill RE, Price DJ. 1999. The transcription factor, *Pax6*, is required for cell proliferation and differentiation in the developing cerebral cortex. Cereb Cortex. 9:627-635.

West JD and Flockhart JH. 1994. Genotypically unbalanced diploid<==>diploid foetal mouse chimaeras: possible relevance to human confined mosaicism. Genet Res. 63:87-99.

Wichterle H, Garcia-Verdugo JM, Herrera DG, Alvarez-Buylla A. 1999. Young neurons from medial ganglionic eminence disperse in adult and embryonic brain. Nat Neurosci. 2(5):461-6.

Wichterle H, Turnbull DH, Nery S, Fishell G, Alvarez-Buylla A. 2001. In utero fate mapping reveals distinct migratory pathways and fates of neurons born in the mammalian basal forebrain. Development. 128:3759–71.

Wonders W and Anderson SA. 2006. The origin and specification of cortical interneurons. Nat Rev Neurosci. 7:687–696.

Wood JG, Martin S, Price DJ. 1992. Evidence that the earliest generated cells of the murine cerebral cortex form a transient population in the subplate and marginal zone. Brain Res Dev Brain Res. 66(1):137-140.

Xu Q, Cobos I, De La Cruz E, Rubenstein JL, Anderson SA. 2004. Origins of interneuron subtypes. J Neurosci. 24:2612–2622.

Xuan S, Baptista CA, Balas G, Tao W, Soares VC, Lai E. 1995. Winged helix transcription factor BF-1 is essential for the development of the cerebral hemispheres. Neuron. 14(6):1141-1152.

Yoon K, Nery S, Rutlin ML, Radtke F, Fishell G, Gaiano N. 2004. Fibroblast growth factor receptor signaling promotes radial glial identity and interacts with Notch1 signaling in telencephalic progenitors. J Neurosci. 24(43):9497-506.

Yoon K and Gaiano N. 2005. Notch signaling in the mammalian central nervous system: insights from mouse mutants. Nat Neurosci. 8(6):709-15.

Yozu M, Tabata H, Nakajima K. 2004. Birth-date dependent alignment of GABAergic neurons occurs in a different pattern from that of non-GABAergic neurons in the developing mouse visual cortex. Neurosci Res. 49:395–403.

Yun K, Potter S, Rubenstein JLR. 2001. *Gsh2* and *Pax6* play complementary roles in dorsoventral patterning of the mammalian telencephalon. Development. 128:193-205.

Yucel G. and Small S. 2006. Morphogens: precise outputs from a variable gradient. Curr Biol. 16:R29-31.

Zembrzycki A, Griesel G, Stoykova A, Mansouri A. 2007. Genetic interplay between the transcription factors Sp8 and Emx2 in the patterning of the forebrain. Neural Dev. 2:8.

Zhong W, Jiang MM, Weinmaster G, Jan LY, Jan YN. 1997. Differential expression of mammalian Numb, Numblike and Notch1 suggests distinct roles during mouse cortical neurogenesis. Development. 124(10):1887-97.

Zhou YH, Tan F, Hess KR, Yung WK. 2003. The expression of PAX6, PTEN, vascular endothelial growth factor, and epidermal growth factor receptor in gliomas: relationship to tumor grade and survival. Clin Cancer Res. 9(9):3369-75.

Zhou YH, Wu X, Tan F, Shi YX, Glass T, Liu TJ, Wathen K, Hess KR, Gumin J, Lang F, Yung WK. 2005. PAX6 suppresses growth of human glioblastoma cells. J Neurooncol. 71(3):223-9.

Zimmer C, Tiveron MC, Bodmer R, Cremer H. 2004. Dynamics of Cux2 expression suggests that an early pool of SVZ precursors is fated to become upper cortical layer neurons. Cereb Cortex. 14(12):1408-20.